UNIVERSIDADE DA CORUÑA

ESCOLA POLITÉCNICA SUPERIOR

Departamento de Ingeniería Naval y Oceánica

A STUDY OF SHIP PARAMETRIC ROLL RESONANCE FOR THE EVALUATION OF PREVENTIVE STRATEGIES

ESTUDIO DEL BALANCE PARAMÉTRICO AUTOEXCITADO DE BUQUES PARA LA EVALUACIÓN DE ESTRATEGIAS PREVENTIVAS

TESIS DOCTORAL

Autor: Marcos Míguez González

Director: Fernando López Peña

Fecha: Junio de 2012

The present work was supported by the Spanish Ministry of Education under the FPU program, grant AP2006-03211, and under MICINN project TRA2009-13805 with EDF funding.

UNIVERSIDADE DA CORUÑA

Fernando López Peña, Profesor Titular de Universidad del Departamento de Ingeniería Naval y Oceánica de la Universidade da Coruña,

CERTIFICA:

Que la memoria titulada:

"*A Study of Ship Parametric Roll Resonance for the Evaluation of Preventive Strategies"*

"Estudio del Balance Paramétrico Autoexcitado de Buques para la Evaluación de Estrategias Preventivas"

ha sido realizada por ***Don Marcos Míguez González***, bajo mi dirección en el Departamento de Ingeniería Naval y Oceánica de la Universidade da Coruña y constituye la Tesis que presenta para optar al grado de Doctor.

Fdo: Fernando López Peña

Director de la Tesis Doctoral

A mis padres, Conchita y Luis

RESUMEN

La resonancia paramétrica es una inestabilidad dinámica que afecta a los buques y que puede generar movimientos de balance de elevada amplitud. El diseño de sistemas de prevención y detección es necesario para evitar las consecuencias de la misma. Los objetivos de la presente tesis doctoral son la caracterización de dicho fenómeno para la elaboración de estrategias de prevención y el desarrollo de un sistema de detección del mismo en el corto plazo. Para determinar la influencia que los distintos parámetros implicados tienen en el desarrollo de dicho fenómeno y analizar el nivel de riesgo del buque en una determinada condición, se han aplicado técnicas numéricas así como ensayos experimentales. Asimismo, se ha desarrollado un sistema de predicción basado en redes neuronales, que a través del análisis del balance del buque es capaz de detectar la aparición del fenómeno de resonancia. Ambas propuestas, basadas en el análisis de dos buques de pesca de tamaño medio, resultarán de directa aplicación para la futura obtención de un sistema de alerta, detección y prevención del fenómeno de balance paramétrico autoexcitado.

RESUMO

A resonancia paramétrica é unha inestabilidade dinámica que afecta aos buques, e que pode xerar movementos de balance de elevada amplitude. O deseño de sistemas de prevención e detección é necesario para evitar as consecuencias da mesma. Os obxectivos da presente tese de doutoramento son a caracterización de devandito fenómeno para a elaboración de estratexias de prevención e o desenvolvemento dun sistema de detección do mesmo no curto prazo. Para determinar a influencia que os distintos parámetros implicados teñen no desenvolvemento de devandito fenómeno e analizar o nivel de risco do buque nunha determinada condición, aplicáronse técnicas numéricas así como ensaios experimentais. Así mesmo, desenvolveuse un sistema de predición baseado en redes neuronais, que a través da análise do balance do buque é capaz de detectar a aparición do fenómeno de resonancia. Ambas as propostas, baseadas na análise de dous buques de pesca de tamaño medio, resultarán de directa aplicación para a futura obtención dun sistema de alerta, detección e prevención do fenómeno de balance paramétrico autoexcitado.

ABSTRACT

Parametric roll is a dynamic stability issue affecting ships that may lead to large amplitude roll motions. The design of prevention and detection systems is necessary to avoid its consequences. The objectives of this thesis are to characterize the phenomenon of parametric roll in order to develop preventive strategies and to design a short term prediction system. In this thesis, both numerical and experimental approaches have been applied to analyze the influence of the different parameters involved in the development and amplitude of the phenomenon and to determine the risk level of the ship in a given condition. Moreover, a preliminary detection system based on artificial neural networks has also been developed. Both proposals, based on the analysis of two fishing vessels, have a straightforward applicability in the development of parametric roll alert, detection and prevention systems.

RESUMEN EN ESPAÑOL

El balance paramétrico autoexcitado, más comúnmente conocido simplemente como resonancia paramétrica, es un fenómeno dinámico que afecta principalmente a los buques portacontenedores, Ro-Ro, de pasaje y de pesca. Más probable en mares longitudinales, es debida a la variación de las fuerzas adrizantes con el paso de las olas y puede provocar, de un modo repentino y en un pequeño espacio de tiempo, movimientos de balance de muy elevada amplitud. Estos pueden derivar en grandes daños materiales al buque y a la carga o en daños a la tripulación y en el peor de los casos, pueden provocar el vuelco y la posterior pérdida del buque.

Aunque conocida desde mediados del siglo XIX, no es hasta finales del siglo XX cuando, debido al accidente del buque portacontenedores APL China en 1998, el estudio de la resonancia adquiere la importancia que, dentro del campo de la estabilidad de buques, tiene hoy en día. En los últimos años, el sector marítimo ha mostrado su interés en el desarrollo de sistemas de prevención y detección en tiempo real, que puedan informar a la tripulación del nivel de riesgo de su buque en una determinada condición de navegación, del cercano desarrollo de un episodio de resonancia paramétrica y que, llegado el caso, pudiesen aplicar las medidas correctivas necesarias para evitar su aparición o minimizar sus consecuencias. Y es en este campo en el que se enmarca esta tesis doctoral.

En la misma se han planteado dos objetivos principales. Por un lado, el estudio y la caracterización del fenómeno de resonancia paramétrica, con el objetivo de

determinar el nivel de riesgo del buque en función de las condiciones meteorológicas en que se encuentre navegando y de su condición de carga y de conocer cuál es la influencia que cada uno de los parámetros definitorios de ambas (altura y frecuencia de ola, rumbo, velocidad y nivel de estabilidad del buque, etc.), tiene en la aparición y en la intensidad del fenómeno.

El segundo de los objetivos comprende el desarrollo de un sistema de predicción de resonancia paramétrica que, a partir del análisis del movimiento del buque, sea capaz de detectar en el corto plazo la aparición de la misma.

La metodología adoptada para la obtención del primero de ambos objetivos se ha dividido entre la realización de ensayos con modelos a escala y en la aplicación de modelos matemáticos del comportamiento del buque. Respecto a los primeros, en la presente tesis se han desarrollado dos campañas de ensayos. En ellas, dos modelos de buques de pesca, uno de ellos diseñado específicamente para este tipo de ensayos en el marco de este trabajo, han sido analizados en condiciones de navegación en olas de proa, tanto regulares como irregulares, propicias para la aparición de resonancia. Respecto a los segundos, dos modelos matemáticos no lineales de comportamiento del buque, con distinto nivel de complejidad, han sido planteados, implementados y validados frente a los datos procedentes de los ensayos en canal, con el objetivo de determinar su precisión para determinar la amplitud del balance paramétrico y su viabilidad para ser utilizados en un sistema embarcado de prevención de resonancia. Asimismo, ambos métodos han sido utilizados para definir los niveles de riesgo del buque en cada condición analizada, mediante la obtención de los diagramas de estabilidad correspondientes y para definir la influencia de los distintos parámetros en la intensidad del fenómeno de resonancia.

En lo que se refiere a los algoritmos de detección, en este trabajo se han utilizado redes neuronales artificiales como base para el desarrollo de un novedoso sistema de predicción del movimiento de balance del buque, a partir del que se pueda detectar la aparición de resonancia paramétrica con diversos niveles de anticipación. La eficacia de dicho sistema ha sido evaluada tanto frente a datos numéricos procedentes de los modelos matemáticos antes planteados, como frente a los datos de balance en olas regulares e irregulares procedentes de los ensayos en canal, que pueden considerarse como una situación muy próxima a la realidad, obteniendo, en ambos casos, resultados muy prometedores.

Los resultados obtenidos en ambas fases serán de gran utilidad para el diseño del sistema de prevención anteriormente descrito. Por un lado, el conocimiento de la influencia que cada parámetro involucrado tiene en el desarrollo de la resonancia, permitirá optimizar el desarrollo de las necesarias estrategias de prevención. Por otro, los modelos matemáticos planteados podrán utilizarse como sistemas embarcados que, a partir de los datos del buque, permitan obtener evaluaciones del riesgo de aparición de resonancia para cada condición. Y por último, los algoritmos de detección diseñados permitirán, una vez implementados en un sistema embarcado, detectar en el corto plazo la aparición del fenómeno.

Además de esta línea principal, la presente tesis doctoral ha permitido la apertura de nuevas vías de investigación. Por un lado, el estudio detallado de la dinámica del buque en olas, a través del análisis de la gran cantidad de datos obtenidos durante los ensayos en canal. Y por otro, el estudio experimental de otras inestabilidades dinámicas, tales como el “broaching”, a través de la utilización del modelo a escala desarrollado durante la misma.

ACKNOWLEDGEMENTS

Firstly, I have to thank Prof. Fernando López Peña, my supervisor, for all the patience, advice and trust put in me during the last years. Moreover, I would also like to thank Prof. Richard Duro. Both of them offered me the opportunity of starting a research career within the Grupo Integrado de Ingeniería which has, in fact, become a second home for me.

The presented work has been partially carried out abroad, where I had the pleasure of working with a wonderful set of people. Prof. Thor Fossen, from the CeSOS of Trondheim, Norway, introduced me into the world of control and parametric roll. Prof. Marcelo Neves, from the UFRJ of Rio de Janeiro, helped me to understand the complexity of ship dynamics; moreover, he provided the three degrees of freedom model used in this work. Prof. Mogens Blanke and Prof. Roberto Galeazzi, from the DTU of Lyngby, Denmark, shed some light in the issue of detection schemes. I am very grateful to all of you for your unselfish guidance and fruitful lessons, but also for the warm welcome you all gave me.

I must also thank Prof. Luis Pérez Rojas and all the people working in the Model Basin of the ETSIN in Madrid. Without your continuous help and advice while carrying out the scale model tests in your lab, a major part of this work (and of my knowledge regarding model testing) wouldn't have been possible. And what is more important, thank you for making me feel completely at home when visiting Madrid.

Heading back to Ferrol, I must thank all the people at the Grupo Integrado de Ingeniería. You all have become more than just colleagues and make working here such a fulfilling experience. I would particularly like to thank Prof. Vicente Díaz, largely responsible for starting my research career and that has contributed to it in many ways, including one month of cold testing in Madrid. It is also necessary to mention the people who were involved in the development and tests of the "UK Trawler" scale model: Blanca, Dani, Fai, Felix and Prof. Alvaro Deibe. Thank you for those endless working days. I know it is difficult to bear with me in certain situations, but I hope you will forgive me. I also have to thank Ahitor Regueiro and Pablo Fernández from the EUDI. The help of Marcos (Lema) with the graphics, the contribution of Juan Carlos in making the thesis cover and the effectiveness of Silvia with the administrative paperwork, also deserve a special mention in this section.

I wouldn't have enough space to name all of the friends I would like to. However, I know you all will feel mentioned in here. Sometimes it is necessary to free the mind after work, and you have always had a minute or two for listening to my problems and encouraging me. To all of you, thank you.

Raquel, your energy and support have made this long journey feel shorter; a great part of the time spent in this work is clearly yours. Thank you for being always so near despite really being so far.

And I would like to make a final mention to my parents, Conchita and Luis. Since I was a child, you have provided me with the best atmosphere anyone could need, you have unconditionally supported my decisions and empowered me in any venture I undertook. And this work, that as you say, it is just the beginning of many others, is as much yours as mine. Thank you for always being there.

PUBLICATIONS

For the development of the present work, the following articles related with the main topic of the thesis have been published:

- Míguez González, M., Caamaño Sobrino, P., Tedín Álvarez, R., Díaz Casás, V., Martínez López, A., López Peña, F. 2012. Fishing vessel stability assessment system. *Ocean Engineering, 41*, 67-78.

- Míguez González, M., López Peña, F., Díaz Casás, V., Pérez Rojas, L. 2012. *Experimental Parametric Roll Resonance Characterization of a Stern Trawler in Head Seas*. Accepted in the 11th International Conference on the Stability of Ships and Ocean Vehicles (STAB 2012). Athens, Greece.

- Míguez González, M., López Peña, F., Díaz Casás, V., Galeazzi, R., Blanke, M. 2011. *Prediction of Parametric Roll Resonance by Multilayer Perceptron Neural Network*. 21st International Offshore (Ocean) and Polar Engineering Conference (ISOPE 2011). Maui, EEUU.

- López Peña, F., Míguez González, M., Díaz Casás, V., Duro, R. J. 2011. *Ship Roll Motion Time Series Forecasting Using Neural Networks*. IEEE International Conference on Computational Intelligence for Measurement Systems and Applications (CIMSA 2011). Ottawa, Canada.

- Míguez González, M., López Peña, F., Díaz Casás, V., Santos Neves, M.A. 2011. *Large Amplitude Roll Motion Forecasting through an Artificial Neural Network System*. 12th International Ship Stability Workshop (ISSW 2012). Washington, EEUU.

- Míguez González, M., López Peña, F., Díaz Casás, V., Santos Neves, M.A. 2010. *An Artificial Neural Network Approach for Parametric Rolling Prediction*. The 11th international symposium on practical design of ships and other floating structures (PRADS 2010). Rio de Janeiro, Brasil.

- Míguez González, M., Caamaño Sobrino, P., Tedín Álvarez, R., Díaz Casás, V., Martínez López, A. 2010. Un sistema embarcado de evaluación de la estabilidad y ayuda al patrón de buques de pesca. *Ingeniería Naval*. Vol. 880.

- Míguez González, M., Díaz Casas, V., Martínez López, A., López Peña, F. 2010. *Inteligencia artificial aplicada a la predicción del balance paramétrico autoexcitado*. 49º Congreso de Ingeniería Naval e Industria Marítima. Bilbao, Spain.

- Míguez González, M., Caamaño Sobrino, P., Tedín Álvarez, R., Díaz Casás, V., Martínez López, A. 2009. *Un sistema embarcado de evaluación de la estabilidad y ayuda al patrón de buques de pesca*. 48º Congreso de Ingeniería Naval e Industria Marítima. Vigo, Spain.

- Míguez González, M., Caamaño Sobrino, P., Díaz Casás, V., Martínez López, A. 2008. *Implicaciones de la Resolución IMO MSC.194 (80) en el Diseño de Buques Ro-Pax*. 47º Congreso de Ingeniería Naval e Industria Marítima. Palma de Mallorca, Spain.

- Míguez González, M., Díaz Casás, V., López Peña, F., Duro, R. J. Buques de Pesca y Eficiencia Energética: Proyecto Peixe Verde. Actividad del Grupo Integrado de Ingeniería. *Ingeniería Naval*. Vol. 857.

LIST OF SYMBOLS

Greek Symbols

β	adimensional quadratic roll damping coefficient
χ	wave encounter angle
Δ	ship displacement ($\Delta = \mathrm{m} \cdot \mathrm{g}$)
$\Delta\phi$	roll decay between consecutive peaks
$\Delta\omega$	irregular waves frequency resolution
δ	ANN output local gradient
ε	irregular waves random phase
ϕ	roll angle
ϕ_{avg}	mean roll amplitude
ϕ_{dev}	roll amplitude standard deviation
ϕ_m	mean roll angle of consecutive peaks
ϕ_{max}	maximum roll amplitude
γ	wave spectrum peak shape parameter (PEF)
λ	wavelength

υ adimensional linear roll damping coefficient

υ_L adimensional purely linear roll damping coefficient

ω_e wave encounter frequency

ω_n natural roll frequency

ω_p wave spectrum peak frequency

ω_{pe} wave spectrum encounter peak frequency

ω_w wave frequency

ψ yaw angle

σ spectral width diameter

θ pitch angle

ζ wave elevation

Roman Symbols

A_{44} roll hydrodynamic added mass

A_w wave amplitude

B ship breadth

B_{44a} roll linear damping coefficient

B_{44b} roll linear quadratic coefficient

b ANN biases

C_{44} roll restoring coefficient

c wave celerity

D ship depth

d water depth

ΔGM ship transverse metacentric height variation in waves

e ANN network error

Fn Froude number

$f()$ ANN activation function

GM_0 still water ship transverse metacentric height

GM_T ship transverse metacentric height (also GM)

GZ ship righting lever

g gravity

H_s significant wave height

H_w wave height

I_{xx} ship mass moment of inertia with respect to OX axis

I_{yy} ship mass moment of inertia with respect to OY axis

K_1, K_2 roll extinction coefficients

KM_L height of ship longitudinal metacenter

KM_T height of ship transverse metacenter

k wave number

k_4 ship transverse radii of gyration

k_5 ship longitudinal radii of gyration

L_{oa} ship overall length

L_{pp} ship length between perpendiculars

m ship displacement (mass)

S_J Jonswap wave spectrum

S_{PM} Pierson-Moskowitz wave spectrum

S_{TMA} TMA wave spectrum

T ship draft

T_e wave encounter period

T_n ship natural roll period

T_p wave spectrum peak period

u ship forward speed

v ANN activation potential

w ANN synaptic weights

x surge displacement

x^l ANN neuron input/output vector

y sway displacement

z heave displacement

CONTENTS

1 INTRODUCTION

The analysis of ship roll motions has been of interest for the marine community since the end of the "Sailing Age", in the mid 19th century, when the development of steam ships (abandoning the stabilizing capabilities of sail rigs and being able to sail in all directions) also led to new technical challenges in the field of seakeeping.

These new challenges included both pitch and heave motions (that increased their importance because ships could now sail in the wave direction) and roll motions (as ships didn´t have sail damping). William Froude was the first scientist in studying ship behaviour in waves and motion stabilization and, in fact, was the first in observing the phenomenon on which this thesis is focused. He realized that, in beam seas and when heave and roll frequencies were in the ratio of 2:1, ships developed higher roll motions than in other conditions (Froude, 1863).

Autoparametric roll resonance, parametric roll resonance or simplifying, parametric roll, could be defined as a ship dynamic instability. It is caused by the variation of ship transversal restoring capabilities when waves pass along the hull, together with the effects of the coupling between roll, heave and pitch motion. It reaches its largest intensity in head or stern seas, when wave height exceeds a given threshold and when ship-wave encounter frequency approximately doubles the ship roll natural frequency.

In these conditions, roll motions could increase rapidly up to very large amplitudes, leading, in the worst cases, to the capsizing of the vessel. The intensity of this phenomenon depends also on many other factors, such as ship hull forms, wave amplitude and frequency, roll damping, etc. Of course, the possible consequences that derive from one of these episodes depend on that intensity, but well known incidents have shown that these can be devastating.

Until the end of the 20th century, no remarkable episodes of parametric roll have been described in the literature. However, economies of scale and cargo containerization have led, in the last few years, to the development of very large containership carriers. As will be seen throughout this work, these ships are very prone to parametric roll resonance due to their hull forms and operational characteristics. A series of accidents involving containerships, which suffered this phenomenon, have brought back parametric roll to the forefront of the interests of the marine research community.

In 1998, the APL China, sailing from Taiwan to Seattle, encountered stormy conditions and experienced sustained violent roll motions of more than 35 degrees, resulting in damage to more than 500 containers and the loss of more than 400. The economic losses were estimated in more than US$ 100 million (France et al., 2003).

This event was followed by some others, involving containerships and other types of ships. All of them had a common characteristic: the crew was completely unaware of the possibility of the appearance of parametric roll resonance. At the same time, its fast appearance made it nearly impossible to take any corrective measure.

As a first reaction, these circumstances led among classification societies, ship-owners, national and international governing bodies and the research

community, to the necessity of developing regulations, recommendations and research projects. These had to be aimed at avoiding resonance conditions during navigation, guiding and training the masters to react against the phenomenon or reducing the sensitivity of new designs to parametric roll. Moreover, the need for a system that could prevent the crews about the possible appearance of roll resonance in the near future, had already been stated by the industry.

As a first approach to the problem, and according to Døhlie terminology (Døhlie, 2006), some first generation parametric roll warning systems were developed. These systems, based on weather forecasts and on measuring ship operational parameters, displayed warning areas along the ship route where parametric roll resonance was likely to occur. Although these systems worked well, their greatest disadvantage was that they didn´t exactly detect when resonance was being triggered. So, and in order to avoid the risk of encountering large roll motions, the master had to modify ship heading or speed. This could lead, in some cases, to delays or larger fuel consumptions, without knowing for sure if real resonant conditions will be really found along the planned route.

That was the reason why the development of a second generation of parametric roll warning systems was proposed. These would differ from the previous ones in that they should be able to produce a real time detection of the resonance phenomenon in a short time horizon, trying to avoid the uncertainty of the longer term predictions. These systems would be supposed to act in the short term, but soon enough so as to alert the crew about a close parametric roll resonance episode, allowing them to take corrective actions. And it is in the field of these second generation systems, where the work carried out in this thesis is framed.

The research presented in this dissertation is focused on the study of parametric roll resonance conditions for a set of ships and the development of a parametric roll prediction and prevention system. Installed onboard, this system should be capable of, on one hand, determining the risk of developing parametric roll in a given seaway and advising the crew about it. In the other hand, it should detect the appearance of parametric roll in the short term and trigger the necessary measures to prevent the development of parametric roll or, if that is not possible, minimize its consequences.

In order to determine the risk situation of a ship sailing under a given set of conditions, it is necessary to know how its behaviour is affected by both the environment and its own characteristics and operational parameters. This analysis has been traditionally carried out from two different viewpoints: experimentally or analytically. The former is the most accurate and realistic method for determining ship performance in waves. Especially, if the phenomenon under analysis has a highly non linear behaviour such as parametric roll. But for sure, cost and time consumption imply serious drawbacks for towing tank tests. On the other hand, the latter represents a cheap and fast tool, able to carry out extensive analysis of different ships with a reduced effort, when compared to scale model testing. However, calibration and tuning are usually difficult tasks and performance may not be adequate if a quantitative analysis needs to be carried out.

Once the risk level of the ship has been obtained, the detection system should operate to determine, from the analysis of the needed parameters, if a parametric roll event is under development in the short term. Finally, if such an event is taking place, adequate measures should be adopted to minimize its consequences or prevent it from fully developing. The ability of a given group of actions for taking the ship out of resonance would again depend on ship

characteristics and the external excitations. The knowledge of the ship motions in waves, previously mentioned, is again of paramount importance for determining what and how these measures would be adopted.

The work described in this dissertation includes the research developed in the first two aforementioned topics, i.e. analysis of ship behaviour under parametric roll conditions and the development of short term detection schemes. Moreover, the bases for the future development of automatic prevention strategies have also been set. It has been divided into five different chapters, including this introductory section, where the structure of the dissertation, the objectives of the work and the methodology followed in their consecution are described.

In the second chapter, the theoretical background and state of the art of the different fields studied here are included. A brief historical overview of the research related to ship roll motions and its stabilization is provided. This is followed by the analysis of the phenomenon of parametric roll resonance. A historical review of parametric resonance, including both ships and other dynamical systems is prsented, together with the mathematical description of the generic phenomenon. A more in depth state of the art study of the mathematical modelling of parametric roll on ships is included in the following section, where the different approaches to the matter are reviewed, from the simplest Mathieu equation to the more complex six degrees of freedom methods. The background analysis is continued by describing the typical ships affected by the phenomenon and the incidents involving parametric roll up to date. Finally, a detailed analysis is carried out of the state of the art in the field of parametric roll detection and prevention, including the current regulatory framework, first and second generation detection schemes and the analysis of the different alternatives taken for the prevention of parametric roll.

The third chapter corresponds to the analysis of the roll motion of the vessel in waves. In this work, two vessels have been selected as base ships for study. Taking into account that research in this field has been historically focused on large vessels such as containerships, two medium-sized vessels were chosen with the objective of obtaining data on the behaviour of smaller ships under parametric roll. These are two stern trawlers, typical of the Spanish and British fleets.

In order to study the influence of the different wave parameters and vessel characteristics on the appearance and amplitude of parametric roll motions, a similar methodology has been applied to both vessels. Firstly, a model scale test campaign has been carried out. On it, the motion of the vessels, sailing at different values of forward speed and loading conditions and under the action of regular and irregular head waves of different frequency and amplitude, has been analyzed. In the first case, a carriage-towed model has been used, where pitch and roll motions together with vertical and transversal accelerations have been measured. In the second case, a self propelled radio controlled model, fully monitored and free to move in the six degrees of freedom, has been designed and built. Data collected from these experiments have been used for analyzing the influence of the different parameters on ship roll motion and obtaining the stability diagrams from each case.

In the second half of the analysis, a mathematical model has been set up for each vessel. In the case of the Spanish-type trawler, a nonlinear “one and a half” degree of freedom roll model has been adopted. On it, non linear damping has been obtained from roll decay tests carried out in the towing tank and the nonlinear restoring term has been computed following the quasi – static look-up table approach. The selected model for simulating the motions of the UK trawler is the well known nonlinear model developed by M.A.S. Neves (M.A.S.

Neves,Rodríguez, 2006), where heave, roll and pitch motions are obtained in a coupled way. Roll damping has also been obtained from roll decay tests. A comparison with values by Ikeda is also included in this section. Both models have been extensively used for reproducing ship motions in different conditions. The results obtained have been validated against those from the towing tank tests and the performance of each model for computing roll amplitude, evaluated. Moreover, the stability areas corresponding to both vessels have been obtained and compared to the ones obtained from the scale model tests. Finally, their usefulness for defining the risk levels of the ship, evaluated.

In the third chapter, the design and development of parametric roll detection schemes is considered. These systems are based on the application of artificial neural networks and their capacity for reproducing the behaviour of non linear systems after a process of training. Their performance for predicting the appearance of parametric roll has been tested in head regular and irregular seas for the two ships analyzed, obtaining, for both of them, very promising results. In the case of the Spanish trawler, data obtained from towing tank tests has been used, while in the UK vessel case, data has been obtained from the three degrees of freedom model.

Finally, the main conclusions of this work, together with the future research lines which have been identified in the development of this thesis, have been stated in the fourth chapter.

1.1 Objectives and Methodology

As may be concluded from the introduction above, the main objectives of this thesis are the following. On one hand, to study the phenomenon of parametric roll resonance, with the aim of being able to determine the risk level of ship in a seaway as a function of the environmental parameters and its own sailing

conditions. On the other hand, designing a system capable of forecasting the ship roll motion and detecting, in the short term, the appearance of parametric roll resonance phenomena. In order to obtain these main objectives, some other sub-objectives have to be accomplished.

Regarding the first of the aforementioned objectives, and taking into account that the analysis of roll resonance will be carried out from two different perspectives, the corresponding sub-objectives were:

- To carry out a scale model towing tank test campaign with a carriage-towed vessel, with the objective of obtaining data of its behaviour in parametric roll conditions for different sailing parameters and wave conditions, including regular and irregular waves.
- The design and development of a self propelled and controlled scale model to carry out a second towing tank test campaign in regular seas, also defining, designing and implementing the necessary monitoring, data acquisition and control systems.
- To design and implement a single degree of freedom nonlinear model of roll motion, capable of simulating parametric roll resonance in head seas. Validate this model against roll decay and roll motion from scale tests and evaluate its performance for different conditions.
- To implement a three degrees of freedom nonlinear coupled model of roll, heave and pitch motions and compare its results to towing tank test data of different sailing conditions. To evaluate its performance and compare the results to the simpler approach of the previous one degree of freedom model.
- To evaluate the applicability range of both mathematical models for determining the risk of parametric roll for the two ships under consideration. Moreover, analyze the influence of the different

parameters involved in the development of parametric resonance on its appearance and intensity.

When considering the second of the two main objectives, which is the development of a parametric roll prediction system, the following sub-objectives have to be taken into account:

- To design and implement an artificial neural network based roll motion forecasting system.
- To evaluate the suitability of the previously developed system for predicting the appearance of parametric roll resonance. This will be done by analyzing its performance against roll motion in regular and irregular head seas, obtained from both towing tank test and mathematical model simulations.

In order to achieve these objectives, it is necessary to follow an adequate methodological strategy; the adopted one could be summarized in the following points:

- Study the background and theoretical basis of parametric roll resonance, in order to define which parameters influencing this phenomenon are the most important regarding its development and intensity.
- These parameters will be measured during towing tank testing and taken into account in the design of the numerical models. These data will be later analyzed in order to determine the influence of each parameter on parametric roll.
- Data from the roll decay tests and the towing tank tests will be applied in the mathematical models, to respectively improve and validate their performance.

- Regarding the roll forecasting algorithms, different alternatives will be systematically implemented and evaluated, in order to select the best performing ones. Data previously obtained from towing tank and mathematical models, will be applied in this step.

2 PARAMETRIC ROLL RESONANCE

2.1 Historical Overview

2.1.1 Ship Roll Motions

If the ship is considered as a rigid body, its motions could be described in six degrees of freedom, considering three translations (surge, sway and heave) and three rotations (yaw, pitch and roll). Among them, roll motion, that is, rotation in the transversal plane, is the most important regarding the safety and operational capabilities of the ship and focus the attention of a great sector of the industry and research community.

Large roll motions could lead to cargo damage, could affect the work of the crew and the comfort of the passengers and could increase the risk of the ship on its seaway due to possible flooding or capsizing if stability levels are not high enough.

However, the analysis of ship roll motions has been only of interest for the marine community since the end of the “Sailing Age”, at the middle of the nineteen century, when the development of steam ships (abandoning the stabilizing capabilities of sail rigs and being able to sail in all directions) also led to new technical challenges in the field of seakeeping (Lloyd, 1989).

These new challenges included both pitch and heave motions (that increased their importance because ships could now sail in wave direction) and the structural challenges that this fact implied and the effects of roll motions, that in

this moment became more noticeable and important as ships didn´t have the damping effects of sails.

The importance of ship transverse stability (closely related to roll), has always been present in the mind of naval architects, but it was not until the mid eighteenth century when the modern ship stability theory was proposed. The increase of size and gun load of the navy ships, also raised the need for safer vessels from the transverse stability point of view. As a response to this need, the scientific community started focusing on this matter (Fincham, 1851).

Pierre Bouguer, in his "Traité du Navire" (Bouguer, 1746), in 1746, establishes the concept of metacenter, while Leonard Euler, in his "Scientia Navalis" (Euler, 1749) and just a few years later (though both works were simultaneously done), proposed the nowadays well known concept of initial stability or transverse stability at small roll angles (Mégel,Kliava, 2009; Nowacki, 2006, 2008; Nowacki,Ferreiro, 2011). Their work related to the static stability was continued by Jorge Juan in his "Examen Marítimo" (Juan,Navia, 1793) and Atwood, that at the end of the 18^{th} century (1796, 1798), successfully developed the theory of stability, settling the principles of large angle stability and introducing the concepts of righting moments and GZ curves (Fincham, 1851).

As can be appreciated, the transverse static stability of the ships was, by that time, starting to become more predictable for naval architects, but the principles of roll motion were still far from been known. The first author in dealing with this issue was Bouguer (Bouguer, 1746), but his principles were based on wrong suppositions.

Daniel Bernoulli was, in fact, the first author in studying with detail the problem of rolling and pitching of ships. In 1755, the Academie Royale des

Sciencies awarded its prize to M. Chauchot, for a memory about the reduction of ship roll and pitch motions. As his results were not totally satisfactory for the Academie, as they lacked precision and detail (Fincham, 1851), a new prize about the same topic was announced for 1757. This prize was won by Daniel Bernoulli with his memoire, were a detailed study was undertaken (Bernoulli, 1810); he begins his work with an analysis of the static stability of ships, to continue with the oscillations of floating bodies, based on the fact that ship motions depended on its stability properties. Bernoulli describes two different types of oscillations: one type he calls "natural oscillations", which period depends on the stability of the ship, and another type of oscillations that are forced by subsequent impulses. Along his work, Bernoulli describes which parameters affect both types of ship motions, based on the comparison with a simple pendulum, and propose alternatives for reducing the roll motion of the ships. He also analyses the influence of stability, ship natural roll period and the influence of external force period and intensity in the amplitude of the roll motion. But as could be seen from above, the roll motion is considered as the effect of a simple action (wave impact on ship sides), and not as a consequence of the water pressure distribution along the hull.

Daniel Bernoulli is considered as the first scientist in directing his efforts to the study of the roll motions of the ship. Although some other scientist after him like Jorge Juan (Juan,Navia, 1793) or Euler (Euler, 1759) considered the issue of high importance and difficulty and continued their studies on the matter, no significant advances could be mentioned, as the effects of waves were still not considered. This fact is clearly stated by Jorge Juan in his Examen Marítimo:

"Of all the theories of a ship´s motions, the most complicated is, without contradiction, that of the rolling and pitching. Without doubt it is for the reason that the most celebrated authors are satisfied with considering the rolling as the

effect of a simple action in a ship […]; but it is clearly seen, that in considering the rolling under this aspect, it would not depend at all upon the action of the waves, whilst it is the wave which produces it, and which can both increase it and diminish it".

D. Jorge Juan deals with the problem of ship roll motions in the 5th Chapter of the 4th book of the second volume of his Examen Marítimo. The author considers the characteristics of the waves (height, length and period) and their influence in the roll behavior of the vessels; however, the need for simplifications due to the difficulties found in dealing with the mathematics of the problem, again lead to not correct conclusions. The work by Jorge Juan was translated by Pierre Leveque and become known in France by 1783.

The end of the sailing age, by the mid nineteen century, led to new challenges for naval architects. The new steam ships were lacking huge sails and masts (and so also their stabilizing capacities) and could sail straight on the waves; roll and pitch motions subsequently dramatically increased their amplitude and generated new problems that until that time haven´t had been significant.

The renewed interest in the rolling of ships started in the 1830´s in Great Britain, as a new class of naval ships designed by that time were found to have very undesired rolling characteristics. This fact could have inspired William Froude, that by the 1850´s started his own research in the field of roll motions, apparently with a lack of knowledge of any other prior work on this matter (Brown, 2006). This work continued in 1857 with the assignment by Isambard Kingdom Brunel, the designer of the Great Eastern (the largest ship by that time), of developing a theoretical study of roll motion.

From the beginning, the work of Froude was focused on analyzing the effect of waves, and he based it on experiencing and observing floats in real wave

conditions. In order to developing the mathematical theory that would fit his observations, Froude was helped by William Bell (a Brunel staff member) and the work done was published in 1861 by the Institution of Naval Architects (Froude, 1861); on it, theory of roll motion in regular waves, without considering roll resistance, had been described.

From this work, Froude extracted three main conclusions: the first one, that the roll of the ship would be the same in identical waves, if the difference of its metacenter (due to ship forms) and centre of gravity (due to weight distribution) was the same, disregarding its absolute height.

The second one is related with the phenomenon of syncronous resonance in beam waves and states that when the natural roll period of the ship is the same of wave encounter, roll amplitude could increase largely.

Finally, the third conclusion deals with the effect of metacentric height (GM) in roll motions. Ships with large natural periods (and small metacentric height), would roll less than those stiff ships with large metacentric heights, that although will roll to smaller angles, would do it more quickly and with more acceleration. This last fact lead to heavy discomfort, heavy loads on masts and structures and bad firing performance, some of the problems that Symonds' ships were suffering from. The compromise between enough stability (large GM, stiff ships) and good roll behavior (low GM) become in that moment an issue of discussion of the marine community; Froude advice to this matter was to make stability adequate for safety, but not excessive.

The work of Froude continued with the study of roll resistance and the development of roll tests, both with scale models and real ships. By the 1870´s, the use of turrets was substituting side cannons, while sail rigs were starting to be in disuse, been replaced by fully steam powered ships. Roll motions of these

kind of ships had became an important design parameter, and demanded more attention from the designers, builders and governments.

The lost of the turreted battleship Captain in 1870, due to stability deficit, set up a Committee on Designs for Ships of War, in charge of analyzing the stability levels of the fleet warships.

Froude was part of this committee, and this allowed him to carry out a vast number of trials, both with scale models and real vessels, in order to analyze the roll characteristics of the different ships. These tests included the first full scale roll trial (HMS Glatton, 1871) or those of the first British ship with no sails (Devastation, 1871 - 1875) (Brown, 2006).

2.1.2 Roll Stabilizing Systems

Devastation test campaign included test with two different scale models (1871) and also real sea trials of the ship (1873-1875). During these tests, Froude discovered that roll resistance was a function of roll speed and tested the efficiency of bilge keels for reducing roll motion; by this time, the need for stable platforms for improving gunnery had become a major issue, and the study of ways for reducing roll motion started. The described use of bilge keels by W. Froude represents the first attempt for designing a roll reduction device.

Roll resistance was quantified in 1875 during the sea tests of two sloops, Greyhound and Perseus, only the first equipped with bilge keels; the effect of this stabilizing device was also verified during sea trials of Shah (1875), tested with and without them. Also in 1875, after the tests of the Fantome, Froude developed the first polar diagram of wave encounter period as a function of heading (Brown, 2006).

In 1877, two years before his death, a Committee with the objective of analyzing the stability of the new battleship Inflexible was set up by the British

Admiralty, both in intact and damaged conditions, by carrying out model tests and theoretical analysis of the vessel. Froude was part of this Committee, while Philip Watts was one of his assistants for accomplishing these studies.

During the experiments, Froude observed that in certain conditions (low number of compartments and with an appropriate filling), the expected roll motions were not reached and that a reduction in the motion amplitude appeared. In the Committee report, it was concluded that the free flowing of the water in the flooded tanks contributed to the increase of the righting levers of the ship, and so stability characteristics were improved (Brown, 2006; Perez, 2005). As a result, in 1880, the ship was fitted with water chambers, and the obtained results reported by Phillip Watts (Watts, 1883, 1885). He was, in fact, the first in applying tanks (in this case free flow tanks) for roll motion reduction (Perez, 2005; Treakle III, 1998).

2.1.3 Autoparametric Roll Resonance

Among the observations made by William Froude, and contained in one of his papers on rolling, there is one that should be mentioned due to its relationship with the main topic of this work.

In 1863, Froude observed that a ship whose linear natural undamped frequency in pitch doubled that in roll, experienced undesirable seakeeping characteristics (I. Oh,Nayfeh, 1996). This undesirable behaviour was, actually, the manifestation of the effects of coupling between these two degrees of freedom that, under a set of given conditions, was showing up.

This phenomenon was a type of internal resonance and, when affecting ship´s roll motion, it is usually called autoparametric roll resonance, parametric roll resonance or, simplifying, parametric roll and is, in fact, the principal issue this

work is about. In the following sections, a description of the phenomenon, its characteristics and importance, will be done.

2.2 Resonance in Dynamical Systems

2.2.1 Resonance & Parametric Resonance

The tendency of a mechanical system to absorb more energy when the frequency of its oscillations coincides with its natural frequency is called resonance. If such a system is excited in that frequency, the amplitudes of the reached oscillations would largely increase. The phenomenon of resonance is well known and considered in many fields of physics and engineering: architecture (buildings), civil engineering (bridges), mechanical engineering (road vehicles, airplanes…) and also in naval architecture.

If we consider the equation of motion of a simple non-damped oscillator,

$$m \cdot \frac{d^2x}{dt^2} + k \cdot x = 0 \tag{1}$$

And the natural oscillation frequency is defined as:

$$\omega_0 = \sqrt{\frac{k}{m}} \tag{2}$$

then

$$\frac{d^2x}{dt^2} + \omega_0^2 \cdot x = 0 \tag{3}$$

In the case the system is excited by a time varying sinusoidal force, $F(t) = F_0 \cdot \sin(\omega \cdot t)$

$$\frac{d^2x}{dt^2} + \omega_0^2 \cdot x = \frac{1}{m} \cdot F(t) = \frac{1}{m} \cdot F_0 \cdot \sin(\omega \cdot t) \tag{4}$$

In this case, if the frequency of the excitation force ω coincides with the natural frequency of the system ω_0, resonance takes place and the amplitude of the motion becomes infinite.

In the more realistic scenario of an under-damped system, also excited by a sinusoidal force:

$$\frac{d^2x}{dt^2} + \frac{c}{m} \cdot \frac{dx}{dt} + \omega_0^2 \cdot x = \frac{1}{m} \cdot F_0 \cdot \sin(\omega \cdot t) \tag{5}$$

$$\frac{d^2x}{dt^2} + 2 \cdot \xi \cdot \omega_0 \cdot \frac{dx}{dt} + \omega_0^2 \cdot x = \frac{1}{m} \cdot F_0 \cdot \sin(\omega \cdot t) \tag{6}$$

$$\xi = \frac{c}{m} \cdot \frac{1}{2 \cdot \omega_0} \tag{7}$$

$$\omega_{res} = \omega_0 \cdot \sqrt{1 - \xi^2} \tag{8}$$

Where ξ is the dimensionless damping ratio (ξ < 1). Again, the amplitude of the motions would be larger when the frequency of the excitation coincides with the resonance frequency, that in this case is influenced by the damping ratio of the system.

The phenomenon of parametric resonance also implies the development of very large amplitude oscillations. From the above, it is clear that resonant oscillations were generated by an external excitation acting on the system. However, in the case of parametric resonance, there is no external excitation, and the oscillations are produced by a periodical change in some of the parameters of the system.

If we consider the equation of the unforced undamped oscillator and consider that the modification of the system parameters leads to a sinusoidal variation of the natural frequency of the system (ω_0) of the form $\omega_0^2 \cdot \left(1 + a \cdot \cos\left(\omega \cdot t\right)\right)$, where ω is the frequency of the parametric excitation, we get

$$\frac{d^2x}{dt^2} + \omega_0^2 \cdot \left(1 + a \cdot \cos\left(\omega \cdot t\right)\right) \cdot x = 0 \tag{9}$$

By making the variable change $\tau = \omega \cdot t$ and dividing all terms by ω^2, we get

$$\frac{d^2x}{d\tau^2} + \frac{\omega_0^2}{\omega^2} \cdot \left(1 + \cos\tau\right) \cdot x = 0 \tag{10}$$

that is the well know Mathieu Equation (Abramowitz,Stegun, 1964), used for describing the behavior of an oscillator which frequency is sinusoidally changing with time:

$$\frac{d^2x}{d\tau^2} + \left(p + q \cdot \cos\tau\right) \cdot x = 0 \tag{11}$$

Where,

$$p = q = \frac{\omega_0^2}{\omega^2} \tag{12}$$

The solutions of the Mathieu differential equation depend on the parameters *p* and *q*, that govern the behavior of the system. The different combinations of the two parameters would lead to bounded solutions (shaded areas of Figure 2.1) or to the existence of at least one unbounded solution (non shaded areas).

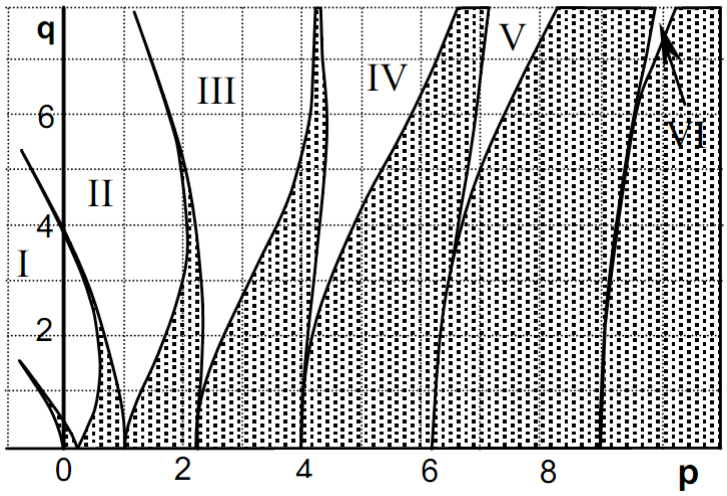

Figure 2.1. Ince-Strutt diagram of Mathieu equation (Shin et al., 2004)

A bounded solution means that a stable steady state would be reached, while no steady state would be achieved for unbounded solutions (V.L. Belenky,Sevastianov, 2007).

The first instability area has its lowest point when $p = 0.25$, which means that the excitation frequency doubles the natural frequency of the system. The second area of instability has its lowest point at $p = 1$, so the system is being excited at its natural frequency.

As will be described in the next section, parametric resonance phenomena could be found in many different mechanical systems and the Mathieu equation can be used to reproduce them. As will be seen, in the case of parametric roll of ships, the nonlinear damped equation of roll motion could be properly transformed into the aforementioned Mathieu equation (Shin et al., 2004).

2.2.2 Parametric Resonance in Mechanical Systems

The phenomenon of parametric resonance was first observed by Faraday in 1831, as he reported that the waves created in the surface of a vertically excited

open air container, partially filled with liquid, had half the frequency of the excitation (Faraday, 1831). Melde, in 1859, observed lateral oscillations of a string longitudinally excited by a tuning fork; those oscillations had half the frequency of the fork, and only appeared under certain conditions (A. H. Nayfeh,Mook, 2004). Those observations were explained by Lord Rayleigh (J.W. Strutt) in 1883 and 1887 (Birikh et al., 2001; A. H. Nayfeh,Mook, 2004), who was the first in proposing a theoretical basis of the phenomena.

Nowadays, parametric resonance is well known and its effects are broadly studied and applied in many contexts of physics and engineering, mostly based on oscillatory mechanical or electrical systems, but also including wave propagation an optical systems. The behavior of most of these systems could be reduced to differential equations, which under the temporal variation of some parameter lead to a parametric resonant response; the paradigmatic repetitive of this kind of equations is the Mathieu equation, that has already been described.

Parametric resonance could be found in mechanical and elastic systems, under the effect of time varying loads. Diverse examples of these fields could be the analysis of vibrating cantilever beams (Oueini,Nayfeh, 1999), ship roll resonance (that will be broadly described in the next chapter), resonance in wave energy converters (Leybourne et al., 2009; Olvera et al., 2001, 2007) or steering instabilities in motorcycles (Evangelou et al., 2006; Salvador,Fabris, 2004; Shaeri et al., 2004; Sharp, 2001).

Electrical oscillating systems are another example of systems where parametric resonance effects are exploited (Butikov, 2005; Damgov, 2004) and also another applications are found in microelectromechanical (MEMS) oscillators (Shaw et al., 2003).

Wave propagation in periodical lens-guide structures, wave evolution in optical resonators (Longhi, 2000) and applications in microscopy (Longhi, 2000; Moreno-Moreno et al., 2006) are among the resonance cases in the field of optics.

For a broader and vast bibliographic analysis on the subject of parametric resonance in different systems, the book by (A. H. Nayfeh,Mook, 2004) "Nonlinear Oscillations" and references therein represent a very good source of information.

2.3 Parametric Roll Resonance on Ships

Ship roll resonance, or synchronous rolling, is a well known matter that was described by Froude in 1861, in his famous work "On the rolling of Ships" and was described in one of the three main conclusions from his theory of ship roll motion; "[…] *one of Froude´s early discoveries was that rolling is worst when the period of the ship is in resonance with that of wave encounter and under such conditions the roll angle can increase alarmingly*" (Brown, 2006).

As has been already said, roll motion due to wave action only started being a matter of study by naval architects when steam become the main source of energy for the propulsion of ships; the worst situation from the rolling point of view was that of the ship sailing in beam seas (where transverse heeling forces were larger). In these conditions, synchronous rolling or resonant rolling took place when wave excitation frequency was the same of the natural roll frequency of the ship, generating very large roll motions that, in certain cases, could lead to capsizing. It is clear that roll resonance was generated by the effect of an external disturbance acting transversally to the ship, the ocean waves.

The phenomenon of parametric roll resonance is different. Although in both cases large roll motions are reached, the latter one can develop when the ship is sailing in pure head or stern seas, with no external transverse excitation causing the motions (although, as will be later described, may also develop in beam seas (Fujiwara,Ikeda, 2007; Skomedal, 1982)). As explained in the previous section, the periodic variations of some internal parameter of the system (in this case the transversal stability of the ship), are producing these large roll motions.

Parametric resonance is most likely to happen when the ship is sailing in head or stern seas, under some specific conditions such as a wave encounter frequency doubling the ship's natural roll frequency, a wavelength almost equal to the ship length and a wave amplitude over a ship dependent threshold. When these conditions are fulfilled, the periodic alternation of wave crests and troughs amidships brings about dramatic changes in ship transverse stability which, in turn, determine a sudden and quick growth of roll oscillations if any external small disturbance (that is always present in a real seaway) starts the motion.

In the following figures, this fact can be appreciated. For a wave of a similar wavelength to the ship length, when the wave crest is situated amidships (Figure 2.2), the waterplane area is minimum and stability parameters (heeling arms curve (GZ) and metacentric height (GM)) are also minimum. On the contrary, when the wave trough is amidships (Figure 2.3), waterplane area and stability parameters reach a maximum.

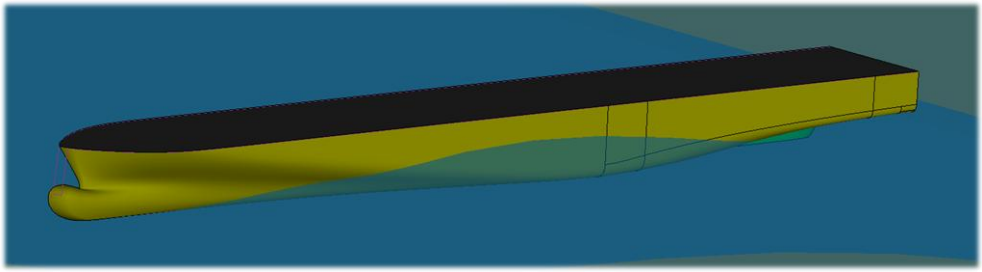

Figure 2.2. Perspective view of a ferry vessel in longitudinal regular waves. Wave crest amidships.

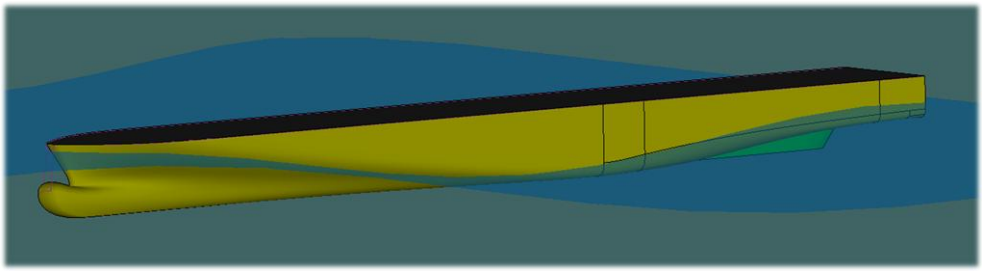

Figure 2.3. Perspective view of a ferry vessel in longitudinal regular waves. Wave trough amidships.

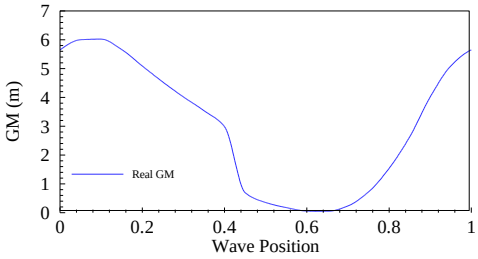

Figure 2.4. GM variation due to wave passing. Ferry vessel.

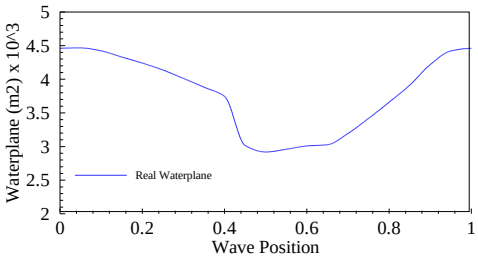

Figure 2.5. Waterplane area variation due to wave passing. Ferry vessel.

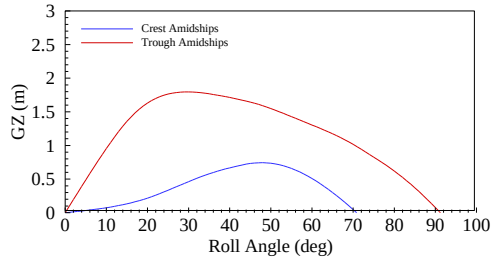

Figure 2.6. GZ curve variation due to wave passing. Ferry vessel.

The variation of waterplane area and metacentric height with the position of wave crest along the hull (0 and 1 represent crests at bow and stern, 0.5 crest at midships) can be seen in Figure 2.4 and Figure 2.5. The GZ curves for the two extreme cases (wave trough and crest amidships), are displayed in Figure 2.6.

In this situation, when this periodic variation of the stability parameters is correctly tuned (the frequency of encounter between ship and waves is twice the natural roll frequency), roll motion starts increasing until the aforementioned necessary conditions disappear, the ships capsizes or roll amplitude is limited by roll damping.

Of course, the effects of such an event could be very different, significantly depending on the violence of the phenomenon itself and the stability levels and roll damping of the ship; in any case, and as will be seen in following sections, extremely dangerous situations could develop, leading to severe cargo and structural damage, personal injuries and even in the worst cases, the capsize and loss of the vessel.

As have already been mentioned, parametric roll resonance was apparently first described by Froude in his papers on rolling (Froude, 1861, 1863). According to (France et al., 2003), the first studies of the stability variations that a ship experiences when sailing in longitudinal seas, date up to the end of the 30´s and the beginning of the 40´s, with the works of Kempf and Graff (Graff,Heckscher, 1941; Kempf, 1938), where the influence of wave passing in the stability levels is investigated. The attention into the parametric roll phenomenon was, by that time, focused on small and medium sized ships, like fishing vessels and coastal carriers, due to some recent accidents, and mainly focused on the case of sailing in following seas and reduced levels of stability.

The aforementioned studies were followed by those of Grim (Grim, 1952), Kerwin (Kerwin, 1955), Paulling and Rosemberg (Pauling,Rosenberg, 1959) or Kinney (Kinney, 1961), which studied the roll behavior of ships in longitudinal waves from a theoretical point of view (I. Oh,Nayfeh, 1996), raising up the effects of couplings between heave and pitch and roll motions.

Research regarding parametric roll resonance in the second half of the twentieth century continued being quite scarce, and was mainly focused in the theoretical analysis and the mathematical modeling of the phenomenon (which will be later treated in this introductory section). Studies in these years are mainly those of Blocki, Nayfeh, Mook or Marshall (Blocki, 1980; Mook et al., 1974; A.H. Nayfeh et al., 1973), from which only Blocki´s one is based on an experimental basis, while the other approaches are mainly focused on the study of heave and pitch couplings with the roll motion. These last research was continued in (A. Nayfeh, 1988; Sanchez,Nayfeh, 1990), where the non linear modeling of ship motions in longitudinal seas was dealt with. Moreover, the work by (I. G. Oh et al., 1993) continued in this line, adding further research by experimental analysis of a tanker model.

However, parametric roll resonance remained as a marginal field until the presentation in the 2001 of the APL China accident case study (France et al., 2003), which showed up the vulnerability of large containerships to developing parametric roll resonance and the dangerous and costly consequences that the phenomenon might lead to.

From this moment on, parametric roll resonance became a matter of great interest for the maritime community and research focused on three main topics: firstly, in the understanding and accurate modeling of the phenomenon, through the use of mathematical models and scale model tests. Secondly, in the study of

preventive strategies and design of warning systems for avoiding the appearance of parametric roll. And thirdly, in the development of stabilizing systems and other control-based approaches with the objective of limiting the consequences of such events.

A more detailed analysis of the historical background and the state of the art of each of these topics, will be done in the subsequent sections of this work.

2.3.1 Parametric Roll Mathematical Modelling

2.3.1.1 Theory of Seakeeping

The problem of determining the behavior of a ship sailing under the effects of waves, also known as seakeeping, is that of determining the pressure field generated by the water flowing around the hull and how the vessel accordingly modifies its position. As for any other type of fluid, this field is governed by the well known Navier-Stokes equations and different approximations have been developed in order to obtain valid solutions to this issue.

Historically, seakeeping analysis was introduced by the studies about roll motion of William Froude at the mid 19th century, that have been previously described in the introductory section of this dissertation. His work was continued along the first half of the 20th century, based on experiments with scale models in the worldwide growing towing tanks, but limited to the simplest cases of regular waves in head, following or beam seas, with no correlation with the ship behavior in a realistic seaway (Lloyd, 1989).

In the 1950´s, two main developments represented a turning point in the research about seakeeping analysis. Firstly, the paper of St. Denis and Pierson (Pierson,St Denis, 1953), where the statistic of ship responses to irregular seas at zero forward speed are computed using spectral methods. Secondly, the development of linear methods for obtaining ship responses in regular seas.

In the first proposal, the authors compute the ship motions at zero forward speed by relating the spectral density of the vessel responses with the wave spectrum of a given seaway. The method was based on two assumptions; on one hand, the sea surface is supposed to be ergodic, Gaussian and with zero mean. On the other hand, the ship is supposed to be a linear system. Under these assumptions, the spectral density of any of the ship responses may be obtained by multiplying the incident wave spectrum by the square of the transfer function (Response Amplitude Operator, RAO) of that response. The RAO represents, for each frequency, the amplitude and phase of the response to regular waves exciting the vessel at that frequency.

Moreover, once obtained that spectral density, the area under this curve is the variance of the probability density function of the response, that under this conditions is fully characterized by this parameter, and that provides all the statistical data of the desired vessel response.

According to this method, the problem of evaluating the motion of a ship at sea is that of knowing the sea spectrum of the seaway and the RAO of the desired responses (Beck,Reed, 2000), that should be computed both by experimental methods (time consuming and expensive) or by analytical ones.

The development of analytical techniques for obtaining the ship responses under the effect of regular waves (and so RAO´s), started at the same time that the spectral theory was presented. All of these theories (and most developments until recent dates) neglected viscosity and applied potential flow. Three main approximations were proposed: the thin ship approximation, the slender body approximation and the strip slender body (usually known as strip theory). The first two didn´t obtain good results, but the latter did and, in fact, evolutions of

the method are widely in use today (Beck,Reed, 2000) and have been used in this work.

Strip theory, as well as the other two approximations, is used for determining the hydrodynamic coefficients of the ship and the exciting wave loads as a function of the frequency, by considering potential flow. This theory has its basis in the work of Ursell about determining the hydrodynamic coefficients of semicircular cross sections oscillating at zero speed in deep waters. Successive works improved the method, by mapping ship sections into those semicircular sections and by including the cases of forward speed and shallow waters (T. I. Fossen,Smogeli, 2004). The most well known strip theory approach is that of (Salvesen et al., 1970), also known as S-T-F, where both forward speed and transom stern effects are accounted for.

Nowadays, strip theory is still the most used method for determining ship motions in waves sailing with forward speed. However, and as will be seen, the fully linear approach that this theory implies, won´t be useful for the adequate modeling of parametric roll resonance.

2.3.1.2 Ship Motion Mathematical Modelling

In order to obtain an approximate solution to the Navier Stokes equations applied to the case of a ship moving in waves, a series of simplifications and assumptions have to be carried out.

First of all, fluid should be considered isotropic and Newtonian, and the effects of viscosity would be neglected (which relevant influence in roll motion will be later revisited). And secondly, fluid is considered irrotational. These two assumptions would transform the vector field of velocities into a scalar field, i.e. potential field.

In order to solve the simpler resulting problem, it is necessary to define the boundary conditions of the system in the free surface of the water, defined by the ocean waves. In this step another simplification should be carried out, consisting in the linearization of this free surface. In order to do this, the height of the wave should be considered small in relation with its wavelength, which is usually true in oceanic waves.

Linear theory is usually adopted, as (Pierson,St Denis, 1953) did for determining ship responses in irregular seas. Under the assumption of linearity of a system, the principle of superposition applies; if two solutions of the system are known, then the summation of both is also a valid solution. Applied to our system, this principle states that the responses of the ship to two or more simultaneous different excitations, would be the same that if the responses to each particular excitations acting separately are computed and then added up (M. A. S. Neves, 2004).

This fact allows us to simplify the problem of ship behavior in waves by dividing it into more simple ones; in particular, forces acting on the ship can be split into different components, proportional to ship accelerations, velocities and displacements, and also in external forces, and by considering that motions in some degrees of freedom have no influence in others (Lewandowski, 2004).

Linear theory for seakeeping has proven to be accurate enough for engineering purposes under the small motions assumption. However, some problems in the field of seakeeping are known to be largely nonlinear, as broaching or surf riding in following seas (Umeda, 1999) and also large amplitude roll phenomena, such us parametric roll resonance. Traditionally, in these cases, instead of tackling the problem from a fully non-linear point of view, the superposition principle and the separation of variables is still applied, and non-

linearities are directly added to the corresponding equations. Although this approach is not correct, in most cases it has been the only way for dealing with the complicated problems derived from the non-linearity of the system, as will be later described in this work (V.L. Belenky,Sevastianov, 2007; M. A. S. Neves, 2004).

If we consider the fully linear approach, the time domain motions of a ship sailing in waves can be described by a Mass – Damper – Spring system, moving in six degrees of freedom, with respect to an inertial reference system OXYZ which moves forward at the ship speed *u*, where the OXY plane coincides with the ship waterplane in still water, the OXZ is the ship´s diametric plane and the OZ axis is in the vertical of the ship´s mean center of gravity; the OX axis is positive in the speed sense, the OY axis is positive pointing to port, and the OZ axis is positive upwards.

In addition to this frame of reference, two other should be taken into account: an earth-fixed one ($SX_0Y_0Z_0$), which SX_0Y_0 plane is in the still water surface, the OX_0 axis is positive in the wave propagation direction (which may deviate of the ship speed direction) and the SZ_0 is positive upwards. And a body fixed frame ($GX_bY_bZ_b$), centered at the ships centre of gravity G, where GX_b is positive in the forward direction, GY_b in the port direction and GZ_b upwards, and the GX_bY_b plane is parallel to the still water surface when the ship is at rest.

The aforementioned six degrees of freedom are three translations of the centre of gravity of the ship, surge in the OX axis, sway in the OY axis and heave in the OZ axis, and three rotations, roll (around OX), pitch (around OY) and yaw (around OZ).

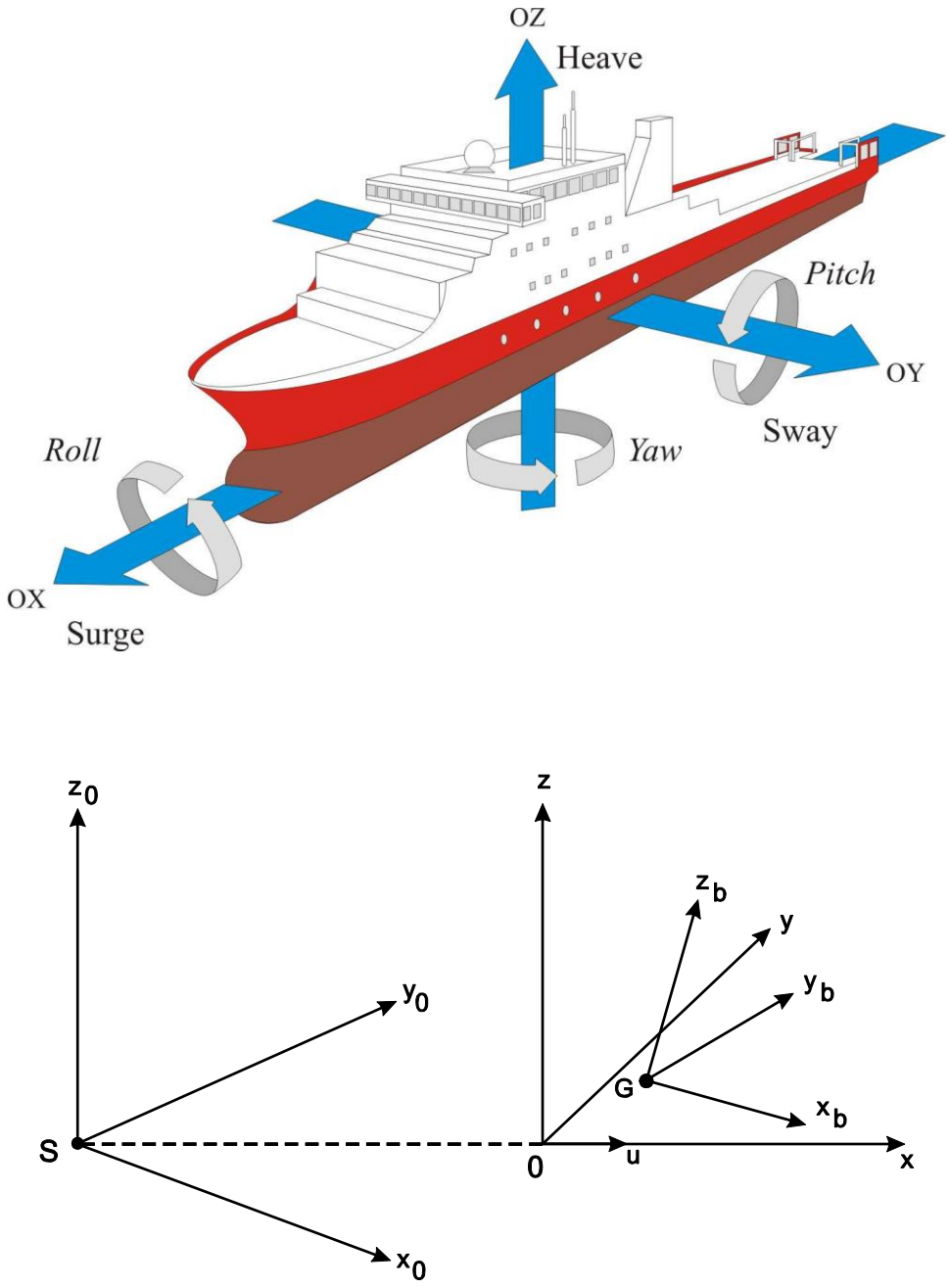

Figure 2.7. Ship motions in 6 degrees of freedom and frames of reference.

If the vector of ship displacements and rotations is defined as $\vec{s}(t) = \left[x(t)\ \ y(t)\ \ z(t)\ \ \phi(t)\ \ \theta(t)\ \ \psi(t)\right]^T$, the linear equations of ship motions in the six degrees of freedom could be written as:

$$\left[M + A\right] \cdot \ddot{\vec{s}} + \left[B\right] \cdot \dot{\vec{s}} + \left[C_{res}\right] \cdot \vec{s} = \overrightarrow{F}_{ext} \tag{13}$$

Where $\left[M\right]$ is the system generalized mass matrix, $\left[A\right]$ represents the hydrodynamic added mass matrix, and $\left[B\right]$ represents the damping matrix. $\left[C_{res}\right]$is the matrix of restoring coefficients and $\vec{F}_{ext}$ represents the external excitation forces and moments.

The term $\left[M\right] \cdot \ddot{\vec{s}}$ represents the inertial force derived from the Newton law. Considering that $\ddot{\vec{s}}$ is the acceleration of the system in the six degrees of freedom, $\left[M\right]$ is a 6 x 6 matrix whose components are the mass of the ship (those relative to linear accelerations) and the moments and products of inertia (relative to angular accelerations).

If the ship fixed axis are selected with its origin in the ship´s gravity center and the vessel has lateral symmetry (as is the case of most surface ships), the mass matrix could be written as:

$$\left[M\right] = \begin{bmatrix} m & 0 & 0 & 0 & 0 & 0 \\ 0 & m & 0 & 0 & 0 & 0 \\ 0 & 0 & m & 0 & 0 & 0 \\ 0 & 0 & 0 & I_{xx} & 0 & -I_{zx} \\ 0 & 0 & 0 & 0 & I_{yy} & 0 \\ 0 & 0 & 0 & -I_{xz} & 0 & I_{zz} \end{bmatrix} \tag{14}$$

The terms $[A]\cdot\ddot{\vec{s}}$ together with $[B]\cdot\dot{\vec{s}}$, are known as radiation forces, and are due to the energy dissipated by the waves generated by the ship when it moves. The term $[A]\cdot\ddot{\vec{s}}$ corresponds to the hydrodynamic inertia forces, known as added mass forces. According to (T. I. Fossen, 2011), "*Hydrodynamic added mass can be seen as a virtual mass added to a system because an accelerating or decelerating body must move some volume of the surrounding fluid as it moves through it. Moreover, the object and fluid cannot occupy the same physical space simultaneously*".

If we consider the vessel port – starboard symmetry and the case of small motions, the added mass coefficient matrix would remain (Lloyd, 1989):

$$[A]=\begin{bmatrix} A_{11} & 0 & A_{13} & 0 & A_{15} & 0 \\ 0 & A_{22} & 0 & A_{24} & 0 & A_{26} \\ A_{31} & 0 & A_{33} & 0 & A_{35} & 0 \\ 0 & A_{42} & 0 & A_{44} & 0 & A_{46} \\ A_{51} & 0 & A_{53} & 0 & A_{55} & 0 \\ 0 & A_{62} & 0 & A_{64} & 0 & A_{66} \end{bmatrix} \tag{15}$$

The term $[B]\cdot\dot{\vec{s}}$ corresponds to the damping forces proportional to the ship speed vector. Taking into account the same considerations as in the case of added mass forces, the matrix of damping coefficients would remain as:

$$[B]=\begin{bmatrix} B_{11} & 0 & B_{13} & 0 & B_{15} & 0 \\ 0 & B_{22} & 0 & B_{24} & 0 & B_{26} \\ B_{31} & 0 & B_{33} & 0 & B_{35} & 0 \\ 0 & B_{42} & 0 & B_{44} & 0 & B_{46} \\ B_{51} & 0 & B_{53} & 0 & B_{55} & 0 \\ 0 & B_{62} & 0 & B_{64} & 0 & B_{66} \end{bmatrix} \tag{16}$$

Finally, $[C_{res}]\cdot\vec{s}$ corresponds to the ship restoring forces, proportional to displacements and rotations, and that oppose the modification of the ship position and orientation. Regarding surge and sway (OX and OY displacements), no other forces are needed to sustain these movements and so, all coefficients related to these degrees of freedom are null. Regarding heave and pitch and under the assumption of port/starboard symmetry, there is no coupling between these motions and lateral plane ones (sway, roll and yaw). The influence of surge is usually very small and so all the corresponding coefficients are null. However, both motions are influenced by each other and a cross coupling restoring coefficient is present. In the case of lateral plane motions and under the port/starboard symmetry and linearity assumptions (small motions), the influence of vertical motions on them may be disregarded and coupling coefficients neglected. Finally and regarding coupling terms between lateral plane motions, the influence of sway and yaw on roll are usually very small and could be neglected, while the influence of sway and roll on yaw should be taken into account through the corresponding coefficients (Lloyd, 1989).

$$[C_{res}]=\begin{bmatrix} 0 & 0 & 0 & 0 & 0 & 0 \\ 0 & 0 & 0 & 0 & 0 & 0 \\ 0 & 0 & C_{33} & 0 & C_{35} & 0 \\ 0 & 0 & 0 & C_{44} & 0 & 0 \\ 0 & 0 & C_{53} & 0 & C_{55} & 0 \\ 0 & C_{62} & 0 & C_{64} & 0 & C_{66} \end{bmatrix} \tag{17}$$

The vector of exciting forces and moments $\vec{F}_{ext}$ could be written as:

$$\vec{F}_{ext} = \begin{bmatrix} F_{ox} \\ F_{oy} \\ F_{oz} \\ M_{ox} \\ M_{oy} \\ M_{oz} \end{bmatrix} \tag{18}$$

These exciting forces could be divided into two terms; the first one is that of wave forces and moments acting on the ship, under the consideration of that it is not affecting the waves by its presence, so incident waves are completely undisturbed. These forces are known as Froude-Krylov forces. The second term is known as diffraction forces, and takes in account effects of the interaction of the waves with the ship, considering it as a non-moving solid (waves generated by the ship motion were accounted for in added mass and damping terms).

Under these suppositions, the linear equations of motion in the six degrees of freedom would remain as:

$$\begin{gathered}
(m + A_{11}) \cdot \ddot{x} + A_{13} \cdot \ddot{z} + A_{15} \cdot \ddot{\theta} + B_{11} \cdot \dot{x} + B_{13} \cdot \dot{z} + B_{15} \cdot \dot{\theta} = F_{ox} \\
(m + A_{22}) \cdot \ddot{y} + A_{24} \cdot \ddot{\phi} + A_{26} \cdot \ddot{\psi} + B_{22} \cdot \dot{y} + B_{24} \cdot \dot{\phi} + B_{26} \cdot \dot{\psi} = F_{oy} \\
(m + A_{33}) \cdot \ddot{z} + A_{31} \cdot \ddot{x} + A_{35} \cdot \ddot{\theta} + B_{31} \cdot \dot{x} + B_{33} \cdot \dot{z} + B_{35} \cdot \dot{\theta} + C_{33} \cdot z + C_{35} \cdot \theta = F_{oz} \\
(I_{xx} + A_{44}) \cdot \ddot{\phi} + (-I_{zx} + A_{46}) \cdot \ddot{\psi} + A_{42} \cdot \ddot{y} + B_{42} \cdot \dot{y} + B_{44} \cdot \dot{\phi} + B_{46} \cdot \dot{\psi} + C_{44} \cdot \phi = M_{ox} \\
(I_{yy} + A_{55}) \cdot \ddot{\theta} + A_{51} \cdot \ddot{x} + A_{53} \cdot \ddot{z} + B_{51} \cdot \dot{x} + B_{53} \cdot \dot{z} + B_{55} \cdot \dot{\theta} + C_{53} \cdot z + C_{55} \cdot \theta = M_{oy} \\
(I_{zz} + A_{66}) \cdot \ddot{\psi} + (-I_{xz} + A_{64}) \cdot \ddot{\phi} + A_{62} \cdot \ddot{y} + B_{62} \cdot \dot{y} + B_{64} \cdot \dot{\phi} + B_{66} \cdot \dot{\psi} + \\
+ C_{62} \cdot y + C_{64} \cdot \phi + C_{66} \cdot \psi = M_{oz}
\end{gathered} \tag{19}$$

The equations above represent the linear motions of the ship in the six degrees of freedom. According to them and as previously described, not all the motions have influence in all the others. Longitudinal plane motions (i.e. surge, heave and pitch), are coupled to each other, happening the same with the three lateral

motions (sway, roll and yaw). However, lateral motions have not influence in longitudinal ones, and viceversa, being uncoupled.

Although these suppositions are valid under the assumptions of linear small amplitude motions, it will be necessary to reconsider them for the case of simulating the phenomenon of parametric roll resonance, as will be described in the following section.

2.3.1.3 Parametric Roll Mathematical Modeling

As in the other fields of seakeeping, one of the main interests of the research community has been that of studying how to precisely simulate the phenomenon of parametric roll resonance. Obtaining a mathematical model that correctly reproduces the motions of a ship under parametric roll resonance, in substitution of towing tank tests, represents a cheaper, easier to use and more extensive tool for determining the likeliness of a ship for suffering the phenomenon, for studying which conditions are more dangerous for it, analyzing how to avoid them and studying the performance of any preventive measures that want to be applied. This issue has been the main topic of the research related with parametric roll resonance in recent years and a large number of approaches are available with different levels of success.

These approaches are usually characterized by the number of degrees of freedom used for computing ship motions and by the adoption of different degrees of non linearities to compute the coefficients involved in the previously seen equations.

On one hand, modern general purpose seakeeping codes of six degrees of freedom, such us LAMP (Shin et al., 2004), FREDYN (France et al., 2003) or HSROLL (Malenica et al., 2006) have been applied for the study of parametric roll. However, the most complex versions of these time-domain codes are based

on 3-D solving of the instantaneous wave-body interaction problem and are very costly and time consuming. Although their performance is good, their time consumption makes then not suitable for very extensive analysis or onboard guidance (Jensen et al., 2008), which is one of the goals of the present work.

On the other hand, many simplified models including multiple degrees of freedom, based on the linear set of equations of motion, have been developed in the last years with the objective of obtaining fast and accurate tools for predicting the large motions that appear in resonant conditions, which are the most suitable for our objectives.

A description of the state of the art in this last field, together with the alternatives adopted in this work, will be done in this section.

2.3.1.4 Uncoupled Roll Equation

The simplest approach to the problem of parametric roll modeling consists on analyzing the equation of roll motion separately from the rest degrees of freedom.

So, initially the three equations of lateral motions (sway, roll and yaw) will be considered separately from those of longitudinal ones (which have been considered decoupled from lateral motions in the previous sections). In the case under study, the effects of yaw could be supposed to be negligible and disregarded from the analysis of the roll motion. Although sway effect is not negligible, roll-sway coupling won´t be explicitly considered (as it can be implicitly considered in the parameters of the one degree of freedom model). So, taking these two facts into consideration, the decoupled linear equation of roll motion will remain the following way:

$$(I_{xx} + A_{44}) \cdot \ddot{\phi} + B_{44} \cdot \dot{\phi} + C_{44} \cdot \phi = M_{ox} \tag{20}$$

While studying parametric roll, the worst case is usually that of head or stern seas; this fact implies that no roll external excitation will be acting on the ship, and so:

$$(I_{xx} + A_{44}) \cdot \ddot{\phi} + B_{44} \cdot \dot{\phi} + C_{44} \cdot \phi = 0 \tag{21}$$

If we still consider the linear approximation, the values of the coefficients of added mass (A_{44}) and roll damping (B_{44}), could be obtained by using potential strip theory. I_{xx} is the ship mass moment of inertia with respect to the longitudinal axis and C_{44} is the roll restoring coefficient.

In normal sailing conditions, the coeffcients shown in the previous equation will remain constant; under these circumstances, and considering that no external excitation is present, it is obvious that no roll motion will develop.

In order to mathematically describe the phenomenon of parametric roll resonance, the uncoupled equation of roll motion of the ship without external excitation, could also be set out by making an analogy with that of the harmonic oscillator shown in Equation (6):

$$\frac{d^2x}{dt^2} + 2 \cdot \xi \cdot \omega_0 \cdot \frac{dx}{dt} + \omega_0^2 \cdot x = \frac{1}{m} \cdot F_0 \cdot \sin(\omega \cdot t) \tag{22}$$

In this occasion, and as a head seas condition is been considered and no external excitation (transversal heeling moment) is present:

$$\frac{d^2x}{dt^2} + 2 \cdot \xi \cdot \omega_0 \cdot \frac{dx}{dt} + \omega_0^2 \cdot x = 0 \tag{23}$$

According to (Shin et al., 2004), if ϕ is the ship roll angle, ω_n the natural roll frequency and δ the dimensional roll damping coefficient and making $x = \phi$, $\omega_0 = \omega_n$ and $\xi \cdot \omega_0 = \delta$, the equation of roll motion could be rewritten as:

$$\frac{d^2\phi}{dt^2} + 2 \cdot \delta \cdot \frac{d\phi}{dt} + \omega_n^2 \cdot \phi = 0 \tag{24}$$

As a simple approximation, for the case of small amplitude linear oscillations, the natural roll frequency could be estimated by:

$$\omega_n^2 = \frac{\Delta \cdot GM_0}{\left(I_{xx} + A_{44}\right)} \tag{25}$$

Where Δ is the ship displacement, GM_0 is the still water transverse metacentric height, I_{44} is the roll inertia and A_{44} is the added roll inertia (due to hydrodynamic effects), and:

$$B_{44} = 2 \cdot \delta \cdot \left(I_{xx} + A_{44}\right) \tag{26}$$

$$C_{44} = \Delta \cdot GM_0 \tag{27}$$

In the case of regular head waves, as can be seen in Figure 2.8, metacentric height changes due to wave passing. In these conditions, its value could be approximated by a sinusoidal variation of the still water metacentric height with a frequency equal to that with which the ship encounter the waves, i.e. encounter frequency, ω_e.

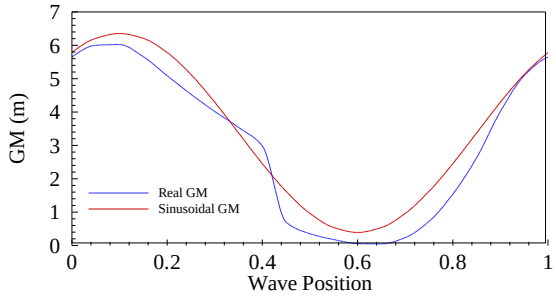

Figure 2.8. GM Variation due to wave passing.
Real GM & sinusoidal approximation.

If we define the amplitude of the variation of the transverse metacentric height as ΔGM , then the value of GM with time remains:

$$GM(t) = GM_0 + \Delta GM \cdot \cos(\omega_e \cdot t) = GM_0 \cdot \left(1 + \frac{\Delta GM}{GM_0} \cdot \cos(\omega_e \cdot t)\right) \quad (28)$$

And the equation of roll motion will remain

$$\begin{aligned} &\frac{d^2\phi}{dt^2} + 2 \cdot \delta \cdot \frac{d\phi}{dt} + \frac{\Delta \cdot GM_0}{I_{xx} + A_{44}} \cdot \left(1 + \frac{\Delta GM}{GM_0} \cdot \cos(\omega_e \cdot t)\right) \cdot \phi = \\ &= \frac{d^2\phi}{dt^2} + 2 \cdot \delta \cdot \frac{d\phi}{dt} + \omega_n^2 \cdot \left(1 + \frac{\Delta GM}{GM_0} \cdot \cos(\omega_e \cdot t)\right) \cdot \phi = 0 \end{aligned} \quad (29)$$

If we first consider the simplified case of an undamped motion with $\delta = 0$ and make the substitution $w_e \cdot t = \tau$, we get:

$$\frac{d^2\phi}{d\tau^2} + \omega_n^2 \Big/ \omega_e^2 \cdot \left(1 + \frac{\Delta GM}{GM_0} \cdot \cos(\tau)\right) \cdot \phi = 0 \quad (30)$$

And if $p = \frac{\omega_n^2}{\omega_e^2}$ and $q = \frac{\omega_n^2}{\omega_e^2} \cdot \frac{\Delta GM}{GM_0}$, then the undamped equation of roll motion in head seas can be transformed into the aforementioned Mathieu equation, described in equation (11).

$$\frac{d^2\phi}{d\tau^2} + \left(p + q \cdot \cos(\tau)\right) \cdot \phi = 0 \tag{31}$$

From Figure 2.1 it can be seen that the Mathieu equation has areas of instability for different values of the parameters p and q , but the widest ones are those for p=0.25 and p=1, which respectively correspond to the "Principal Parametric Resonance" and the "Fundamental Parametric Resonance" areas (Hayashi, 1964; A. H. Nayfeh,Mook, 2004).

From those areas of instability, the most frequent and where we will focus our analysis, is the one correspondent to the principal resonance (p=0.25). In order to satisfy this condition, $p = \omega_n^2 / \omega_e^2 = 0.25$ and so $\omega_e = 2 \cdot \omega_n$, that is, wave encounter frequency should double ship natural roll frequency. Under this premise, and as could be seen in Figure 2.1, the presence or not of an unbounded solution also depends on the parameter q, which represents the amplitude of the metacentric height variation due to wave passing together with the effects of the frequency ratio. In the proximity of the case of principal resonance, nearly all values of the q parameter lead to unbounded solutions and so, to the development of large roll motions.

In order to include the effects of roll damping, we consider equation (30) with a non null damping coefficient $\kappa = \delta / \omega_e$:

$$\frac{d^2\phi}{d\tau^2} + 2 \cdot \kappa \cdot \frac{d\phi}{d\tau} + \omega_n^2 / \omega_e^2 \cdot \left(1 + \frac{\Delta GM}{GM_0} \cdot \cos(\tau)\right) \cdot \phi = 0 \tag{32}$$

If now we consider $\phi(\tau) = x(\tau) \cdot e^{(-\kappa \cdot \tau)}$, the previous equation becomes

$$\frac{d^2\phi}{d\tau^2} + 2\cdot\kappa\cdot\frac{d\phi}{d\tau} + \omega_n^2 \Big/ \omega_e^2 \cdot \left(1 + \frac{\Delta GM}{GM_0}\cdot\cos(\tau)\right)\cdot\phi = 0 \qquad (33)$$

$$\frac{d^2x}{d\tau^2} + \left(\left(\frac{\omega_n^2}{\omega_e^2} - \kappa^2\right) + \frac{\omega_n^2}{\omega_e^2}\cdot\frac{\Delta GM}{GM_0}\cdot\cos(\tau)\right)\cdot x = 0 \qquad (34)$$

$$p = \frac{\omega_n^2}{\omega_e^2} - \kappa^2 \text{ and } q = \frac{\omega_n^2}{\omega_e^2}\cdot\frac{\Delta GM}{GM_0} \quad , \qquad (35)$$

$$\frac{d^2x}{d\tau^2} + \left(p + q\cdot\cos(\tau)\right)\cdot x = 0 \qquad (36)$$

As can be seen in Figure 2.9, the effect of damping in the areas of instability mostly consists, especially in the two first areas, on an upwards displacement of their lower vertex. This displacement implies that their lower limits are now separated from the horizontal axis and that a higher value of the parameter q (and so a higher value of the variations in GM, i.e, higher excitations) is needed for entering an unstable zone. The appearance of parametric roll resonance is thus retarded for the same conditions by the effect of damping.

Moreover and by analyzing this equation, the main parameters influencing the appearance or not of a phenomenon of parametric roll resonance could be defined.

First of all, and if we consider the "Principal Parametric Resonance" area and that the effect of damping is negligible for determining the lateral position of its lower vertex, then $p = 0.25 \approx \frac{\omega_n^2}{\omega_e^2}$ and $\omega_e = 2\cdot\omega_n$.

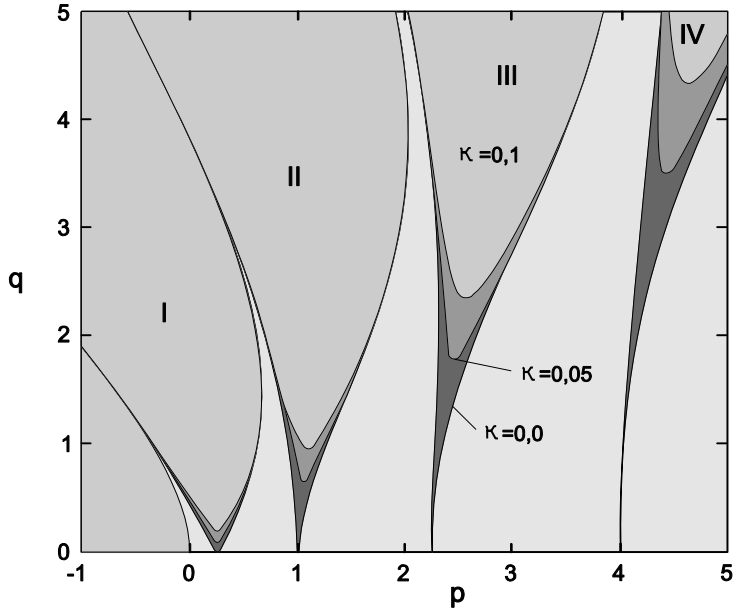

Figure 2.9. Damped Mathieu equation. Areas of Stability (Insperger,Stépán, 2003).

Encounter frequency ω_e is the frequency with which the ship encounters the waves, and generally is the one that should be taken into account while considering the effects that waves have on ship motions ((Lloyd, 1989). Encounter frequency depends on ship speed *u*, ship heading related to the direction of wave propagation χ and absolute wave frequency ω_w (see Figure 2.10). Under the deep seas assumption, it can be computed the following way:

$$\omega_e = \omega_w - \frac{\omega_w^2}{g} \cdot u \cdot \cos(\chi) \tag{37}$$

Regarding the influence of encounter frequency, it could then be concluded that for a given seaway condition, ship speed and heading are the "controllable" parameters affecting the possible appearance of parametric roll, while wave frequency (and of course the other wave characteristics), are the "non controllable" parameters.

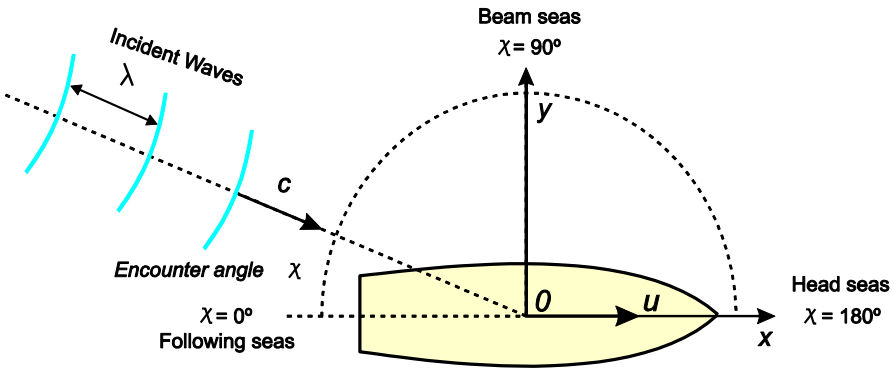

Figure 2.10. Ship-wave encounter frequency diagram.

Other variable influencing the parameter p is the natural roll frequency ω_n. From its definition (see Equation (25)), it can be appreciated that it depends on ship displacement, metacentric height and transverse mass and added mass moments of inertia. Ship displacement and the transverse mass moment of inertia only depend on the ship loading condition, while the added mass moment of inertia also depends on roll frequency and submerged hull forms. As metacentric height depends on the vertical positions of the centre of gravity and buoyancy and on the metacenter position, this parameter is also a function of loading condition and underwater hull forms. All of these parameters are dependent on ship weight distribution, loading condition and hull forms and although the value of natural frequency could change between different loading conditions, this change would be small with time and can be considered constant for the periods of time that will be considered in this work. In any case, natural roll frequency could be considered as a "non controllable" parameter regarding roll resonance (always considering that no active stabilizers are under operation, as is the case).

Finally, the last variable to be considered while analyzing p is roll damping κ.

$$p = \frac{\omega_n^2}{\omega_e^2} - \kappa^2 \tag{38}$$

As have been already said, an increase in roll damping will imply that a higher excitation is needed for triggering resonance at a given frequency ratio. Although roll damping is theoretically a non controllable parameter, as it depends on ship hull forms and forward speed, together with other motion parameters (Valle Cabezas, 1999), the use of some stabilizing systems may affect ship roll damping (such as the deployment of fin stabilizers), and this effect could be applied to reducing roll amplitude. However, and along this work, roll damping will be considered as non controllable parameter.

So, from the analysis of the previously seen equation, it can be concluded that for a given ship with no stabilizing devices, which is sailing under a certain set of environmental excitations and in a given loading condition, forward speed and heading are the only parameters on which the master may actuate in the short term to avoid a possible resonance episode.

Although equation (36) represents the simplest approximation to the simulation of parametric roll in longitudinal seas, it has been successfully applied by many authors and is in fact the basis for carrying out theoretical studies regarding the phenomenon, such us vulnerability analysis (France et al., 2003), studying the GM influence on parametric roll development (L.S. McCue et al., 2007; Thomas et al., 2008) or roll motion stability analysis.

However, the accuracy of this model for simulating roll resonance in a realistic scenario is limited due to some of the simplifications undertaken in its development. Linearity implies limited motions and, while dealing with resonance, this is hardly the case.

2.3.1.5 Nonlinear Uncoupled Roll Equation

In order to improve the accuracy of the model while trying to simulate the motions of a real ship, it is necessary to carry out some modifications on the previous case.

On one hand, the previous equation, where restoring coefficient has been taken as GM dependant, is valid for reduced roll angles; from classic transverse stability theory, it is well known that large angle stability is governed by the restoring arms or GZ´s, which are nonlinearly dependent of roll angle (Figure 2.11).

If GZ´s are included into equation (21), the large amplitude nonlinear roll motion of the ship could be represented as:

$$(I_{xx} + A_{44}) \cdot \ddot{\phi} + B_{44} \cdot \dot{\phi} + \Delta \cdot GZ(\phi) = 0 \tag{39}$$

where $GZ(\phi)$ is roll angle dependant restoring arm. In the same way as in the linear roll motion case, the parametric excitation, needed for the simulation of the phenomenon, should come from the time variation of the restoring term (in this occasion the GZ´s), which will reproduce the effects of wave passing along the hull.

Taking this into account, equation (39) could be transformed into

$$(I_{xx} + A_{44}) \cdot \ddot{\phi} + B_{44} \cdot \dot{\phi} + \Delta \cdot GZ(\phi, t) = 0 \tag{40}$$

where $GZ(\phi, t)$ represents the time and roll angle dependant restoring arm. From the analysis of the previous equation, it can be concluded that a realistic definition of the time dependency of the restoring term will be mainly responsible of the performance of the model.

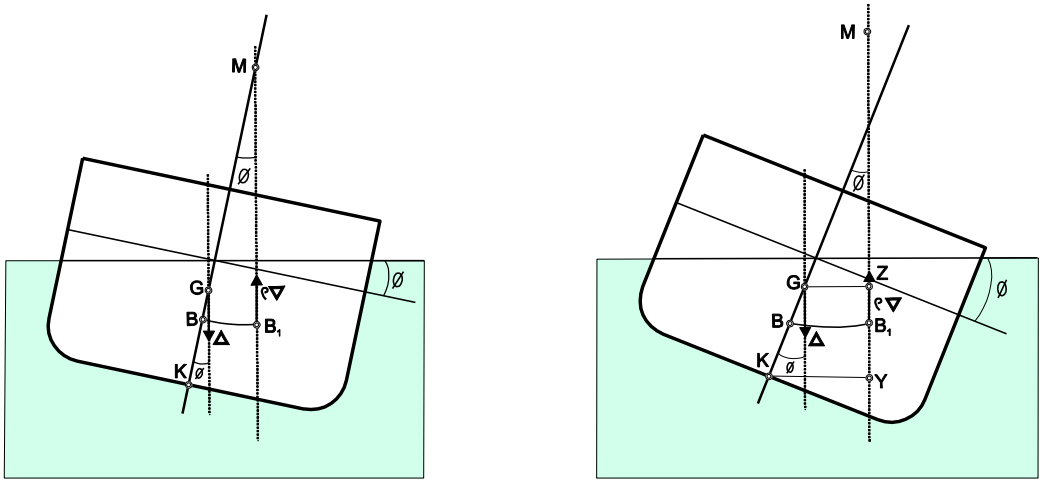

Figure 2.11. Ship static transverse stability. Small roll angles (left) and large angles (right).

Moreover, another mention should be done regarding roll damping. Although considering damping to be linear in most degrees of freedom have been demonstrated to be a valid supposition in the vast majority of conditions, linearity in roll damping only remains true for small motions and only in limited cases. Largely influenced by viscosity, vortex shedding and turbulence, an accurate modeling of roll damping, especially while dealing with large amplitudes, should be nonlinear, as is explained in the well known Himeno work (Himeno, 1981).

These two considerations have been broadly adopted by the research community; the vast majority of the authors take the previous equation as a starting point and focus their efforts in modeling in the most realistic way the nonlinear restoring term, together with the adoption of different degrees of nonlinearities in roll damping (normally linear plus quadratic or linear plus cubic alternatives).

As examples of this, the following references can be mentioned; in (Francescutto, 2001), Mathieu equation is taken as a basis, together with a nonlinear approach of GM variation in waves and third order roll damping, for

evaluating the roll parametric threshold for a destroyer, obtaining good results in comparison to experimental testing. In (Francescutto et al., 2004), a linear plus cubic damping and cubic restoring moment is adopted for further study of resonance threshold. In this case, an additional term is taken into account. Considering that vertical motions also influence restoring arm variation (as they effectively modify ship flotation), a vertical motion dependant coefficient is included into the restoring term. This model was told to be a 1.5 degree of freedom model, as vertical plane motions were considered into the evaluation of roll resonance but from a quasi-static way.

In (Bulian, 2005, 2006a, 2006b; Bulian et al., 2004) and references therein, the later development of the previous model is described. The authors propose a look-up table approach for the GZ curve, where by applying hydrostatical computations and adopting a quasi-static approach, the effects of heave and pitch on time dependence of the restoring term in waves are taken into account. Finally, a highly nonlinear analytical alternative is proposed for fitting this GZ surface, showing accurate results for predicting roll amplitude under parametric roll in regular and irregular seas.

This approach is also taken in (de Juana Gamo et al., 2005), where such a model, including linear plus quadratic damping, is set up for simulating roll resonance of a medium size trawler, obtaining accurate results in comparison to towing tank tests of the same vessel.

Moreover, these methods have also been applied in the guidelines published by the American Bureau of Shipping (ABS, 2004) and the International Towing Tank Conference (ITTC, 2005), for predicting the appearance of roll resonance from the early design stages of the ships. The first one, based on the paper (Shin et al., 2004), handles a two-level methodology; in a first stage, parametric roll

susceptibility is evaluated from a Mathieu – type method; and secondly, and if the ship turns out to be prone to resonance, an analysis based on the nonlinear GZ look-up table approach, as that proposed in (Bulian, 2006a), should be done. In the same way, the ITTC method is based on the aforementioned reference (Francescutto et al., 2004) and also in (K. J. Spyrou, 2005). In both cases, roll damping is linearly considered.

In (Hashimoto,Umeda, 2004; Umeda et al., 2004), the restoring term variation in waves is obtained following two different approaches, with the objective of studying the stability of roll motion in resonance conditions for a containership both in head and stern ships. On one hand, the Froude-Krylov assumption was evaluated, showing to amplify restoring term variations, especially at low speeds and resulting as not able for parametric roll computations. On the other, a direct GZ measurement from towing tank tests was used for determining GZ in waves, which was subsequently applied for the stability analysis carried out in the work.

In (Munif et al., 2005), the authors apply the one degree of freedom model, with linear plus cubic damping and up to seventh order fitting of the GZ curves, for the prediction of parametric roll in beam waves of a modern cruise ship. The results of the three year research project in which both scale model tests were carried out together with analysis using this mathematical model, are contained in (Ikeda et al., 2008).

Finally, in (Umeda et al., 2008), the authors apply a one degree of freedom model for evaluating the performance of different systems for reducing parametric roll amplitude. In this model, the restoring term was nonlinearly modeled by taking into account the restoring term time variation through systematic hydrostatic calculations at different wave heights and a fixed

wavelength, and the application of Grim´s effective wave height. Moreover, it was coupled to an anti-roll tank model.

2.3.1.6 Nonlinear Coupled Roll Equation

Although the described one degree of freedom models are quite simple, easy to handle and some of them have shown shown to be in many cases accurate, they have a clear drawback. When the six linear equations of motion were obtained (see equation (19)), the system was divided into two different sub-systems, that under the small motions assumption were supposed to be independent. However, when the ship sails into head seas, heave, pitch an also surge motions may become quite large; under these conditions, the coupling between the vertical plane motions and roll turns out to be non-linear. An un-coupled model of roll, under these circumstances, may fail in correctly simulating the phenomenon of parametric roll resonance, as the dynamic contributions from heave and pitch motions, together with their hydrostatic contributions, are disregarded (M. A. S. Neves,Rodriguez, 2007; I. G. Oh et al., 2000).

The need for such a model, where the influence of vertical plane motions was taken into account, has been stated form the early days of the research in the field of parametric roll (Pauling,Rosenberg, 1959). Increasing the number of degrees of freedom (d.o.f.) considered into the model would imply an increase on its complexity and many approaches have been adopted where different combinations of motions are taken into account. While aiming to simulate parametric roll, heave and pitch are accounted for in most cases (3 d.o.f. models), while some others also include surge (4 d.o.f.) or the complete set of motions (6 d.o.f.).

However, there exist other models where only roll, together with surge, are considered, as can be the case of (K.J. Spyrou, 2000), in which the author

analyzes the influence of the asymmetry in surge motion on the development of parametric roll in following seas of a purse-seiner.

Regarding the multi-degree of freedom models, (Tondl,Nabergoj, 1990; Tondl et al., 2000) displayed two simplified mechanical models, which were dynamically equivalent to ship motion equations. These two models considered on one hand, a 2 d.o.f. heave and roll coupled motion. The second model was a fully coupled 3 d.o.f. approach to compute roll, pitch and heave motions. In both cases, they were used for studying the appearance of roll motions, i.e. stability analysis, but not for analyzing its later development.

From the three degrees of freedom models, one of the the most well known is that proposed in (M.A.S. Neves,Rodriguez, 2005; M.A.S. Neves,Rodríguez, 2006). On it, the nonlinear coupled restoring actions on heave, roll and pitch are computed following a methodology based on Taylor Series expansions of up to third order, where hull forms and wave shape are taken into account; moreover, linear plus quadratic damping is considered. This model is the evolution of the 3 degrees of freedom model presented in (M. A. S. Neves et al., 1999). Both approaches have been extensively applied to the evaluation of the behaviour under parametric roll in regular head seas of two similar fishing vessels. In (M. A. S. Neves et al., 2003), the eldest model is used; in (M.A.S. Neves, J.A. Merino, et al., 2009; M.A.S. Neves et al., 2007), the latest approach is coupled to a model of a U-Tank stabilizer, and in (M. A. S. Neves,Rodriguez, 2007; M. A. S. Neves et al., 2009; M.A.S. Neves, C.A. Rodríguez, et al., 2009; Vivanco, 2009), the stability behaviour of a fishing vessel with and without the U-Tank stabilizer is evaluated. Finally, in (C.A. Rodríguez et al., 2007), the same model is applied for computing roll motions of a containership under head seas parametric roll. In all cases, the model has performed accurately when

compared to data from towing tank tests. This same model has been also used in this work, and a broader description of it could be found in Section 3.3.

Regarding some examples of the full six degrees of freedom approaches, the following works could be mentioned.

The ROLLS model, developed in (Kroeger, 1987; Petey, 1988), is a 6 d.o.f. code, where non linear roll and surge motions are coupled with linear sway, heave, pitch and yaw computed by using a strip theory method (it may be described as a 2 + 4 d.o.f. code, where 2 motions are nonlinearly obtained and the rest are based on linear theory). It has been applied in some works for analyzing the performance of ships in parametric roll resonance, both in regular and irregular seas. For example, in (Chang, 2008), ROLLS is applied to analyze parametric roll in regular head seas of a Ro-Ro.

In (Spanos,Papanikolaou, 2005), the authors apply a 6 d.o.f. nonlinear model to complement an experimental study of the TS fishing vessel also analyzed in (M.A.S. Neves,Rodriguez, 2005), with the objective of determining vessel responses as a function of wave height, although no comparison is made between the two approaches. Regarding the basic hydrodynamics, this is a linear model based on potential theory, while non linearities are included, such as large amplitude excitations or body effects. Both incident and hydrostatic forces are obtained through direct integration of dynamic and hydrostatic pressure fields on instantaneous wetted surface, and radiation forces are obtained from a panel code. Non linear effects in roll damping are also taken into account.

In (Cipriano Quinteros, 2005), the coupled non linear 3 d.o.f. model developed by (M.A.S. Neves,Rodriguez, 2005) is completed up to 6 d.o.f. by including coupled equations in surge, sway and yaw, together with an auto-pilot model.

The model is compared with towing tank tests of a purse-seiner in roll decay, beam and quartering seas, obtaining good results, although no parametric roll experiments were carried out.

A 5 d.o.f. (sway, heave, roll, pitch and yaw) non linear approach is presented in (Ribeiro e Silva et al., 2005), where heave, pitch and roll restoring forces are computed under the quasi-static approach for the instantaneous wave elevation along the hull (including possible deck submergence), and nonlinear roll damping is taking into account. Comparison with scale model tests of a container ship in regular seas of different heading is presented, showing good agreement. Moreover, a numerical analysis of the same ship in irregular head seas is also described, demonstrating the model capability for predicting parametric roll in both cases. In (Ribeiro e Silva,Guedes Soares, 2008) an extension of this model is presented, where strip theory and instantaneous integration techniques over real waterline and ship position are used for determining hydrodynamic and restoring coefficients and excitation forces at each time step. In (Ribeiro e Silva et al., 2010) this model is also applied to parametric roll sensitivity analysis of the C11 class containership.

In (Munif,Umeda, 2006), the comparison of two models is carried out for analyzing parametric roll on an Icelandic trawler with no variation of its GM in waves; on one hand, a 1 d.o.f. where balanced heave and pitch are considered for computing the GZ curve. On the other, a 6 d.o.f model, where heave and pitch are linearly computed and coupled with roll. Both models are compared taking as a basis regular head seas towing tank test at zero speed. Under these assumptions, the 1 d.o.f. fails to simulate parametric resonance, while the 6 d.o.f. shows a good performance.

Finally, in (Jensen, 2007; Jensen et al., 2008; Vidic-Perunovic, 2009; Vidic-Perunovic,Jensen, 2009), a simplified version of the non linear 6 d.o,f. seakeeping code ROLLS is adopted for simulating parametric roll resonance of a containership in an irregular head seas seaway. On it, 4 d.o.f are taking into consideration: sway and yaw motions are disregarded and surge is considered uncoupled from the other motions; moreover, heave is considered as linearly dependant on wave amplitude and pitch is quasi statically considered on the computation of the time dependant GZ curve, which is obtained for a given wave height; linear dependency between GZ curve and wave height is supposed for obtaining the GZ curve for other values of wave height.

As could be seen from the above, a large variety of different methods have been developed to predict the phenomenon of roll resonance. However, in order to determine the real performance of the different models in comparison to the others, some common benchmark results are needed. Such a study was carried out in the frame of the SAFEDOR project, and is included in the work (Spanos,Papanikolaou, 2009). On it, the roll predictions made by several numerical models in different conditions of parametric resonance are compared to the corresponding towing tank tests. This work provides a very useful reference to analyze which approximations are those performing better for a given set of conditions.

The benchmark vessel is a 150 m long container ship and the carried out tests included 22 conditions, defined by different values of GM, forward speed, heading, wave height, frequency and type (regular, group waves and irregular).

Among the 13 tested models, are some of those previously mentioned in this section, but there are some other approaches such as those of (Ovegård, 2009)

or (Schreuder, 2008), which descriptions are included within the references of the benchmark study.

In this test, the performance of the different models was evaluated in two ways. Firstly, by their capacity for predicting the steady state amplitude of parametric roll resonance. And secondly, by only predicting the appearance of the phenomenon, disregarding the roll amplitude. The results showed an accuracy of approximately the 80 % for the best performing models in predicting resonance and a mean deviation of 6.4º and a correlation coefficient of 0.64 for predicting the steady state roll amplitude. These values are supposed to represent the state of the art of parametric roll modeling.

However and although the different methods are not identified in the study, it could be shown that among the best performing ones in both analyses, representatives of all the categories described in this section are present (1, 3 and 6 d.o.f. models, based on linear and non-linear strip theory or 3D methods, etc.), which could mean that, instead of the complexity of the proposed structure, an adequate modeling of the parameters involved in the phenomenon seems to be the most important issue while designing this kind of methods.

2.3.2 Most Affected Ships

As have been analyzed in the previous section, the intensity of the phenomenon of parametric resonance mainly depends, for a given set of sailing conditions (ship speed and heading, encounter frequency and wave height), on the variation of the roll restoring capacities with wave passing and on the effects of vertical motions. The amplitude of this variation largely depends on the hull forms of the ship, as metacentric height depends on waterplane area. Those ships with a large increase or deacrease of waterplane area between different flotation levels would be more affected by resonance.

Regarding large restoring terms variations, from the above it could be seen that those ships with hull forms rapidly changing from full to slim lines would be the most affected by parametric roll resonance. This type of hull forms is nowadays mostly typical of containerships and car carriers. These ships are designed to have a high cruising speed (usually of more than 20 knots), but at the same time they need large deck areas for stowage of cars and containers. The first requirement is fulfilled by using thin lines at the bow and stern at the design draft level, while the large deck areas are obtained by nearly full-breathed forms near above the flotation level. This hull forms are usually characterized by very large bow flares and overhanging sterns. As can be appreciated in Figure 2.12, small variations in fore and after drafts (induced by wave elevation), would lead to large increasing or decreasing of waterplane area. In a similar situation could be also found the modern cruise ships, car carriers or ferries.

Historically, the effects of parametric resonance have been limited to small and medium sized vessels with low metacentric heights, where resonance was produced mostly due to the reduced stability instead of due to the variation of this parameter, and mainly in stern seas at low speeds. The typical types of ships fulfilling these constraints were the fishing vessels, which were supposed to experience the phenomenon. However, and as will be seen in this section, no reference has been found to a real episode of parametric roll of a fishing vessel, although model tests have undoubtedly shown this possibility.

The case of container ships and car carriers is slightly different. Cargo containerization dates from the late fifties and the use of the aforementioned large bow flared hull lines dates only from the last twenty years, coinciding with the full development of container shipping and the increase of speed and cargo capacity requirements.

Figure 2.12. Modern containership (CMA CGM Columbia).
Note large bow flare and hanging stern. www.shipspotting.com.

Together with this fact, in the last years a large growth of the containership fleet has been experienced. Both elements have lead to a scenario where the probability of any of these vessels suffering parametric roll resonance has largely increased, as more ships are operating and a larger percentage of them have resonance – prone hull shapes.

The interest of the research community and the maritime industry on the phenomenon of resonance has been empowered by the aforementioned facts, but also due to the extremely large economical consequences that a fully developed parametric roll episode can have if suffered by one of these ships. The case of the APL China, that in 1998 lost or had damaged more than 1.500 containers of a total load of 5300, is considered as the starting point of the consideration of parametric roll resonance as a serious issue while designing and operating containerships and other similarly hull shaped vessels.

In the following subsections, the most affected vessels and the known episodes of parametric roll resonance until the date will be described.

2.3.2.1 Containerships

As have been mentioned above, containerships are among the vessels with higher probabilities of suffering parametric roll resonance, mainly due to the

large bow flares and hanging sterns designed to maximize container stowage surface on deck and keep low resistance and so, reduced fuel consumptions.

Although these vessels are supposed to be prone to developing the phenomenon if the necessary conditions are present, it is normally quite difficult to exactly determine if the cause of some large roll motion episodes is parametric roll resonance, the effect of large waves acting on the ship side, confused irregular seas or any other similar event, as usually no real time monitoring of incident waves, ship loading condition and other sailing parameters, are simultaneously present onboard the vessels. Moreover, if no substantial damage results from the event, no following investigation will be carried out and no news of the event will be known by the community. This may be one of the reasons why information regarding parametric roll resonance events is so scarce.

Up to the author´s knowledge, only three references exist regarding parametric roll resonance real events on container ships and that include the incidents of the APL China in 1998 (France et al., 2003), of the Maersk Carolina in 2003 (Carmel, 2006) and that of the Nedlloyd Genoa in 2006 (MAIB, 2006).

APL China is a 4800 TEU Post-Panamax containership, built in HDW shipyards in Kiel in 1995, having a length of 262 m and a speed exceeding 24 knots. It belongs to the APL C11 class containerships, having five other sister ships. This class was the evolution of the first Post-Panamax container carriers, the APL C10 class. In October of 1998, on route from Taiwan to Seattle, the ship was hit by the typhoon Babs. Despite the severity of the seas and wind conditions, with significant wave heights exceeding 13 m, the more relevant fact of the incident were the large motions generated, that in the case of roll reached more than 35 degrees, especially if it is considered that the master always tried to keep the bow into the swell direction.

Figure 2.13. APL China. 2008. www.shipspotting.com.

As a result of this event, of the 1300 containers carried on deck, about 400 were lost and around 500 more were damaged, together with other ship structural damages. Insurance claims were reported to be of up to US$ 100 million, being considered as the worst incident within container shipping industry.

By the time of the construction of the vessel, no consideration was given to parametric roll resonance in head seas. In fact, the appearance of parametric roll in following seas had been studied in the design stage of the C10 class containerships, predecessors of the C11´s, by the application of mathematical models, showing roll angles at the worst conditions of up to 35 degrees. Model testing of both designs prior to construction also showed large rolling angles due to synchronous roll (roll resonance), reaching 30 degrees in following and stern-quartering seas. No tests analyzing the head seas condition were carried out.

The causes and consequences of the accident were extensively studied in the work by France et al. (France et al., 2003), presented at the 2001 SNAME annual meeting, where it was concluded that parametric roll was the most probable cause of the APL China incident and some recommendations to face this phenomenon were included, regarding container lashing equipment, consideration of parametric roll in head seas and guidance to master.

Figure 2.14. APL China on the port of Seattle in October 1998, after the parametric roll event. International Longshore and Warehouse Union Auxiliary, Seattle, Washington, USA. http://www.ilwu19.com/.

This work has subsequently become as the beginning of the modern research in the field of parametric resonance in head seas and the consideration of the phenomenon as a real and important issue affecting the design and operation of containerships.

The case of Maersk Carolina in 2003 is quite similar to that of APL China. Maersk Carolina is a 4300 TEU Panamax containership of 292 m length, built in Hyundai shipyards in 1998. On January of 2003, on her route from Algeciras (Spain) to Halifax (Nova Scotia), it encountered bad weather, with 40+ knots winds and waves of up to ten meters. While trying to keep on head seas, the ship experienced very heavy roll motions of up to 47 degrees, together with strong pitching and heaving. According to the descriptions of the crew (Carmel, 2006):

"The vessel was running at reduced speed to minimize pounding with courses such that the sea was on the bow at various angles to minimize rolling. […]. The vessel was rolling and pitching moderately with a consistent motion. Then with no warning the vessel began to roll and pitch heavily, with maximum rolls developing in only a few roll cycles. […]. After several cycles of extreme motion (during which the containers were lost) the vessel returned to her previous roll / pitch motion. The entire event lasted only a couple minutes and did not appear to have been caused by any action on the part of the vessel –no course or speed changes were made and there was no change in the prevailing weather.

The described event fits perfectly in the description of a parametric roll resonance phenomenon. The consequences of this episode were 133 containers lost overboard and more than 50 damaged, together with moderate ship structural damage which had to be subsequently repaired. More than US$ 4

million were estimated only in cargo claims. The aforementioned work by Carmel (Carmel, 2006) studied the incident, concluding that an episode of parametric roll resonance was its most probable cause, stating also the need of guiding systems which inform the crew about the risk of appearance of this phenomenon.

The incident of Nedlloyd Genoa in January 2006 is different to the two other passages described above, as it is not probed that parametric roll resonance was its cause and it is only considered by the investigators of the accident as one possibility, as all conditions were very close to the optimum for this phenomenon to develop.

Nedlloyd Genoa (now Maersk Phuket) is a 2900 TEU containership built in 1998 in Rostock, Germany, of 210 m length and a maximum speed of 23.5 knots. On January of 2006, in her Atlantic voyage between Le Havre and Newark, she was hit by stormy weather, facing winds of more than 65 knots and waves of up to 12 meters height according to the crew descriptions. While trying to keep head seas at reduced speed, the ship faced a series of waves that induced a few large amplitude roll cycles of around 30 degrees. Due to these large motions and the associated accelerations, 27 40 foot containers were lost overboard and 32 were damaged, after the collapsing of some containers in one of the ship bays.

An investigation of the Marine Accident Investigation Branch of the United Kingdom government followed the incident (MAIB, 2006), analyzing the causes of the large roll motions that lead to the container damage. The conclusions of this report showed that the possibilities could include either the appearance of an episode of parametric roll resonance or the pure effects of an abnormal wave hitting the ship in her port bow quarter. In the moment of the

accident, the ship had reduced its speed and according to the analysis carried out in the report, both sea and sailing conditions (wavelength, natural roll and encounter frequencies) were very near of that were parametric roll is more likely to happen. The report states that:

"P&O Nedlloyd Genoa's master was aware of the hazards of parametric and synchronous rolling. […]. When the roll amplitude became untenable in the deteriorating weather, a course which placed the ship's head more into the swell was adopted, together with a reduction in speed to prevent slamming. Also, 1104 tonnes of water ballast was loaded into the double bottom, which increased the ship's GM […]. By increasing the GM, the master decreased the roll amplitude, but the natural roll period was getting closer to twice the encountered wave period, and therefore the risk of parametric rolling would have been increased. Slowing down increased the encountered wave period bringing it even closer to half the vessel's natural roll period. […].

In this incident, the sea conditions do not appear to have been steady enough to induce parametric rolling. Additionally the ship's natural roll period appears at the time to have been just outside the limits for parametric rolling to occur. However, the master's actions were generating the pre-conditions for parametric rolling – something he could have avoided had ship specific advice on the phenomenon been available to him".

It can then be concluded that parametric roll could have been the cause of this accident, although this point have not been demonstrated. Moreover, the report states again (as in the case of Maersk Carolina) the need of the masters for advice parametric regarding roll resonance to avoid these events, fact that mostly inspires the present PhD thesis and that will be further analyzed in forthcoming sections.

CMA CGM Otello is a 8200 TEU containership, built by Hyundai shipyards in 2005, 319 meters long and with a speed of 25 knots. Its case is very near in time and position to that of Nedlloyd Genoa, as it occurred on the 17th of February of 2006, while sailing from Malaysia to Le Havre. In the Bay of Biscay, the ship faced rough weather, experiencing large pitch and roll motions that lead to the loss of 50 containers at sea and to the damage of other 20. According to the inquiry developed by the French government (state flag of the ship) through its Marine Accident Investigation Office (BEAmer, 2006), the ship experienced heavy pitching and rolling (15-20 degrees) in 5-6 meter nearly head waves. Although no final conclusion is obtained in the report about the cause of the heavy motions, parametric roll is stated as a possibility:

"The platform motions of the Otello, however pronounced they may have been, seem to belong to the gamut of the "normal" motions described in § 8.1.1 (platform motions due to the weather conditions: wind, wind waves, swell, cross seas/swell, abnormal waves, to say nothing of rogue waves), but were "unusual" (closely linked to the hull forms of container ships. […]. Fluctuations in their GM. […]. Parametric rolling) in that there was a series of pronounced pitching motions followed by a series of pronounced rolls. They nonetheless contributed to the loss of the containers. The pitching undoubtedly caused damage to the deck cargo lashing and securing systems, which was further amplified by the subsequent rolling – reaching at least 20° - causing several seriously weakened container stacks to topple over".

However, no detailed analysis of ship loading condition (natural roll frequency), encounter frequency or wave length is included in the report.

Figure 2.15. CMA CGM Otello. Port of Valencia. 2011. Photo courtesy of M. Hernández Lafuente.

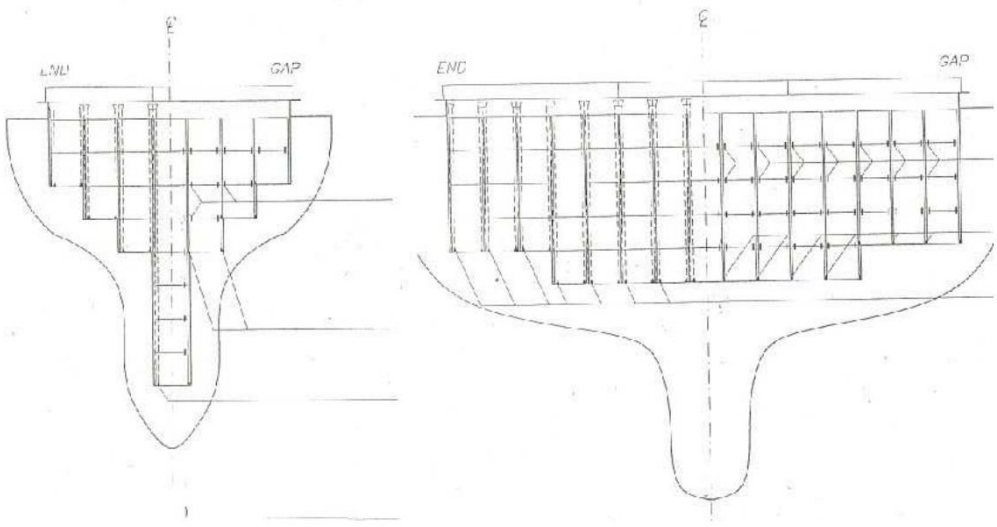

Figure 2.16. CMA CGM Otello bow (left) and stern (right) shapes. (BEAmer, 2006).

As a curiosity, the same day the CMA CGM Otello experienced the described incident, two other ships in the same or very near positions, P&O Nedlloyd Mondriaan (8400 TEU) and CMA CGM Verdi (5800 TEU), also experienced similar incidents which lead to the loss of respectively 50 and 80 containers.

The above described cases are those in which some report or research work has been found, and where a more or less detailed analysis of the event was reported. However, parametric roll resonance could have taken place in some

other events where don´t exist cargo loss or damage, or where no subsequent investigation is carried out or have been found. As an example, the case of OOCL America, that in 2000 lost 300 containers, is supposed to have been due to parametric roll resonance, but no evidence has been found about this fact.

Anyway, from the described cases it can be concluded that parametric roll resonance is not such an isolated issue affecting modern containerships, and that all of them follow a very similar sequence of actions. In a bad weather situation, with heavy seas, the master reduces speed aiming to reduce bow slamming and tries to keep the ship in a head seas situation in order to reduce the roll motion excited by waves hitting the ship sideways. Both actions, together with a proper natural roll frequency, set up the likely conditions for parametric roll resonance to develop. Although masters are usually aware of this fact, its main concern is avoiding the structural damage that could be generated by heavy pitching. Moreover, the need for onboard guidance systems that warn them about the high risk of appearance of parametric roll has been also stated as a fundamental issue for avoiding this kind of incidents.

2.3.2.2 Pure Car and Truck Carriers. Ro-Ro Ships.

Pure Car and Truck Carriers (PCTC) are a special type of ship intended to transport mainly cars, trucks, bus and other heavy wheeled machinery. Cargo is loaded in full lengthed and breathed decks, that are interconnected by internal ramps or elevators. In order to maximize the available surface of these decks and so cargo capacity, the superstructure of these ships is clearly box-shaped, while due to carrying a relatively light cargo its hull forms are quite slender and heavily bow flared, with large breath gradient while increasing draft. As seen in the previous chapter, these kind of hull shapes are very similar to those of containerships. Overhanging sterns are also present in PCTC, but not as sharp as in the case of containerships.

Figure 2.17. PCTC Courage (formerly Aida) in Antwerp (Belgium), 2008. Note the large bow flare and hanging stern. Photos courtesy of J. Willaert.

Moreover, roll damping in these kind of ships is sometimes small, making them even more sensitive to any dynamic issue involving roll motion such as, for example, parametric roll resonance (Windén, 2009).

The most representative examples of parametric roll resonance events on PCTC are those of M/V Aida and M/V Fidelio, that took place in 2003 and 2004 (Aida) and 2009 (Fidelio). The case of Aida, as will be seen, is quite representative, as the whole 2004 event was recorded by an onboard sensing system, being the first time this was done for a real ship.

M/V Aida is a 1991 built PCTC (now renamed as Courage and operated by ARC), with a length of 200 m and the capacity to carry 4850 cars at a speed of 20 knots. In February of 2003, roll angles of up to 50 degrees where reached while sailing in head seas of a significant height of around 5.5 meters. The owner and operator of the vessel at that time, Wallenius Wilhelmsen, after analyzing the event, concluded that parametric rolling was likely its cause, installing an onboard decision support system that should analyze and record ship motions and weather forecasts in order to determine risk areas on ship route. This system had implemented the IMO MSC/Circ. 707 which, as will be described in following sections, didn´t account for the head seas case while analyzing parametric roll resonance.

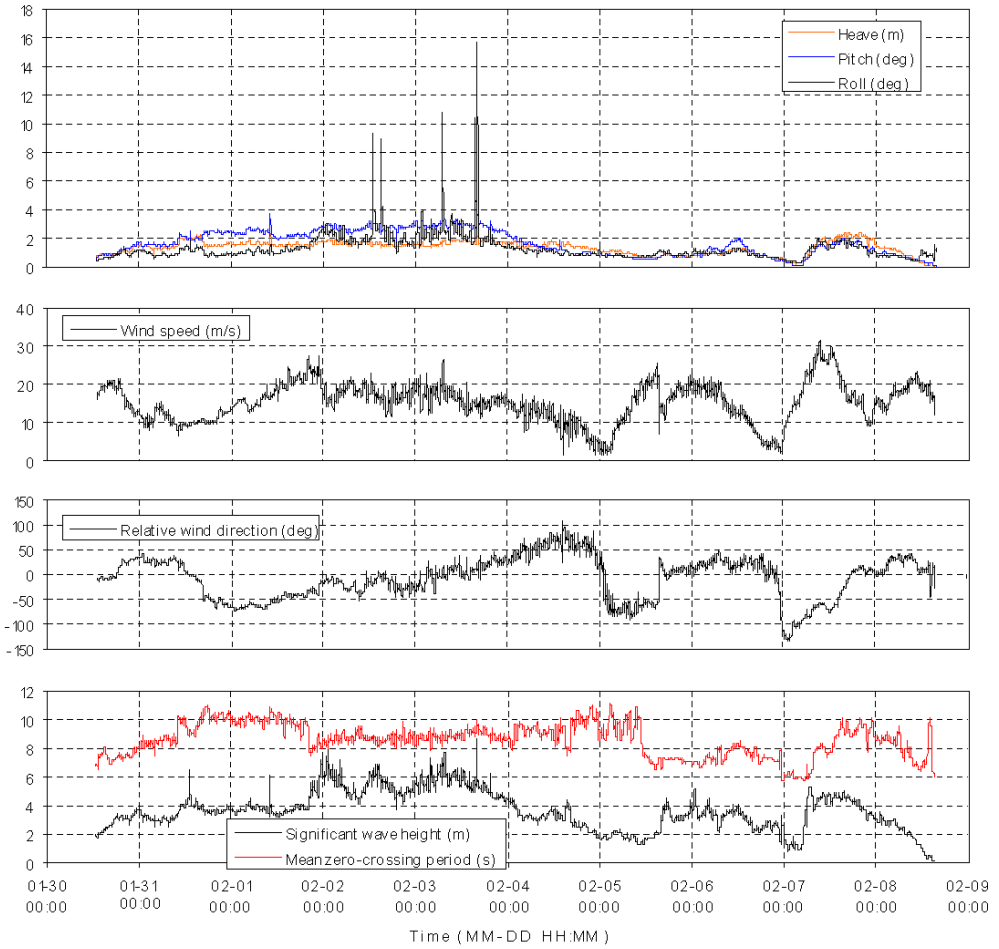

Figure 2.18. Recordings of parametric roll events onboard M/V PCTC Aida in 2004 (Palmquist,Nygren, 2004).

In 2004, and while sailing in very similar conditions to those of the 2003 event (similar load case, speed and wave parameters and head seas situation), five events of parametric roll resonance were recorded in the space of 30 hours between the 2nd and 3rd of February, reaching maximum roll angles of 17 degrees. The whole episode was recorded by the onboard guidance system and subsequently carefully studied. The results of this analysis can be found in (Palmquist,Nygren, 2004). From this work it has been extracted Figure 2.18,

where the five events of parametric roll resonance can clearly be appreciated. This reference will be revisited in following sections of this work.

PCTC M/V Fidelio is a slightly larger car and truck carrier than M/V Aida, as it is 220 m long and can carry up to 8000 cars. It was delivered to Wallenius Wilhelmsen in 2007. According to (Windén, 2009) and references therein, the ship experienced a severe episode of parametric roll resonance in December of 2009, reaching roll angles of 35 degrees and damaging cargo. Masters of Fidelio and her sistership Faust, have claimed in 2008 the need for an stabilizing system to avoid unlikely roll motions in rough weather and cargo damages.

Apart from PCTC, other Ro Ro ships, like cargo and cargo-passenger ferries, could be affected by parametric roll resonance. These types of ships are intended to carry rolling cargo of any kind and sometimes also passengers, leading again to relatively light loads and slender hull forms, although no so much as those of containerships and PCTC, as their cruising speed is usually less than in the later cases. Although no parametric roll events are recorded affecting these types of ships, the large variation of restoring capabilities also affecting them can be illustrated by the case of the M/V Finnbirch ferry vessel, (Krüger et al., 2008), which capsized and sank in following seas in 2006 mainly due to reduced stability levels and the roll generated by righting lever variation with wave passing.

2.3.2.3 Cruise Ships

The case of cruise ships is again similar to that of containerships and PCTC´s; in the last years, the needs for higher cruising speeds that could reduce the distance between stops in visiting harbors and higher deck areas that could increase the number of passengers and facilities, have led to very slender hull

forms, that rapidly get full as distance to flotation increases. As have been already mentioned, this type of hull raises the possibilities of the ship suffering from parametric roll resonance.

The only case in which parametric roll resonance has been confirmed among the cruise ships is that of the Costa Voyager; moreover, it is the only real case event that has been fully video recorded, as it was filmed from a SAR helicopter that came following the distress call of the ship.

Costa Voyager is a 180 m long cruise ship, able to carry up to 920 passengers, and was built in 2000 in the Blohm & Voss shipyards in Hamburg, Germany. One of the special features of this vessel is its maximum speed, being able to sail up to 28 knots due to its thin hull forms, that together with its roll damping characteristics (that led to heavy passage discomfort while on anchor and with no stabilizing capabilities (noticiasdecruceros.com, 2011)), may have been the causes of the parametric roll event that will be subsequently described. Nowadays, since 2011, it is operated by the Italian company Costa Crociere; the ship has had several names, depending on the operator, having been called Olympic Voyager, Olympia Voyager, Voyager (at the time of the accident) and Grand Voyager.

At the time of the accident, in February 2005, it was operated by Iberojet Cruises. While on route from Tunis to Barcelona, on the 14th of February and near the island of Menorca, the ship encountered heavy weather and reduced speed, proceeding head seas at between 3 and 4 knots.

Under these conditions, a large wave broke one of the bridge front windows, letting water in and disabling all source of power, stopping the main engines and retracting the fin stabilizers, heavily rolling in beam seas.

Figure 2.19. Grand Voyager (formerly Voyager). 2007. Photo courtesy of M. Hernández Lafuente.

Figure 2.20. Video captures of the heavy roll motion event of Voyager (2005). Note heavy head waves (left) and retracted stabilizers and huge roll amplitude (right).

After this situation, apparently once propulsive power was partially recovered and while making very low speed in head seas, the vessel suddenly heavily rolled for several times, experiencing fully developed parametric roll resonance. The event was fully recorded by the Cagliari S.A.R. helicopter that proceeded to the ship after its distress call, made following the power breakdown.

The vessel then proceeded to the port of Cagliari, with the result of several passengers injured (one of whom died some days later, (Europa-Press, 2005)) and heavy material damage. Although the official investigation report made by the Bahamas Maritime Authority (BMA, 2007) is only focused on the window

breakage issue (also suffered from Voyager sistership Explorer one month before) and makes no reference to the heavy roll motions, it is possible that the event was caused by the reduced ship speed in head seas (that led to encounter frequency – natural roll frequency tuning) and the reduced damping capabilities of the ship due to the failure of the fin stabilizers.

The second documented case of parametric roll resonance affecting a cruise ship is that of Pacific Sun in 2008, while on route from Mystery (Anatom) Island to Auckland, as a part of a cruise around South Pacific Islands. Pacific Sun (formerly MS Jubilee) is a 1985 built cruise ship, 223 m long, with a maximum speed of 18 knots and a capacity of 1900 passengers and operated by P&O Cruises Australia.

On the 28th of July, 2008, the ship was sailing form Mystery Island to Auckland as the final step of a cruise around South Pacific islands, when it faced heavy swells generated by an approaching storm, with only the starboard fin stabilizer under operation (as port stabilizer was housed due to breakdown). The ship was sailing with seas on the starboard quarter and rolling up to 10 degrees, when the master, at dusk, and aiming to reduce roll motion, decided to reduce speed (to about 6 knots) and heave on to head seas.

Under these conditions, the ship suddenly rolled up to 14 degrees. The master tried to modify heading to stabilize the ship, but before doing so, a very heavy pitching motion was followed by three new roll cycles, reaching up to 31 degrees, as confirmed by video footage captured by the CCTV system (Figure 2.22). Heading was then modified and de-ballasting in order to increase GM was ordered, stabilizing the roll motion in an average of 10 degrees. Starboard stabilizer was malfunctioning (being unknown if it stopped working before,

during or after the large roll event) but was kept extended to act as a passive stabilizer.

Although no major structural damage was sustained, very heavy damage to internal furniture and equipment occurred, both in public spaces, cargo handling areas, communication locals and others. Moreover, from the 1730 passengers and 671 crew onboard, a number of 77 injured people were recorded, three of them seriously, mostly due to furnishing hits and falling, as at the time of the incident most passengers were in the recreation spaces having dinner.

In the investigation report carried out by the UK Marine Accident Investigation Branch (MAIB, 2009) (Annex 5), an initial study of the sea and ship conditions in order to study the possible appearance of parametric roll resonance was prsented. At the moment of the incident, the ship natural roll period was about 17.3 seconds and was sustaining a speed of 6 knots. Under these conditions, parametric roll could have been expected in head seas for wave periods between 10 and 11 seconds, being the later the most critical, as the resulting wavelength was of 189 m, nearly equal to ship length. Taking into account that the weather routing information contained in Annex 1 of the same report, informed of waves of 7 m height and periods of between 10 and 11 seconds two hours prior the accident, parametric roll resonance could clearly be considered as a possible cause of the accident, as is concluded in the mentioned investigation. Moreover, other determining factors could have influenced the appearance of the phenomenon, like the reduced roll damping characteristics of the ship due to the breakdown of the fin stabilizers.

Figure 2.21. Pacific Sun. 2009. Photo courtesy of www.shipspotting.com.

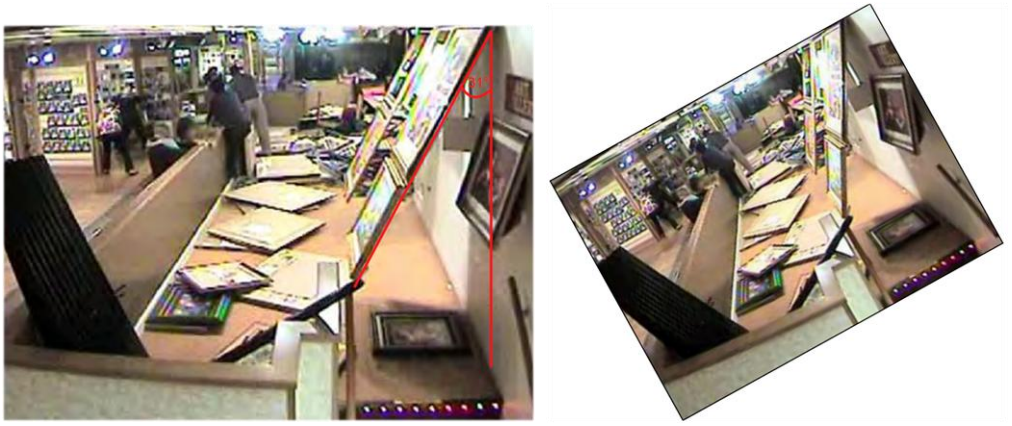

Figure 2.22. Ship Art Gallery at the moment of the largest roll amplitude (MAIB, 2009).

Figure 2.23. Resulting damages in different spaces after rolling (MAIB, 2009).

However, it is also stated that a detailed analysis of the susceptibility of the Pacific Sun hull to parametric roll would be needed to confirm this point, and that other possible cause of the three large roll events could be the action of some abnormally higher and steeper wave (MAIB, 2009).

2.3.2.4 Fishing Vessels

The last type of ship that has been historically related to parametric roll resonance is that of fishing vessels. One of the main characteristics of this kind of ships is its heterogeneity, as their typology largely changes depending on the fishing equipment used (trawlers, purse seiners, longliners, etc.) and also depending on the geographical location under analysis (as the arrangement of the ship also depends on the regulatory framework and the tradition of each location).

However and regarding parametric roll resonance, one main common characteristic may be highlighted, that is that fishing vessel hull forms don´t usually present very pronounced bow flares, as was the case of the other type of ships previously analyzed, although in many occasions transom and overhanging sterns are present.

In fact, in some occasions, as shown by (Munif,Umeda, 2006) , the changes in GM with wave passing are very small by themselves, and heave and pitch motions have more influence for triggering roll resonance.

An example of transom stern fishing vessel, likely to suffer the phenomenon, is that of the traditional Spanish trawler, which presents a transom stern, where the trawling ramp is usually included and trawling doors are stowed.

Figure 2.24. Typical arrangement of a Spanish mid-sized stern trawler. www.shipspotting.com.

Until today, and as far as the author is concerned, no parametric roll events affecting fishing vessels have been reported. However, this fact does not imply that parametric resonance doesn´t appear on these ships, as will be subsequently explained.

Fishing vessels usually have reduced stability levels (sometimes just fulfilling the minimum requirements) and crew training capabilities are much lower than those corresponding to larger merchant ships. Taking these two facts into account, if a large amplitude parametric roll event takes place, there are many possibilities that the ship capsizes and sinks and, if not, it is also possible that crew are not able to distinguish parametric roll as itself and could be described as wave impacts or other stability or seakeeping issues.

Whatever the case is, parametric roll of different fishing vessels has been studied by many authors, probing that parametric rolling is likely to affect them.

For example, a comparison of the behavior in longitudinal head seas of two sistership typical UK trawlers, only differing in the stern type (round and

transom stern), characterizing its influence on the amplitude of the developed parametric roll, was made in (M. A. S. Neves et al., 1999), while in (S. Neves et al., 2003; Pérez Meza,Sanguinetti, 2006) both vessels were separately studied. This same transom stern ship was also studied by (Spanos,Papanikolaou, 2005) and (Míguez González, López Peña, Díaz Casás, Galeazzi, et al., 2011).

Actually, this ship has become a very know example of fishing vessel hull form with a high tendency to developing parametric roll resonance; in fact, its seakeeping characteristics have been studied since mid 70´s until 2011, as it sank in 1974 possibly due to bad seakeeping capabilities in certain seas, and investigations about this fact have recently been concluded (Gimson, 1975; Paffett, 1976; Young, 2011).

In (de Juana Gamo et al., 2005), the authors studied the behavior in longitudinal head seas of the aforementioned Spanish medium-sized trawler, demonstrating that parametric roll resonance is likely to be suffered under the analyzed conditions.

In (K.J. Spyrou, 2000), parametric roll resonance of a purse-seiner in following seas is analyzed.

Finally, in (Umeda et al., 2002) the authors compare the likeliness of two different types of fishing vessels (a Japanese one versus an Icelandic one) to developing parametric roll, concluding that the Icelandic hull forms are more prone to suffering roll resonance, although the Japanese design could also experiment it under certain conditions. The Icelandic fishing vessel was also subsequently analyzed in detail in (Munif,Umeda, 2006).

Moreover, the first two ships (the UK transom stern trawler and the Spanish one), will also be studied along this work, demonstrating its clear tendency to developing the phenomenon.

2.4 Parametric Roll Prediction and Prevention

2.4.1 Introduction

One of the main characteristics of parametric roll is its very sudden onset and fast development. As it has been described, it is a sudden phenomenon that fully develops in just a few rolling cycles, and there are few signs that can timely suggest the crew that the resonance is occurring.

The possible consequences of an incident involving parametric roll resonance could go from just a scary episode to huge cargo or ship damage, and even casualties or vessel capsizing, as have been seen above. Therefore, the need for a system that could advice and warn the masters and crews about the possibility of appearance of the phenomenon and that could allow them, or an automatic system, to take corrective actions to prevent large rolling, is clear.

On the forthcoming sections, the state of the art in this matter is analyzed. On one hand, the different alternatives developed for assessing the probability of a ship suffering from parametric roll resonance, for guiding the masters to avoid the phenomenon and to detect it in case it finally developed, are presented. On the other hand, the strategies focused on preventing parametric roll resonance once it is developing, and that include ship speed and/or heading control and the use of different stabilizing systems, are described.

2.4.2 Prediction of Parametric Roll Resonance

2.4.2.1 Regulatory Framework

Ship dynamic instabilities have always been a concern for the governing bodies, especially those related to following and quartering seas conditions. Being aware of the fact that ships could be facing several dangerous situations while sailing on the swell direction and that stability standards were limited to static stability criteria, the Marine Safety Committee of the International Maritime Organization, on its 65th session (May 1995), approved the 707 MSC Circular, entitled "Guidance to the Master for Avoiding Dangerous Situations in Following and Quartering Seas" (IMO, 1995).

This guide was intended to provide the master with a set of basic principles for avoiding the risky situations that could appear while sailing in heavy stern seas and that included surf-riding and broaching, reduced stability while wave riding, synchronous roll and parametric roll. Guidance is based on ship speed, length and natural roll frequency and wave length, height and frequency. Polar diagrams are included indicating the master, as a function of ship heading related to waves (encounter angle) and the aforementioned parameters, risk areas where dynamic unwanted phenomena are likely to occur. Guidelines for measuring and estimating from observations the necessary ship and wave parameters were also within the document.

Although parametric roll was included in these guidelines, it was only indicated that parametric roll was likely to occur when wave encounter period was near half the natural roll frequency. For avoiding those conditions, and as only stern seas situations were considered, the recommendation was to reduce ship speed after the estimation of encounter period. Literally:

"The master should prevent a synchronous rolling motion which will occur when the encounter wave period T_E is nearly equal to the natural rolling period of ship T_R. Large rolling motions which occur under the condition of $T_E \approx T_R/2$, that is the parametric rolling should be also prevented. The encounter wave period T_E is a function of V/T as shown in figure 3. By using this relation, the master can know whether his ship will encounter the synchronous and parametric rolling or not.

When reducing speed in order to avoid any of above critical conditions, the master should take into consideration the minimum speed required for maintaining course control in waves and wind."

As the polar diagrams present on the guidelines were only referred to surf – riding and encountering high wave group instabilities, that recommendation was the only information masters received for avoiding the appearance of parametric roll resonance in stern seas. No guidance at all was provided for avoiding parametric resonance in head seas.

Coinciding with the development of large containerships and car carriers, a series of incidents involving very large roll motion in head seas (that have already been described in this work) turned the sector attention back to the parametric roll phenomenon and to the need of providing the masters with more information to avoid it, especially when facing head seas, situation not considered in the 707 MSC Circular.

In 2002, during IMO Sub-committee on Stability and Load Lines and on Fishing Vessels (SLF) 45th session and in the frame of the review of the Intact Stability Code (SLF 45/6) being undertaken at that time, two documents were submitted for their consideration related to head seas parametric roll and IMO 707 MSC Circular (IMO, 2002a).

In SLF 45/6/2 (IMO, 2002b), Germany proposed the revision of the 707 MSC Circular, in order to include the dangerous situations that new designs were facing in head seas (IMO, 2002b):

"[...] Intact stability, however, governs the behavior of the ship at all times. Thus a better understanding of dynamic effects in irregular seas should not be limited to developing stability criteria. The development of physically sound criteria by itself is considered a first step forward. The next step has to be to continue the development of guidance to the master currently contained in MSC/Circ. 707 [...]".

"At the time of development of this circular, it was accepted that problems with dynamic effects would be observed only in following and quartering seas. This is no longer the case. The more recently designed vessels with large bow flares and high deck loading capacities are additionally considered vulnerable in encountering seas. Thus Germany proposes to revise MSC/Circ. 707in the light of the additionally gained experience".

In SLF 45/6/7 (IMO, 2002a), the US submitted the France et al. article "An Investigation of Head-Sea Parametric roll and its Influence on Container Lashing Systems" about APL China accident (France et al., 2003), where it was finally concluded that:

"The IMO should consider enhancing MSC Circular 707 [...] to incorporate guidelines for operating vessels prone to head sea parametric rolling".

In 2004, and after PCTC Aida incident, Sweden submitted to the IMO SLF committee, on its 47th session and together with document SLF 47/6/6, the article "Recordings of head sea parametric rolling on a PCTC" (Palmquist,Nygren, 2004), where the real measurements of a head seas

parametric rolling episode on that PCTC were described. In this article, the authors stated, along with other conclusions, that:

"The need to extend MSC/Circ.707 to cover also head sea regarding parametric rolling has already been addressed within IMO […]. It is a fact that the properties that make, for instance, RoRo and container ships sensitive to parametric rolling and pure loss of stability are inherent in the actual concept of those ship types.

As operational aspects are vital, it is the authors' opinion that the main target should be further development of methods for short-term risk assessment that can be put into practice in ship operation, for instance implemented in operational decision support systems. Such methods should deal with the specific hull form, taking factors like wave direction, wave spectra bandwidth and multiple wave systems into account".

From the aforementioned references, three main conclusions could be obtained:

1. The sector was, by 2004, completely aware of the importance of parametric roll resonance in head seas, and that the current guidelines and stability criteria were not enough for facing the new challenges.
2. Head sea parametric rolling was an inherent characteristic of new Ro-Ro, containerships and cruise vessels.
3. It was necessary to provide the masters with new guidelines and short-term risk analysis to face possible parametric roll events.

Taking in consideration these three conclusions, the IMO SLF subcommittee continued with the revision of stability criteria and MSC/Circ. 707.

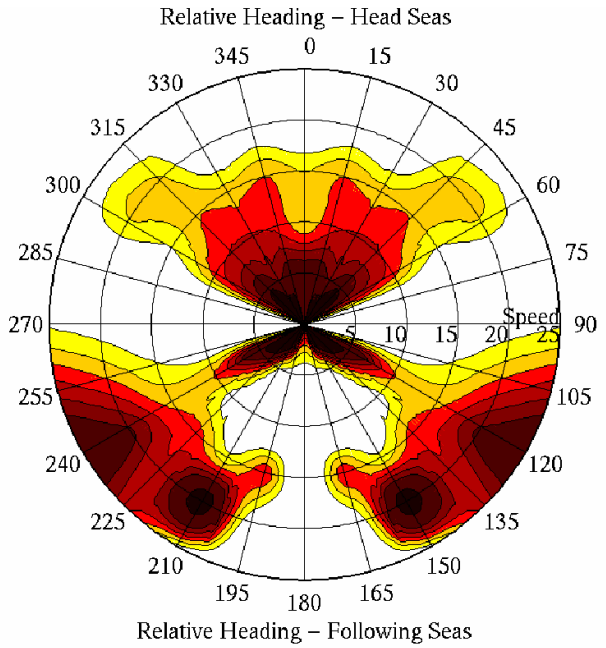

Figure 2.25. Polar diagram showing resonance risk areas in head and quartering seas. (V. L. Belenky et al., 2006).

At the same time, the American Bureau of Shipping (ABS), Classification Society that in that moment was classing the majority of large and new ultra large containerships (ABS, 2000), established a new optional class notation (PARR – N, PARR – C1 and PARR – C2). This notation could be assigned to all the vessels which satisfied a number of requirements described in (ABS, 2004). Mainly based on the work by Shin et al. (Shin et al., 2004), the objective of this notation is to assess if the ship under consideration is likely to developing the phenomenon and, if so, how large would the roll amplitudes be.

If the ship is found to be prone to parametric roll, it is required to supply the master with an operational guidance. It would be based on polar diagrams, where as a function of ship speed and course (from head to stern), and for different loading conditions and sea states, attained roll angles are plotted in different colors (Figure 2.25).

As it could be seen, this new notation was trying to fill the regulatory gap regarding parametric roll resonance that existed in that moment. On one hand, it tried to address in the design stage how that "inherent" characteristic of containerships would be affecting the operation of the ship in the future, by determining if it was or not likely to suffer from head seas parametric roll. And on the other hand, the requirement of an operational guidance for the affected ships was the evolution of the MSC/Circ. 707 into the head seas case. The first vessels that obtained this notation were the containerships Hyundai Forward (4700 TEU) and Hyundai Faith and Force (8600 TEU) in 2008 (ABS, 2008). They were awarded the PARR C1 class, that is, the vessel is prone to parametrically roll, numerical tests have been carried out and a Guide to the Master has been placed onboard.

The work done by that time in the International Towing Tank Conference was also oriented into the first of these alternatives, i.e. addressing the possible appearance of parametric roll from the design stage. In ITTC document 7.5 – 02 – 07 – 04.3, "Testing and Extrapolation Methods Loads and Responses, Stability. Predicting the Occurrence and Magnitude of Parametric Rolling" (ITTC, 2005), approved in the 24th ITTC Conference in 2005, again some numerical criteria were proposed to evaluate the susceptibility of a ship to parametric roll resonance. Although the process was very similar to the numerical evaluation carried out in the ABS guidelines, some very interesting statements were included within the ITTC document, regarding the influence of realistic seaways in the appearance of roll resonance and the difference between susceptibility to parametric roll, probability and risk of parametric roll:

"Despite the progress a few issues remain open, such as the development of effective criteria for the prevention of parametric rolling by design, the assessment of the effects of coupling with other motions, and last but not least,

the derivation of optimal experimental/numerical procedures for safety assessment in a realistic sea […]. In general, the development of a criterion that is suitable for a realistic sea is still open. […] Integration of the above assessment of parametric rolling within a risk assessment procedure entails specification of the consequences. As it well-known, risk is defined as the product of the probability of occurrence times the consequences. It is not appropriate, even in a liberal sense, to consider as identical the "probability of parametric roll" with the "risk of parametric roll". The consequences of parametric roll could vary qualitatively as well as quantitatively. Ship capsize should be considered as rare whilst more likely should be damage to the cargo. This damage should be quantified in order to determine the risk. Furthermore, the susceptibility to parametric rolling should be distinguished from the probability of parametric rolling; because in addition to how prone a ship is to parametric rolling, the latter contains also the probability of encounter of critical environmental conditions. At this stage, it is untimely to propose a detailed guidance for carrying out risk assessment of parametric rolling as the field is currently under development".

These guidelines were complemented in 2008 by the revision during the 25th ITTC Conference of the procedure 7.5 – 02 – 07 – 04.1, "Model Tests on Intact Stability" (ITTC, 2008a), where detailed instructions were given for carrying out the towing tank tests in parametric rolling conditions that, for example, are recommended in the ABS Guidelines (*"Indicated severity is to be considered as a warning of a possible problem with parametric roll, which has to be addressed during further design. Sophisticated numerical simulations and model tests are to be considered")* or that may be carried out by any designer or shipbuilder that wanted to evaluate the behavior of a given ship in such conditions.

Regarding the IMO again, the work in revising the MSC/Circ. 707 ended in January of 2007, with the approving of the MSC.1/Circ.1228, "Revised Guidance to the Master for Avoiding Dangerous Situations in Adverse Weather and Sea Conditions" (IMO, 2007).

Although in this revised version of the Guide the problem of parametric roll in head seas is mentioned, the description and the preventive measures that are proposed are still very limited, at least compared to those proposed by the ABS. The description of the phenomenon and the guidance included in the MSC.1/Circ.1228 to avoid head seas parametric rolling is the following:

"Other than in following or quartering seas, where the variation of stability is solely effected by the waves passing along the vessel, the frequently heavy heaving and/or pitching in head or bow seas may contribute to the magnitude of the stability variation, in particular due to the periodical immersion and emersion of the flared stern frames and bow flare of modern ships. This may lead to severe parametric roll motions even with small wave induced stability variations.

For avoiding parametric rolling in following, quartering, head, bow or beam seas the course and speed of the ship should be selected in a way to avoid conditions for which the encounter period is close to the ship roll period or the encounter period is close to one half of the ship roll period".

The aforementioned rules, recommendations and guides, compose the regulatory framework dealing with parametric roll resonance in head seas that are nowadays in force. As it could be seen, the probability and severity of the consequences of parametric roll resonance in the modern design of certain types of ships have been assumed, together with the need for addressing the tendency

of a ship of developing the phenomenon and providing the masters with a series of guidelines that could help them to prevent its appearance.

However, and taking into account that the proposed Guidelines are mainly based on the "manual" observation of ship sailing conditions (i.e. waves, ship speed and heading, natural roll frequency, loading condition parameters, etc.), they just could be used as an indication of a possible risk situation, with a high degree of uncertainty. At the same time, the more complete this guidance was, the more complicated would be the evaluation of the contained information by the master. This fact was also observed by the ABS in its Guidelines, allowing the use of computerized or electronic systems for displaying the information contained in the guides, together with the polar diagrams, that could be developed following, for example, the guidelines contained in (V. L. Belenky et al., 2006).

So, the next step ahead was then clear and consisted, taking profit of new meteorological analysis systems, on electronic onboard systems, that based on those guidelines but with improved characteristics, would provide the masters with real time information regarding the risk situation of their ships.

2.4.2.2 First Generation Detection Systems

As it has been seen in the previous section, the use of onboard computer systems where guidance to master instructions were implemented, was the industry answer to the problems of ship behavior in heavy seas and other dynamic issues such as parametric roll resonance.

This kind of software have been in use since the IMO MSC Circ./707 entered into force. Most of them were implementing the requirements of this circular, but including some improvements regarding the evaluation of ship sailing conditions and other important parameters.

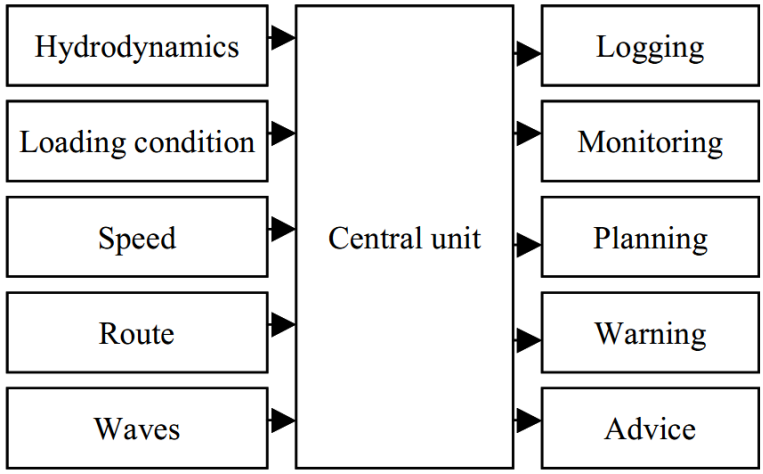

Figure 2.26. GL HRSRA System Scheme.

The main concept beyond these systems could be obtained from the Germanischer Lloyd certification guidelines for Hull Response Monitoring Systems, in the section referred to Shipboard Routing Assistance Systems (HRSRA) (GL, 2011).

The system is based on a central unit that using a numerical seakeeping code and a hydrodynamic database, processes the information received from the ship navigation systems (speed and course), wave monitoring or forecasting and loading condition, to estimate real time and future ship motions.

These estimations could be used to provide routing assistance to the crew, warning them against potentially dangerous conditions and providing advice.

In the case of parametric roll resonance, and considering the highly nonlinear behavior of roll motion in these circumstances and the irregularity of real seaways, these warnings should be based on the analysis of the sea state and ship sailing parameters described in the 707 Circ., but with the main advantage of that in this case, these values could be automatically obtained from the HRSRA system.

AMI SeaWare Enroute Live (AMI, 2001) could be perfectly taken as a representative example of this kind of systems, of their advantages and disadvantages. A wide and deep description of its main working principles, operation and results of a real case could be found in the paper (Palmquist,Nygren, 2004), where the measurements obtained from PCTC Aida during her parametric rolling event, previously cited in this work, are described.

As it has been previously said, the main parameters used for evaluating the possible appearance of roll resonance, both by IMO and ABS Guides, are the value of ship-wave encounter frequency and ship natural roll frequency. According to those guidelines, these parameters should be evaluated from observation of wave conditions (encounter frequency) and from the analysis of ship roll motion in calm seas (natural roll frequency). As it could be easily understood, this procedure could lead to significant errors, both in the evaluation of wave frequency and in the natural roll frequency, especially if this last value was trying to be obtained with the ship sailing in open seas and subjected to wave excitation.

Among the main advantages of this kind of automatic systems is that, based on the use of motion sensors and its connection with onboard navigation systems, the values of natural roll frequency and incident wave spectra could be determined in real time. Once these parameters are known, the software is able to generate warnings corresponding to different dynamic instabilities after considering a set of given criteria. It is also able, based on the received weather forecasts, of making estimations of future sea state and consequently, through the numerical seakeeping code, to determine future warning zones.

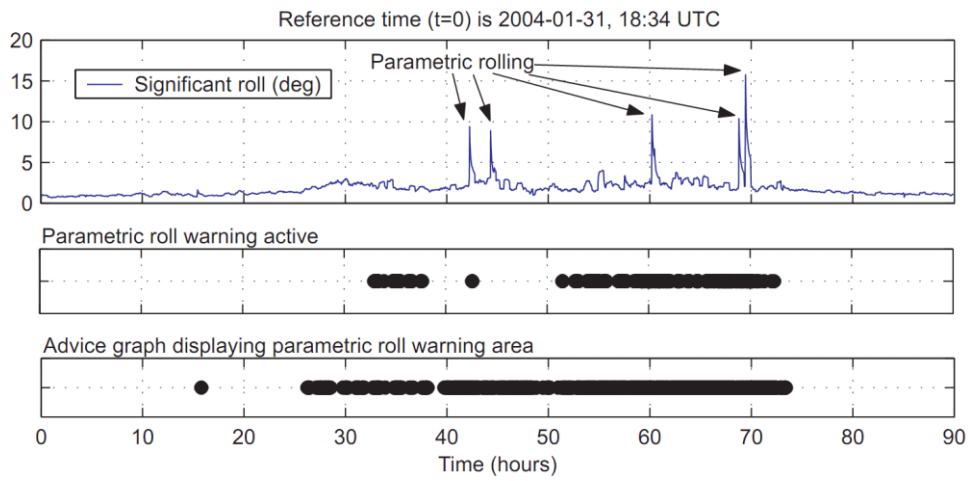

Figure 2.27. SeaWare EnRoute Live parametric roll warnings (Palmquist,Nygren, 2004).

In the case under study, at the time of the measurements, the system was operating under MSC Circ./707 criteria and so, taking into account that according to this circular head seas condition is not a risky situation regarding parametric roll resonance, no warnings were displayed and the parametric rolling event finally occurred.

In any case, the playback mode of the described software allowed the authors to study the behavior of the system overriding MSC Circ./707 criteria and allowing it to display warnings when head seas parametric rolling was likely to happen.

From Figure 2.27, by comparing both real time warnings and predicted warning timelines with the real parametric roll events, two conclusions could be obtained. Firstly, that both the real time and the predicted warnings were displayed when roll resonance occurred and so indicating the master that corrective measures were needed. But when the warnings along timeline are analyzed, it can also be seen that while only five parametric rolling episodes

happen, lasting about 7 minutes each, real time warnings were displayed for more than 20 hours, while predicted warning areas lasted more than 40 hours.

If countermeasures, as a reduction of ship speed, had been undertaken, parametric rolling events would surely have been avoided. But these measures, at the same time, would have implied a reduction of speed and so, a delay of the ship voyage and an increase of the shipping costs; for sure they would have been necessary a short time before roll resonance, but not during the whole length of the warning area where no resonance developed.

This fact illustrates the need of a short term detection system, that could detect that a parametric rolling event is on course shortly before it appears. These kind of systems would be described in next chapter.

In order to include a further analysis of these onboard guidance systems, some other approaches could be mentioned, apart from SeaWare EnRoute Live. Amarcon Octopus-Onboard (Amarcon-BV, 2011b) is another of these packages, intended to support the master´s decisions about dynamical stability. In this case, loading condition and navigation data and measured and forecasted weather excitations are used for computing ship motions through a hydrodynamic library and a 3D potential theory numerical code. From these values of motion, together with measured data, different warnings are displayed for the main dynamic instabilities, including head seas parametric roll resonance. Basically and regarding parametric roll resonance, its philosophy is equivalent to that of SeaWare EnRoute.

Another example is that of ADOPT DSS which is intended to act as an engineering tool in the first stages of the ship design, as a training tool for crews and as a guidance system while installed onboard. The system is based on the previously described ROLLS seakeeping code and on an real time measurement

system of the environmental conditions (Günther et al., 2008; Krüger,Kluwe, 2008; Krüger et al., 2008).

Marsig´s ARROW is slightly different to the aforementioned softwares, as it is mainly a tool to generate polar diagrams from user input data according to IMO guidelines. All details could be found in (Marsig, 2011).

Although in general, the described decision support systems have been of great help to the masters, regarding parametric roll resonance they still have some drawbacks, especially those related to the fact that they do not provide a short term real time warning, although they have, at least, generated a general sense of awareness about the phenomenon on the maritime community.

2.4.2.3 Second Generation Detection Systems

As it has been mentioned in this work, and was stated by (Døhlie, 2006), classification societies as Det Norske Veritas have pointed out the need for second generation warning systems, that complement current systems based on polar diagrams that have been the first response of the maritime industry to the call for decision support systems, which could help the master in counteracting the onset of parametric roll.

The main feature of these novel systems should be the capability to predict/detect the onset of parametric roll in a short time horizon (few minutes) just shortly before it develops, allowing the crew to take immediate corrective actions, or to trigger a system that could automatically take the ship out of the risk area.

In response to this need, some research tanks have pursued different lines of research aiming at obtaining a real-time detection system, which analyzes the ship's motions and detects the possible occurrence of parametric resonance. Thus, preventive actions would be taken only when parametric roll is certainly

developing, avoiding the potential drawbacks derived from taking unnecessary countermeasures. Model based approaches have been proposed by (Holden et al., 2007; L. S. McCue,Bulian, 2007), whereas a signal based approach is at the core of the methods in (R. Galeazzi et al., 2009a, 2009b).

(Holden et al., 2007) proposed an observer-based predictor. Assimilating ship roll motion to a second order oscillatory system, the detection method is based on the analysis of the eigenvalues of the system. Thus, if those values move into the instability area, the system will generate a warning alerting of the probability of roll resonance, that is, that roll motion has became unstable.

In order to obtain the time varying parameters of the oscillatory system and so to be able to compute the eigenvalues for defining the stability of the system, the authors propose three different alternatives: a discrete Kalman filter, the recursive least squares method and a particle filter method. The three methods were tested using experimental data from towing tank tests of a containership, both in regular and irregular head seas, in resonant and non resonant conditions. The three methods obtained very similar predictions, being very accurate in regular seas, but generating some misdetections or false positives in the irregular wave case.

(L. S. McCue,Bulian, 2007) studied the possible evaluation of Finite Time Lyapunov Exponent (FTLE) time series to detect the occurrence of parametric roll resonance. The system was tested using a mathematical nonlinear model of 1.5 degrees of freedom (roll motion plus heave and pitch, being these two last degrees of freedom computed by a quasi-static assumption) of a RoRo ship in irregular seas, where parametric excitation was obtained through the variations in restoring arms according to Grim´s effective wave amplitude. Different roll motion time series were obtained for testing the capabilities of the method, both

for zero and non-zero forward speed, in head irregular seas according to a Bretschenider spectrum in parametric roll resonance conditions.

Although the analysis of FTLE time series has demonstrated to identify indicators of increasing roll motion and capsizing, it was also concluded that these indicators were mostly qualitative and that, in many times, they were too close or too far to the beginning of the parametric roll event as to trigger any kind of alarm or preventive measure or as to be certain that roll resonance was developing.

As it has been described, none of the aforementioned methods had been able to accurately detect the appearance of parametric roll resonance in realistic seaways, and in both cases, the authors claimed for future developments and improvements in their methods in order to obtain better results.

The only alternative that has demonstrated to work fine in the whole range of operational conditions is that presented by Galleazzi et al. In fact, and by the time of writing this work, this system has been patented and recent works have been initiated in order to implement the detection strategies into the onboard guidance system Amarcon Octopus Onboard, previously described in this work (Amarcon-BV, 2011a).

Galleazzi et al. present two complementary detection schemes, one working in the frequency domain and the other in the time domain. In (R. Galeazzi et al., 2009a), the frequency domain alternative is presented. It is based on the analysis of the power spectrum of heave, pitch and roll motions. By analyzing the two first spectra, the ship-wave encounter frequency is determined. If resonant conditions are met, the system starts monitoring the roll spectrum. The author presents two methods for determining if parametric roll is developing from the analysis of roll power spectrum. On one hand, the first method is

based on sinusoidal signal detection in white noise and the evaluation of energy increasing in the aforementioned spectrum. On the other, the second method is based on the energy transfer between pitch and roll spectra that takes places while resonance develops, using an energy flow coefficient.

In (R. Galeazzi et al., 2009b), the time domain option is presented. It is based on the fact that, while parametric roll resonance is developing, pitch and roll time series peaks get aligned (every second peak of pitch time series gets in phase with the peak of roll), and that when this alignment disappears, roll amplitude decreases. Thus, the detection is based on analyzing changes on the variance of a signal (signal power) that has information about pitch and roll phases, and that is obtained by the product of roll angle and the square of pitch angle. A Generalized Log-Likelyhood Ratio Test (GLRT) technique is used for change detection in the driving signal.

Both alternatives were separately tested against experimental data of towing tank testing of a containership in both regular and irregular head seas. The obtained results showed a very good performance, especially in regular waves, while some false positives appeared in the irregular case, but still maintaining good prediction accuracy.

These two methods have been merged within a monitoring system for the early detection of parametric roll and the vast testing done on experimental and full scale data of container ships in transit assessed the good capabilities to timely detect the onset of parametric roll and the robustness against false alarms due to e.g. synchronous roll (R. Galeazzi et al., 2012; R. Galeazzi,Perez, 2011).

In this work, another approach for parametric roll detection will be presented, based on the novel application of artificial neural networks for forecasting ship roll motions. It will be described in Chapter 4 of this dissertation.

2.4.3 Prevention of Parametric Roll Resonance

2.4.3.1 Introduction

As it has been already described, parametric roll resonance could generate large roll motions and lead to fatal consequences. The need for a detection system, and even for a guidance system, has been explained in the previous chapter. However, the main goal is to obtain systems that could, in a first stage, detect the appearance of parametric roll resonance, but that could, in a second stage, prevent it from developing.

As mentioned, there are some specific conditions that have to be present for parametric roll to appear, regarding both ship and waves characteristics. Wave encounter frequency should be around twice the ship natural roll frequency, their amplitude should be over a certain threshold that depends on ship characteristics, and their wavelength should be near ship´s length. Ship roll damping should be small enough not to dissipate all the energy that is generated by the parametric excitation. And finally, ship restoring arm variations due to wave passing along the hull, should be large enough as to counteract the effect of roll damping.

If parametric roll resonance wants to be prevented, it´s obvious that there are three main approaches that could be dealt with, and that consist on avoiding at least one of the aforementioned conditions to be present.

The first alternative consists on acting on ship damping components, or using stabilizing forces that oppose the heeling arms generated during the resonance process. In this group, the use of bilge keels and the different stabilizing systems would be included.

The second alternative, aimed at reducing the amplitude of restoring arm variations, necessarily implies introducing modifications in hull forms or adding additional structural elements, such us sponsons.

Finally, the third alternative is focused on avoiding that wave encounter frequency is twice the ship natural roll frequency. If we consider a ship sailing at a given loading condition (and so with a constant natural roll frequency) in a specific seaway (frequency and amplitude), the only way of acting on the frequency ratio is modifying encounter frequency. So, this alternative would be based on ship speed and heading variations that take the vessel out of the risk area defined by $\omega_e / \omega_n = 2$.

2.4.3.2 Stabilizing Systems

The different ship stabilizing systems, mostly aimed at reducing roll motion, are divided into two groups, passive and active, and their main working principle consists on increasing ship roll damping or generating properly tuned forces that counteract those ones that generate ship roll motions.

These systems have been extensively studied and tested and most of them have a good performance in a typical ship operational condition. Nevertheless, their stabilizing performance during parametric roll episodes uses to be unsatisfactory. For this reason not much less research effort has been focused on studying roll stabilization devices for parametric roll resonance. The main publications about this matter will be described below.

Among passive stabilization devices, bilge keels, or passive anti rolling tanks are the most representative. The main objective of bilge keels is increasing roll damping; they do not need any specific tuning, and the only consideration that has to be taken into account is if they´re properly designed as to increase this

damping up to a level that could dissipate all the energy generated during the resonance process. The case of anti rolling tanks is slightly different. These systems are designed in such a manner that water flows from one side to the other at a period equal to the natural roll period of a ship, but with a difference in phase. This lag, allows tank created moments to counteract heeling moments, thus generating a reduction in roll amplitude.

Regarding passive systems, the most complete work is that of (Umeda et al., 2008). In this work, the authors study the performance of side sponsons and bilge keels in parametric roll resonance conditions, and also the use of a passive U-type anti roll tank. The behavior of the different stabilizers is analyzed using both numerical and scale model tank testing of a 6600 TEU containership in regular head seas.

The main objective of side sponsons (prismatic-like side structures fitted along the waterline), is to increase buoyancy while a wave crest is amidships, thus reducing the variation of GZ curve with wave passing and so the probability and amplitude of roll resonance. The study concludes that side sponsons alone could reduce the amplitude of roll motions, but not completely preventing it. At the same time, the effect of an increase of the size of the original bilge keels of the ship is studied. Although the linear damping is increased by an 80 %, neither prevention nor significant reduction in resonant roll amplitude was obtained.

In the case of stabilizing tanks, results are shown for just one sea condition, with different filling levels of water in the tank. For this situation, the tank filled in more than a 40 % (which means an increase of more than a 300 % in linear damping) prevents resonance from appearing. However, no other sea conditions are presented.

As could be seen, results obtained with bilge keels and sponsons are not very satisfactory from the prevention of resonance point of view. Apart from this fact, installing sponsons has other drawbacks in addition to their economical cost, as increasing of resistance and complicating drydocking and loading/unloading operations (increased distance ship-quay).

Although the results regarding anti roll tanks seem to be good, the authors also state one of the main drawbacks of these systems, which is the reduction on the ship loading capacity that they imply.

For a more detailed study of passive anti roll tanks and their influence in ship stability in parametric roll conditions, the work by Neves et al. (M.A.S. Neves, J.A. Merino, et al., 2009) should be considered. There, the application of a passive U-tank (although it is defined as active, it´s considered as purely passive along the study) to a fishing vessel very likely of developing parametric roll resonance, is described. A coupled nonlinear mathematical model of three degrees of freedom (heave, roll and pitch), taking into account the influence of the tank, is used for studying the obtained roll reduction at different wave conditions and filling levels of the tank. As the authors point out, for a given set of tank parameters, its performance in preventing the appearance of parametric resonance largely depends on wave conditions. In some situations, the tank is able to completely counteract its effects, while in others, only reductions of a 50 % or even no reduction at all could be obtained. In order to determine the influence of the tank parameters on its performance for different wave conditions, the concept of maps of stability described in (M. A. S. Neves,Rodriguez, 2007) is revisited. In this occasion, a complete study of the influence of tank filling (mass), damping ratio, natural frequency and tank vertical position for different wave frequencies and amplitudes is accomplished, concluding that the most affecting parameters are the correct tuning between

tank frequency and ship natural roll frequency and the tank water level assessment.

Taking this last consideration into account, it could be concluded that the best option for stabilizing roll resonance (regarding anti roll tanks) could be that of a tank that could automatically adjust its natural frequency to the natural roll frequency of the ship. These would lead us to the use of active anti roll tanks.

These same conclusions were obtained by (Windén, 2009), where different type of stabilizers where tested for using onboard a RoRo ship for preventing parametric roll resonance. The main problem of passive tanks was found to be the frequency tuning; in some conditions, the tank made roll motions even larger than in the case without it. The solution came with the use of active tanks, able to be tuned for the different encountered conditions.

Regarding the study of active tanks for stabilization of roll resonance, and apart from the previously mentioned reference, the research about active anti rolling tanks and their control strategies for its application to prevent parametric roll resonance, is quite scarce.

The main reference about this topic is that of (Holden et al., 2009), where the application of nonlinear control Lyapunov strategies is studied for control of active U-tanks in parametric roll resonance conditions in head seas and regular waves.

In this work, the passive U-tank model presented in (Lloyd, 1989), was complemented in order to deal with the large roll amplitudes due to roll resonance and to be actively controlled. The fluid flow is modified by the use of a controlled pump, placed at the center of the bottom duct. The fluid motion is governed by a simplified Euler equation, where only the water surface level in each of the tank vertical reservoirs is taken into account. The results of the

system were tested against a nonlinear coupled three degrees of freedom model of a 4400 TEU containership described in (C.A. Rodríguez et al., 2007). Although just one sea condition is presented, the roll motions obtained with the active tank are compared against the ones obtained with a passive tank and with no stabilization, showing a better performance of the active stabilizer compared to that of the passive one, at least for the presented sea state. Moreover, in (Holden et al., 2011) two nonlinear models of U- tanks, applicable to large roll angles (and so to the possible stabilization of parametric rolling), are presented.

Talking about other active stabilizing systems applied to parametric roll resonance conditions, fin stabilizers and rudder roll stabilization should be studied.

In the field of fin stabilizers, (R. Galeazzi,Blanke, 2007) studied the ability of fin stabilizers controlled by a roll rate feedback controller to reduce parametric roll resonance amplitude. Only one sea condition (head seas, regular waves) was evaluated, using a 4 d.o,f. nonlinear containership model; the performance of the system depending on the roll angle at which the system was activated was studied. The results showed that the stabilizer was able to damp roll resonance relatively quickly if activated when roll amplitude was increasing; however, if it was activated when roll resonance was completely developed, the time to reduce the roll motions considerably increased.

In (R. Galeazzi, Holden, C., Blanke, M., Fossen, T. I., 2009), the same author studied the use of fin stabilizers to prevent parametric roll resonance, as an isolated system or together with a speed control system that would be later revisited in this work. In this paper, the performance of a pair of nonlinearly backstepped controlled fin stabilizers is tested, using the aforementioned 3 d.o.f mathematical model of a containership (C.A. Rodríguez et al., 2007), in head

regular waves. Again, only one sailing condition is presented, and fin stabilizers were not able, by themselves, to prevent parametric roll resonance, as only small amplitude reductions were obtained.

However, the effect of fin stabilizers not only depends on the controller, as their capacity for reducing roll motions is proportional to the generated stabilizing forces, that are also dependant of fin surface and ship forward speed. Although a brief analysis of ship forward speed influence in fin performance is included in this work, further work is still needed to deeply study the influence of both speed and fin size in parametric roll stabilization.

2.4.3.3 Speed/Heading Control

As described in the introductory section, parametric roll resonance appears when some conditions are met at the same time. One of these conditions is that the ratio between encounter frequency and ship natural roll frequency should be around 2. As it also has been described, one of the methods for trying to prevent roll resonance is de-tuning this ratio, that is, modifying encounter frequency (as natural roll frequency could be considered a constant value) in order to place the ship outside the risk area.

Taking into account that encounter frequency depends on wave frequency, ship speed, and incidence wave angle, and that it is not possible to act on wave parameters, the only strategy to modify encounter frequency is controlling ship speed and heading.

Although this strategy is the one recommended on IMO guidelines and is the one used by the first generation warning systems presented in the previous section (as polar diagrams are based on studying the mentioned frequency ratio), not many research could be found about the performance of an automatic

system which objective is to prevent parametric roll resonance by acting on ship speed and heading.

The most active research groups about this topic are those of NTNU Centre for Ships and Ocean Structures (CeSOS) of Trondheim, Norway, lead by Professor Fossen, and DTU Department of Electrical Engineering, lead by Professor Blanke. Among their related references, (D. Breu, Fossen, T. I, 2010), (R. Galeazzi, Holden, C., Blanke, M., Fossen, T. I., 2009), (van Laarhoven, 2009) and (D. A. Breu,Fossen, 2011) could be mentioned. Moreover, in (T. I. Fossen, Nijmeijer, H., 2012), their latest research in this field could be found.

In (R. Galeazzi, Holden, C., Blanke, M., Fossen, T. I., 2009), the authors study the feasibility of preventing roll resonance by using a combination of fin stabilizers and speed control, although both contributions are also separately considered. For developing the speed controller, a nonlinear coupled surge – roll model and Lyapunov stability theory are applied; this controller is just designed to maintain a constant speed while the ship sails in head seas; the variations on forward speed have to be externally defined, as the system is not autonomous for computing the value of the speed change that would detune the frequency ratio. Although just one sailing condition is evaluated, some interesting results are presented. The only case that considers speed control on its own, evaluates the influence of a speed reduction in the development of parametric resonance. In the presented case, the speed reduction only leads to a slight reduction of roll amplitude. The other two cases include also an active fin stabilizer, while an increasing and decreasing of forward speed is done. Although in both cases the whole system is able to stabilize roll resonance, it was concluded that the increase of forward speed, mainly due to the correspondent rise in the performance of the fin stabilizer, is more effective.

A similar approach is the one considered by (van Laarhoven, 2009). A simple speed controller is used to test the influence that a increasing or decreasing on forward speed has on the behavior of a ship sailing in fully developed parametric rolling. The author concludes that although reductions in speed always lead to a reduction in roll angle, increasing speed not always did so, even considering that the new set up speed implied a detuned condition of frequency ratios. However, again no automatic control was considered.

Lately, the work by (D. Breu, Fossen, T. I, 2010), deals with some of those missing topics, such us the automatic speed and heading control. In this work, an extreme seeking adaptive control method is used to design a speed and heading control system, that, once parametric roll resonance has started, acts on these two parameters such as to modify encounter frequency, de-tune the frequency ratio and prevent the development of large roll angles. This strategy is tested with a nonlinear mathematical model of a containership, used for obtaining ship roll, surge and yaw motions, in head seas and regular waves. The results obtained for the only condition presented are quite good, presenting a quick reduction of roll amplitude once the control system starts to work. In (D. A. Breu,Fossen, 2011), some modifications to the previous approach, by applying adaptive control, are also described.

Although within the presented works a good approach to the problem has been done, there still are some important issues to be analyzed. Some more testing is needed to evaluate the performance of these systems in more realistic seaways. Both tests in irregular seas and in other sea conditions in regular seas (different frequencies and wave amplitudes) would be necessary to accurately evaluate their performance.

In addition, one consideration should be taken into account while designing speed controllers. While sailing in head seas, especially in bad weather, ships motion lead to violent bow slamming that could lead to severe structural and cargo damage. Taking into account that the intensity of bow slamming is very dependent on the ship hull forms, size, etc., it would be necessary to include this parameter while designing automatic speed controllers, especially when considering that, in order to de-tune the frequency ratio, either an increase or a decrease of ship speed could be adopted.

3 PARAMETRIC ROLL STABILITY ANALYSIS

3.1 Introduction

As has been previously described, when the ship is sailing the risk of parametric roll resonance may rise up. This risk is created by the simultaneous appearance of various factors, both from the ship and the environment, that create the suitable conditions for parametric roll to develop. Among these factors, and as previously described, it could be found wave height, wave frequency, ship speed, heading and loading condition, all together with a specific type of hull forms.

In order to take preventive strategies to avoid the development of parametric roll without unnecessarily altering ship normal sailing parameters, two main steps should be taken. On one hand, it is necessary to determine if the ship is sailing into a risk area, which will depend on the environmental conditions and on the operational situation of the vessel. And on the other hand, it is necessary to know the vessel response under given set of conditions, once it has entered a risky area. This knowledge is also of paramount importance for determining which preventive measures will be optimal for taking the ship out of this risk situation, ensuring its safety with a minimal disturbance to its normal operation.

The study of the ship dynamical behaviour under the conditions where parametric roll resonance is more likely to take place, is what has been called in this work “Parametric Roll Stability Analysis”. On it, the ship roll motion

response in longitudinal head seas has been studied to characterize the influence of parametric roll resonance on its operation.

As have been previously described, parametric roll resonance usually affects large ships as containerships, Ro-Ro´s or cruise vessel, where documented resonance episodes are included among this work references. However, fishing vessels are also known to be prone to parametric roll and although no real cases have been reported to date, many research works have shown this possibility.

In Spain, fishing activity has a major importance. It represents a contribution of 0.2% of the Spanish Gross Domestic Product and employs about 70.000 people, having a distinctly regional character, with GDP contributions in highly dependent zones of up to the 15%. Although the number of workers is relatively small, is one of the sectors with more industrial accidents. The same happens in other countries, like Great Britain or the USA. And most of these accidents, are related to stability issues, especially in small-medium sized vessels (Míguez González et al., 2012).

Taking into account the aforementioned facts and considering that due to their usually low stability and incorrect operation a parametric roll event affecting one of these ships may be fatal, it has been decided to focus this study into this type of ships. Moreover, this work runs in parallel to the development of a fishing vessel stability guidance system in which the author is also involved (Míguez González et al., 2012).

In this section, the parametric roll stability analysis of two small-medium sized fishing vessels has been carried out, applying the same methodology in both studies.

The first analyzed case is that of a medium size stern trawler, that could be a clear representative of the current Spanish fleet fishing at the Great Sole bank.

From now on, this vessel will be designated as “Spanish Trawler”. This ship is the same that has been studied by (de Juana Gamo et al., 2005), work that has been already presented in Section 2.3.2.4.

The second case is another medium size trawler, with the typical design of the 80´s British fleet, very similar to current Dutch beam trawlers and that has already been broadly studied by many authors (Míguez González, López Peña, Díaz Casás, Galeazzi, et al., 2011; Pérez Meza,Sanguinetti, 2006; Spanos,Papanikolaou, 2005) and specially by M.A.S. Neves (M. A. S. Neves et al., 1999), as such a ship has been involved in an stability related incident described in Section 2.3.2.4. In the following sections, we will refer to this vessel as “UK Trawler”.

In both cases, the objective of this section was to analyze the conditions in which parametric roll resonance is more probable, the corresponding severity of the phenomenon and to analyze the contribution of the different parameters involved, in order to establish the optimum corrective actions that could be taken in each case.

The applied methodology has been very similar in the two cases. The first step has consisted in carrying out a series of towing tank tests in head seas in parametric roll resonance conditions, for a broad set of combinations of the different parameters involved in the phenomenon, i.e. wave characteristics, ship speed and loading condition, etc. Scale model tests are the most accurate way of obtaining realistic data of the behaviour of a given ship in a seaway. However, they´re expensive and time consuming and so their extension is limited. The results obtained from the towing tank tests have been used for determining the relationship among the different parameters involved in the development of parametric rolling for a realistic scenario, including regular and irregular waves.

Considering the limitations of scale model tests in order to carry out an extensive analysis or a detailed evaluation of the risk of the ship under a given set of conditions that had not been tested in the towing tank, it has been necessary to consider mathematical models of ship motion.

Such tools, capable of simulating the parametric roll phenomenon, have been set up for each vessel. These models have been used for obtaining the ship motions in head regular waves, as will be later described in this section. The mathematical model approach is the simplest, cheapest and more extensive tool available for evaluating the phenomenon of roll resonance, as the number of conditions that could be evaluated is much larger than carrying out towing tank tests. Moreover, these models may be implemented in onboard guidance systems, that could provide the crews with information about the risk of roll resonance in a real scenario. The validation process of the results obtained by the model has been done by using the data obtained from the scale model tests.

Apart from being used for determining the limits of stability of the two vessels, the roll motion data obtained in this section (from both the mathematical models and the towing basin experiments), will also be used in this work to test the performance of the parametric roll prediction schemes developed in Chapter 4.

3.2 Spanish Trawler

3.2.1 Description

The ship selected for this first analysis is a typical Spanish trawler, representative of the large Spanish fleet fishing at the Southern Ireland banks of the Great Sole. These ships are stern ramp trawlers, usually two decked and with the bridge placed in the forward part of the ship, immediately afterwards the forecastle deck.

They´re medium sized vessels, with an average overall length of 35 meters, a breadth of around 8 meters and an average tonnage of about 350 GT (Miguez González et al., 2008).

In order to maximize hold capacity, their hull forms are quite full amidships; bow hull forms are usually flared (including bulbous bows in many occasions), although in a much more reduced manner as containerships or PCTC´s, while transom sterns are normally present.

Stability levels are regulated by IMO Torremolinos Protocol, including the following minimum values:

Table 3.1. Minimum stability requirements for Spanish fishing vessels larger than 24 m length.

Minimum initial metacentric height (GM_T)	0.350 m
Minimum GZ at a heeling angle of 30 º or more	0.200 m
Minimum heel angle corresponding to maximum GZ	25 degrees
Minimum area under GZ curve between 0º and 30º	0.055 m.rad
Minimum area under GZ curve between 0º and 40º or flooding angle	0.090 m.rad
Minimum area under GZ curve between 30º and 40º or flooding angle	0.030 m.rad

These type of ships usually present a lack of static stability, due to its arrangement and weight distribution (traditionally with large superstructures and heavy fishing equipment placed quite high).In order to satisfy these criteria, ships are usually fitted with a box keel, that filled with concrete or steel scrap, runs entirely from the bow to the rudder toe. This low weight reduces the

vertical position of the centre of gravity of the ship, increasing its stability levels (GM_T, maximum GZ and positive GZ range).

As have been described in Section 2.3.2.4, no cases of parametric resonance on these kind of vessels have been reported to date, although many incidents involving capsizing in waves and sinking are known. The most frequent causes are loss of stability in stern seas or loss of watertight integrity and flooding due to bad operation (Míguez González et al., 2012), but cases involving parametric roll may have been hidden due to the fact that crews usually don´t know the phenomenon, its causes or consequences and are not able to distinguish it from another dynamical issues.

The ship under analysis in this work has been previously studied in head regular seas by (de Juana Gamo et al., 2005), demonstrating that these type of hull forms are very prone to developing parametric rolling.

The ship´s general arrangement, hull forms and main dimensions and characteristics are shown in the following figures:

Table 3.2. Spanish trawler main characteristics.

Overall Length	34.50 m
Length Between Perpendiculars	29.00 m
Breadth	8.00 m
Depth to Main Deck	3.65 m
Depth to Upper Deck	5.80 m
Design Draught	3.60 m
Design Displacement	514.0 t
Gross Tonnage	332 GT

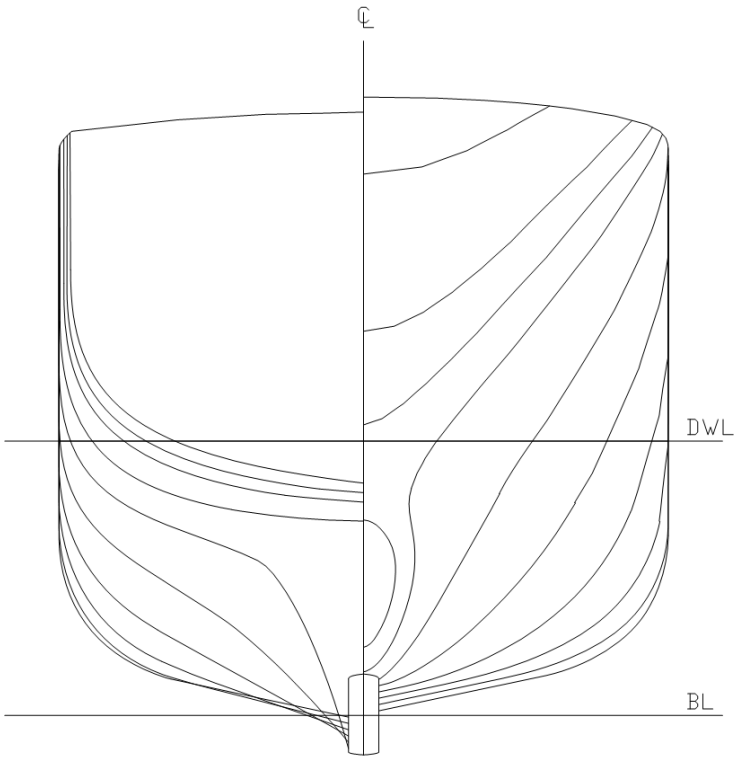

Figure 3.1. Spanish trawler hull forms.

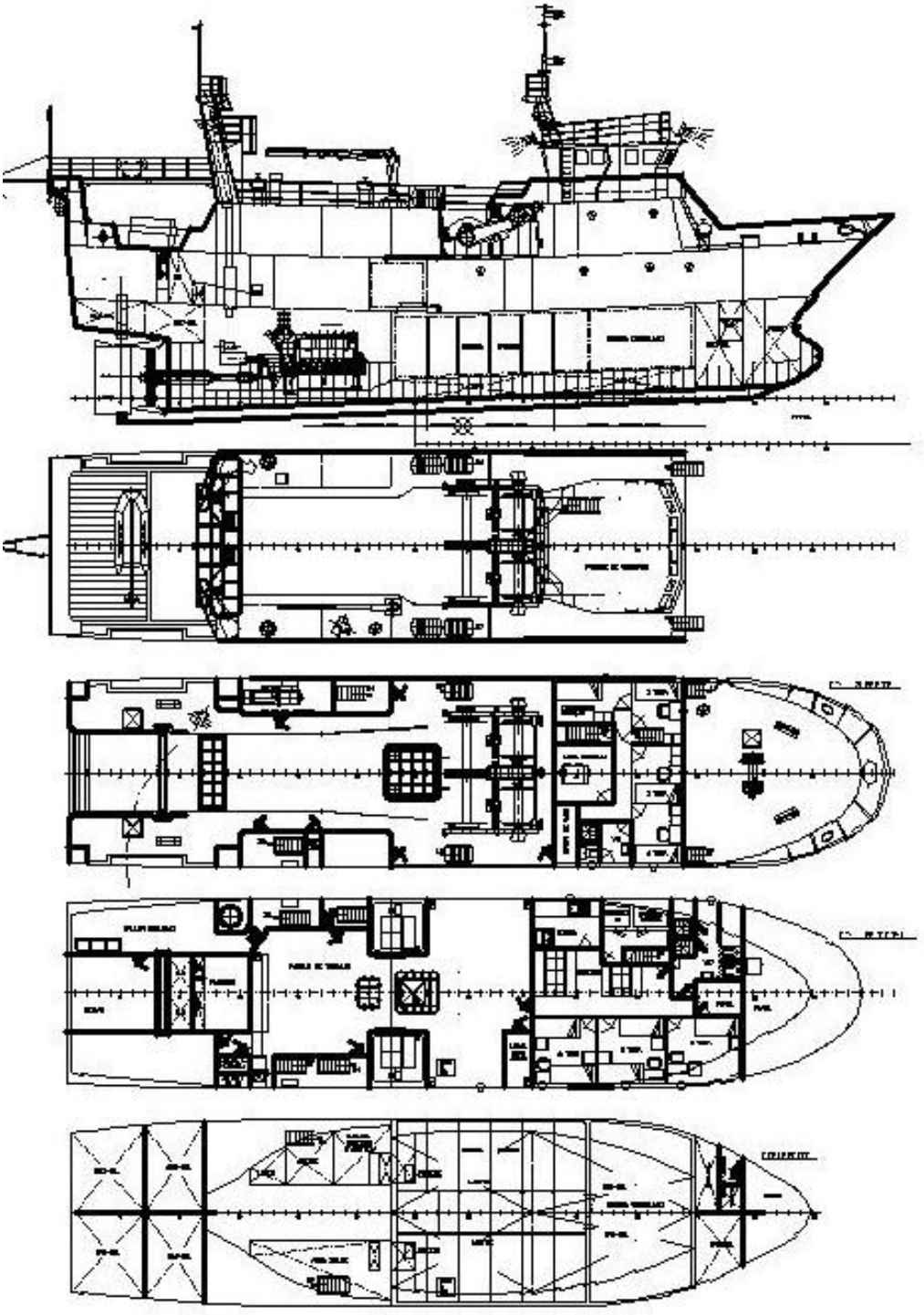

Figure 3.2. Spanish trawler general arrangement.

3.2.2 Towing Tank Tests

The first approximation to the analysis of roll resonance of the Spanish Trawler includes an extensive towing tank test campaign of a 1/18.75th scale model of the ship.

Along these tests, the ship was tested against regular head waves of different frequency and amplitude and also in irregular seas, generated according different wave energy spectra, in both cases at different ship forward speeds.

In addition to these experiments, roll decay tests at the different forward speeds have also been carried out, together with a stability test in order to check that the loading condition and static stability parameters are set up correctly.

3.2.2.1 Experimental Arrangement

The aforementioned scale model tests have been carried out in the test basin of the Escuela Técnica Superior de Ingenieros Navales of the Polytechnic University of Madrid. This towing tank is 100 meters long, 3.8 meters wide and 2.2 meters deep. It is equipped with a screen type wave generator, directed by an AwaSys[1] wave generation program, capable of generating longitudinal regular and irregular waves according to a broad set of parameters and spectra. The basin is also equipped with a towing carriage able to develop a speed of up to 4.5 m/s (see Figure 3.3 and Figure 3.4).

The scale model is a wooden one with adjustable weights; roll and pitch angles, together with lateral and vertical accelerations at three different locations have been measured at a 50 Hz frequency through three onboard mounted accelerometers. Wave elevation has also been measured, using a carriage mounted wave probe which registers wave elevation at a distance of 3.90 meters ahead of the ship forward perpendicular.

[1] http://www.hydrosoft.civil.aau.dk/AwaSys/

Figure 3.3. ETSIN test basin.

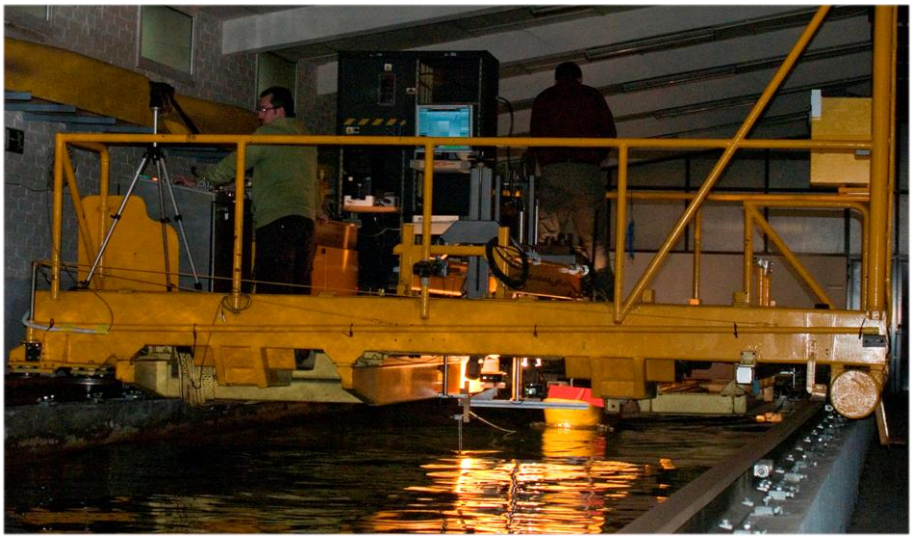

Figure 3.4. ETSIN towing carriage during tests.

Taking into account that surge, sway and yaw influence in the development of parametric roll resonance may be neglected compared to that of heave, roll and pitch (M.A.S. Neves,Rodríguez, 2006), the model restraining devices were fitted to try to limit the first three motions to the minimum possible (although this assumption will be later revisited).

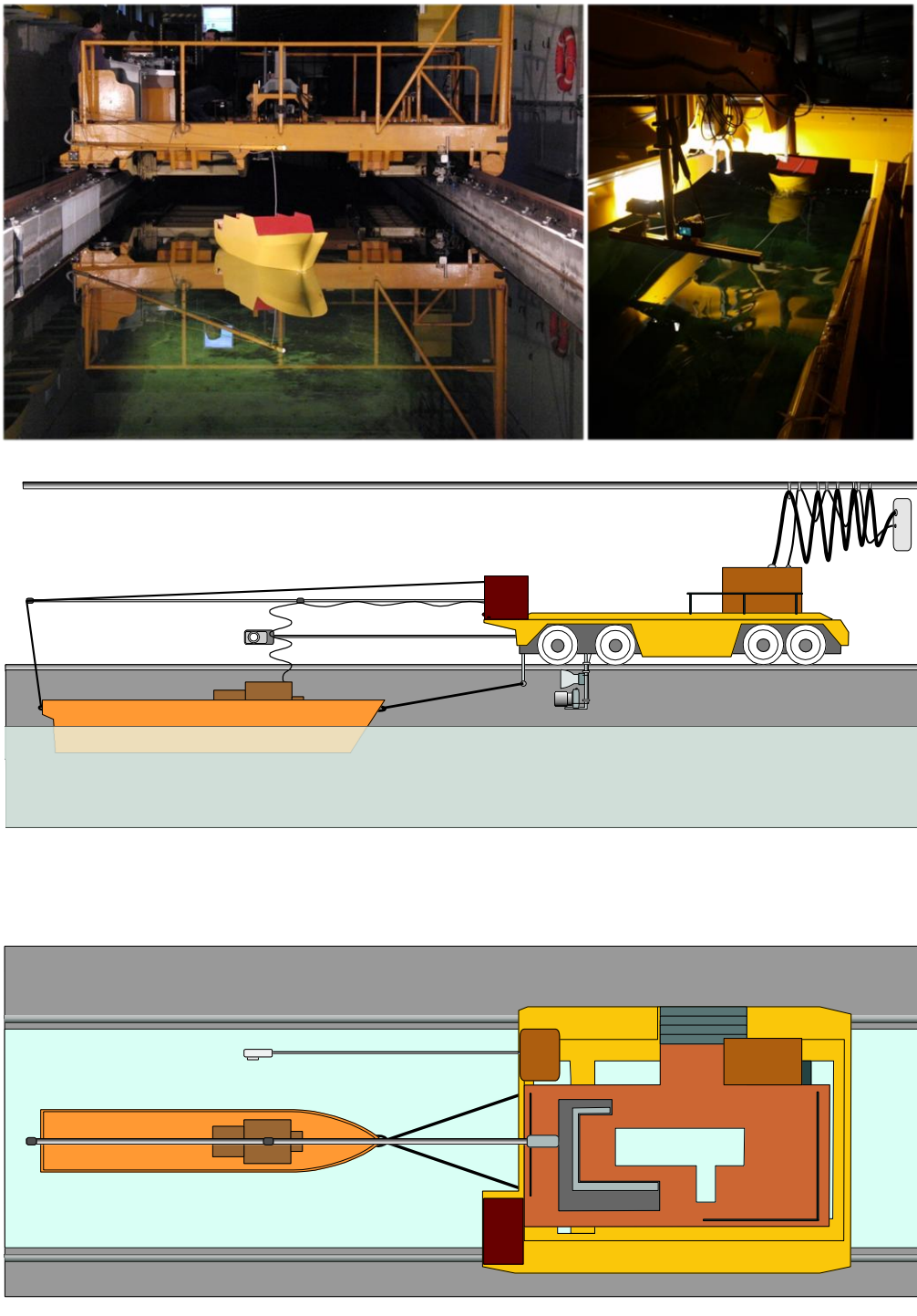

Figure 3.5. Model arrangement. Zero speed (model at rest) (Up-left) and forward speed (Up-right and center-down).

These restraining devices consisted in two semi elastic ropes fixed to an articulation in the bow, at waterline level, while another one was fitted at the same level of the stern.

While carrying out the experiments at zero speed, the forward ropes were fastened to the sides of the basin, forming an isosceles triangle, while the stern one was fastened to the towing carriage, situated immediately after the model.

In the case of the forward speed experiments, bow ropes were fastened to the carriage, while the stern one was holding from a beam extending after the carriage from its rear part (see Figure 3.5).

Regarding the roll decay tests, in the cases with forward speed, the arrangement of the model was the same as the one used for the parametric roll tests with forward speed. When the desired speed was reached, under no waves, the ship was displaced from its equilibrium position and then released, trying not to induce any initial angular speed. For developing the roll decay tests at zero speed, the model was placed complete free in the middle of the basin, in a transverse position related to the tank walls, with the objective of avoiding wall interference in the roll motion.

Finally, static stability tests and longitudinal mass moment of inertia measurements were carried out following the well known methodology of weight displacement and corresponding roll angle measurement and the use of an inertia board respectively.

3.2.2.2 Experiment Development

The main objective of the tests was to study the development of the parametric roll resonance phenomenon under different sailing situations, from the simplest

to more realistic ones, including the analysis of the influence of forward speed and wave parameters on the intensity of the phenomenon.

The test campaign was divided in two. On one hand, the ship has been tested in longitudinal small steepness waves (that could be modeled by linear Airy theory), for different values of encounter frequency-natural roll frequency ratio, wave amplitude and forward speed. The main objective of this first part was to determine the influence of encounter frequency/natural roll frequency ratios, forward speed and wave amplitude on the severity of rolling motions.

On the other hand, the model has also been tested under irregular waves conditions. This is a more realistic case, as usually these are the waves that the ship could be facing during a real case navigation. Moreover, these tests would provide us with information about the development of parametric rolling in irregular seas, that would be later used for testing the roll forecasting algorithms. In this second half of the campaign, different spectra and their characteristic parameters have been applied to study the ship behaviour for again four forward speeds, in order to analyze how the spectrum parameters affect the development of parametric roll resonance.

In these experimental analysis, only one loading condition has been tested, as the influence of GM in the development of parametric rolling won´t be analyzed in these first test campaign. The details of the selected condition are included in Table 3.3

Table 3.3. Spanish trawler loading conditions parameters

Draught	3.290 m
Trim	0 m
Displacement	448.0 t
KM_T	4.131 m
GM_T	0.350 m
ω_n	0.563 rad/s
Transverse radii of gyration	3.128 m (39 % B)
Longitudinal radii of gyration	9.112 m (31 % L_{pp})

3.2.2.3 Regular Waves

As has been previously described, the main parameter affecting the appearance of parametric roll resonance is the ratio between encounter frequency and natural roll frequency. Theoretically, the most critical value is around 2, but experience has shown that nonlinear resonance is also likely for ratios between 1.9 and 2.2 and even more (Bulian, 2006a; Sadat-Hosseini et al., 2010). Once this condition is satisfied, other parameters are also needed to trigger resonance. Wave amplitude should be over a given threshold and regarding wavelength, the more similar to ship length, the larger the developed roll motions will be.

Moreover, ship speed influence is mainly due to two facts: the variation of roll damping terms, that as have been described, are strongly speed dependant (apart from the fact that it also influences the encounter frequency, and so the tuning

ratio). And the intensity of pitch and heave that, due to coupling, influence roll motion.

Regarding wave parameters, the wave generator followed the Airy linear wave theory for determining the wave profile. Under the deep water assumption, the only parameters on which it depends are wave amplitude and frequency, taking into account that wavelength, under these hypotheses, is dependant of wave frequency.

In order to this supposition to remain valid, the ratio between water depth and wavelength should be approximately greater than 0.50 (Lloyd, 1989). Taking this into account and that the towing tank water depth is 2.2 m, this supposition would remain valid for all wavelengths under 82.5 m (4.4 m in model scale). If tables in Appendix A are observed, it can be seen that most test cases fall within this range. So, the deep water approach will be considered valid for all the experiments.

Under these constraints, for each value of ship speed, the different experiments consisted in generating waves with different combinations of frequency and amplitude.

The proposed test matrix includes, at four different forward speeds, test cases for combinations of frequency ratios between 1.7 and 2.3 and wave heights between 0.5 m and 3.0 m; the complete test set is composed of 24 different combinations for the zero speed case, 16 for Froude 0.1, 15 for 0.2 and 13 for the Froude 0.3 case.

The different combinations of wave height and encounter frequency/ natural roll frequency ratios tested for each forward speed, could be seen in Table 3.4. The full set of wave parameters and the obtained roll dta for each combination are included as Appendix A.

3.2.2.3.1 Limits of stability

One of the main objectives of this study was to determine the areas in which, as a function of wave height and encounter frequency – natural roll frequency ratio and for different forward speeds, parametric roll takes place (limits of stability). From the analysis of these regions, the risk state of the ship at every moment could be determined.

In Figure 3.6, Figure 3.7, Figure 3.8 and Figure 3.9, the obtained results for the four tested forward speeds are presented. On them, the areas on which the vessel roll motion is stable (no resonance takes place) or unstable, could be appreciated and the influence of forward speed on those areas determined

Analyzing these results, it can be seen that the unstable region lower vertex appears to be nearer to the horizontal axis in the zero speed case and the whole area moves upwards as speed increases. This behaviour could be expected from the previously described influence of damping in the stability regions of the Mathieu equation (see Section 2.3.1.4). The unstable area moves upwards as damping is increased, which in our case is due to the effects of the forward speed (that increase roll damping). This fact would mean that for lower speeds, resonance would develop at lower wave heights. However, it can also be appreciated that in the zero speed case, the unstable area is narrower than in the other cases; it extends between frequency ratios of 1.9 and 2.1 (at least for wave heights under 1.5 m), while in the forward speed cases it clearly extends to the right, between ratios of 1.9 and 2.3.

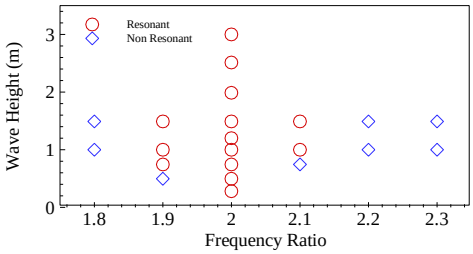

Figure 3.6. Limits of Stability. Fn = 0.

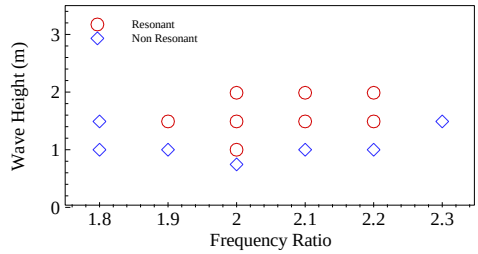

Figure 3.8. Limits of Stability. Fn = 0.2.

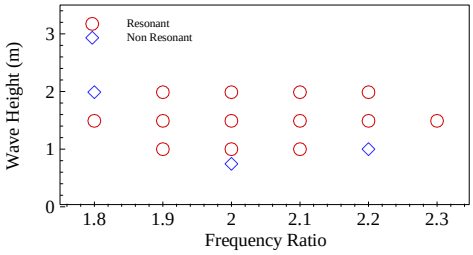

Figure 3.7. Limits of Stability. Fn = 0.1.

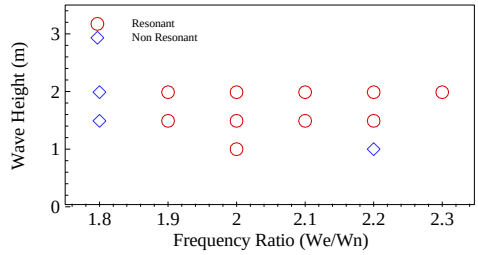

Figure 3.9. Limits of Stability. Fn = 0.3.

This effect has been already described in (M. A. S. Neves,Rodriguez, 2007) for the “UK Trawler” that will also be studied in this work, and is due to the strong coupling between vertical motions (heave and pitch) and roll. This fact implies that for frequency ratios in the vicinity of the unstable area vertex, resonance develops at lower wave heights for lower speeds, but for larger ratios, resonance may develop at smaller wave heights for higher speeds. On the other hand, and once parametric rolling is developing, it was also needed to determine how the different involved parameters influence the amplitude of the generated roll motions. So, and analyzing the results obtained from the towing tank tests, the influence of forward speed, wave height and wave encounter frequency – natural roll frequency ratio on the maximum roll angle on the reached steady state motion, will be studied.

Table 3.4. Regular wave test cases. Tested wave conditions.

Wave Heigth (m)	ω_e/ω_n	Fn 0	Fn 0.1	Fn 0.2	Fn 0.3
0.281	2.00	✓			
0.497	1.90	✓			
	2.00	✓			
0.745	1.90	✓			
	2.00	✓	✓	✓	
	2.10	✓			
1.000	1.70	✓			
	1.80	✓		✓	
	1.90	✓	✓	✓	
	2.00	✓	✓	✓	✓
	2.10	✓	✓	✓	
	2.20	✓	✓	✓	✓
	2.30	✓			
1.200	2.00	✓			
1.491	1.70	✓			
	1.80	✓	✓	✓	✓
	1.90	✓	✓	✓	✓
	2.00	✓	✓	✓	✓
	2.10	✓	✓	✓	✓
	2.20	✓	✓	✓	✓
	2.30	✓	✓	✓	

Wave Heigth (m)	ωe /ωn	Fn 0	Fn 0.1	Fn 0.2	Fn 0.3
1.988	1.80		✓		✓
	1.90		✓		✓
	2.00	✓	✓	✓	✓
	2.10		✓	✓	✓
	2.20		✓	✓	✓
	2.30				✓
2.513	2.00	✓			
3.000	2.00	✓			

3.2.2.3.2 Forward speed and wave height influence

In order to analyze the effects of forward speed and wave height on the amplitude of the roll motion in parametric roll conditions, the value of the maximum reached roll angle depending on the wave height has been plotted for the different forward speeds tested, while the frequency ratio has been kept constant. The obtained results corresponding to four different frequency ratios are presented in Figure 3.10, Figure 3.11, Figure 3.12 and Figure 3.13.

In Figure 3.11 the results for a frequency ratio of 2.0, are presented. From the observation of this figure, it can be concluded that an increase in wave height implies, for all the tested speeds, an increase in the amplitude of the steady state roll motion. Referring to forward speed, it has been observed that at the lowest wave heights, higher speeds imply smaller roll angles, although the difference is not very significant at the smaller Froude numbers. However, at larger wave heights, it has been observed that the increase of speed could lead to an amplification of roll motion, as could be appreciated for the Fn = 0.1 and Fn =

0.2 cases, in which roll amplitude is larger than in the case with no forward speed.

A similar behaviour regarding the influence of wave height could be observed for the frequency ratios of 2.1 and 2.2 (Figure 3.12 and Figure 3.13). In both cases, an increase in the wave height implies an increase in roll amplitude, with the exception of the Fn 0.1 case for the 2.1 ratio condition, in which roll amplitude seems to attenuate for the larger heights. The influence of forward speed for these two ratios seems to be different as frequency ratio is increased.

For a tuning factor of 2.1, an increase in forward speed implies smaller roll amplitudes, with the exception of the zero speed case, which behaves similarly to the previous case and shows smaller amplitudes than Fn = 0.1 and 0.2 conditions. This tendency seems to dramatically change when the tuning ratio is increased to 2.2, where higher speeds imply higher roll angles, especially as wave height is increased.

Finally, and regarding the lowest tuning ratio (1.9), a reduced amplification of the phenomenon with wave height seems to be present for the lowest and highest values of speed (Fn = 0 and Fn = 0.3), where roll amplitude decreases as wave height rises. However, this tendency is not present for Fn = 0.1, which follows the relationship appreciated in the 2.0 tuning ratio case.

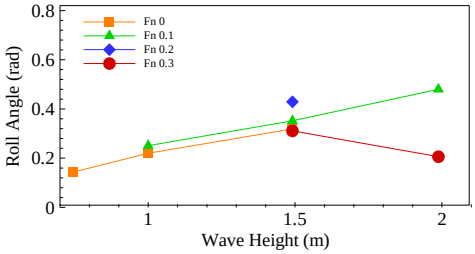

Figure 3.10. Max. Roll Angle. Frequency ratio = 1.9.

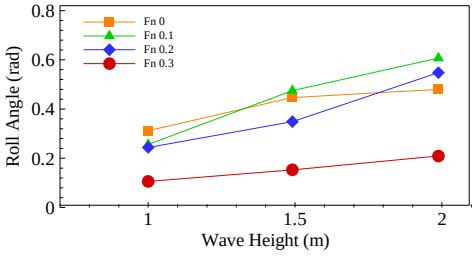

Figure 3.11. Max. Roll Angle. Frequency ratio = 2.0.

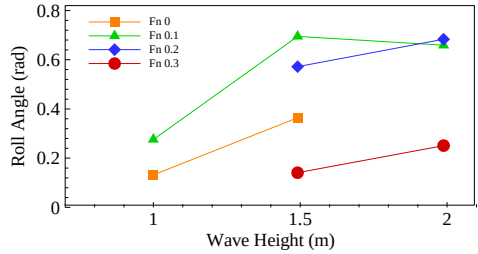

Figure 3.12. Max. Roll Angle. Frequency ratio = 2.1.

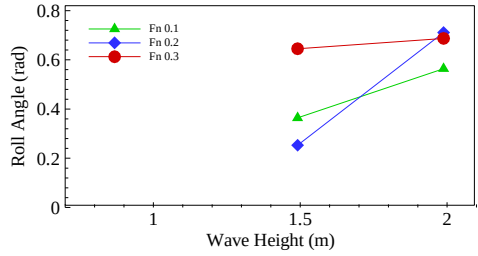

Figure 3.13. Max. Roll Angle. Frequency ratio = 2.2.

3.2.2.3.3 Frequency ratio and wave height influence

In the following figures, the roll amplitude under parametric resonance has been plotted against wave height, but unlike what has been done in the previous analysis, the different tuning ratios are now presented while keeping the forward speed constant, with the objective of determining the influence of the ratio in the amplitude of the roll motions for the different speed values.

In the zero speed condition (Figure 3.14), the largest amplitudes take place at a frequency ratio of 2.0, particularly as wave height increases. This amplification is observed for the other two tuning ratios, although the influence of wave height in roll amplitude seems to be larger for the highest tuning ratio (2.1), as roll angle largely amplifies with wave increase.

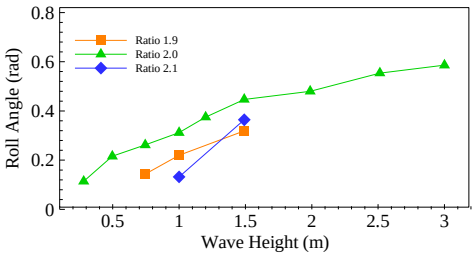

Figure 3.14. Max. Roll Angle. Fn = 0.

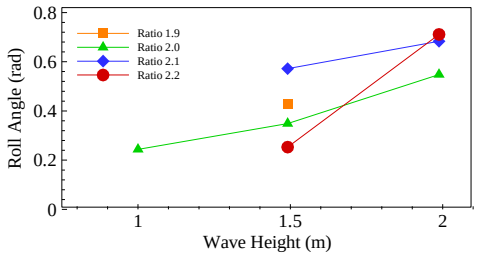

Figure 3.16. Max. Roll Angle. Fn = 0.2.

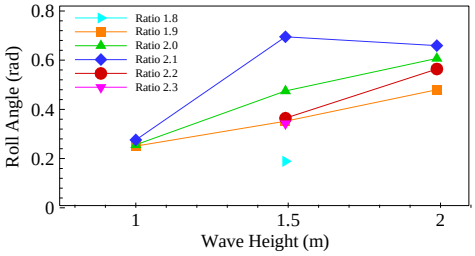

Figure 3.15. Max. Roll Angle. Fn = 0.1.

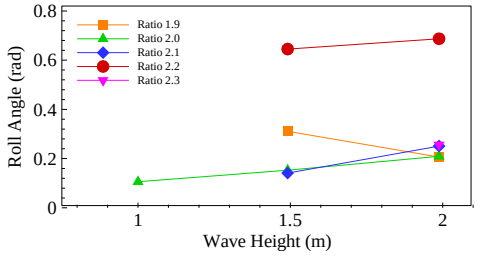

Figure 3.17. Max. Roll Angle. Fn = 0.3.

For a forward speed corresponding to a Froude number of 0.1 (Figure 3.15), roll amplitude does not depend much on frequency tuning for the lowest wave heights.

However, for the intermediate wave heights, this dependence turns out to be very strong, as the largest amplitudes are reached for a tuning ratio of 2.1, fact that is maintained for the largest waves. Moreover, the roll amplification at a tuning factor of 2.2 also increases, while at 2.1 it stabilizes.

The observed behaviour gains importance as forward speed increases. In Figure 3.16 and Figure 3.17, corresponding to Froude numbers 0.2 and 0.3 respectively, it can be observed that the largest roll amplitudes are reached at the highest tuning ratios (up to the limit frequency ratio of 2.3), particularly as wave height increases. In the Froude = 0.2 case (Figure 3.16), the largest roll angles are reached for the 2.1 tuning ratio for the lower wave heights, while for the higher waves, the 2.2 ratio is the most critical situation.

Moreover, a very large amplification of the phenomenon could be observed especially for this ratio as wave height increases. In the last case (Fn = 0.3, Figure 3.17), the described tendency could also be observed, as the largest roll motions correspond to the largest tuning ratio (again up to 2.3, where roll amplitude is smaller) and the biggest amplifications with wave height also correspond to these values (tuning ratios of 2.1 and 2.2).

As could have been seen, the previously described fact of that the theoretical tuning ratio of 2.0 may not be the worse regarding roll amplitude under nonlinear parametric roll, has been illustrated in this section, as larger roll motions were obtained for higher ratios (specially at the higher speeds and wave heights, where motion coupling and nonlinearity becomes more evident).

3.2.2.3.4 Forward speed and frequency ratio influence

If wave height is kept constant, the aforementioned behaviour could be better appreciated. In Figure 3.18, the roll amplitudes for different frequency ratios and forward speeds, corresponding to a wave height of 1.5 m, are presented. As can be seen in this figure, the most critical frequency ratio increases with speed for all speed ranges, and this fact is especially noticeable for the Fn = 0.3 case. Moreover, an amplification of roll motion could also be observed if frequency ratio is diminished, but only for the highest speeds. For the lowest speed values, the behaviour is the opposite, experiencing a smaller amplification as the ratio is reduced.

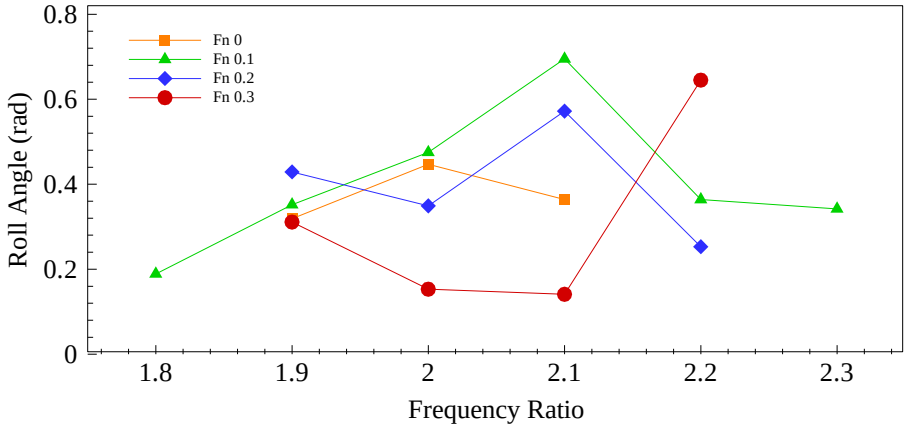

Figure 3.18. Max. Roll Angle. Wave height = 1.5 m.

3.2.2.4 Irregular Waves

In this second step of the towing tank experimental campaign, the scale model has been tested under irregular waves. Again, four different values of the vessel forward speed have been selected, including the zero speed case together with speeds corresponding to Froude numbers 0.1, 0.2 and 0.3.

Irregular seas may be modeled by using different wave spectra (which reproduce the conditions of a given area or type of swell). In our case, the TMA spectrum (Bouws et al., 1985) has been selected for wave generation.

This spectrum is a variation of the very well known Jonswap spectrum, but including a wave depth dependency. It could be applied both for deep and shallow waters, and leads to a wider spectrum when the shallow waters approach is taken.

If $S_J(\omega)$ is the Jonswap spectrum for a given wave frequency ω (described in Section 4.4.2 of this work), the TMA spectrum would be (DNV, 2007):

$$S_{TMA}(\omega) = S_J(\omega) \cdot \Phi(\omega) \tag{41}$$

Where $\Phi(\omega)$ is the depth (d) function, defined as

$$\Phi(\omega) = \frac{\omega^5 \cdot \frac{\partial k}{\partial \omega}}{2 \cdot g^2 \cdot k^3} \tag{42}$$

that taking into account the following dispersion relation

$$\omega^2 = g \cdot k \cdot \tanh(k \cdot d) \tag{43}$$

could be written as

$$\Phi(\omega) = \frac{\cosh^2(k \cdot d)}{\sinh^2(k \cdot d) + \omega^2 \cdot d / g} \tag{44}$$

As well as the Jonswap spectrum, it is characterized by a parameter, the Peak Enhancement Factor (PEF) (also known as Peak Shape Parameter), which determines the sharpness of the spectral peak and that in the North Sea (where data for both spectra was collected) goes from 1 to 7, averaging 3.3. Moreover and as have already been seen, apart from the common spectral characterizing values (peak frequency and significant wave height among others), water depth is also needed for the definition of the TMA spectrum. In addition to the TMA spectrum, a limited number of tests cases, for the zero forward speed case, have also been carried out with the Jonswap spectrum.

As have been done in the first step of the test campaign with regular waves, the objective of this second step is to analyze the influence of the wave parameters that characterize a given sea condition, in the development of parametric roll. Making an analogy with the regular wave case, the parameters that will be considered are the significant wave height, the ratio between the peak encounter frequency and natural roll frequency and the spectrum peak enhancement

factor, unique parameter of the irregular wave case. Moreover, and as aforementioned, different forward speeds have been considered.

In this second part of the test campaign, a total of 81 experiments have been carried out. In these experiments, combinations of significant wave heights from 1 to 2.5 meters, encounter peak frequency – natural roll frequency ratios from 1.9 to 2.3 and peak enhancement factor of 3.5, 5 (only for the Jonswap spectrum) and 7, have been considered.

As have been already said, the vast majority of the tests cases correspond to the TMA spectrum, as only four combinations have been done using the Jonswap one.

All the experiments with forward speed have been carried out at a constant significant wave height (1.490 m). After some preliminary testing, this height was found to be the minimum for stimulating parametric roll in some cases, and the maximum for avoiding too large waves that could damage the model (as maximum wave height may double significant wave height (Faltinsen, 1993)). These data have been used for analyzing the influence of frequency tuning ratio, PEF and forward speed on parametric rolling intensity.

At the zero forward speed case it has been possible to test different wave heights, for a constant tuning ratio of 2.0. These experiments have been used for analyzing the influence of significant wave height on the phenomenon.

Taking into account the randomness of the characteristics of the waves generated under one of the spectra stated above and the limited testing time while dealing with forward speeds, most of the combinations have been tested two or more times, in order to obtain more realizations of time series with the same combination of parameters.

In the case of the zero speed experiments, the test runs have been extended as much as possible before wave reflections affected the model, providing long testing times averaging 30 minutes in model scale (approximately 130 min in real scale). However, the duration of the test runs with forward speed is much shorter. The length of the typical Fn = 0.1 run is 180 s in model scale (13 minutes in full scale), 110 s for Fn = 0.2 (8 minutes in full scale) and 80 s for Fn = 0.3 (5.8 minutes in full scale).

In order to characterize the behavior of roll motion for the different combination of parameters, traditional temporal averaging of the different runs corresponding to the same set of parameters has been done, computing the mean and standard deviation of the roll motion, together with the maximum roll amplitude achieved at each run. On one hand, the maximum roll values indicate the maximum reached amplitude during a parametric roll event occurring during the tests; on the other, an analysis of the mean roll motion together with the standard deviation can be an indicative of the number and intensity of parametric roll events along the run.

Regarding the use of temporal averaging as estimators of roll motion statistics, a brief note has to be done. Their use is correct if ship motions are supposed to be ergodic, which is usually true under the linear seakeeping theory and for analyzing sufficiently long runs. However, large amplitude roll motion, and specially parametric rolling, are known to be highly non linear and the ergodicity assumption may be discussed, leading to unreliable results if temporal averages are used. In (Bulian et al., 2006; Bulian et al., 2008), the issue of non-ergodicity of roll motion together with the reliability of temporal averaging for obtaining the statistical information from a set of experiments is studied in detail. By using both numerical and experimental data sets, large uncertainties in the estimation of roll statistics have been shown, together with

the presence of long transient stages which influence roll motion and largely depend on initial conditions.

From the results shown in the references above, and taking into account the short length of the test runs carried out with forward speed, the results that will be presented in this section will have to be taken with care for quantitative analysis, in especial those corresponding to forward speed tests, where the influence of initial conditions and transients could be larger.

In Table 3.5, all the combinations and the number of runs for each one are presented, and the whole set of combinations and their corresponding results have been included in Appendix A..

3.2.2.4.1 Significant wave height influence

For analyzing the influence of wave height in the amplitude of the reached roll motion, the four TMA spectrum time series corresponding to the tests at zero forward speed, a peak frequency – natural roll frequency ratio of 2, a PEF of 7 and four different values of wave height, have been used.

The achieved values of the average and maximum roll amplitudes in the different test cases are presented on Figure 3.19.

From its analysis, it can be concluded that the effects of an increase in significant wave height in the irregular wave case, are the same as those observed in regular waves regarding roll motion, including the reduced amplification at the largest values of wave height for the maximum roll values. Moreover, it can also be observed that maximum roll amplitudes are very similar (although slightly slower) to those corresponding to the regular wave case of equivalent wave height and ratio (see Figure 3.14).

Table 3.5. Irregular wave test cases. Tested wave conditions.

Spectrum	Significant Wave Heigth (m)	ω_e/ω_n	PEF	Fn 0	Fn 0.1	Fn 0.2	Fn 0.3
TMA	0.993	2.00	7.0	✓			
TMA	1.490	1.90	3.5			✓ (x 4)	
			7.0			✓ (x 2)	
		2.00	3.5		✓ (x 4)	✓ (x 4)	✓ (x 6)
			7.0	✓	✓ (x 5)	✓ (x 6)	✓ (x 8)
		2.10	3.5			✓ (x 4)	✓ (x 4)
			7.0		✓ (x 2)	✓ (x 7)	✓ (x 4)
		2.20	3.5		✓ (x 2)	✓ (x 4)	
			7.0		✓ (x 2)	✓ (x 4)	
		2.30	7.0				
TMA	1.987	2.00	3.5	✓			
			7.0	✓			
TMA	2.437	2.00	7.0	✓			
Jonswap	1.800	2.00	5.0	✓			
Jonswap	1.987	2.00	3.5	✓ (x 3)			

This is due to the fact that those values are achieved during parametric roll events, caused by the most energetic waves in the vicinity of the peak spectrum and with a height similar to the significant one, which could be assimilated to a regular wave of those characteristics.

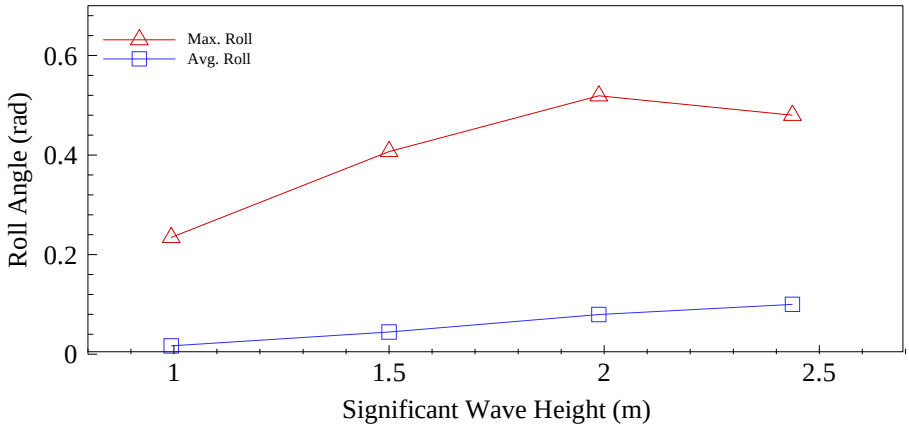

Figure 3.19. Roll Angles. Fn = 0.

3.2.2.4.2 Frequency ratio and PEF influence

In order to study the influence of frequency ratio and peak enhancement factor on the amplitude of parametric roll, the results obtained for the experiments with the TMA spectrum and the three different forward speeds have been considered. These tests consist of a total of 72 runs carried out at an encounter peak frequency – natural roll frequency ratios between 1.9 and 2.2, peak enhancement factors of 3.5 and 7 and a significant wave height of 1.49 meters. The results of the average mean and maximum roll amplitude for each parameter combination are presented in Figure 3.20, Figure 3.21 and Figure 3.22.

From the analysis of the aforementioned graphs, and regarding the effects of the peak enhancement factor, it can be observed that higher PEF values imply both higher average and maximum roll amplitudes. Taking in account that a higher PEF implies a sharper spectrum (and so more energetic waves in the vicinity of the peak frequency) and that roll motion in these experiments is mainly produced by the effects of head waves with frequencies within this narrow band, these results could be expected.

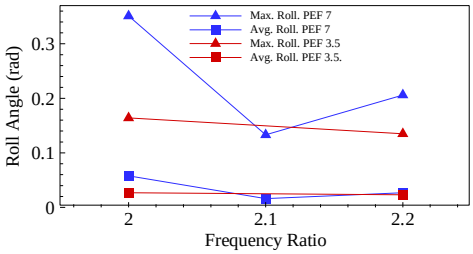

Figure 3.20. Roll Angles. Fn = 0.1.

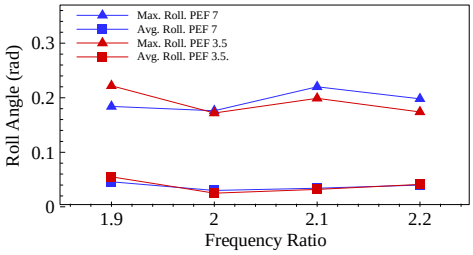

Figure 3.21. Roll Angles. Fn = 0.2.

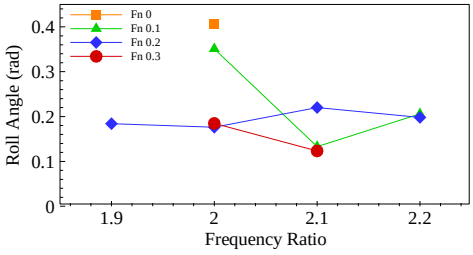

Figure 3.23. Max. Roll Angle. PEF = 7.

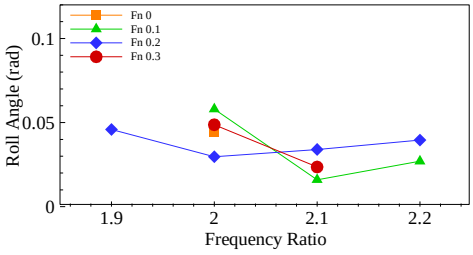

Figure 3.24. Avg. Roll Angle. PEF = 7.

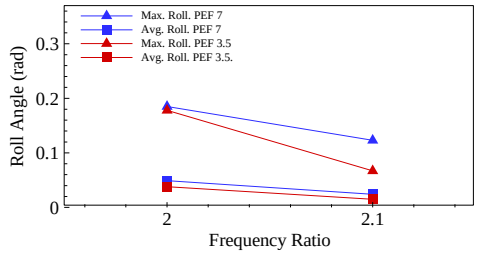

Figure 3.22. Roll Angles. Fn = 0.3.

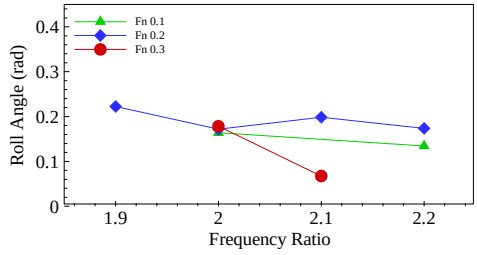

Figure 3.25. Max. Roll Angle. PEF =3.5.

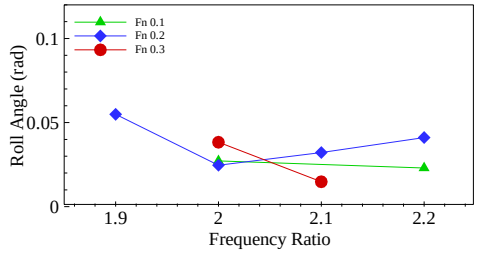

Figure 3.26. Avg. Roll Angle. PEF = 3.5.

Regarding the influence of the tuning ratio, for a Froude number of 0.2, the behaviour is basically the same that has been observed for the regular wave case (see Figure 3.18), where the highest roll values appear at frequency ratios different from the theoretical ratio of 2.0 (2.1 and 1.9). In the highest speed case, the maximum amplitude is reached at a 2.0 ratio, decreasing for the 2.1 case. However, no tests have been carried out for the 2.2 ratio and the amplification experienced in the regular wave case for this value cannot be confirmed in the irregular wave case. In any case, data show the same tendency at the available combinations. Finally, and talking about the Fn = 0.1 tests, the maximum amplitude has moved to the 2.0 ratio, unlike what happened in the regular wave case and more similar to those cases with a higher forward speed. The described behaviour is, in all cases, independent of the peak encounter factor.

3.2.2.4.3 Frequency ratio and forward speed influence

Finally, the influence of forward speed has been analyzed through Figure 3.23, Figure 3.24, Figure 3.25 and Figure 3.26 where, for a given PEF, maximum and average roll angles as a function of frequency ratio and Froude number have been plotted.

From these graphs, it could be appreciated that regarding the maximum roll amplitudes (and so roll episodes during parametric roll), lowers speeds imply larger roll angles (or very similar ones, as could be seen in Figure 3.25 for a PEF of 3.5) at the lowest frequency ratios (2.0 tuning ratio). However, as the ratio is increased, this relationship is modified in a very similar way to what happened in the regular wave case (see Figure 3.18), both for the broader (PEF 3.5, Figure 3.25) and the slender (PEF 7, Figure 3.23) spectra.According to this, an increase in the frequency ratio up to 2.1, implies a decreasing of the maximum amplitude both for the lower (Fn = 0.1) and higher (Fn = 0.3) speeds,

while it increases for the intermediate speed value (Fn = 0.2), which is exactly the same behaviour observed for regular waves.

If the tuning ratio is increased even more, up to 2.2, the regular wave tendency is maintained for the intermediate speed at both PEF values, as roll motion amplification is reduced. In the case of the lower speed, this fact is only true for the broader spectrum, as for the PEF 7 case and Froude number of 0.1, roll amplitude increases again.

As have been already said, no data is available for the highest Froude number of 0.3 and the 2.2 tuning ratio, and so the possible large amplification of parametric roll at high tuning ratios for high speed, that has been appreciated to happen in regular waves, cannot be confirmed for the irregular wave case.

3.2.3 Mathematical Model

The second step in this section has been to set up a mathematical model that could accurately reproduce the phenomenon of parametric roll resonance for the ship under analysis, in the head seas condition and under the effect of regular seas. Such a model will be useful for carrying out extensive analysis, aimed at analyzing the possible tendency of a given ship from the design stage, or even for its use within an onboard guidance system.

In this first case, a model of one degree of freedom has been used. As it has been explained in Chapter 2, parametric roll resonance can be simulated by using a non linear mathematical model where roll motion is computed in an uncoupled way from the other five degrees of freedom of the system. Taking into account that parametric rolling is produced by the variations of the righting moments due to wave passing, it is necessary to include this effect through a time dependant restoring term, which represents the influence of the wave motion and also the effects of heave and pitch motions in the appearance of

parametric rolling. Moreover, the effect of non linearities in the damping and restoring terms should also be considered to accurately reproduce the large amplitude motions that take place during parametric roll.

The proposed one degree of freedom non linear coupled model has the following structure:

$$(I_{xx} + A_{44}) \cdot \ddot{\phi} + B_{44,T}(\dot{\phi}) \cdot \dot{\phi} + C_{44}(\phi, t) = 0 \tag{45}$$

Where I_{xx} and A_{44} are respectively the mass and added mass moments of inertia in roll, $B_{44,T}(\dot{\phi})$ represents the nonlinear damping term and $C_{44}(\phi, t)$ is the time varying nonlinear restoring coefficient. The definition and methods used for determining the different components of the model will be described below.

3.2.3.1 Moment and Added Moment of Inertia

The moment and the added moment of inertia have been obtained by measuring the natural roll frequency from the zero speed roll decay test that will be described in Section 3.2.3.3, and that could be seen in Figure 3.38. Considering that natural roll frequency could be expressed as:

$$\omega_n = \sqrt{\frac{C_4}{I_{xx} + A_{44}}} \tag{46}$$

And that for small roll angles,

$$\omega_n = \sqrt{\frac{\Delta \cdot GM}{I_{xx} + A_{44}}} \tag{47}$$

The value of $I_{xx} + A_{44}$ could be obtained for a frequency equal to that of the roll motion (natural roll frequency), which is the one that will be experienced in parametric rolling.

In order to determine the dry mass moment of inertia in roll I_{xx}, not measured in the scale model, it has been necessary to estimate the value of the added mass term (A_{44}).

It is generally accepted that for the computation of the added mass terms, the results obtained by potential theory methods are accurate enough (M.A.S. Neves,Rodríguez, 2006). In order to obtain the frequency dependant coefficients, the software Amarcon-Office[2] has been used, where the strip theory code Seaway (Journee,Adegeest, 2003) is included, and the effects of roll-sway coupling have also been taken into account.

The obtained added mass in roll (a_{44}), sway (a_{22}) and cross-coupling terms (a_{24} and a_{42}) at the considered draught, for an encounter frequency equal to the natural roll motion of the vessel and for zero forward speed, are shown in figures from Figure 3.27 to Figure 3.30.

Taking into account that these coefficients are computed in a reference frame with its origin in the still water surface, the roll added mass term referred to G A_{44}, should be obtained by transforming these coefficients the following way (Lloyd, 1989):

$$A_{44} = a_{44} + \overline{OG} \cdot a_{42} + \overline{OG} \cdot a_{24} + \overline{OG}^2 \cdot a_{22} \qquad (48)$$

Where $\overline{OG}$ is the distance between mean water level and the vessel centre of gravity.

Once computed the roll added mass, the dry mass inertia could be obtained. In order to check the validity of the results, the obtained dry inertia in roll was

[2] www.amarcon.com

compared to the results from the approximate formula proposed by the ITTC (ITTC, 2008b) or (Krüger,Kluwe, 2008).

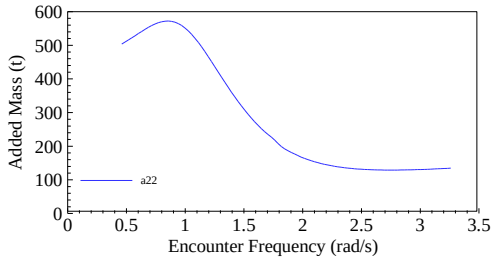

Figure 3.27. Added inertia term a_{22}.
T = 3.30 m. ω_e = 0.563 rad/s. Fn = 0.

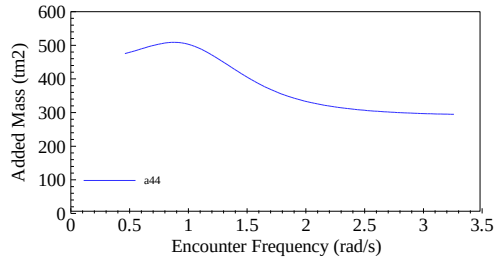

Figure 3.29. Added inertia term a_{44}.
T = 3.30 m. ω_e = 0.563 rad/s. Fn = 0.

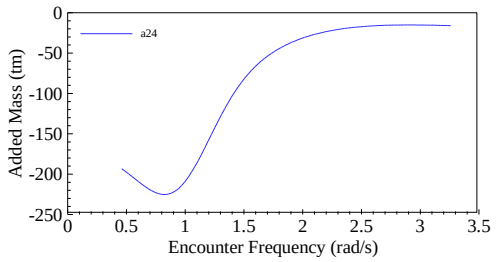

Figure 3.28. Added inertia term a_{24}.
T = 3.30 m. ω_e = 0.563 rad/s. Fn = 0.

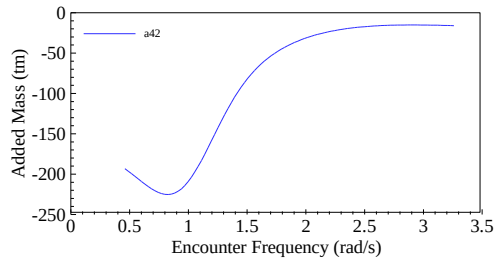

Figure 3.30. Added inertia term a_{42}.
T = 3.30 m. ω_e = 0.563 rad/s. Fn = 0.

According to this, the transverse radii of gyration k_4 is approximately 0.40 times the breadth of the ship, and so:

$$I_{xx} = m \cdot k_4^2 = m \cdot 0.4^2 \cdot B^2 \tag{49}$$

The obtained results presented in Table 3.6, show the adequacy of the added mass term estimation.

Table 3.6. Roll moment and added moment of inertia.

$(I_{xx} + A_{44})_{EXP.}$	4852.86 t m^2
A_{44}	469.26 t m^2
I_{xx}	4383.60 t m^2
k_4	3.128 m
k_4 / B	0.391

3.2.3.2 Restoring Term

As have been described in the Chapter 2, while dealing with small rolling angles, the roll restoring coefficient C_{44} could be supposed to be constant and independent of ship roll angle, leading to a linear restoring term. However, it is well known that when dealing with larger roll angles, transverse stability (and so the restoring coefficient) depends on roll angle, and this dependence is non linear. In fact, the well known transverse curves of stability (GZ curves) are those where, for a given loading condition (and usually in still water), restoring coefficient GZ is related to roll angle.

While trying to model parametric roll resonance, it has been seen that both heave and pitch motions have a clear influence in the appearance of the phenomenon, together with the effects of wave moving along the hull. This fact has lead to the development of the three degrees of freedom models, such as that of (M.A.S. Neves,Rodriguez, 2005), that has been mentioned in the Chapter 2 and that will be later used in this work.

However, and although a more simplified approach wants to be taken in the form of a single degree of freedom roll model, the effects of those motions, together with the effects of wave passing along the hull, should also be included to maximize the accuracy of the proposed structure. This should supersede the "Mathieu equation" approach of considering a sinusoidal variation of the restoring term (that implies parametric excitation due to only wave passing effects along the hull).

In this work, the quasi-static "look up table" approach, described by (Bulian, 2005, 2006a) and required by the ABS Guidelines (ABS, 2004) for modelling the variation of the ship restoring capabilities in longitudinal waves, has been followed.

According to it, and for every wave and loading condition that wants to be analyzed, GZ values as a function of roll angle have been computed following standard hydrostatic computations, where the ship is free to trim and sink, for different positions of the wave crest along the hull.

This approach considers that for each wave crest position and roll angle, trim and sinkage are able to change up to a static stability position, while heave and pitch motions are statically balanced. This approach has been successfully applied at the long encounter frequencies typical of following seas and in wave lengths larger than ship length (where heave and pitch motions are supposed to be quasi-static), but has also proven to be quite accurate for the head wave case that is analyzed in this work (Bulian, 2006a).

For a given loading condition and wave characteristics (frequency, height and wavelength), the procedure for setting up the GZ "look up" table, includes computing the righting lever values for a set of roll angles and different wave

positions along the hull. This leads to a matrix of GZ values as a function of roll angle in a “wave crest position” domain.

The GZ look up table in the “wave crest position” domain, should be transformed into the time domain to be used in the proposed mathematical model. In order to do this, wave crest position as a function of time, should be determined for each time step.

As have been said, regular Airy waves have been considered in this section. According to this theory, wave celerity, as a function of water depth d, could be written as

$$c = \sqrt{\frac{g \cdot \lambda}{2 \cdot \pi} \cdot \tanh\left(\frac{2 \cdot \pi \cdot d}{\lambda} \right)} \tag{50}$$

In the case under analysis, the “deep water” assumption may be used; this consideration is valid when the hyperbolic tangent term of the previous equation is near 1, which occurs approximately when $\frac{d}{\lambda} > 0.50$ (Lloyd, 1989). Under the deep seas assumption, that would be considered true all along this work, wave celerity may then be computed as:

$$c = \sqrt{\frac{g \cdot \lambda}{2 \cdot \pi}} \tag{51}$$

The most important wave parameter in the analysis of parametric resonance is, together with wave amplitude, wave frequency (or encounter frequency, if the ship is moving), both of which are known for every test that is carried out.

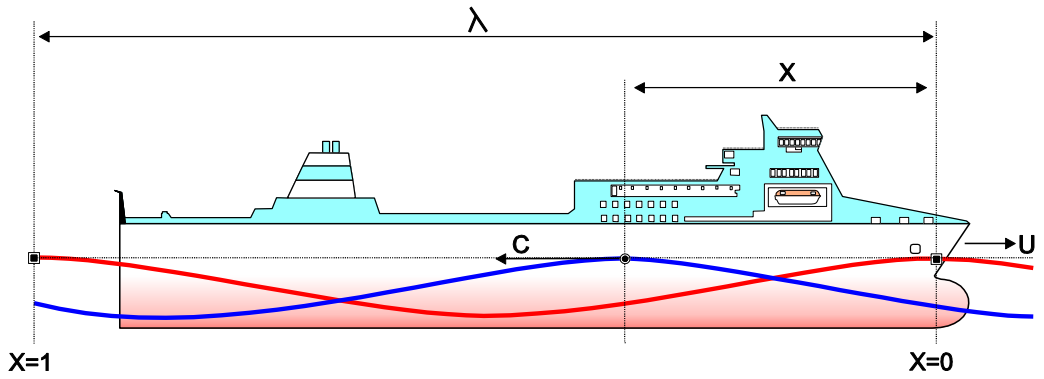

Figure 3.31. Wave position along the hull.

In order to determine the wave position along the ship, it is necessary to know the wave celerity and wavelength, that can be determined by using the previous relationship and the one relating wave period and wavelength $\left(c = \frac{\lambda}{T_w} \right)$.

If the effects of the ship forward speed u and heading are considered, the position of the wave for each time step could be determined by using the encounter period T_e, as will be later described.

Wave position along the hull has been computed in six different offsets related to wavelength, between 0 and 1. For 0 and 1 values, a wave crest is supposed to be in the ship forward perpendicular. Intermediate values represent the different positions of the wave profile along its whole wavelength in this same point. For example, if wavelength equals ship length, an offset value of 0.5 represents two wave crest at both perpendiculars and a through amidships (see Figure 3.31)

The results of some of these GZ computations, corresponding to a wavelength of 40 meters and wave heights of 1, 2 and 3 meters, compared to those of the still water case, are displayed on Figure 3.32 (still water condition), Figure 3.33, Figure 3.34 and Figure 3.35. On Figure 3.36, the interpolated GZ surface for the 2 meters height case and the different wave positions is also presented.

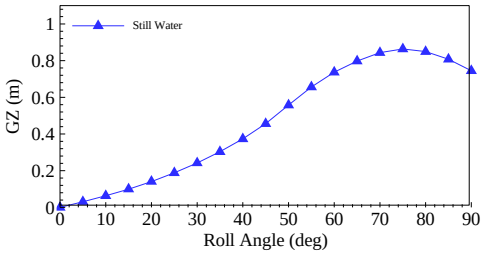

Figure 3.32. GZ curve. λ=40 m. Still water.

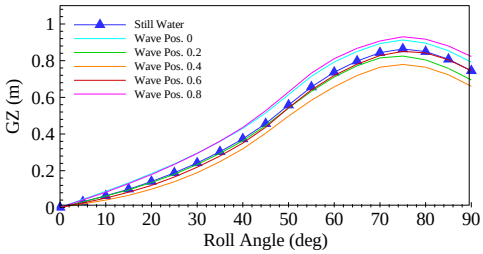

Figure 3.33. GZ curve. λ=40 m. H_w= 1 m.

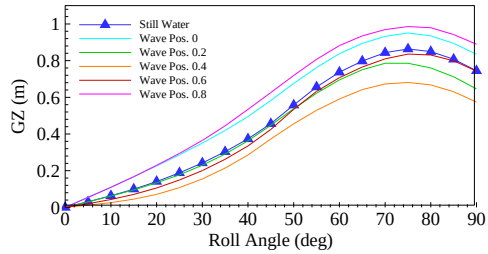

Figure 3.34. GZ curve. λ=40 m. H_w= 2 m.

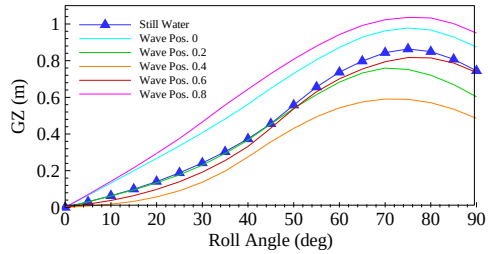

Figure 3.35. GZ curve. λ=40 m. H_w= 3 m.

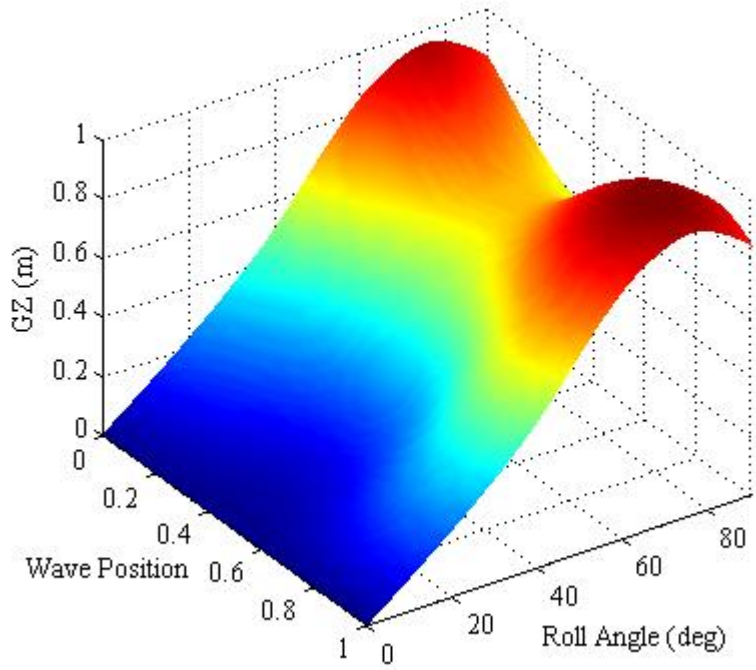

Figure 3.36. GZ variation due to wave passing. λ=40 m. H_w= 2 m.

In the figures above, the variations in righting levers due to wave passing can be appreciated. In the presented condition, wave length is similar to ship length, the worst situtation relating parametric roll development. When wave crest is at the bow or stern (wave position 0), stability levels are maximum related with the still water case, and are minimum when wave crest is amidships (wave position 0.5). As could also be appreciated, this variation increases with wave height, and so the intensity of the phenomenon.

In order to obtain the wave position in the time domain, the time used by the wave to travel its own wavelength, from the point of view of an observer onboard the ship, should be considered. This time is the encounter period T_e.

The relative travelling speed of the wave could be defined as

$$V_R = (c - u \cdot \cos\chi) \tag{52}$$

Where c is wave celerity $\left(c = \sqrt{\frac{g \cdot \lambda}{2 \cdot \pi}} = \frac{g}{\omega_w} \right)$, u is the vessel speed and χ is the angle between incident waves and ship heading (Figure 2.10).

Considering that encounter period could be defined as $T_e = \frac{\lambda}{V_R}$ and that the value of wavelength under the deep water assumption was defined as $\lambda = \frac{2 \cdot \pi \cdot g}{\omega_w^2}$, the value of the encounter period remains:

$$T_e = 2 \cdot \pi \cdot \left(\omega_w - \frac{u \cdot \omega_w^2}{g} \cdot \cos\chi \right)^{-1} \tag{53}$$

which is the inverse of the well known formula of the encounter frequency, already mentioned in this work.

Considering then that from the point of view of an observer onboard the ship, the wave travels a wavelength in an encounter period, the wave position as a function of time (x) may be determined by computing the modulo of t/T_e by 1, so that:

$$\text{Wave position} = \text{mod}\left(\frac{t}{T_e}, 1\right) \tag{54}$$

Finally, the roll restoring term $C_{44}(\phi, t)$ will remain as:

$$C_{44}(\phi, t) = \Delta \cdot GZ(\phi, t) \tag{55}$$

Where $GZ(\phi, t)$ are the time varying and roll angle dependant righting levers, computed as indicated above.

3.2.3.3 Roll Damping

Damping may be considered linear and within the limits of potential theory (and so independent of fluid viscosity), in the motions where wave damping component is very large and dominates over the viscous effects, such us pitch, heave or surge motions. However, the case of roll is different. Wave damping in roll motion for slender bodies is quite low, and so the viscous components become more significant. Viscous roll damping is due to many causes, and skin friction, flow separation, vortex generation or the effects of appendages (such as rudder or bilge keels), have to be taken into account to accurately reproduce the roll motion of a ship (Himeno, 1981). As could be seen, in all these components fluid viscosity is involved and so potential theory approaches are not suitable for the roll case. Moreover, forward speed, roll amplitude and frequency, also have a paramount influence on the roll damping, as is shown, for example, in (Valle Cabezas, 1999).

In addition to this, it is known that for large roll motions, strong nonlinear effects are present in roll damping. This effects are of huge importance while dealing with parametric roll resonance, where a correct modelling of the nonlinearities both in roll damping and restoring terms, is essential to accurately reproduce the phenomenon.

In order to account for these nonlinearities, roll damping has been decomposed in two terms, one linear component, which is supposed to be dominant at small roll angles, and a quadratic one, which is necessary to model the effects of damping at large roll angles. This approach has also been applied by many authors for modelling parametric roll, i.e. (M.A.S. Neves,Rodríguez, 2006), with accurate results. According to this structure, roll damping term would remain as:

$$B_{44,T}(\dot{\phi})\cdot\dot{\phi} = B_{44a}\cdot\dot{\phi} + B_{44b}\cdot\dot{\phi}\cdot\left|\dot{\phi}\right| \tag{56}$$

In order to determine the two damping coefficients (B_{44a}, B_{44b}) in the most accurate way, roll decay tests for different forward speeds have been carried out in still water for the loading condition under analysis. The procedure followed for determining the damping coefficients from these tests is that described in (Bhattacharyya, 1978) or (Himeno, 1981). On it, data of roll decrement ($\Delta\phi$) between consecutive extremes of the roll decay time series, should be plotted against the mean roll angle (ϕ_m), and a quadratic polynomial should be fitted to them, so that:

$$\Delta\phi = K_1\cdot\phi_m + K_2\cdot\phi_m^2 \tag{57}$$

Where K_1 and K_2 are called the extinction coefficients. In order to obtain the damping terms from the extinction coefficients, the expressions found in

(Himeno, 1981) may be used, which were obtained after integrating the equation of roll motion with no excitation over half a roll cycle and considering that the energy dissipated by damping equals the work done by the roll restoring term:

$$K_1 = \frac{\pi}{2} \cdot \frac{\omega_\phi}{\Delta \cdot GM} \cdot B_{44a} = \pi \cdot \nu \tag{58}$$

$$K_2 = \frac{4}{3} \cdot \frac{\omega_\phi^2}{\Delta \cdot GM} \cdot B_{44b} = \frac{4}{3} \cdot \beta \tag{59}$$

Where ω_ϕ is the roll frequency, obtained from the test that is been analyzed and ν and β are respectively the linear and quadratic nondimensional damping coefficients, obtained from combining equations (45) and (56),

$$(I_{xx} + A_{44}) \cdot \ddot{\phi} + B_{44a} \cdot \dot{\phi} + B_{44b} \cdot \dot{\phi} \cdot \left|\dot{\phi}\right| + C_{44}(\phi, t) = 0 \tag{60}$$

dividing all terms by $(I_{xx} + A_{44})$,

$$\ddot{\phi} + \frac{B_{44a}}{(I_{xx} + A_{44})} \cdot \dot{\phi} + \frac{B_{44b}}{(I_{xx} + A_{44})} \cdot \dot{\phi} \cdot \left|\dot{\phi}\right| + \frac{C_{44}(\phi, t)}{(I_{xx} + A_{44})} = 0 \tag{61}$$

and making

$$2 \cdot \nu \cdot \omega_\phi = \frac{B_{44a}}{(I_{xx} + A_{44})} \tag{62}$$

$$\beta = \frac{B_{44b}}{(I_{xx} + A_{44})} \tag{63}$$

As previously mentioned, in the present work roll decay tests have been carried out for different forward speeds. Three runs have been done for the zero speed case, four for the Froude = 0.1 case, three for a Froude of 0.2 and two for 0.3.

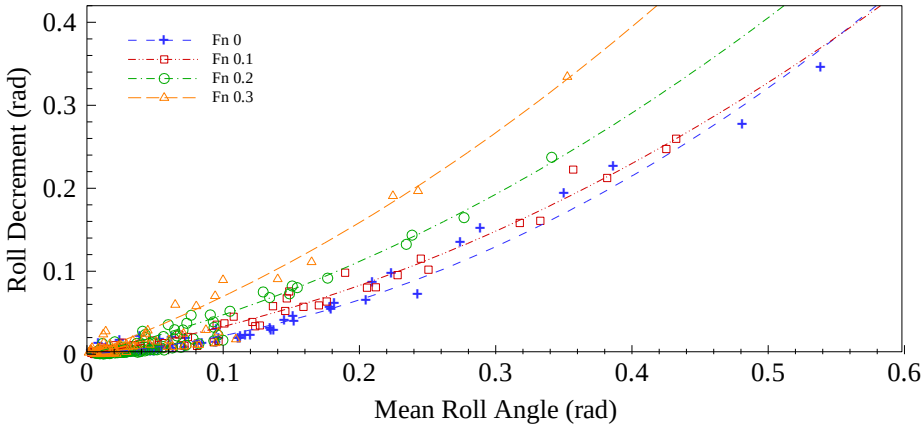

Figure 3.37. Roll decrement data (scatter points) and fitting quadratic polynomial (lines) from roll decay tests.

Damping coefficients have been obtained following the methodology described above, by considering the whole data set obtained from the different tests at the same speed.

In Figure 3.37, the roll decrement data from the roll decay tests for the four forward speeds is shown, together with the quadratic polynomial used for fitting the data and obtaining the extinction coefficients. In Table 3.7 and Table 3.8, the obtained results for the values of the damping coefficients at the four Froude numbers are shown. Moreover, and for the sake of reference, the purely linear damping coefficient, obtained from the linear fitting of the data above, is also included.

The obtained damping data behave as expected in relation with ship forward speed, and as speed rises roll damping also does. It could also be appreciated that this increase is larger for the higher speeds, and becomes smaller as speed decreases. In fact, for the largest values of roll angles, roll damping is almost the same for the lowest speed conditions (zero speed and Fn = 0.1).

Table 3.7. Damping coefficients.

	Damping Coeff.	Fn 0	Fn 0.1	Fn 0.2	Fn 0.3
Quadratic Damping	B_{44a} (t·m^2/s)	99.85	221.62	346.73	498.75
	B_{44b} (t·m^2)	1864.50	1507.2	1640.14	1652.46
Purely Linear Damping	B_{44} (t·m^2/s)	372.04	423.58	510.98	700.13

Table 3.8. Adimensional damping coefficients.

	Damping Coeff.	Fn 0	Fn 0.1	Fn 0.2	Fn 0.3
Quadratic Damping	ν	0.0187	0.0404	0.0620	0.0953
	β	0.3932	0.3008	0.3158	0.3631
Purely Linear Damping	ν_L	0.0697	0.0772	0.0914	0.1338

In order to validate the obtained damping results, the mathematical model has been used for simulating, for each speed value, one of the corresponding roll decay tests carried out in the towing tank, and the results have been compared. As can be appreciated in Figure 3.38, Figure 3.39, Figure 3.40 and Figure 3.41, the time series obtained from the mathematical model accurately track the real roll decay tests, and the results could be considered as correct.

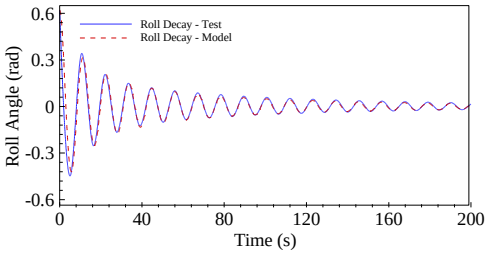

Figure 3.38. Roll decay tests. Fn = 0.

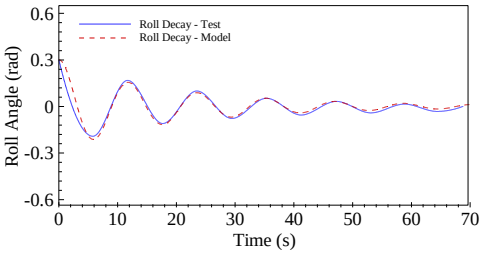

Figure 3.40. Roll decay tests. Fn = 0.2.

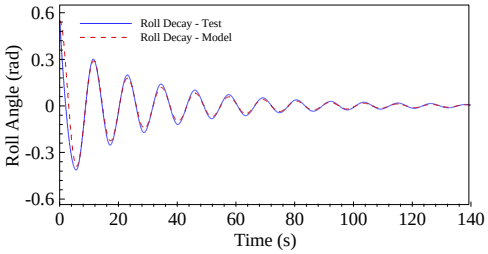

Figure 3.39. Roll decay tests. Fn = 0.1.

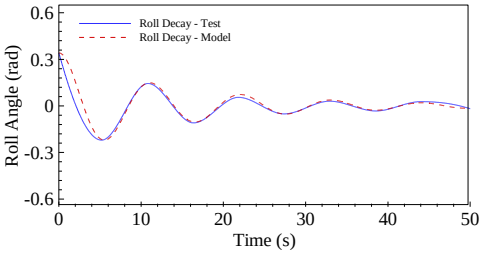

Figure 3.41. Roll decay tests. Fn = 0.3.

3.2.3.4 Model Validation

Once the model has been set up, its behaviour has to be validated, in order to determine if it performs adequately in the different conditions where parametric roll is present and also in those where it is not.

The benchmark data used for the validation have been those described in the previous section, corresponding to the towing tank tests carried out at the ETSIN model basin. Four different values of forward speed and one loading condition (see Table 3.9) have been tested, in head regular waves.

From Figure 3.42 to Figure 3.45, the results obtained with the mathematical model at zero forward speed, a frequency ratio of 2 and wave heights of respectively 0.745 m, 1.000 m, 1.491 m and 1.988 m, are compared to the corresponding results from the towing tank experiments.

Table 3.9. Spanish trawler loading condition parameters.

Draught (m)	3.290
Trim (m)	0
Displacement (t)	448.0
KM_T (m)	4.131
GM (m)	0.350
ω_n (rad/s)	0.563
Transverse radii of gyration (m)	3.128 (39 % B)
Longitudinal radii of gyration (m)	9.112 (31 % Lpp)

Wavelength has been computed following the deep seas assumption, and set to a value of 48.640 m, equivalent to that used in the scale model tests. As can be appreciated, this value is far from the worse possible condition regarding parametric roll, which would be in the vicinity of the ship length (29 m).

Observing the results displayed in the aforementioned figures, it can be concluded that the correspondence between the mathematical model and the real behaviour of the ship for the described conditions is good, as the model accurately tracks the transient phase and steady state motion of the resonant rolling. However, it also has to be mentioned that, in all cases, the mathematical model slightly underestimates the steady state roll amplitude.

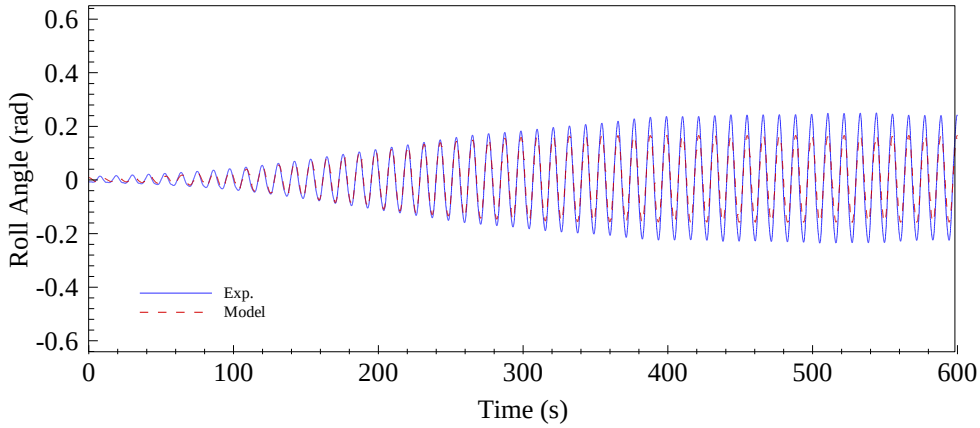

Figure 3.42. Roll data. Fn = 0. Frequency Ratio = 2.0. H_w = 0.75 m. λ = 48.640 m.

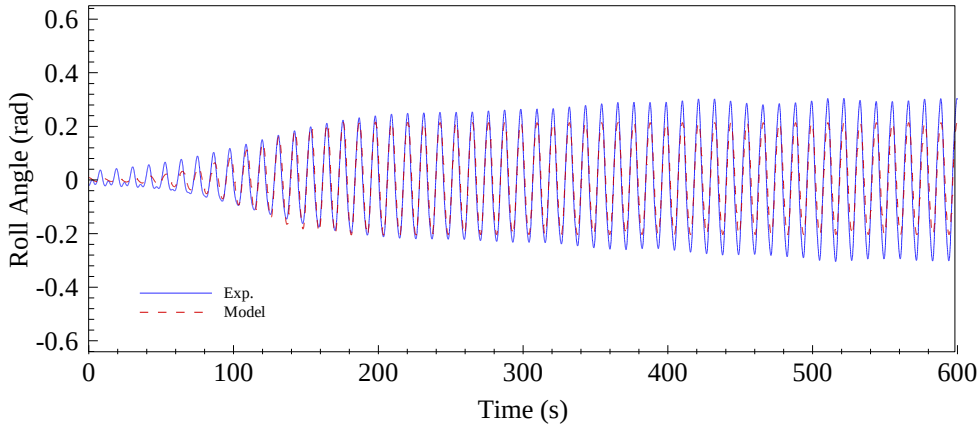

Figure 3.43. Roll data. Fn = 0. Frequency Ratio = 2.0. H_w = 1.00 m. λ = 48.640 m.

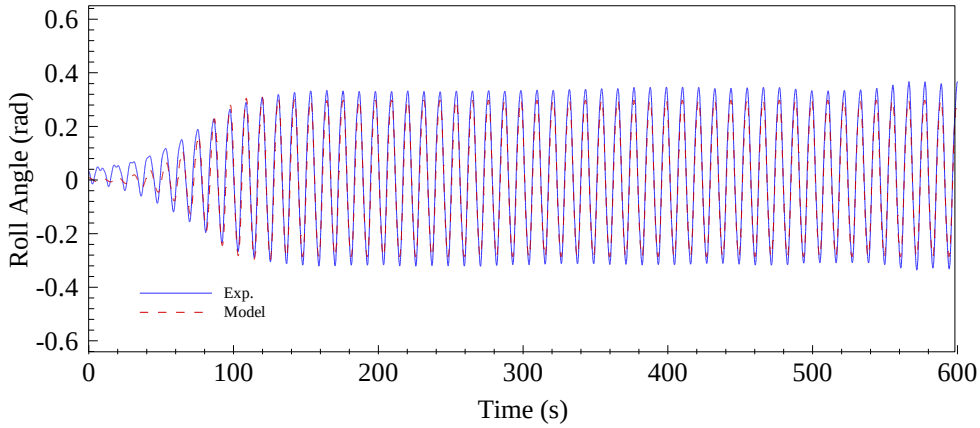

Figure 3.44. Roll data. Fn = 0. Frequency Ratio = 2.0. H_w = 1.491 m. λ = 48.640 m.

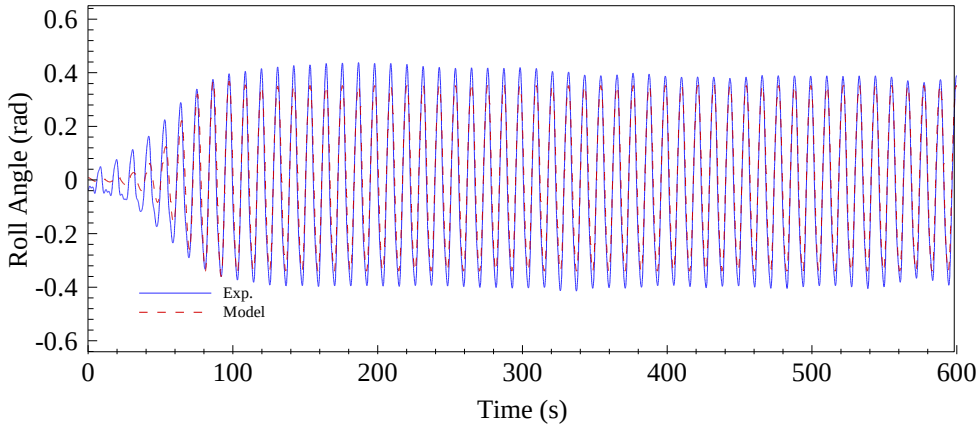

Figure 3.45. Roll data. Fn = 0. Frequency Ratio = 2.0. H_w = 1.988 m. λ = 48.640 m.

In Figure 3.46, Figure 3.47 and Figure 3.48, the mathematical model roll time series obtained for a forward speed equivalent to a Froude number of 0.1, the same frequency ratio of 2 and wave heights of 1.000 m, 1.491 m and 1.988 m, are plotted against the corresponding towing tank results. In this case, as speed has been increased, wave frequency has been reduced to maintain the frequency ratio constant. As a result, wavelength has been increased up to a value of 66.145 m, which is nearly the double of ship length.

As could be appreciated, again and in the three cases, the model performance may be considered as satisfactory. Although due to the forward speed effects and the towing arrangement, which allows certain surge and yaw motions, the vessel response from the towing tank tests looks somewhat irregular, the transient period and the average steady state motion are well reproduced by the mathematical model.

However, it could be also appreciated that, in most cases, the mathematical model is again underestimating the steady state amplitude.

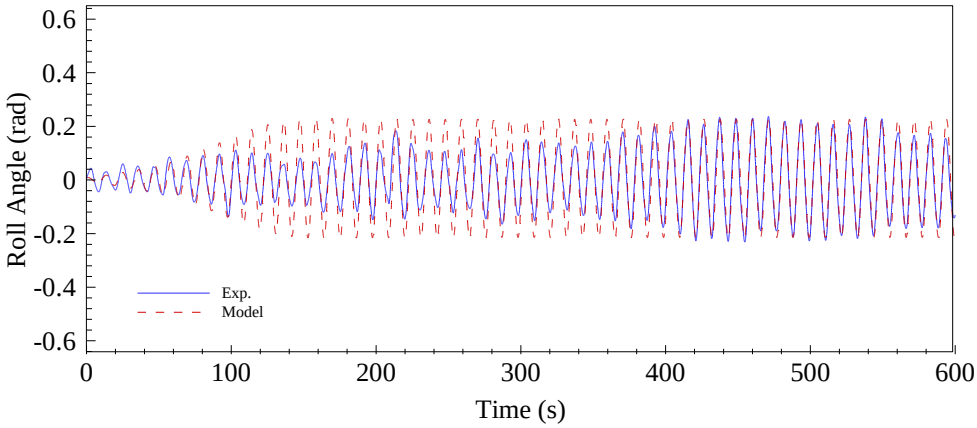

Figure 3.46. Roll data. Fn = 0.1. Frequency Ratio = 2.0. H_w = 1.000 m. λ = 66.145 m.

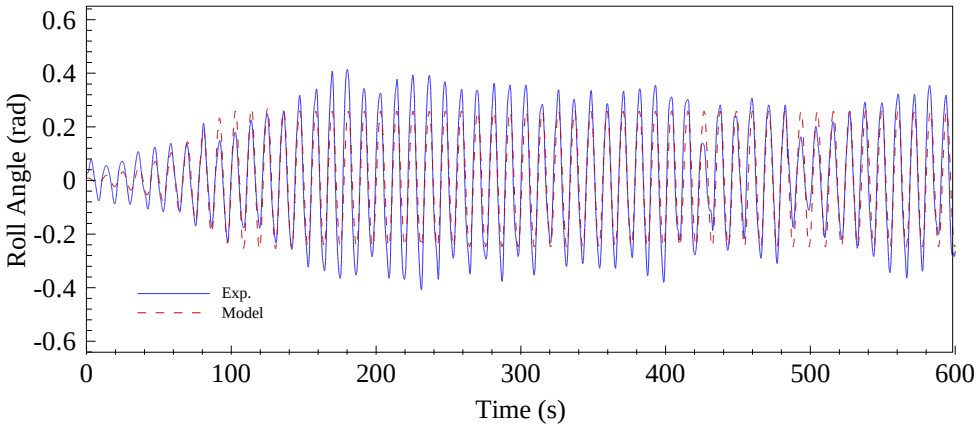

Figure 3.47. Roll data. Fn = 0.1. Frequency Ratio = 2.0. H_w = 1.491 m. λ = 66.145 m.

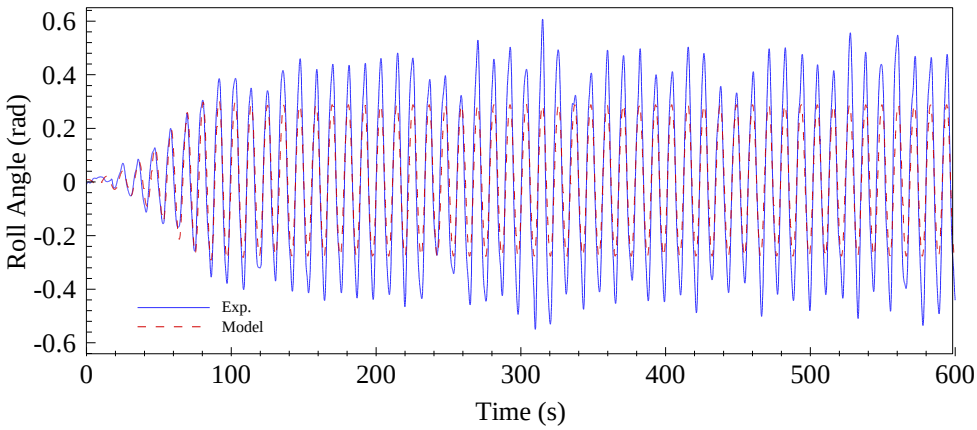

Figure 3.48. Roll data. Fn = 0.1. Frequency Ratio = 2.0. H_w = 1.988 m. λ = 66.145 m.

In the lowest wave height case (Figure 3.46, H_w = 1.000 m), this effect is not appreciated. In fact, the model overestimates the vessel response along a period (approximately between seconds 100 and 350) where resonance does not reach the steady state amplitude. From second 350 and so on, resonance is fully developed in the scale model tests, and math model response accurately tracks it.

Nevertheless, as wave height is increased, the difference between the mathematical model and the scale model tests also grows, as can be seen in Figure 3.47 and Figure 3.48, although the results could also be considered as quite accurate.

This fact becomes more critical when ship speed is increased up to Froude numbers 0.2 and 0.3, in lower wave frequencies and much longer wavelengths. In these conditions, the mathematical model is unable to simulate any of the parametric rolling events that effectively take place in the different towing tank tests, under the parameters shown in Figure 3.6 and Figure 3.9.

The explanation to this behaviour could be related to the quasi static approach adopted for taking in account the effects of heave and pitch motions. As have been explained in Section 2.3.1.5, heave and pitch motions are computed in a quasi static approach when GZ curve is calculated for each wave position, disregarding any possible dynamical effect. As is stated in (Bulian, 2006a), this approximation has proved to be correct especially in following waves, which implies low encounter frequencies and quasi-static variations of heave and pitch, and also in head long waves, where again, hydrostatic effects dominate over hydrodynamic ones. Moreover, in the mentioned work, accurate results of this model are presented for four different vessels, at wavelengths similar to ship length.

In the case under analysis in this work, the model is capable of reproducing resonance for maximum wavelength values of around the double of the ship length, while it fails for the higher wavelengths which correspond to the vast majority of wave combinations in Froude 0.2 and 0.3 test runs.

Although in these cases of large wavelength, heave and pitch motions should behave quasi statically and the hydrostatic assumption should be valid (and so no parametric roll should be present), large heave and pitch motions have been appreciated in the towing tank tests, even for the largest values of wavelength.

In Figure 3.49 the pitch and roll time series from the towing tank test corresponding to a Froude number of 0.2, a frequency ratio of 2 and a wave height of 1.988 m are shown. The wavelength in this run is 81.965 m. Moreover, a sequence taken from the video recording of the test is shown in Figure 3.50, where a whole roll cycle has been captured.

As could be seen both in the video clip capture and in the pitch time series, pitch motions have a large amplitude (the maximum pitch amplitude is 0.187 rad and the average value is 0.052 rad), even though wavelength is larger than in previous cases (Froude numbers 0 and 0.1).

In the described conditions, where wavelength largely exceeds ship length, pitch and heave motions according to the quasi static approach are supposed to be small, waterplane variations due to wave passing (the main cause of parametric roll) should also be small and no resonant motion should develop.

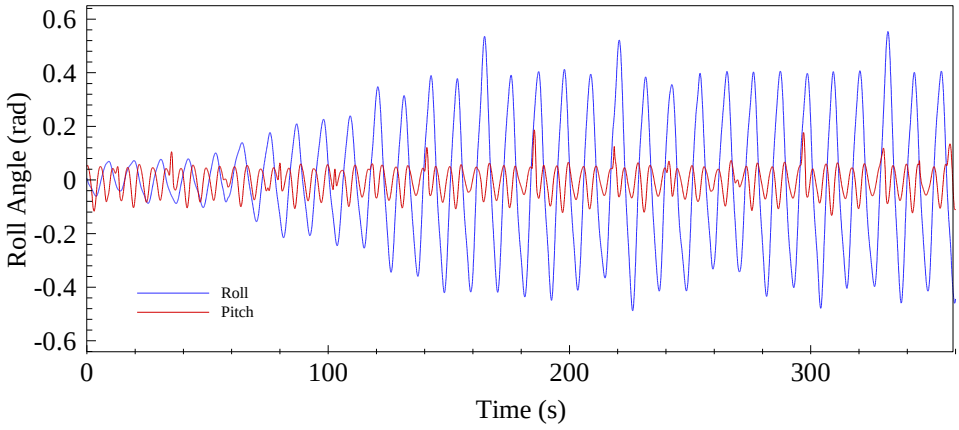

Figure 3.49. Roll and pitch data. Fn = 0.2. Freq. Ratio = 2.0. H_w = 1.988 m. λ = 81.965 m.

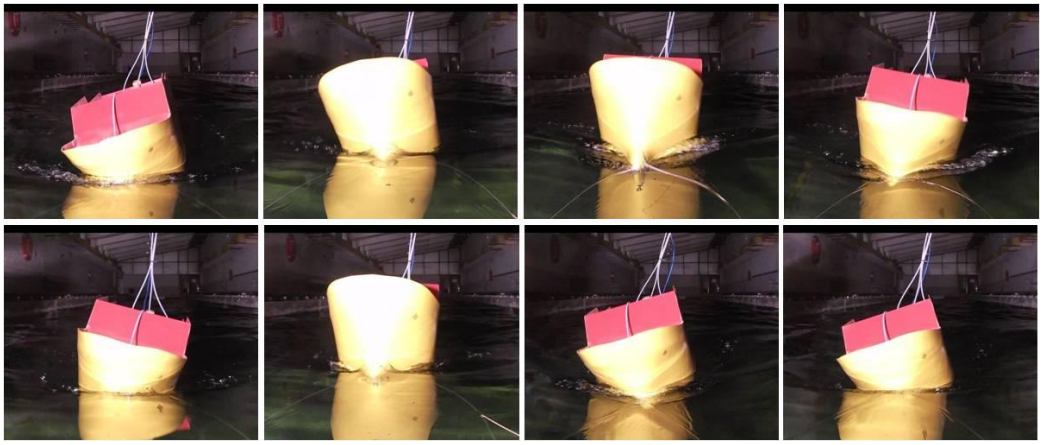

Figure 3.50. Roll cycle sequence. Fn = 0.2. Frequency Ratio = 2. H_w = 1.988 m. λ = 81.965 m.

However, from the video clip and the pitch time series above, it could be observed that pitch motions are intense, and are implying large variations in the water plane area which are surely the cause of the development of the phenomenon in such long wavelength conditions.

In order to obtain a broader view of the performance of the model in the whole set of conditions tested in the towing tank tests, the stability diagrams corresponding to the four forward speed conditions have been computed by using the mathematical approach.

These diagrams represent, for each value of speed, the steady state roll amplitude that is obtained for each combination of encounter frequency – natural roll frequency ratio and wave height, and provide a clear view of the areas where parametric roll resonance takes place and its severity.

By comparing these graphs to the results obtained in the towing tank tests, a global view of the performance of the model may be obtained. This information will be very useful for determining under which conditions the model could be used for providing accurate advice about the risk level of the ship.

In order to build these stability diagrams, the model has been run several times for different values of frequency ratio and wave height, for the four values of speed considered in this work (zero speed and Froude numbers 0.1, 0.2 and 0.3). Wave height ranged between 0.25 m and 3.00 m, while frequency ratio ranged between 1.65 and 2.45, so that the whole set of combinations of the scale tests have been covered. As have already been said, wavelength is been considered dependant on wave frequency, and so a different value of wavelength corresponds to each value of encounter frequency.

In figures from Figure 3.51 to Figure 3.54, the obtained results are presented for each value of forward speed. These data will be compared to the limits of stability obtained in the towing tank tests that have already been shown from Figure 3.6 to Figure 3.9. For simplifying this comparison, the experimental results obtained in the previous section have been superimposed on the mathematical model plots. Green dots represent those conditions where no parametric roll develops, while red dots are those in which the phenomenon takes place.

Figure 3.51 represents the math model stability diagram obtained for the zero speed case. The wavelength values corresponding to this value of speed are the

shorter ones in comparison to the cases with forward speed. So, and according to what has been observed regarding the performance of the model, this should be the condition in which the best approximation is obtained. If this stability diagram is compared to that of Figure 3.6, this fact is confirmed. The limiting edges of both unstable areas are very similar; the lowest vertex is approximately placed at a frequency ratio of 2 in the two cases, and practically no resonance takes place for values of frequency ratios under 1.9. The main difference appears in the shape of the stability diagram to the right of the lowest vertex. According to the diagrams, parametric rolling is predicted at lower wave heights by the math model for frequency ratios over 2.1. It may also be highlighted that a narrow low amplitude resonance band, centered at a frequency ratio of 1.7, may be appreciated in the math model results. No scale tests have been carried out for this range of frequencies, so no equivalence can be analyzed. However, the general correspondence between the model and the towing tank tests appears to be good.

Regarding the Froude = 0.1 case, the results from the mathematical model are displayed in Figure 3.52, while the limits of stability obtained in the towing tank test have been included in Figure 3.7. The main differences in the shapes of the stability areas appear on the left hand side of the lowest vertex of the unstable region. While the right side of the unstable area have been well simulated by the mathematical model, the left side is limited by a frequency ratio of about 1.85. However, it could be seen that some resonance takes place for ratios under this value (1.8) in the towing tank tests. If it is considered that reduced frequency ratios imply longer wavelengths (in this case between 70 m and 80 m), the observed behaviour of the math model at long wavelengths may be shown here, also considering that speed has been increased from the previous case (zero speed).

Finally, in Figure 3.53 and Figure 3.54, the stability diagrams corresponding to Froude numbers 0.2 and 0.3 are shown. As can be appreciated, only a small area of resonance appears for the lowest Froude number, while no resonance at all is predicted for the highest speed. If these results are compared to the ones obtained in the towing tank tests (Figure 3.8 and Figure 3.9), it could be seen that resonance develops in a much wider area, contrary to what the math model shows. Wavelength values in these tests are much longer than in the previous ones, and range from 65 m to more than 100 m, which is more than three times the ship length. The quasi static approach fails, as have been previously said, in predicting the appearance of roll resonance in such conditions.

So, as a conclusion from the validation process, it may be stated that, on one hand, the proposed model is not able to reproduce parametric roll resonance in the conditions where wavelength largely exceeds ship length, at least in this type of small vessel, which shows large pitch motions even in long head seas.

However, on the other hand, it has been shown that in the conditions where wavelength is the range of ship length and even longer (see the results for Froude number of 0.1 in Figure 3.46, Figure 3.47 and Figure 3.48) the model accurately predicts the appearance of roll resonance, and seems to be useful for obtaining guiding information for evaluating the vessel risk of resonance in a seaway.

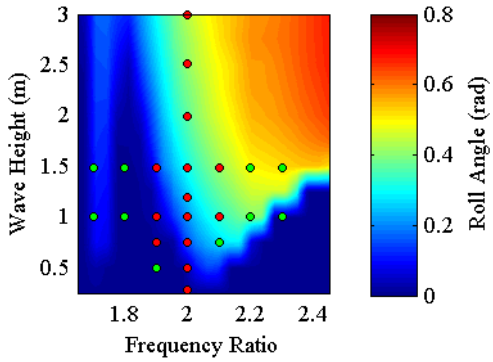

Figure 3.51. Stability diagram. Fn = 0. Variable wavelength.

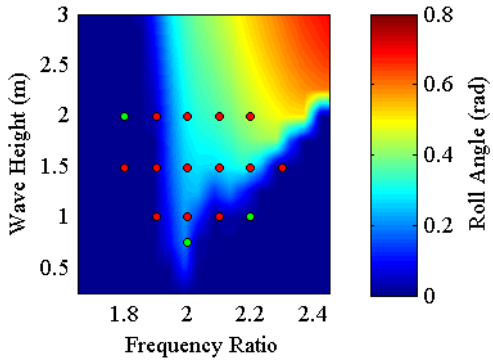

Figure 3.52. Stability diagram. Fn = 0.1. Variable wavelength.

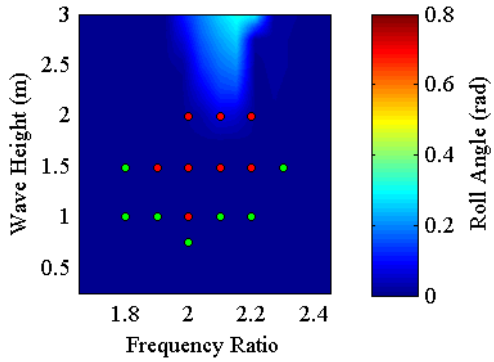

Figure 3.53. Stability diagram. Fn = 0.2. Variable wavelength.

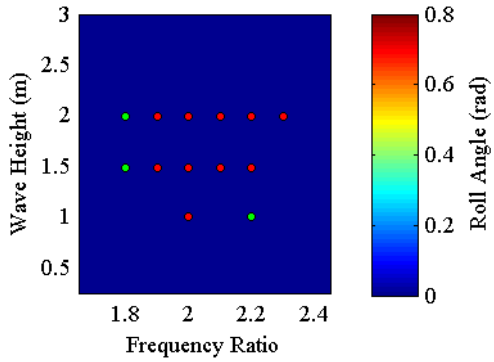

Figure 3.54. Stability diagram. Fn = 0.3. Variable wavelength.

3.2.3.5 Ship Stability Analysis. Regular Waves

In the previous section, the performance of the mathematical model for simulating the appearance of parametric roll resonance in regular waves, at different values of forward speed and wave frequency and height, has been evaluated.

In those tests, wavelength has been computed following the deeps seas approach, as a function of wave frequency. For the ship under analysis, a small-medium sized trawler, typical of the Great Sole bank Spanish fishing fleet, the

deep seas assumption may be considered correct for the vast majority of its operational life. The selected conditions are so the most adequate for evaluating the real risk of experiencing parametric roll for this type of ship.

Although these conditions are supposed to be more realistic, from the point of view of parametric roll resonance amplitude, they are not the most dangerous. As have been already seen, wavelengths similar to ship length are those which imply largest variations in stability characteristics with wave passing and so are the ones leading to the largest roll motions.

Taking into account that the math model has shown a remarkable accuracy in simulating parametric rolling for wavelengths of about the ship length, in this section the stability diagrams corresponding to a fixed wavelength equal to ship length have been computed. Again, and for the sake of comparison, the experimental results obtained for the same combinations of frequency ratio and amplitude, have been superimposed on the math model graphs.

These diagrams will complement the realistic data obtained from the towing tank tests, with those corresponding to the worst possible conditions regarding parametric rolling.

It has to be mentioned that in the vast majority of the references analyzing parametric roll resonance, this is the selected option, i.e., fixed wavelength equal to ship length. For large ships, these conditions may be easily present in a real seaway. However, in the case under analysis, and as can be seen in the tables in Appendix A, these conditions may only be present sailing at reduced speeds (which may be the case of rough weather), but are not probable at higher forward speeds, as very shallow waters should be needed to reduce wavelength to that extent.

So, the following analysis will show the worst possible conditions the analyzed vessel could be facing, although the most probable will be those considered in the towing tank experiments.

Regarding the zero speed case (Figure 3.55), the obtained results are very similar to those of the variable wavelength analysis, as the latter are those of the whole test matrix with shorter wavelengths. The main difference appears to be at the smaller frequency ratios (larger wavelengths), as the unstable region slightly extends to the left in comparison with the previous case. Moreover, the narrow resonance band previously present around a frequency ratio of 1.7, has now disappeared.

As forward speed is increased, differences between the variable and the fixed wavelength analysis also increase. For a Froude number of 0.1 (Figure 3.56), the unstable area is larger, as resonance is now present at the highest frequency ratios for smaller wave heights and also for the whole range of wave heights at frequency ratios under 2. In comparison with the zero speed case, the unstable area has been slightly reduced and moved “upwards”, although the differences are not very large. Moreover, no significant differences in roll amplitude may be appreciated.

For the highest values of speed, the comparison with the previous cases makes no sense, as no parametric roll has been previously predicted in these cases.

In both conditions (Figure 3.57 and Figure 3.58), the evolution of the unstable region is very similar. As speed rises, the area of instability reduces and is displaced upwards, rising its lower vertex.

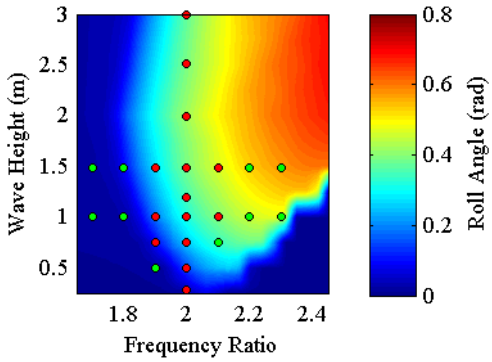

Figure 3.55. Stability diagram. Fn = 0.
Fixed wavelength. λ = 30 m.

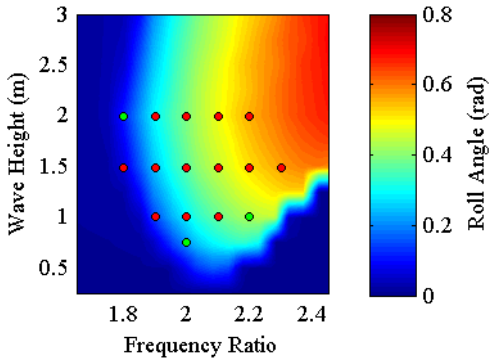

Figure 3.56. Stability diagram. Fn = 0.1.
Fixed wavelength. λ = 30 m.

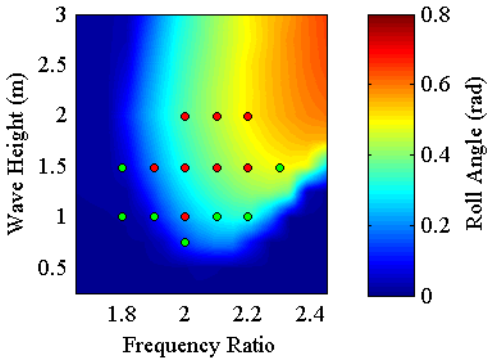

Figure 3.57. Stability diagram. Fn = 0.2.
Fixed wavelength. λ = 30 m.

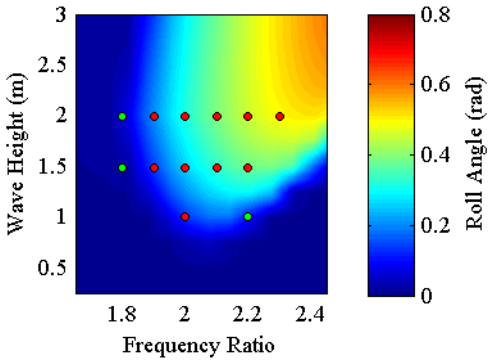

Figure 3.58. Stability diagram. Fn = 0.3.
Fixed wavelength. λ = 30 m.

As an example, while for the zero speed case resonance develops at frequency ratios of 2.1 at waves of less than 0.5 meter height, these value has moved to approximately 0.6 for Froude = 0.2 and to more than 1 meter for Froude = 0.3. Moreover, a significant reduction of steady state roll amplitude could be especially seen for the highest speed tests.

If the experimental results are compared to the mathematical model results, it can be observed that the areas of stability obtained by this approach fit the scale model results with reasonable accuracy, in special for the highest values of

speed. The possible larger pitching and heaving considered in the math model for this condition may compensate the underestimation of the previous case, leading to more accurate results. However, further analysis of the pitch motion both form the experiments and the numerical model, is needed as to conclude about this matter.

3.2.4 Discussion

From the towing tank tests results presented in this section, it can be concluded that the analyzed design, typical of the Spanish fishing fleet, is very prone to developing parametric roll resonance (at least at the tested loading condition), even for very low wave heights. Although the minimum threshold wave amplitudes are found for the zero forward speed case, where parametric roll is only likely for a relatively narrow frequency band, as speed is increased the range of frequencies also grows, and with it the number of possible dangerous sailing conditions.

Moreover, it has been confirmed that in most conditions, a frequency ratio of 2.0 does not imply the worst situations regarding the intensity of parametric roll resonance. In this ship, the worst condition tends to shift to higher frequencies as speed is increased. This fact will be of importance when analyzing possible preventive measures; trying to prevent resonance by increasing speed may, under this conditions, lead to higher amplitudes instead of avoiding the phenomenon.

As have been also stated, the experiments carried out for irregular seas have a limited application. Although those corresponding to zero advance speed are long enough and could provide valuable information, those corresponding to forward speeds seem to be very short and the results subjected to the influence of transient stages.

Finally, and regarding the scale model tests, it has to be underlined that some disturbances have been detected in pitch and roll motions due to the effect of the towing arrangement (the “peaks” in the pitch time series presented in Figure 3.49 are due to this matter). Moreover, surge motion has not been totally restrained, and a slight variation of forward speed with wave passing has also been observed. In order to try to avoid these effects, the use of a self propelled model for the stability analysis of the second trawler was proposed. Such a model is described in the following section.

Respecting the possible application of the mathematical model for its use within an onboard guidance system, it has been seen that, when variable wavelengths are considered, the predictions of roll amplitude obtained for the lower speeds are accurate, but the model is unable to reproduce parametric rolling at the highest speeds and the corresponding stable and unstable areas. Nevertheless, if a fixed wavelength is selected, the stability areas are correctly estimated by the model, though the accuracy of the roll amplitude has not been evaluated. This last fact leads to the possibility of applying the proposed model into the aforementioned guidance system. It could be used for computing and evaluating the resonance risk of a given sailing condition, disregarding, by now, the amplitude of the possible parametric roll event.

As previously stated, the study of pitch and heave data from the scale experiments would be necessary for improving the performance of the mathematical model in all the tested conditions and will be presented as a future work line

3.3 UK Trawler

3.3.1 Description

In this second part of the parametric roll stability study, another fishing vessel has been chosen. The selected ship is other stern trawler, but not equipped with a ramp, as in the previous case. This ship is a representative of the typical UK trawler from the 80´s, and that is also similar to current Dutch-type beam trawlers, having a single deck, the navigation bridge placed abaft and a forecastle forward.

As have already been already mentioned, the selected hull forms are those corresponding to the MFV Trident (Figure 3.59), a British trawler which sank in October 1974 off Wick, Scotland. According to the reports of the investigations which followed the sinking (Gimson, 1975; Young, 2011), the Trident was lost while sailing in stern-quartering seas of up to approximately 2.6 meters of significant height, conditions that aforehand didn´t have to be dangerous for the ship. The scale model tests carried out by the NMI in 1976 (Paffett, 1976), included in the aforementioned investigation, showed that reduced intact stability characteristics and a natural tendency to broaching may be among the causes of the lost of the ship. Moreover, the comparison with a twin vessel but with round stern design (instead of the transom stern of the Trident), showed the worse seakeeping characteristics of the latter one. According to the research carried out by MARIN (Maritime Research Institute Netherlands) in 2009, within the rehearing of the investigation (Young, 2011) and where scale model tests were included, although the ship was unlikely complying with some of the minimum intact stability requirements of IMO (Table 3.1) , the most probable cause of the lost of the Trident may had been its own dynamic stability characteristics, which most probably lead to a capsize in the prevailing sailing conditions.

But apart from the mentioned investigation which mainly studied its behaviour while sailing in stern or near stern seas, this vessel has also been subjected to extensive research in order to determine its head seas sailing characteristics, and specially its tendency to developing parametric roll resonance in these conditions. Under this framework, both towing tank testing and setting up of mathematical models for simulating the ship behaviour have been carried out, specially by research groups of the Federal University o Rio de Janeiro and the Austral University of Chile.

As an example of this research work, the following references could be mentioned. In (M. A. S. Neves et al., 1999), an extensive comparison of the behaviour of the UK Trawler and the twin vessel design with round stern in parametric roll conditions is done for the zero speed case, based on the analysis of the towing tank tests and also in an uncoupled model of the vessel roll motion. In this case, two different values for the GM of the UK Trawler (0.35 m and 0.85 m) were considered.

In (M.A.S. Neves et al., 2002), a similar approach is taken but, in this case, the effects of forward speed in the development of the phenomenon are also taken into account, in a study only based on the analysis of towing tank tests of both vessels. In this occasion, the UK Trawler was tested in two different loading conditions (GM = 0.37 m and GM = 0.50 m), using a similar towing arrangement to that described in Section 3.2.2 of this work. More information regarding these experiments may also be found in (Pérez Meza,Sanguinetti, 2006) or (M. A. S. Neves et al., 2003). References included within these works provide a broad description of the underdone research involving the UK trawler design.

Finally, in (M.A.S. Neves,Rodriguez, 2005; C. A. Rodríguez, 2008, 2010) and references therein, the work for developing a three degrees of freedom coupled model, and its validation and application to the case of the UK trawler, is presented. Moreover, in (M.A.S. Neves, C.A. Rodríguez, et al., 2009), the limits of stability of the same vessel are studied from a fully non-linear point of view, by using the model described in the previous references.

As could be seen from the above, and also by some of the references included in Sections 2.3.1 and 2.3.2.4 of this work, this vessel has become one of the benchmarks regarding the study of parametric roll resonance. However, only data from the towing tank tests carried out in the Austral University of Chile (Valdivia, Chile) are available today. These tests were carried out by using a towing arrangement similar to that applied in the “Spanish trawler” section of this work, and only a limited set of data were obtained from them.

The main objective of this second part, is to study the phenomenon of parametric roll resonance for the UK trawler design, by using an advanced scale model, completely self propelled, sensorized and free to move in the six degrees of freedom. The objective of using this model is essentially to avoid all the effects of the towing devices on the ship behaviour.

Tests will be done at different forward speeds and loading conditions, in order to provide highly realistic data of the behaviour of all the variables involved in the phenomenon, where the contributions of the whole set of motions in parametric rolling could be analyzed, and that could complement the research and information available today.

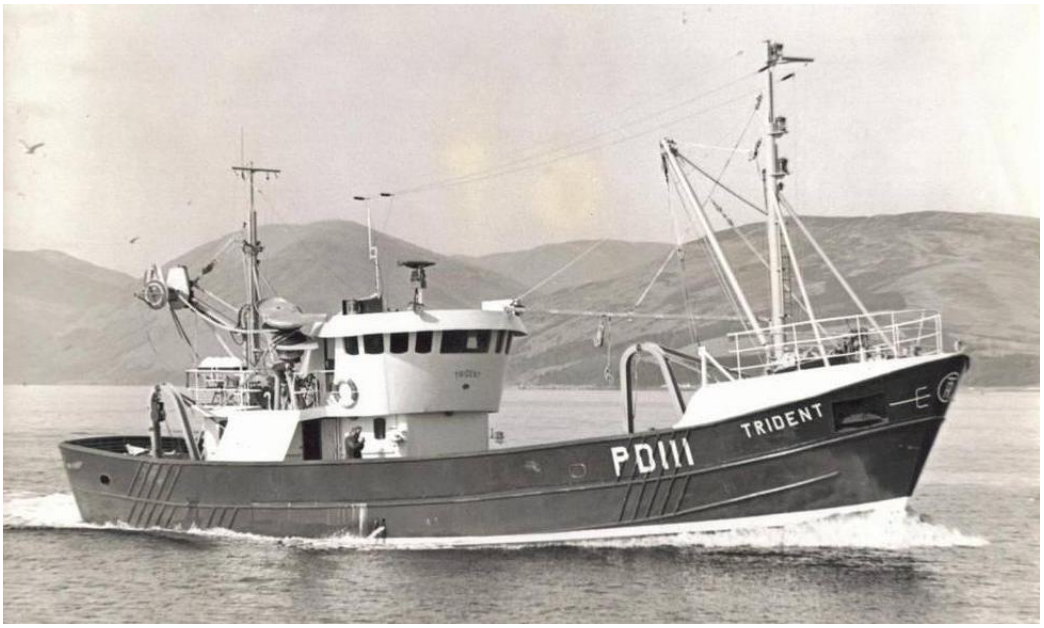

Figure 3.59. M.F.V. Trident. Courtesy of www.trawlerphotos.co.uk.

Moreover, these data will also be used to compare the results obtained with the three degrees of freedom coupled model developed by (M.A.S. Neves,Rodriguez, 2005) and that will be applied later in this work for studying the performance of the parametric roll detection schemes.

Therefore, the ship that has been used in this work is the well studied trawler design with transom stern, and that has been demonstrated to have a natural tendency to easily developing parametric rolling in not very heavy sea states.

The vessel hull forms are presented in Figure 3.60, while its general arrangement is included in Figure 3.61 and its main characteristics in Table 3.10.

3.3.2 Towing Tank Tests

The towing tank test campaign corresponding to this second trawler, has also been done in the towing tank of the Escuela Técnica Superior de Ingenieros

Navales of the Polytechnic University of Madrid, which main characteristics have already been described (Section 3.2.2).

In this case, the tests have been carried out at three different forward speeds and also at zero speed, in head regular waves of different frequency and amplitude and for two different loading conditions. Moreover, roll decay tests at the four speed values plus another additional one have also been done.

The objective of these tests is again to analyze the influence that the different parameters have in the development and amplitude of parametric rolling, including wave amplitude and frequency, ratio between encounter frequency and natural roll frequency, ship forward speed and also metacentric height, which has not been analyzed in the tests of the Spanish trawler.

In addition to this, the design of a scale model that could be capable of self propelling and being auto controlled and positioned and with the capacity of measuring most of the parameters involved in the analysis of its dynamic stability has also been done. This model should also be watertight, as it has been intended to be used in all kind of seakeeping analysis, such us the presented parametric rolling tests, broaching analysis, loss of stability, etc.

Table 3.10. UK trawler main characteristics.

Overall Length	25.91 m
Length Between Perpendiculars	22.09 m
Breadth	6.68 m
Depth to Main Deck	3.35 m
Design Draught	2.48 m
Design Displacement	170.3 t

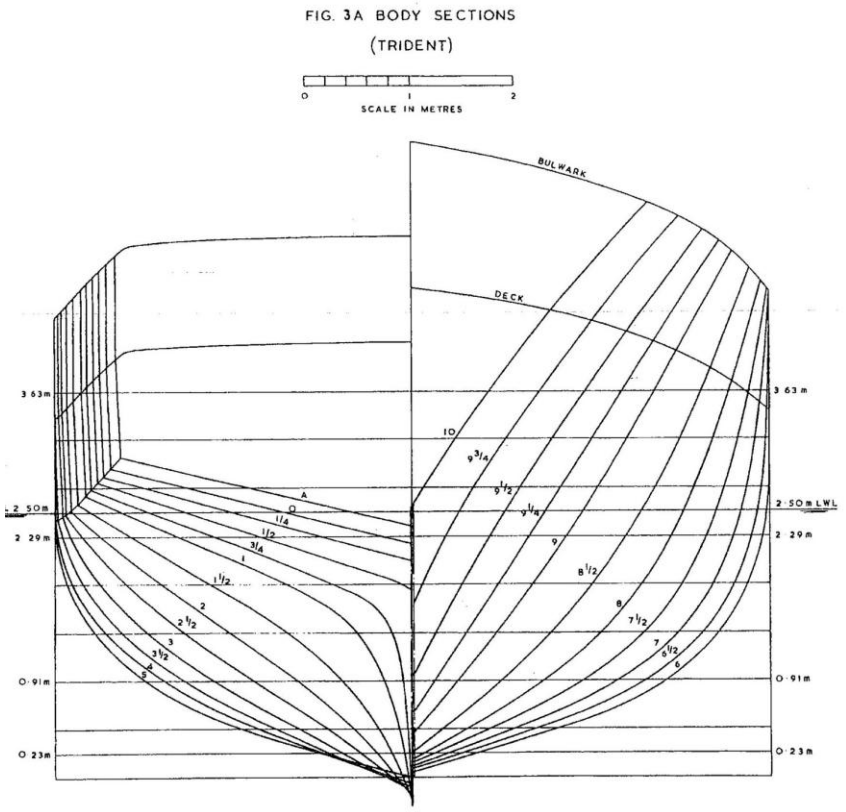

Figure 3.60. UK trawler hull forms (Paffett, 1976).

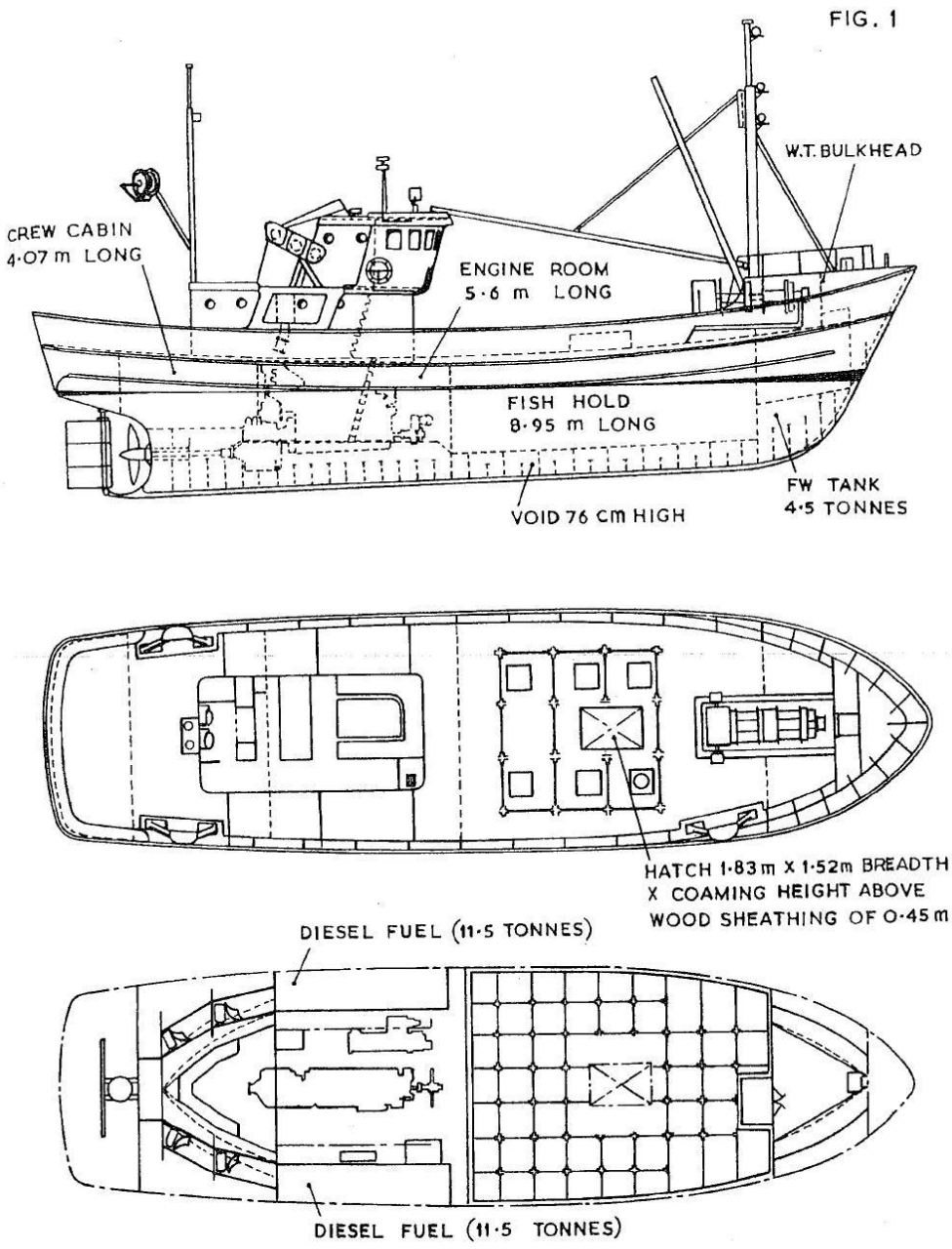

Figure 3.61. UK trawler general arrangement (Paffett, 1976).

3.3.2.1 Experimental Arrangement

The UK trawler scale model has been machined from high density (250 kg/m^3) polyurethane blocks to a scale of 1/15th, painted and internally covered by reinforced fiberglass. Mobile lead weights have been installed in PVC foam supporting elements, allowing longitudinal, transverse and vertical displacements for a correct mass arrangement. Moreover, two small weights have been fitted into a transverse slider for fast and fine tuning of the position of the transverse centre of gravity and the mass moment of inertia.

The propulsion system consists of a three-phase electric motor and two cascaded planetary gearboxes, which move a four bladed propeller. The rudder is actuated by an electronic servo, which may be controlled either using an external transmitter or by the own model control system.

In order to obtain data of all the representative parameters which have importance in the dynamic behaviour of the ship, the following sensors have been installed onboard:

- Inertial Measurement Unit (IMU): has nine MEMS embedded sensors, including 3 axis accelerometers, 3 axis gyros and 3 axis magnetometers. The IMU provides information of accelerations in the OX, OY and OZ axis, angular rates around these three axis and quaternion based orientation vector (roll, pitch, yaw), by using Kalman filtering techniques. This sensor has been placed approximately in the center of gravity of the ship with the objective of improving its performance.
- Thrust sensor: a thrust gauge has been installed to measure the thrust generated by the propeller at the thrust bearing.

- Revolution and torque sensor: in order to measure the propeller revolutions and the torque generated by the engine, a torque and rpm sensor has been installed between both elements.
- Sonars: intended to measure the distance to the towing tank walls and feed an automatic heading control system.

Data acquisition is made through an onboard mounted PC, placed forward on the bottom of the model. The software in charge of the data acquisition and processing and engine speed and rudder control (Matlab based code, developed by GII[3] members), is also installed in this PC. However, if needed the system may be controlled from another external workstation by using Wi-Fi connection.

An overview of the model where its main components are shown, is included in Figure 3.62.

The speed control of the model is done by setting a rpm command, which keeps engine revolutions constant by using a PI controller programmed in the governing software. Alternatively, a servo command may be used for setting a constant power input for the engine. Regarding heading control, IMU and sonar data are used for keeping the model direction along the towing tank. In case these values are not accurate enough, heading control may be switched to a manual mode and an external RC transmitter could be used for course keeping.

The power for all the elements is provided by two 12 V D.C batteries, placed abaft in the ship, providing room in their locations for longitudinal and transverse mass adjustment. These batteries have enough capacity for a whole day of operation.

[3] Integrated Group for Engineering Research. University of A Coruña. www.gii.udc.es

Two adjustable weights have been placed in both sides of the model, and another one has been placed forward in the centerline. In both cases, enough room has been left as to allow transversal and vertical mass adjustment. Moreover, two sliders with 0.5 kg weights have been installed for fine tuning of the mass distribution.

3.3.2.2 Experiment Development

As have already been mentioned, in this test campaign trials at different forward speeds and also at zero speed have been carried out. The experimental arrangement for carrying out the zero speed runs has been similar to that used in Section 3.2.2. In order to keep the model in position and to try to avoid as much as possible any interferences of the restraining devices in the ship motions, two fixing ropes with two springs have been tightened to the sides of the basin and to a rotary element fixed to the model bow. Moreover, another restraining rope has been fitted between the stern of the model and the towing carriage, stowed just behind of it. However, this last rope has been kept loosen and partially immersed, being enough for keeping the model head to seas without major influence on its motions.

In the forward speed test runs, the model has been left sailing completely free, with the exception of a security rope that would be used just in case the control of the ship could be lost. In all tests, the course keeping of the model has been done manually by using the RC transmitter; however, the directional stability of the model has been quite high in all tests, and rudder control has been reduced to the minimum, hardly introducing any disturbance on the development of parametric roll.

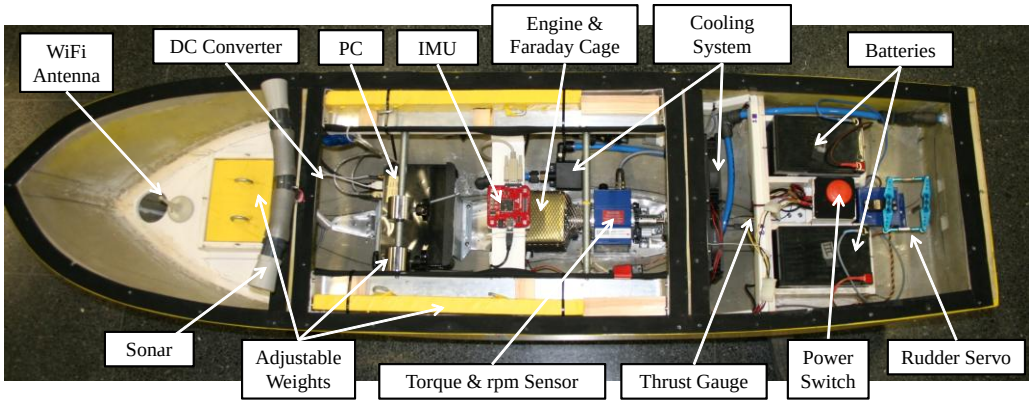

Figure 3.62. UK trawler scale model overview.

Figure 3.63 Scale model. Up left: prior to painting. Up Right: general view under stability test. Centre Down: ready for testing.

In order to set the adequate speed for each test run, a previous calibration for different wave conditions has been carried out, to establish the needed engine output power (engine servo command) for reaching the desired speed as a function of wave height and frequency. The measuring of the exact speed value developed in each of the test runs, has been done by following the model with the towing carriage, providing the instantaneous speed along the run. The calibration curve was updated as the different runs were completed, providing more information for the subsequent tests. However and considering that the model is free to move in the six degrees of freedom, the instantaneous speed of the model may be affected by surge motion, especially at the conditions with highest waves.

In this work, only the results corresponding to the roll motion will be presented. As have already been mentioned, the IMU measured and recorded accelerations, angular rates and magnetic field intensity in the three axis. The attitude of the model (yaw, roll and pitch) is obtained after the processing of the measured data by an IMU-embedded Kalman filter, though raw values from all the three sensors have also been recorded.

In the calibration stage of the model, a clear interference of the tank carriage rails on the IMU magnetic field measurement was observed. So, Kalman filter parameters were modified to remove the magnetic field contribution to the attitude solution. Because of this fact, yaw results showed a continuous drifting due to the gyro yaw rate absence of reference, which also affected the filtered roll and pitch measurements. As a consequence, the roll data presented in this work has been obtained after using the IMU three axis accelerometer as a classical inclinometer, from which also pitch angle has been computed. The results obtained using this approach have been compared to the Kalman filtered ones from an undisturbed IMU test, showing an adequate performance.

Anyway, further processing of the IMU raw data will be needed to combine both gyro and accelerometer data into an undisturbed complete attitude vector.

Regarding the ship loading condition, the main parameters have been set equal to those selected in (M.A.S. Neves et al., 2002), for the sake of comparison of the obtained results. Moreover, two stability levels have been considered, with the objective of also analyzing the influence of the loading condition on the development of parametric roll. Following the approach of (M.A.S. Neves et al., 2002), which carried out towing tank tests of the same design, both a low and a high GM have been selected.

The low GM case, corresponding to a GM of 0.370 m, coincides with the one selected by the aforementioned authors. As well as being used for analyzing the behaviour of the vessel in a reduced-stability condition, in the vicinity of the non-compliance with the IMO intact stability requirements, this condition will be also taken as the reference value for comparing the results obtained in this work with the ones previously obtained by those authors.

On the other hand, a higher GM value of 0.436 m has been selected. Taking into account that the higher GM used in (M.A.S. Neves et al., 2002) was 0.500 m, an intermediate value has been chosen, with the objective of providing information not available up to date and avoiding data redundancy.

The parameters of the two loading conditions tested in this section (in real scale), are included in Table 3.11.

In this study, the vessel has been tested in head regular waves with different combinations of wave height and frequency and at different speeds. Apart from these, roll decay tests have also been carried out, for the two loading conditions and four Froude numbers (0, 0.1, 0.20 and 0.30). In Section 3.3.3, the results

obtained from these experiments and the corresponding analysis will be presented.

Table 3.11. UK Trawler loading conditions parameters

	Low GM	High GM
Draught	2.475 m	
Trim	0.000 m	
Displacement	170.30 m	
KM_T	3.705 m	
GM_T	0.370 m	0.436 m
ω_n	0.839 rad/s	0.913 m rad/s
Transverse radii of gyration	1.920 m (28 % B)	
Longitudinal radii of gyration	6.507 m (29 % Lpp)	

3.3.2.3 Regular Waves

A total number of 105 test runs have been carried out for the head seas regular wave case. Different combinations of wave height (ranging from 0.255 m to 1.245 m) and ratio between encounter frequency and natural roll frequency (from 1.80 to 2.30) have been considered, for three different values of forward speed (Froude numbers 0.1, 0.15 and 0.2) and zero speed, and two different values of metacentric height (0.370 m and 0.436 m). From the whole set of test runs, 55 correspond to the 0.370 m GM case, while 50 correspond to a GM of

0.436 m. The selected parameters for the different test runs are described in Table 3.12 (GM = 0.370 m) and Table 3.13 (GM = 0.436 m).

The full set of wave parameters and the obtained roll motions for each combination are included in Appendix B.

Table 3.12. Tested wave conditions. GM 0.370 m.

Wave Height (m)	ω_e/ω_n	Fn 0	Fn 0.1	Fn 0.15	Fn 0.2
0.375	1.80		✓		
	1.90				✓
	1.95			✓	
	2.00	✓	✓		
	2.05		✓		
	2.10		✓	✓	✓
	2.25		✓		
0.495	2.00	✓ (x2)			
0.630	1.90	✓		✓	
	1.95			✓	
	2.00	✓	✓		✓
	2.05		✓	✓	✓
	2.10	✓	✓	✓	
	2.20	✓			
	2.25		✓		

Wave Height (m)	ω_e/ω_n	Fn 0	Fn 0.1	Fn 0.15	Fn 0.2
0.75	1.85		✓		
	1.90		✓	✓	
	1.95				✓
	2.00	✓	✓	✓	✓
	2.05			✓	
	2.10	✓	✓	✓ (x2)	
	2.15			✓	
	2.20	✓	✓		
	2.30		✓		
1.005	1.90	✓			
	2.00	✓	✓ (x2)		
	2.10	✓			
	2.20	✓			
1.125	1.90	✓			
	2.00	✓ (x2)			
	2.10	✓			
	2.20	✓			
1.245	2.00	✓			

Table 3.13. Tested wave conditions. GM 0.436 m.

Wave Height (m)	ω_e / ω_n	Fn 0	Fn 0.1	Fn 0.15	Fn 0.2
0.255	2.000	✓			
0.375	1.900	✓			
	1.950		✓		
	2.000	✓	✓ (x2)		
	2.050				✓
	2.100	✓	✓		
	2.150		✓	✓	
	2.200				✓
	2.300		✓		
0.495	1.900	✓			
	1.950			✓	
	2.000	✓	✓		✓
	2.100	✓			
	2.150		✓		
0.630	1.900	✓	✓	✓	
	1.950			✓	✓
	2.000	✓	✓		
	2.050				✓
	2.100	✓			✓

Wave Height (m)	ω_e / ω_n	Fn 0	Fn 0.1	Fn 0.15	Fn 0.2
0.75	1.800		✓	✓	
	1.850		✓	✓	
	1.900			✓	
	1.950			✓	
	2.000	✓			
1.005	1.800		✓		
	1.900		✓		✓
	1.950		✓		
	2.000	✓			✓
	2.050				✓
	2.100	✓			
	2.200				✓
1.125	1.800		✓		
	1.900	✓			
	2.000	✓			
	2.100	✓			

3.3.2.3.1 Limits of stability

Again, and as has been done for the Spanish trawler, the data obtained from these tests will be used for analyzing the influence of the different parameters (both wave characteristic and ship sailing conditions) in the development of parametric rolling, with the objective of studying the application of possible preventive measures for avoiding the phenomenon.

As a first step, the limits of stability of the UK trawler for the two loading conditions have been set up. In these graphs, the appearance or not of parametric roll is indicated for the different combinations of wave height and frequency ratio, for each forward speed and loading condition.

These could be seen for the 0.370 m GM case from Figure 3.64 to Figure 3.67, while the GM = 0.436 m results are included from Figure 3.68 to Figure 3.71.

Regarding the zero speed case, it could be appreciated that the unstable region is quite narrow for both GM values, restricted to frequency ratios higher than 1.9 and lower than 2.2. For the lowest GM (Figure 3.64), the unstable area lowest vertex seems to correspond to a relatively large wave height; in fact, the increase in stability due to the larger GM of the 0.436 m case (Figure 3.68), implies a decreasing of the unstable area lowest vertex wave height. Another remarkable difference between the two cases, appears in the upper limit of the unstable region for the higher GM- At the pure resonance ratio (2.0), the unstable area seems to be limited at a wave height of 1.005 m, while this limit is not present in the GM 0.370 m case.

For the low GM case, an increase in speed up to a Froude number of 0.1 implies, just as happened for the “Spanish Trawler”, an extension of the unstable area to both higher (2.2) and lower (1.9) frequency ratios (Figure 3.65). However, and opposite to that case, the unstable area lowest vertex now moves down, implying that parametric roll would develop at lower wave heights than for zero speed. Regarding the 0.436 m GM stability diagram (Figure 3.69), it could also be seen that the unstable region slightly extends to the left, although the inferior vertex seems to remain at the same position that in the previous case (no much data is present in the right hand side of the diagram).

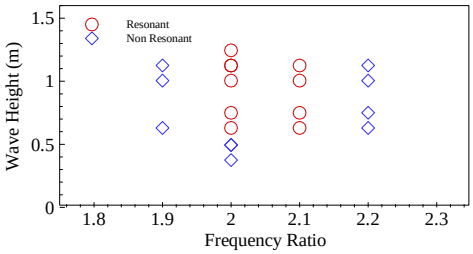

Figure 3.64. Limits of Stability. Fn = 0. GM = 0.370 m.

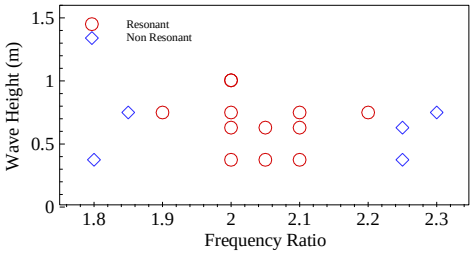

Figure 3.65. Limits of Stability. Fn = 0.1. GM = 0.370 m

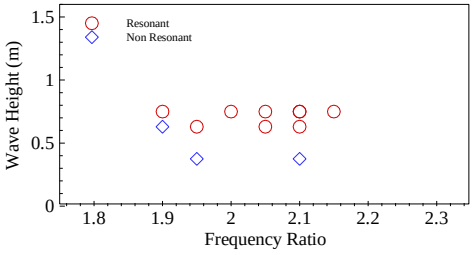

Figure 3.66. Limits of Stability. Fn = 0.15. GM = 0.370 m.

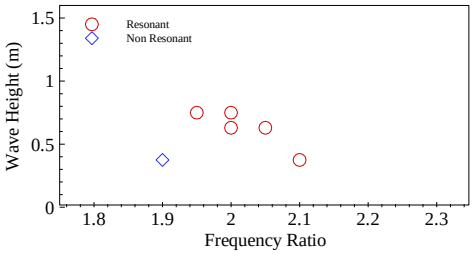

Figure 3.67. Limits of Stability. Fn = 0.2. GM = 0.370 m.

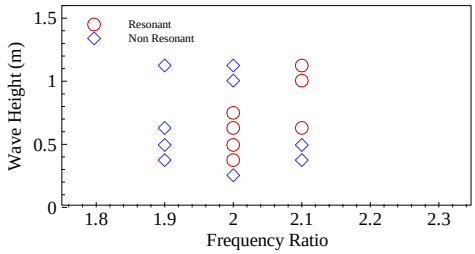

Figure 3.68. Limits of Stability. Fn = 0. GM = 0.436 m.

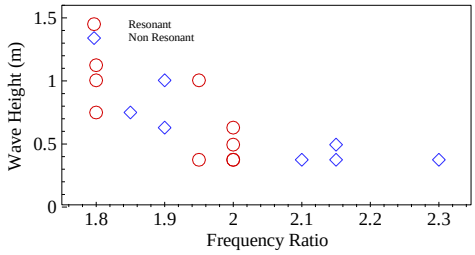

Figure 3.69. Limits of Stability. Fn = 0.1. GM = 0.436 m.

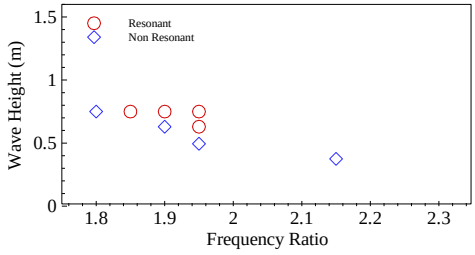

Figure 3.70. Limits of Stability. Fn = 0.15. GM = 0.436 m.

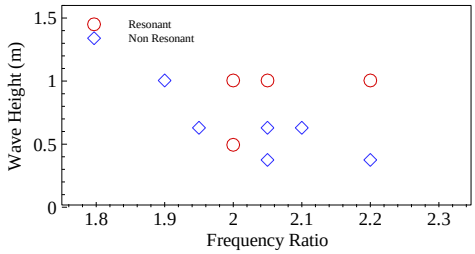

Figure 3.71. Limits of Stability. Fn = 0.2. GM = 0.436 m.

Moreover, a narrow resonant area appears now at a frequency ratio of 1.80, extending along a wide range of wave heights. The influence of wavelength may be the reason for the appearance of this unstable band.

If speed is increased again, up to a Froude of 0.15, the rising of the unstable region could be clearly appreciated for both levels of stability (Figure 3.66 and Figure 3.70), as resonance does not develop for any frequency ratio at wave heights of less than 0.500 m. Moreover, the unstable band described in the previous case for the frequency ratio of 1.8 has now disappeared.

Finally, the highest speed tests (Froude number of 0.2, Figure 3.67 and Figure 3.71), show a very different behaviour depending on the vessel stability level. On one hand, for the highest GM value (Figure 3.71), the unstable region has been limited even more, having its main area for wave heights above 1.00 m at most frequencies (except for a frequency ratio of 2.0, where minimum wave height is 0.5 m), which is the usual behaviour as speed, and so roll damping, increases. But on the other hand and for the lowest GM (Figure 3.67), the resonant area has moved downwards again and parametric roll now occurs at a minimum wave height of 0.5 m and for a frequency ratio of 2.1. However, not much data are available for this condition and it is not possible to obtain a complete representation of the whole unstable region.

3.3.2.3.2 Forward speed and wave height influence

Following the same methodology applied in the “Spanish Trawler” analysis, the maximum roll motion for each test run has been plotted against wave height for different values of forward speed, while keeping the frequency ratio constant. The objective of this section is to analyze the influence of forward speed and wave height on the amplitude of the parametric roll phenomenon.

It has to be noted that in the presented figures, maximum roll values of approximately under 0.1 radians are normally corresponding to non-resonant conditions, and caused by the natural roll motion of the free sailing ship in a head seas seaway. However, the appearance or not of parametric roll in a given run, may be determined from Figure 3.64 to Figure 3.71.

Regarding the low GM case (0.370 m), in Figure 3.73 and Figure 3.74 is where the dependence of parametric roll amplitude on forward speed and wave height may be better appreciated.

When the frequency tuning ratio is 2.0, it could be seen that roll amplitude increases with wave height for the lowest speeds, but only up to a limit, from which roll amplitude starts decreasing, largely for the zero speed case. This dependence seems to be not so strong for the Froude 0.15 case, while at the highest forward speed (Fn = 0.2), roll amplitude decreases with wave height.

If the frequency tuning ratio is increased up to 2.1, the described tendency remains the same for the Froude = 0.1, but the maximum roll amplitude is reached at smaller wave heights. The intermediate speed value (Fn = 0.15) has now a very similar behaviour to Fn = 0.1 case. Regarding the zero speed test, it can be seen that although roll amplitude follows a similar pattern to the previous case (with a maximum value at a wave height of 1.00 m), wave height has much less influence on roll motion.

Regarding roll amplitude, the largest values correspond, for both frequency ratios, to the Froude = 0.1 case (which is coherent with the larger unstable area shown in Figure 3.65). For a frequency tuning ratio of 2.0, roll amplitudes for the zero speed case are also quite large, while for higher speeds the roll amplification is reduced.

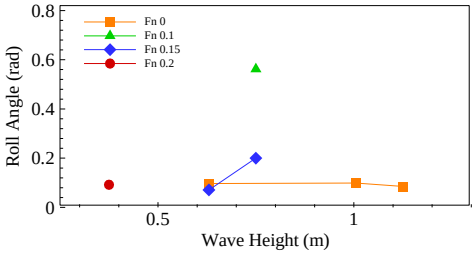

Figure 3.72. Max. Roll Angle.
Freq. ratio = 1.9.GM = 0.370 m.

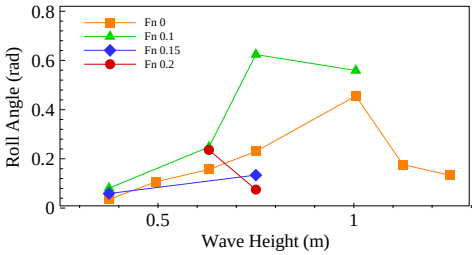

Figure 3.73. Max. Roll Angle.
Freq. ratio = 2.0.GM = 0.370 m.

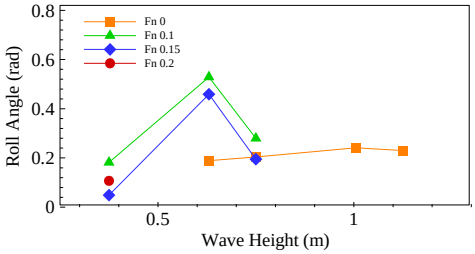

Figure 3.74. Max. Roll Angle.
Freq. ratio = 2.1.GM = 0.370 m.

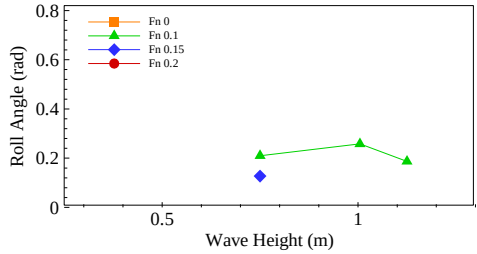

Figure 3.75. Max. Roll Angle.
Freq. ratio = 1.8.GM = 0.436 m.

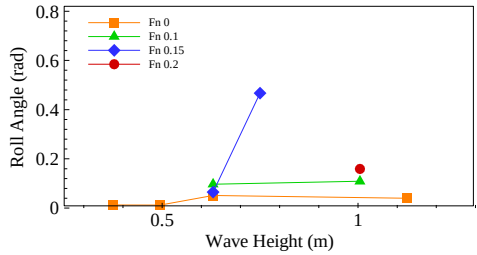

Figure 3.76. Max. Roll Angle.
Freq. ratio = 1.9.GM = 0.436 m.

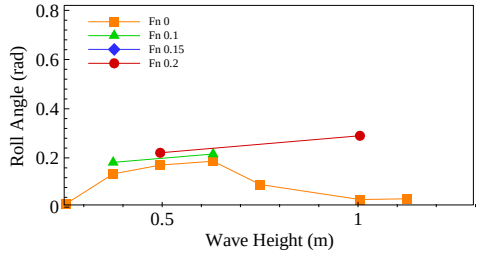

Figure 3.77. Max. Roll Angle.
Freq. ratio = 2.0.GM = 0.436 m.

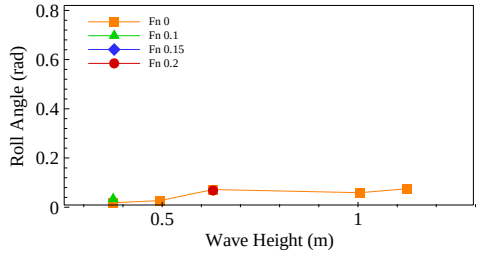

Figure 3.78. Max. Roll Angle.
Freq. ratio = 2.1. GM = 0.436 m.

When frequency ratio is increased (Figure 3.74), roll amplification at zero speed is reduced and intermediate speeds are those in which the largest amplitudes are reached. Finally, in most cases roll motions for the highest forward speed of Froude = 0.2 are not among the most intense.

When the ship stability is increased (GM = 0.436 m, Figure 3.75 to Figure 3.78), the previously observed intense amplification of the parametric roll amplitude due to larger wave height may not be appreciated, with the exception of the Fn = 0.15 case at a frequency ratio of 1.9 (Figure 3.76). This behaviour could also have been observed in Figure 3.72 for the lower GM case.

However, and although the intensity of the amplification is less in comparison to the previous case, in the test runs where parametric roll is present the same relationship between wave height and parametric roll motion has been observed: roll amplitude rises with wave height up to a limit, from which roll amplitude starts decreasing (see for example Fn = 0.1 case in Figure 3.75 or Fn = 0 in Figure 3.77).

On this analysis, two facts should be highlighted; on one hand, the narrow band of resonance present for a frequency ratio of 1.8 and Fn 0.1, that has been already described in the corresponding stability region and that will have to be further analyzed. And on the other hand, the resonant runs that appear at 2.1 frequency ratio for the zero speed case (see Figure 3.68 and Figure 3.78). Although the maximum roll amplitudes are quite small, which may lead to think that no resonance takes place, from the analysis of the time series it can be concluded that parametric rolling is present, and that´s why they have been included in the unstable region of Figure 3.68.

3.3.2.3.3 Frequency ratio and wave height influence

In order to better analyze the influence of the frequency ratio on parametric roll severity, maximum roll amplitude has been plotted against wave height, for different frequency ratios and for a given forward speed which has been kept constant. The results are shown in Figure 3.79 to Figure 3.86.

Regarding the low metacentric height case (Figure 3.79 to Figure 3.82), it could be seen that, for zero forward speed (Figure 3.79), the tuning ratio of 2.0 is that where the largest roll amplitudes take place at the majority of wave heights.

As forward speed is increased, and for intermediate values (Fn = 0.1 and Fn = 0.15), the same tuning ratio remains the worst regarding roll resonance at the higher values of wave height. However, for smaller waves, the largest amplitudes are reached at the higher tuning ratio of 2.1. If speed is increased even more, up to Fn = 0.2, the largest roll values are again reached at the 2.0 frequency ratio.

An increasing of the stability levels of the ship (Figure 3.83 to Figure 3.86) implies, for the zero forward speed case, a reduction of maximum roll amplitude for all tuning ratios, being the 2.0 case again the most critical one. The same occurs with the Fn = 0.1 case, although an important resonance event occurs at the 1.80 ratio, with a relatively high intensity. If forward speed continues rising, roll amplitude seems to increase for the lower frequency ratios, especially at the largest wave heights. Finally, and for the largest value of forward speed (Fn = 0.2), the highest roll amplitudes are reached at the highest frequency ratios for the larger waves, while the 2.0 tuning case is still the most critical at low waves.

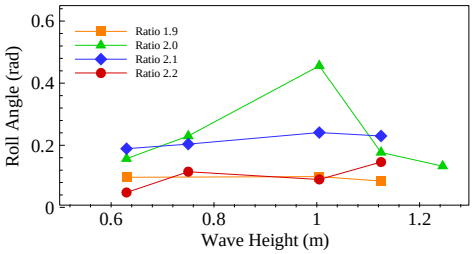

Figure 3.79. Max. Roll Angle. Fn = 0. GM = 0.370 m.

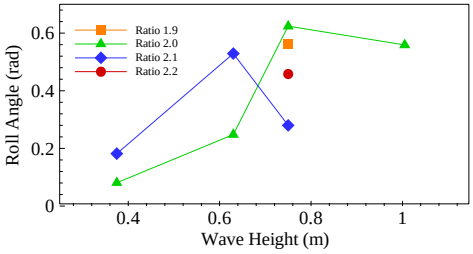

Figure 3.80. Max. Roll Angle. Fn = 0.1. GM = 0.370 m

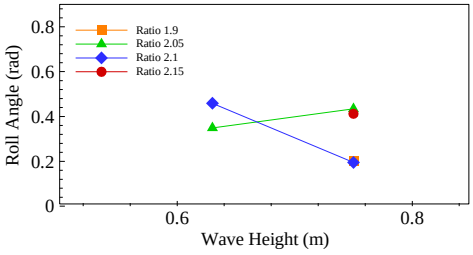

Figure 3.81. Max. Roll Angle. Fn = 0.15. GM = 0.370 m.

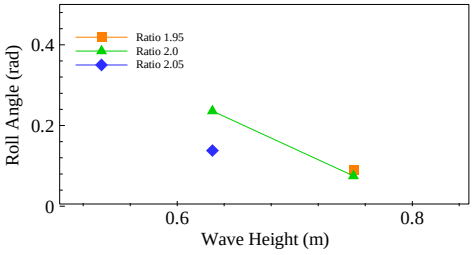

Figure 3.82. Max. Roll Angle. Fn = 0.2. GM = 0.370 m.

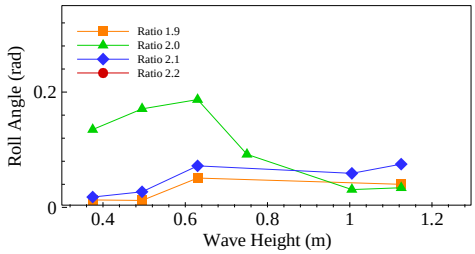

Figure 3.83. Max. Roll Angle. Fn = 0. GM = 0.436 m.

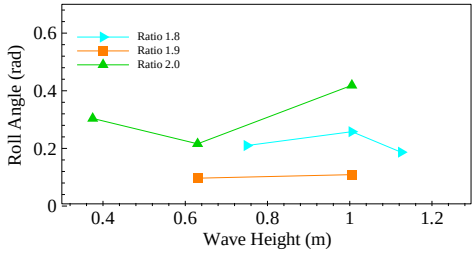

Figure 3.84. Max. Roll Angle. Fn = 0.1. GM = 0.436 m.

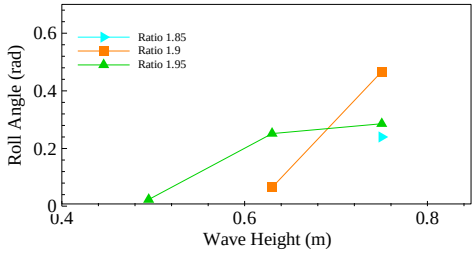

Figure 3.85. Max. Roll Angle. Fn = 0.15. GM = 0.436 m.

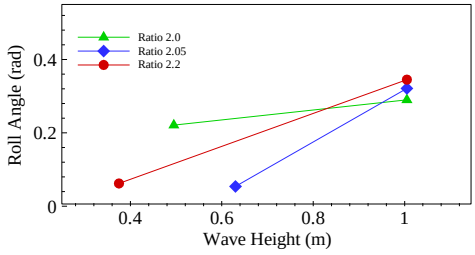

Figure 3.86. Max. Roll Angle. Fn = 0.2. GM = 0.436 m.

3.3.2.3.4 Forward speed and frequency ratio

In order to investigate the influence of forward speed and frequency ratio, without considering the effects of wave height, steady state maximum roll angle has been plotted against frequency tuning ratio for different values of forward speed, keeping wave height and GM constant.

In Figure 3.87, the results obtained for a GM of 0.370 m and a wave height of 0.75 m are included. From it, it could be concluded that largest roll motions correspond to a speed of Fn = 0.1 and a tuning ratio of 2.0. At this value of speed, a minimum roll angle is reached at a tuning ratio of 2.1, increasing again for a frequency relationship of 2.2. Such V-shape behaviour also appears for the Fn = 0.15 case; from a minimum roll angle at a frequency ratio of 2.0, roll amplitude rises up to a maximum at a 2.05 ratio, then decreases and rises again at 2.15. Both the zero speed and the Fn = 0.2 case seem not to be largely affected by the tuning ratio, as roll amplitude slightly decreases from a maximum value (tuning ratios of 2.0 and 1.95 respectively) as the frequency ratio is increased.

In the case shown in Figure 3.88, both metacentric and wave height have been increased, up to 0.430 m and 1.005 m respectively. For the three forward speed values shown in the figure, the behaviour is quite similar to that appreciated in the previous case. On one hand, the variation of roll amplitude with frequency ratio for Froude numbers 0.2 and 0 is again quite low. However, in this second case roll angle rises as tuning ratio is increased, instead of the previously observed decreasing. Moreover, the roll amplitude present for the Fn = 0.2 case, is much larger in comparison to the other speed values than what has been previously seen. Finally, and regarding the Fn = 0.1 case, it could be said that the V-shape behaviour of roll amplitude observed in Figure 3.87 is repeated now, although the lower vertex has moved from a high ratio of 2.1 to 1.9.

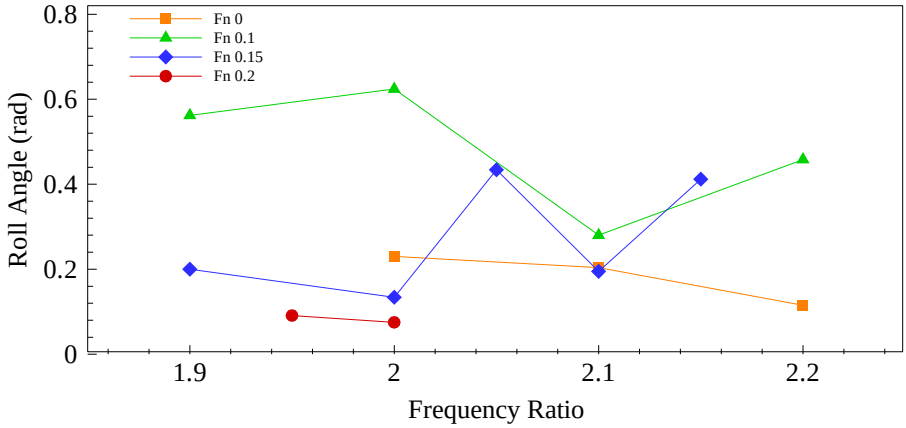

Figure 3.87. Max. Roll Angle. GM = 0.370 m. H_w = 0.75 m.

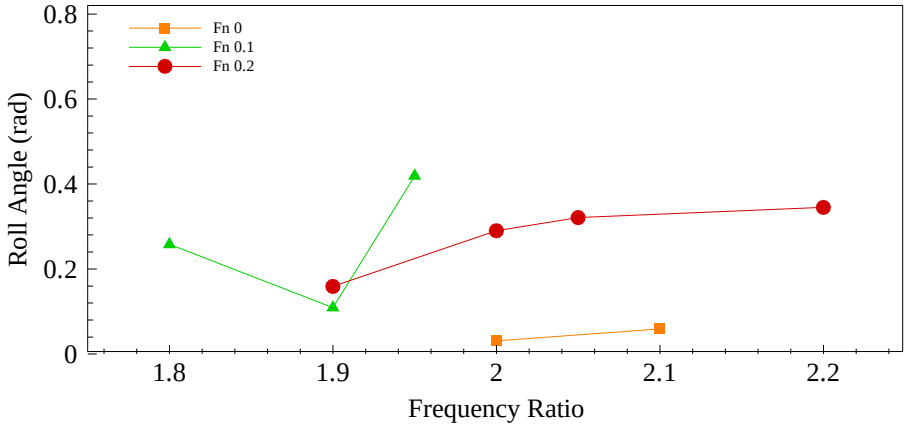

Figure 3.88. Max. Roll Angle. GM = 0.436 m. H_w = 1.005 m.

3.3.2.3.5 Metacentric heigth influence

To end with the analysis of the influence of the different determining factors in the development of parametric roll resonance, the comparison of the obtained values of roll amplitude for the two tested metacentric heights for the same group of parameters has been done. In figures from Figure 3.89 to Figure 3.96, maximum roll amplitude for the two tested metacentric heights (0.370 m and 0.436 m) is plotted against frequency ratio, for different combinations of wave height and forward speed.

From these graphs, it can be concluded that, in most conditions, the reduction in metacentric height from 0.436 m to 0.370 m implies a clear increase in resonance amplitude. The exceptions appear in Figure 3.89 and Figure 3.93. In these two cases, maximum roll amplitude is almost the same for both stability levels; the main difference comes from the position of these maxima. When stability is larger (GM = 0.436 m), the roll peak value takes place at lower frequency ratios (2.0 in Figure 3.89 and 1.9 in Figure 3.93), moving right as ship stability is increased (2.1 in Figure 3.89 and 2.05 in Figure 3.94). This fact seems to be present also in Figure 3.90, Figure 3.92 and Figure 3.95, but the lack of data for these sets of parameters, especially for the larger GM case, avoids us for extending this conclusion.

3.3.3 Mathematical Model

From the towing tank tests described in the previous section, the influence of the different conditions involved in the development of parametric roll has been studied. Although the results obtained provide an important knowledge about the phenomenon, they´re limited to a reduced number of forward speeds and loading conditions.

It is well known that the use of towing tank tests for carrying out intensive seakeeping analysis is not viable, due to their high cost and time consumption. As have already been mentioned in this work in Section 3.2, the use of mathematical models for studying the dynamic behaviour of vessels on a seaway is broadly extended among the marine community. The complexity and difficulty on developing and tuning these models is, of course, related to the complexity of the dynamic phenomena which the model is intended to reproduce.

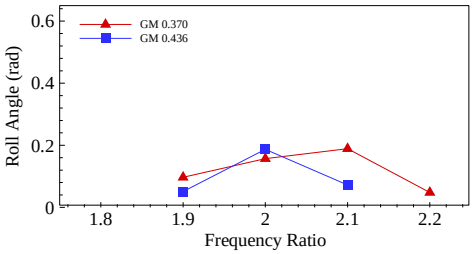

Figure 3.89. Max. Roll Angle. Fn = 0.0. H_w = 0.630 m.

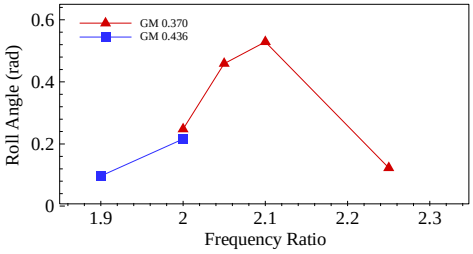

Figure 3.90. Max. Roll Angle. Fn = 0.1. H_w = 0.630 m.

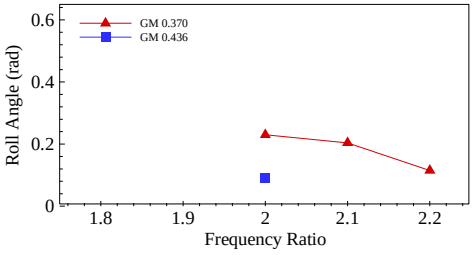

Figure 3.91. Max. Roll Angle. Fn = 0.0. H_w = 0.750 m.

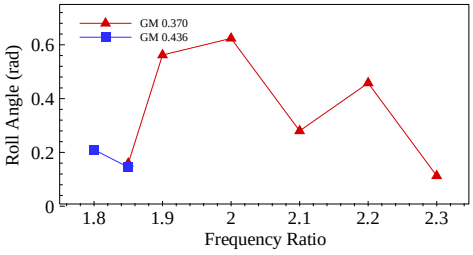

Figure 3.92. Max. Roll Angle. Fn = 0.1. H_w = 0.750 m.

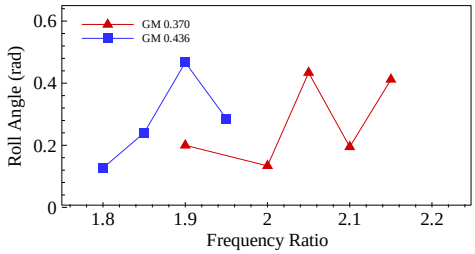

Figure 3.93. Max. Roll Angle. Fn = 0.15. H_w = 0.750 m.

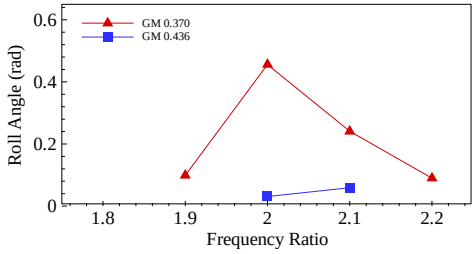

Figure 3.94. Max. Roll Angle. Fn = 0.0. H_w = 1.005 m.

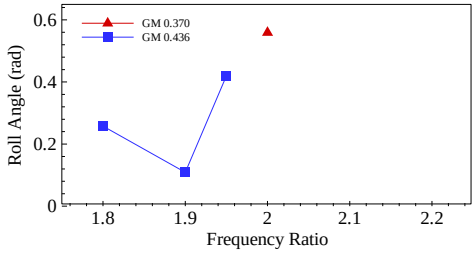

Figure 3.95. Max. Roll Angle. = 0.1. H_w = 1.005 m.

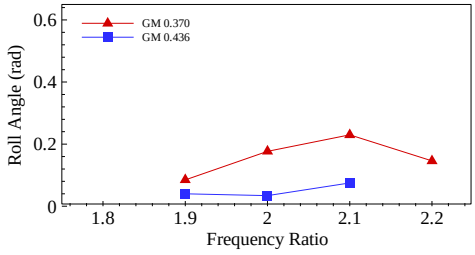

Figure 3.96. Max. Roll Angle. Fn = 0.0. H_w = 1.125 m.

In order to set up preventive strategies or a guidance to the master system that could help avoiding the development of parametric rolling in a real seaway, it is necessary to carry out such a previous intensive analysis of the different sailing conditions the ship could be facing and where roll resonance may take place; the best alternative is the use of a mathematical model.

The main objective of this section, as the one referring to the Spanish trawler model (Section 3.2.3), is to set up such a mathematical model that could reproduce the phenomenon of parametric roll resonance in head seas and validate its performance against the data obtained from the towing tank tests. Moreover, this model will be also used for evaluating the performance of the parametric rolling detection schemes that have been developed in this work and that will be subsequently presented.

In the section corresponding to the Spanish trawler (3.2.3), a one degree of freedom model has been set up, capable of simulating parametric roll in regular head seas. In this model, roll motion is computed completely uncoupled from the other degrees of freedom, taking into account the nonlinear behaviour of the damping and restoring terms. The parametric excitation is considered through the restoring term, which is time dependant following the wave motion along the hull. Moreover, the necessary contribution of heave and pitch motions has been taken into account following a quasi-static approach for the computation of the restoring arms.

In this section, the non linear model developed by (M.A.S. Neves,Rodríguez, 2006) has been used. This model computes, for regular head seas, the ship motions in three degrees of freedom (heave, roll and pitch) in a coupled way, thus considering the effects that longitudinal displacements and rotations (heave and pitch) have on roll motion and so, on the development of parametric roll.

This model is based on a third order Taylor series expansions of the position dependant forces and moments, from where the different nonlinear forcing and restoring terms are derived.

To describe ship motions in these three degrees of freedom, two orthornormal reference systems are stated, one fixed at the mean ship motion (ship speed) and another fixed to the ship, with its OXY plane coinciding with the sea surface in the absence of excitations or disturbances, and with the OZ axis pointing upwards and containing the centre of gravity (Figure 2.7). The ship equations of motion, considering the three degrees of freedom, can be written this way:

$$(M+A)\cdot\ddot{\vec{s}}+B(\dot{\phi})\cdot\dot{\vec{s}}+\vec{C}_{res}(\vec{s},\zeta)=\vec{C}_{ext}(\zeta,\dot{\zeta},\ddot{\zeta}) \tag{64}$$

Where $\vec{s}(t)=\left[z(t)\ \ \phi(t)\ \ \theta(t)\right]^T$ is the position vector (including heave translation and roll and pitch rotations), M is the system mass matrix, and A and $B(\dot{\phi})$ respectively represent the frequency dependant hydrodynamic added mass and damping matrices. $\vec{C}_{res}(\vec{s},\zeta)$ is the vector of non-linear restoring actions, dependant on the relative motions between ship hull and wave elevation $\zeta(t)$. The vector $\vec{C}_{ext}(\zeta,\dot{\zeta},\ddot{\zeta})$ represents the external excitation forces, including Froude – Krylov and diffraction forces, dependent on wave direction, encounter frequency ω_e, amplitude A_w and time, so that:

$$\vec{C}_{ext}(\zeta,\dot{\zeta},\ddot{\zeta})=\vec{C}_{ext(FK)}(\zeta)+\vec{C}_{ext(Diff.)}(\dot{\zeta},\ddot{\zeta}) \tag{65}$$

In this case, linear Airy Theory is used for modelling wave elevation. Taking also into account that the head seas case is being considered (and thus longitudinal waves), the equation of wave elevation at a given longitudinal position x is:

$$\zeta(x,t) = A_w \cdot \cos\left[k \cdot x + \omega_e \cdot t\right] \tag{66}$$

Where k is the wave number ($k = \frac{2 \cdot \pi}{\lambda}$).

In order to derive the aforementioned forcing and restoring terms in a coupled way, a vector $\vec{C}_{Pos}$ of forces and moments depending on ship position (but also considering the effects of wave elevation along the hull), may be defined and decomposed up to the third order in a Taylor Series expansion. If a generalized vector $\vec{q} = \left[\vec{s}, \zeta\right]^T$ is defined, then that $\vec{C}_{Pos}$ vector may be expressed in the following way:

$$\vec{C}_{Pos} = \sum_{i=1}^{4} \frac{\partial \vec{C}_{Pos}}{\partial q_i}\bigg|_0 q_i + \frac{1}{2}\sum_{i=1}^{4}\sum_{j=1}^{4} \frac{\partial^2 \vec{C}_{Pos}}{\partial q_i \partial q_j}\bigg|_0 q_i q_j + \frac{1}{6}\sum_{i=1}^{4}\sum_{j=1}^{4}\sum_{k=1}^{4} \frac{\partial^3 \vec{C}_{Pos}}{\partial q_i \partial q_j \partial q_k}\bigg|_0 q_i q_j q_k \tag{67}$$

From the previous equation, the terms that are not dependent on $\vec{s}(t) = \left[z(t) \;\; \phi(t) \;\; \theta(t)\right]^T$, represent the linear and non-linear Froude-Krylov forces and can be expressed as follows:

$$\vec{C}_{ext(FK)}(\zeta) = \frac{\partial \vec{C}_{Pos}}{\partial \zeta}\bigg|_0 \cdot \zeta + \frac{1}{2}\frac{\partial^2 \vec{C}_{Pos}}{\partial \zeta^2}\bigg|_0 \cdot \zeta^2 + \frac{1}{6}\frac{\partial^3 \vec{C}_{Pos}}{\partial \zeta^3}\bigg|_0 \zeta^3 \tag{68}$$

Taking this into account, the restoring forces vector could be written as

$$\vec{C}_{res} = \vec{C}_{pos}(z \;\; \phi \;\; \theta \;\; \zeta) - \vec{C}_{ext(FK)}(\zeta) \tag{69}$$

As have been already mentioned, diffraction forces and moments, not dependant on ship motions, have been included in the $\vec{C}_{ext}(\zeta, \dot{\zeta}, \ddot{\zeta})$ term, and considered only up to first order.

Regarding the non linear forcing terms proportional to the relative displacement between hull and waves (wave passing effects) up to third order, the authors have placed them into the $\vec{C}_{res}(\vec{s},\zeta)$ vector, due to their similarities with the classical hydrostatic restoring actions, where hydrostatic actions in calm water are also included up to third order.

In this model, all terms in matrices A and B are calculated using potential theory, except for the case of roll damping $B_{44}(\dot{\phi})$ where, as have been described in the previous section, non-linear contributions up to the second order have to be included for properly simulating parametric roll, so that

$$B_{44}(\dot{\phi})\dot{\phi} = B_{44a}\dot{\phi} + B_{44b}\dot{\phi}\left|\dot{\phi}\right| \tag{70}$$

In (M.A.S. Neves,Rodríguez, 2006), the authors have followed the empirical Ikeda approach for computing roll damping terms (Himeno, 1981). In this work, damping coefficients have been obtained from roll decay tests carried out in the towing tank, with the objective of increasing the accuracy of the model.

Regarding wave excitation forces (Froude – Krylov and diffraction), they have also been computed by potential flow approximation. For the computation of the non linear effects of wave passing along the hull, the instantaneous sea surface and the flare and breadth distribution of the different hull sections have been considered. Finally, this flare distribution has also been taken in account for obtaining the restoring terms in calm water.

Therefore, equation (64) presents a nonlinear model where, unlike other approaches, roll motion is coupled to the other two degrees of freedom. All the details of this development, together with the description, computation and discussion of all the parameters and coefficients involved, may be found in the

aforementioned work (M.A.S. Neves,Rodríguez, 2006) and the same authors´ references therein.

3.3.3.1 Roll Damping

As have been indicated above, roll decay tests have been carried out in the test basin with the objective of determining the two components in which the nonlinear roll damping has been divided.

The followed methodology has been the same as explained for the "Spanish trawler" case. On one hand, roll decay tests have been carried out for four different values of forward speed, and for the two loading conditions which are being considered in this work (a high metacentre one (GM = 0.436 m) and a low metacentre condition (GM = 0.370 m)). Regarding the low GM case, four runs have been done for zero forward speed, two runs for Fn = 0.1 and 0.2 cases and one for Fn = 0.3. In the high GM condition, three runs have been carried out for the zero speed case, two runs correspond to Fn = 0.1 and 0.2 and another one has been carried out for the highest speed (Fn = 0.3).

The procedure for determining the damping coefficients consisted again on setting up the roll decrement curves for each condition and, by using a quadratic fitting, determining the corresponding extinction coefficients from which the damping terms will be obtained (see Section 3.2.3.3).

In Figure 3.97 and Figure 3.98, the obtained roll decrement data for the four considered speeds and the two GM´s are presented, together with the quadratic fitting used for computing the corresponding extinction coefficients.

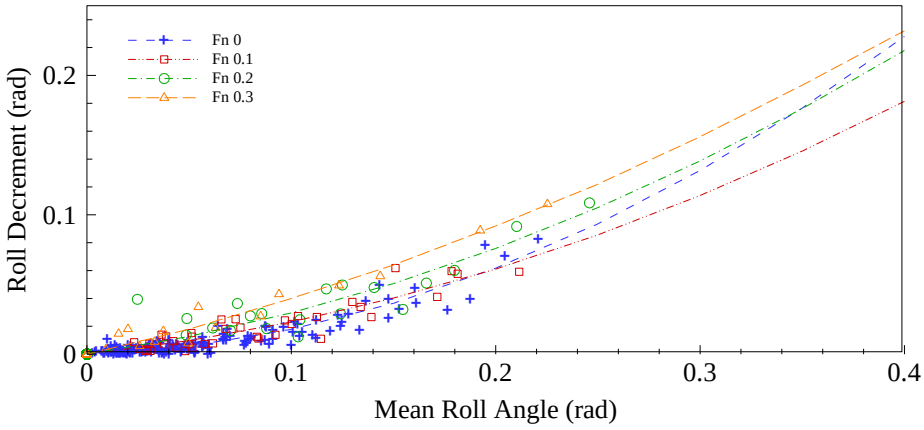

Figure 3.97. Roll decrement data (scatter points) and fitting quadratic polynomial (lines) from roll decay tests. GM = 0.370 m.

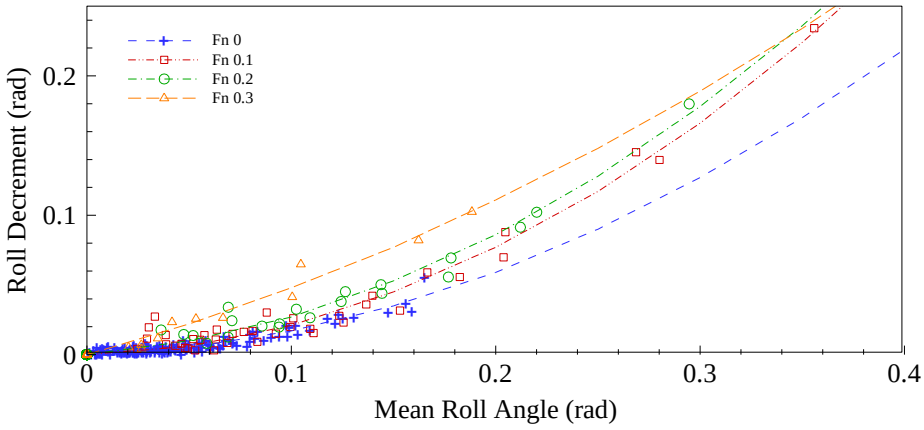

Figure 3.98. Roll decrement data (scatter points) and fitting quadratic polynomial (lines) from roll decay tests. GM = 0.436 m.

The damping coefficients obtained from the aforementioned data, are included in Table 3.14, Table 3.15, Table 3.16, and Table 3.17, for the two metacentric heights considered. Moreover, the corresponding purely linear damping coefficients have also been included. Finally, a comparison of the damping moments obtained by using the damping coefficients from the roll decay tests and those computed by using the Ikeda approach, for the GM 0.370 m case, is presented in Figure 3.99, Figure 3.100, Figure 3.101 and Figure 3.102.

Table 3.14. Damping coefficients. GM = 0.370 m.

	Damping Coeff.	Fn 0	Fn 0.1	Fn 0.2	Fn 0.3
Quadratic Damping	B_{44a} (t·m^2/s)	10.85	35.68	47.79	69.84
	B_{44b} (t·m^2)	404.32	228.10	246.84	160.30
Purely Linear Damping	B_{44} (t·m^2/s)	47.90	58.80	78.09	91.24

Table 3.15. Damping coefficients. GM = 0.436 m.

	Damping Coeff.	Fn 0	Fn 0.1	Fn 0.2	Fn 0.3
Quadratic Damping	B_{44a} (t·m^2/s)	11.09	10.47	28.13	98.04
	B_{44b} (t·m^2)	422.76	574.92	542.76	233.61
Purely Linear Damping	B_{44} (t·m^2/s)	42.34	104.42	106.39	125.17

From the observation of the results of these analyses, one fact may be highlighted. While for the high GM case the four decrement curves run approximately parallel, representing higher damping values as speed is increased, in the low GM case this fact is not exactly true. Although the decrement curves corresponding to Fn = 0.1, 0.2 and 0.3 follow this same behaviour, roll damping corresponding to the zero speed case grows faster with average roll angle than those corresponding to the moving ship. In fact, roll damping at zero speed exceeds that of the Fn = 0.1 case for angles above 0.2 rad, and even equals that of the Fn = 0.2 case for roll angles over 0.35 rad.

Table 3.16. Adimensional damping coefficients. GM = 0.370 m.

	Damping Coeff.	Fn 0	Fn 0.1	Fn 0.2	Fn 0.3
Quadratic Damping	ν	0.0076	0.0250	0.0341	0.0533
	β	0.4895	0.2776	0.3100	0.2308
Purely Linear Damping	ν_L	0.0335	0.0412	0.0557	0.0696

Table 3.17. Adimensional damping coefficients. GM = 0.436 m.

	Damping Coeff.	Fn 0	Fn 0.1	Fn 0.2	Fn 0.3
Quadratic Damping	ν	0.0069	0.0065	0.0174	0.0637
	β	0.4737	0.6414	0.6056	0.2871
Purely Linear Damping	ν_L	0.0263	0.0646	0.0658	0.0813

This fact could explain the behaviour observed from the analysis of the results of the towing tank tests, regarding the differences of the unstable regions between the Fn = 0 and 0.1 cases (Figure 3.64 and Figure 3.65).

According to the usual dependence of damping with speed, the increase in speed would also imply an increase in damping; so, the unstable region corresponding to the higher speed should have moved “upwards” in comparison to that of the zero speed case.

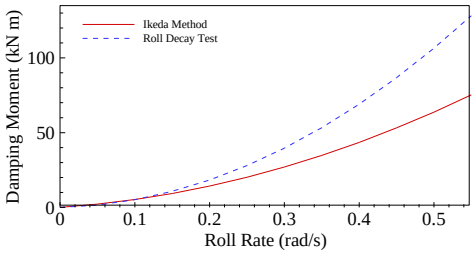

Figure 3.99. Roll Damping Comparison. Fn = 0.0. GM = 0.370 m.

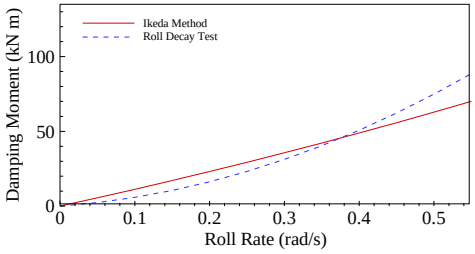

Figure 3.100. Roll Damping Comparison. Fn = 0.1. GM = 0.370 m.

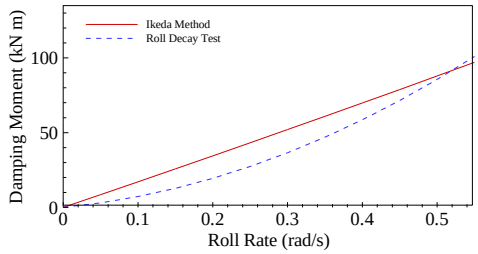

Figure 3.101. Roll Damping Comparison. Fn = 0.2. GM = 0.370 m.

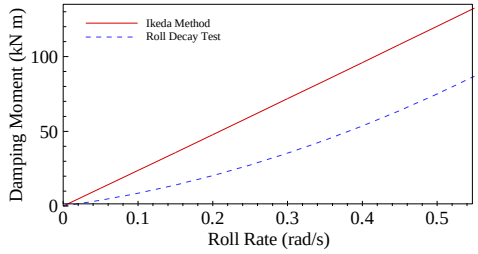

Figure 3.102. Roll Damping Comparison. Fn = 0.3. GM = 0.370 m.

The behaviour observed in the present tests, where the lower vertex of the Fn = 0.1 unstable area takes place at lower wave heights than that of the zero speed case and that is apparently opposite to the standard behaviour, could then be explained by this damping response.

At the same time, the relatively low roll amplitudes observed for the zero speed cases in comparison to that of the cases with forward speed, as could be observed, for example, in Figure 3.87, are also explainable taking in account the aforementioned behaviour of roll damping at zero speed.

Regarding the comparison of the results obtained by the roll decay tests and those from the Ikeda empirical method, it could be concluded that, for the cases where forward speed is present, the Ikeda damping seems to be quite accurate, obtaining very similar results to those form the decay testing, with the exception of the highest speed case, where Ikeda method over predicts roll damping for all roll values. In addition, and regarding the zero forward speed

case, roll damping is under predicted by the Ikeda method, especially at large roll rates. The obtained damping curve is less steep than the real one and, in fact, follows the expectable results that could be seen, for example, in the GM = 0.436 m case (Figure 3.98).

Finally, the validation of the results has been carried out by comparing the data obtained from the roll decay tests with the time series obtained by using the proposed mathematical model, for the three values of forward speed considered and the two metacentric heights. These results are presented in Figure 3.103 to Figure 3.110. From them, it could be concluded that the damping model is quite accurate, as good results have been obtained in all the tested conditions, at least for the roll amplitudes under consideration.

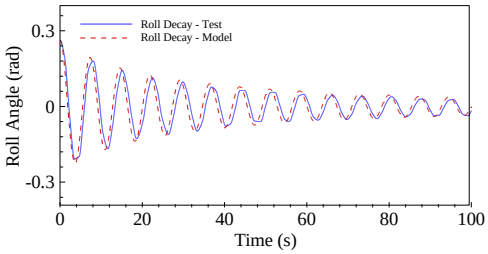

Figure 3.103. Roll decay tests. Fn = 0. GM = 0.370 m.

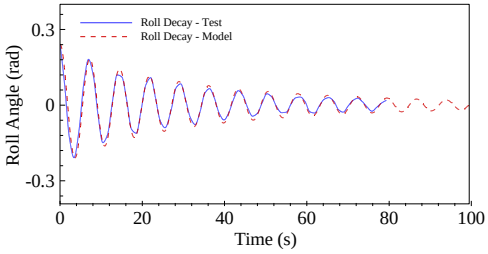

Figure 3.104. Roll decay tests. Fn = 0.1. GM = 0.370 m.

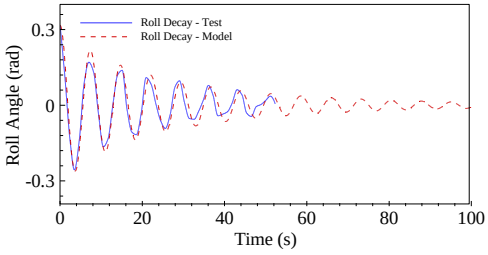

Figure 3.105. Roll decay tests. Fn = 0.2. GM = 0.370 m.

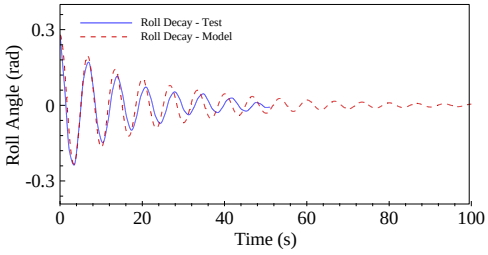

Figure 3.106. Roll decay tests. Fn = 0.3. GM = 0.370 m.

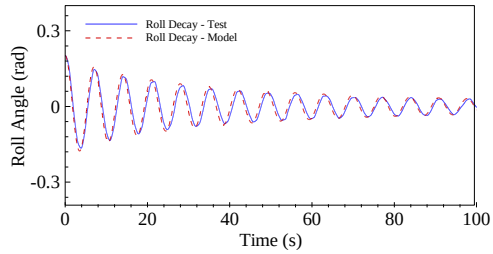

Figure 3.107. Roll decay tests. Fn = 0. GM = 0.436 m.

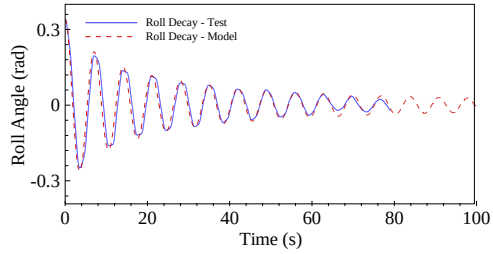

Figure 3.108. Roll decay tests. Fn = 0.1. GM = 0.436 m.

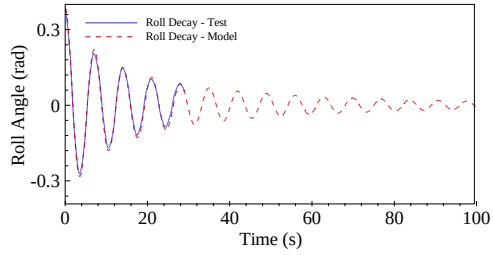

Figure 3.109. Roll decay tests. Fn = 0.2. GM = 0.436 m.

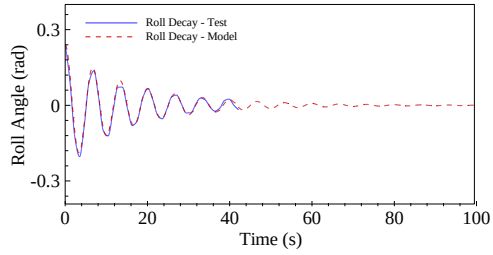

Figure 3.110. Roll decay tests. Fn = 0.3. GM = 0.436 m.

3.3.3.2 Model Validation.

As have previously been done in the case of the Spanish trawler, the results obtained in the towing tank tests have been compared to those computed using the mathematical model, in order to study its performance in the different conditions.

The two analyzed loading conditions are those also considered in the towing tank tests (see Table 3.11) and four different speed values have been taken into account, corresponding to Froude numbers of 0, 0.10, 0.15 and 0.20.

In figures from Figure 3.111 to Figure 3.125, the time series obtained both from the towing tank tests and the mathematical model for the high GM condition (GM = 0.436 m) are presented. In figures from Figure 3.126 to Figure 3.131 , the results corresponding to the low GM loading condition (GM = 0.370 m) are shown.

Regarding the high GM case with no forward speed (Figure 3.111 to Figure 3.117), two different facts should be highlighted regarding the behaviour of the mathematical model. On one hand, and for frequency ratios of 2.0 and lower, no parametric resonance events are predicted by the model. Although in all cases parametric roll resonance takes place, its amplitude is very low and may be due to an over excitation generated by a small misalignment of the model with the pure head waves situation.

On the other hand, when frequency ratio is increased to 2.10 (Figure 3.114, Figure 3.116 and Figure 3.117), the low amplitude resonance present in the towing tank test is over predicted by the model, which predicts a quite large amplitude roll resonance.

When the vessel speed is increased to a Fn = 0.10, the model still under predicts roll motions for the lowest frequency ratios (in this case only those under 2.0, Figure 3.118 and Figure 3.121), but obtains better results for the higher tuning ratios, especially for the largest wave heights (Figure 3.120).

If speed is increased up to a Froude number of 0.15 (Figure 3.122 to Figure 3.124), the results turn out to be accurate in all conditions, regardless of the frequency ratio; finally, and for the maximum forward speed considered (Figure 3.125), the results are again quite accurate.

Regarding the low GM loading condition (Figure 3.126 to Figure 3.131), the results are very similar to those of the previous case. When no forward speed is present (Figure 3.126 to Figure 3.128), the parametric rolling events which took place in the towing tank tests are not predicted by the math model. In the Froude 0.1 case, although the model predicts the development of parametric rolling, the obtained amplitude is much less than that observed in the scale model tests. Finally, when forward speed is increased up to a Froude number of 0.15, and in the same way that it did for the high GM condition, the mathematical model predicted parametric rolling in all cases and the maximum steady state roll amplitude was accurately computed.

In (M.A.S. Neves,Rodríguez, 2006), model and experiment results of this same ship, for the GM = 0.370 m condition, a frequency ratio of 2.0 and Froude numbers of Fn = 0.15 m, Fn = 0.20 and Fn = 0.30 are presented. In this reference, model performance appears to be very good in all conditions, although some underestimation is observed for the highest wave heights. This fact is also observed in the data presented in this thesis; see for example, Figure 3.122 and Figure 3.123 or Figure 3.111, Figure 3.112 and Figure 3.113.

On the other hand, model results presented in the reference above seem to fit experimental results more accurately than those presented herein. In addition, experimental results also present a clear steady state motion after the transient period, while in the experimental results presented in this section the motion seems to be more variable. This fact may be explained by the influence of the six degrees of freedom motions in which the UK Trawler model developed in this section is free to move, and which induce more irregularities in the roll motion. The fact that the data presented in Section 3.2 clearly resemble those obtained in (M.A.S. Neves,Rodríguez, 2006) and that the experimental arrangement in both cases is very similar, may also support the conclusion above.

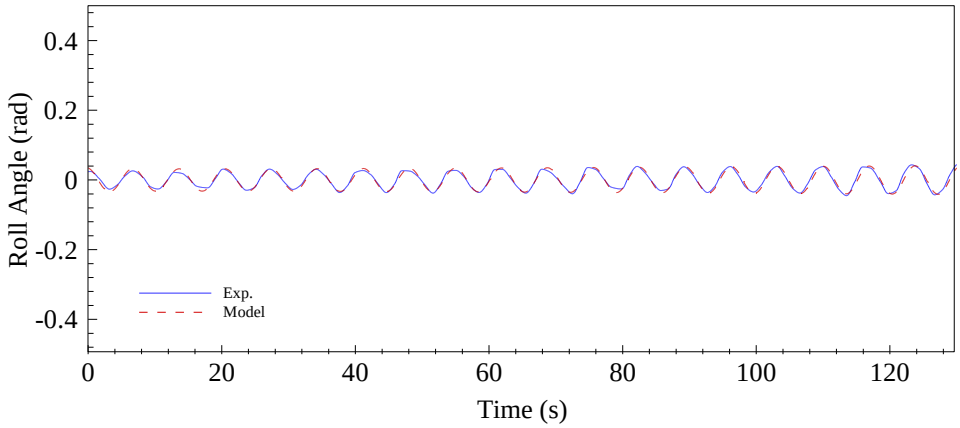

Figure 3.111. Roll data. GM = 0.436 m. Fn = 0. Freq. Ratio = 2.0. H_w = 0.375 m. λ = 18.4 m.

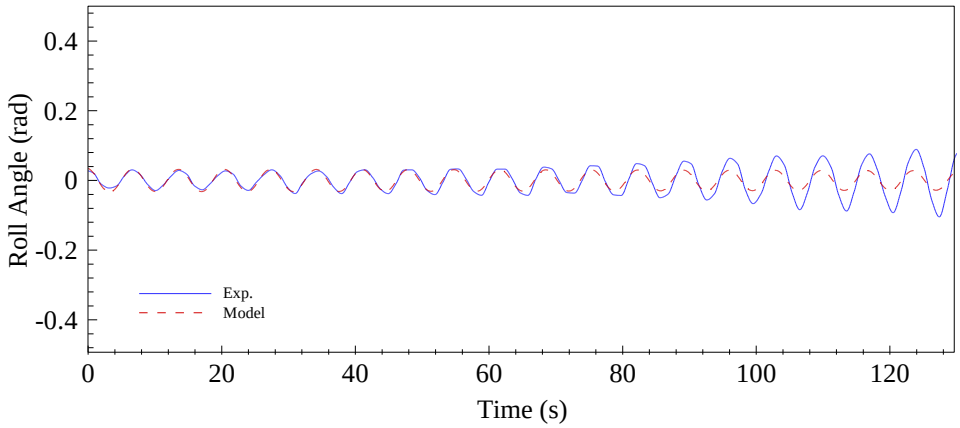

Figure 3.112. Roll data. GM = 0.436 m. Fn = 0. Freq. Ratio = 2.0. H_w = 0.495 m. λ = 18.4 m

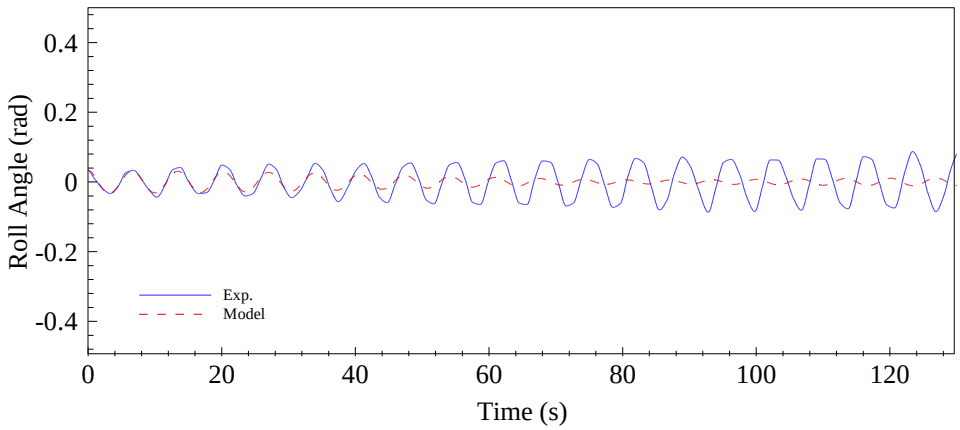

Figure 3.113. Roll data. GM = 0.436 m. Fn = 0. Freq. Ratio = 2.0. H_w = 0.630 m. λ = 18.4 m.

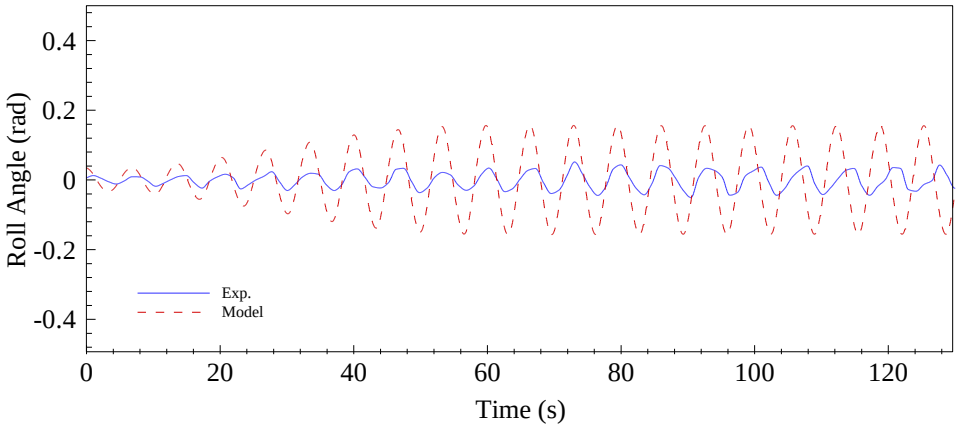

Figure 3.114. Roll data. GM = 0.436 m. Fn = 0. Freq. Ratio = 2.1. H_w = 0.630 m. λ = 16.7 m.

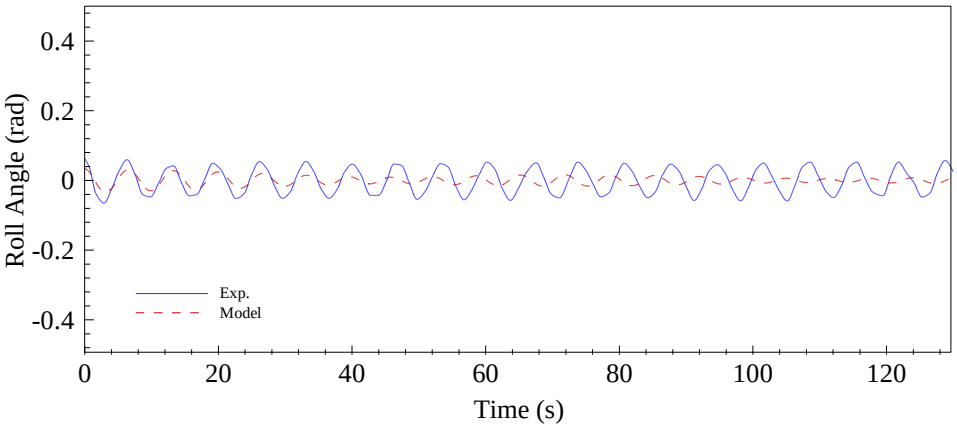

Figure 3.115. Roll data. GM = 0.436 m. Fn = 0. Freq. Ratio = 2.0. H_w = 0.750 m. λ = 18.5 m.

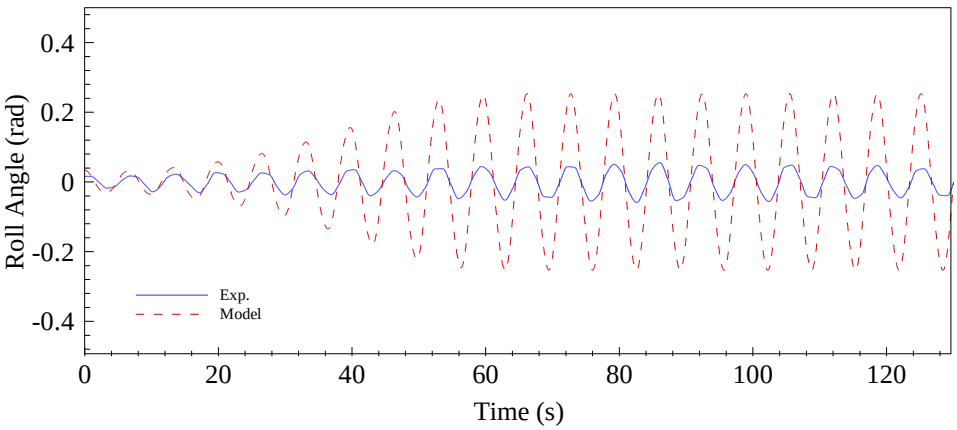

Figure 3.116. Roll data. GM = 0.436 m. Fn = 0. Freq. Ratio = 2.1. H_w = 1.005 m. λ = 16.7 m.

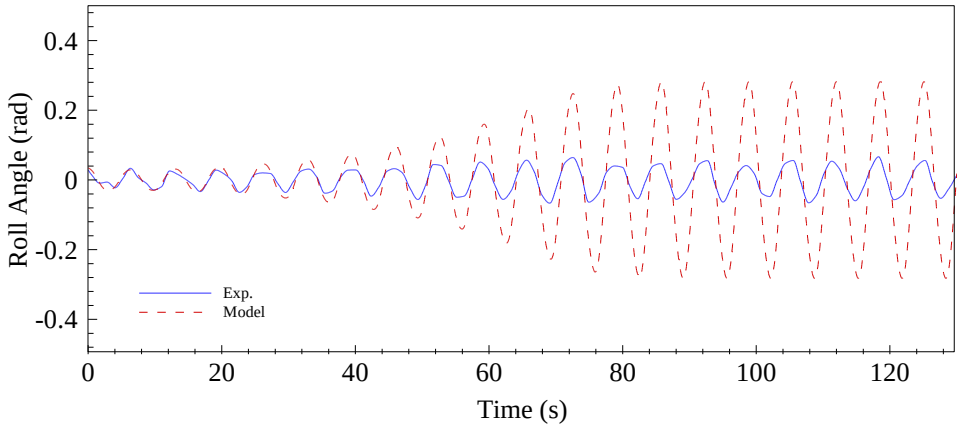

Figure 3.117. Roll data. GM = 0.436 m. Fn = 0. Freq. Ratio = 2.10. H_w = 1.125 m. λ = 16.5 m.

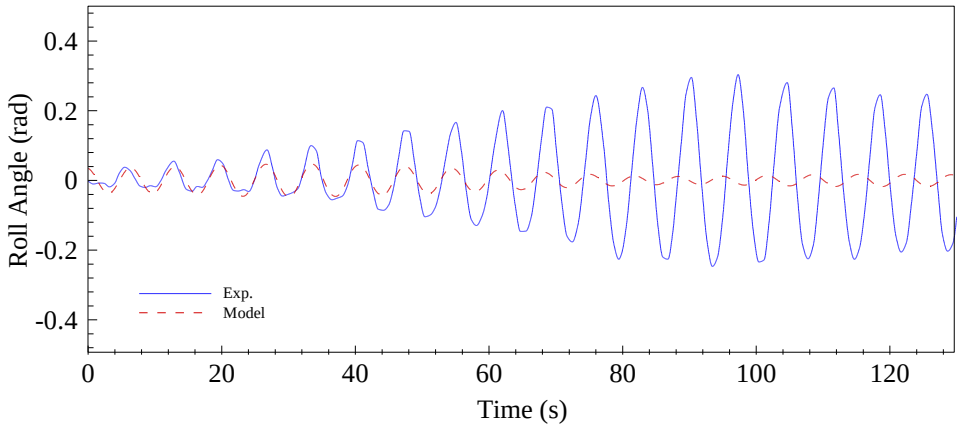

Figure 3.118. Roll data. GM = 0.436 m. Fn = 0.1. Freq. Ratio = 1.95. H_w = 0.375 m. λ = 27.5 m.

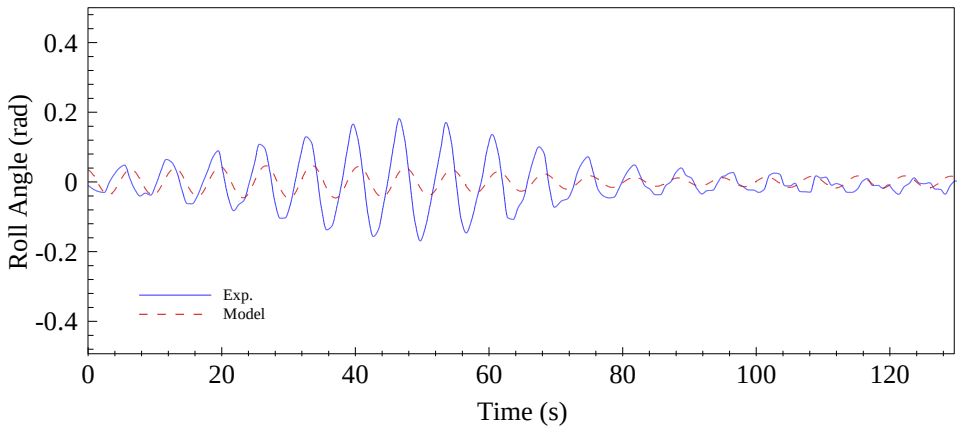

Figure 3.119. Roll data. GM = 0.436 m. Fn = 0.1. Freq. Ratio = 2.00. H_w = 0.375 m. λ = 27.5 m.

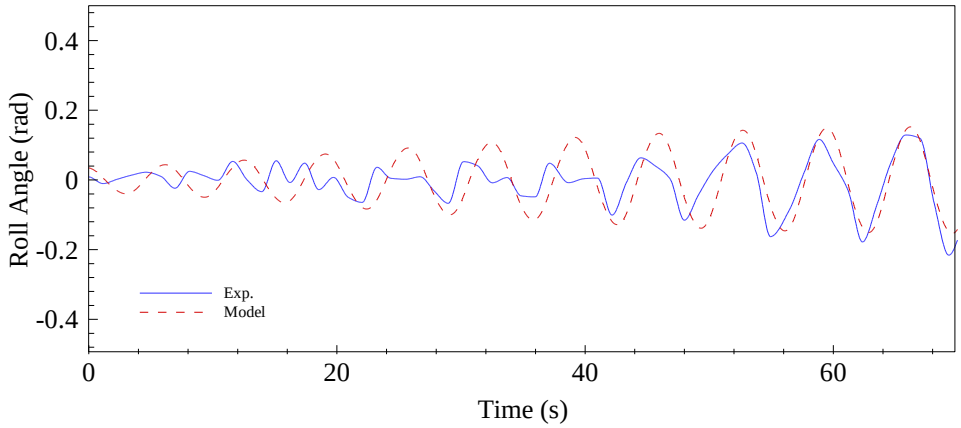

Figure 3.120. Roll data. GM = 0.436 m. Fn = 0.1. Freq. Ratio = 2.00. H_w = 0.630 m. λ =27.5 m.

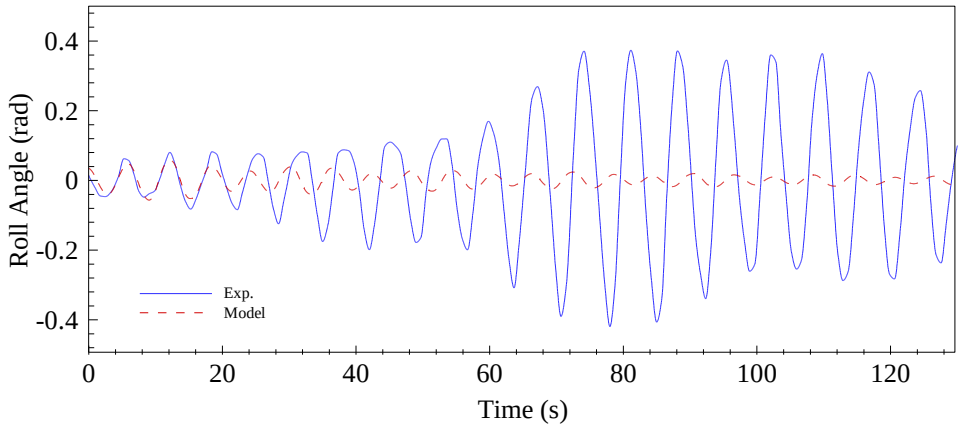

Figure 3.121. Roll data. GM = 0.436 m. Fn = 0.1. Freq. Ratio = 1.95. H_w = 1.005 m. λ =27.5 m.

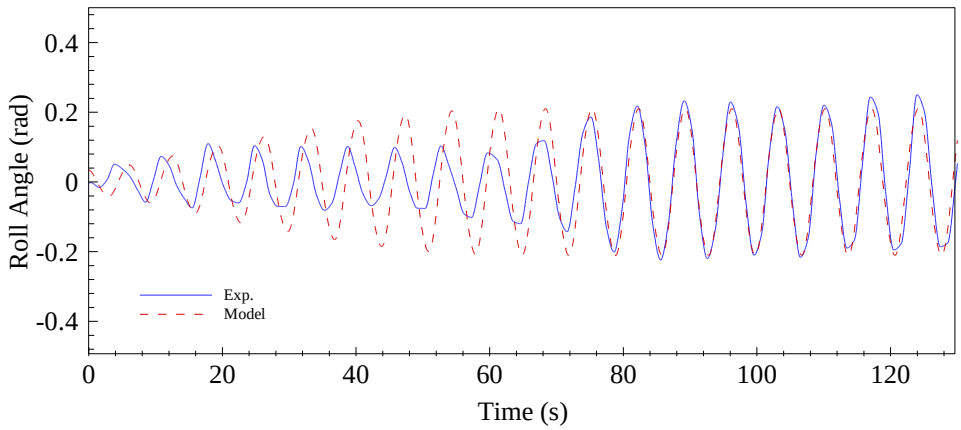

Figure 3.122. Roll data.GM = 0.436 m. Fn = 0.15. Freq. Ratio = 1.95. H_w = 0.630 m. λ =31.7 m.

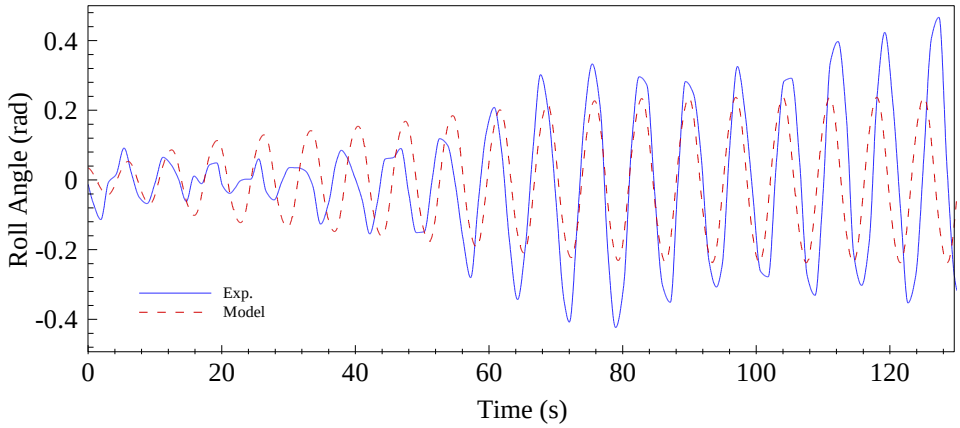

Figure 3.123. Roll data.GM = 0.436 m. Fn = 0.15. Freq. Ratio = 1.90. H_w = 0.750 m. λ =31.7 m.

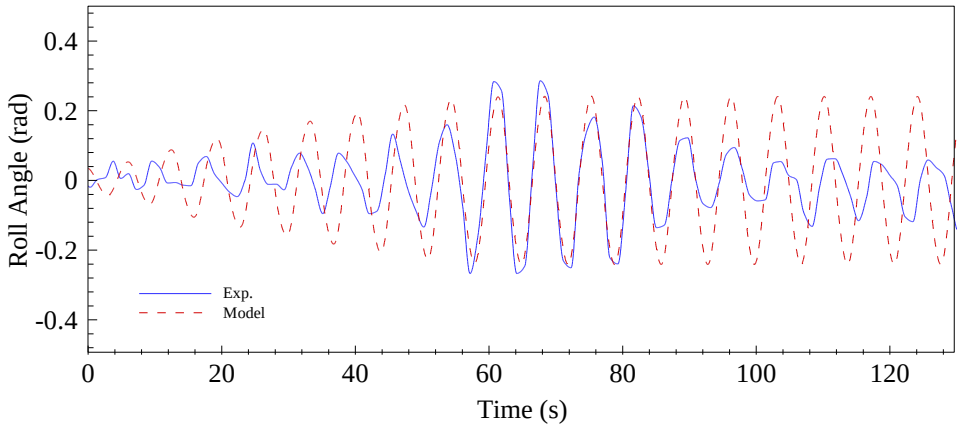

Figure 3.124. Roll data.GM = 0.436 m. Fn = 0.15. Freq. Ratio = 1.95. H_w = 0.750 m. λ =31.7 m.

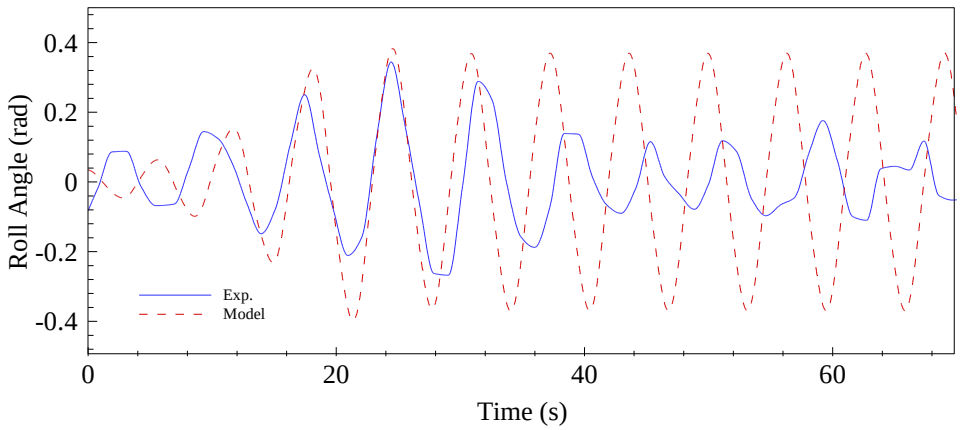

Figure 3.125. Roll data.GM = 0.436 m. Fn = 0.20. Freq. Ratio = 2.20. H_w = 1.005 m. λ =31.7 m.

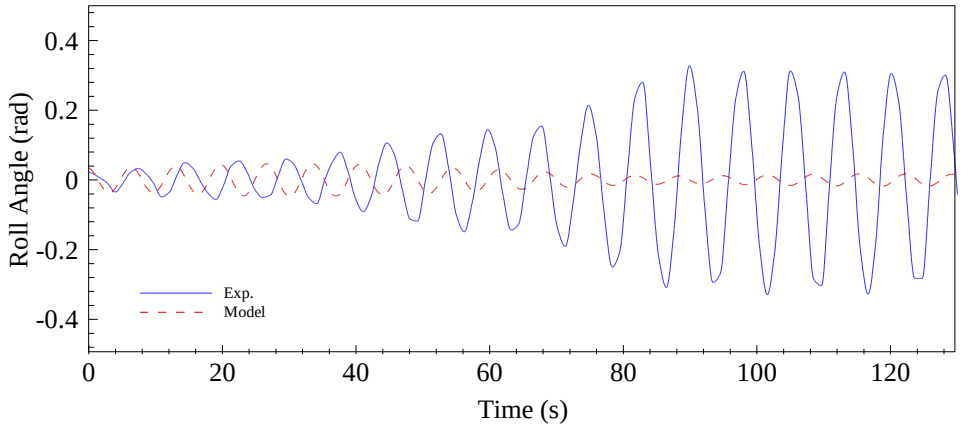

Figure 3.126. Roll data. GM = 0.370 m. Fn = 0. Freq. Ratio = 2.00. H_w = 1.005 m. λ = 21.9 m.

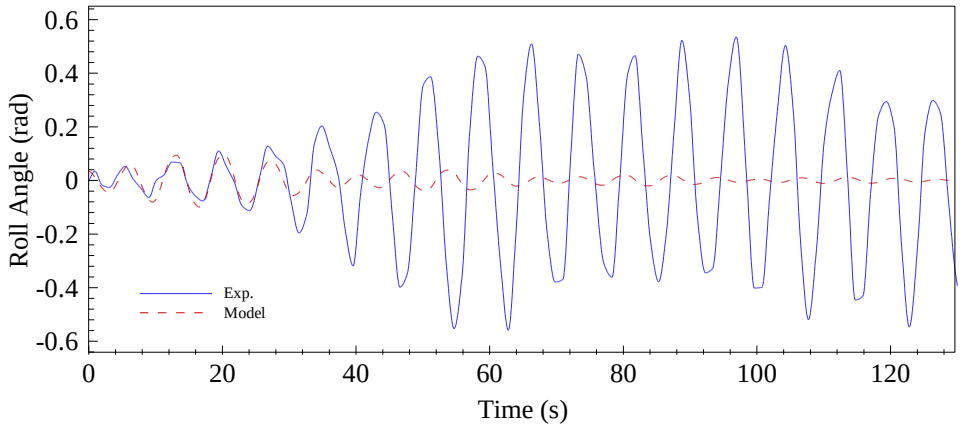

Figure 3.127. Roll data. GM = 0.370 m. Fn = 0. Freq. Ratio = 2.00. H_w = 1.005 m. λ = 32.0 m.

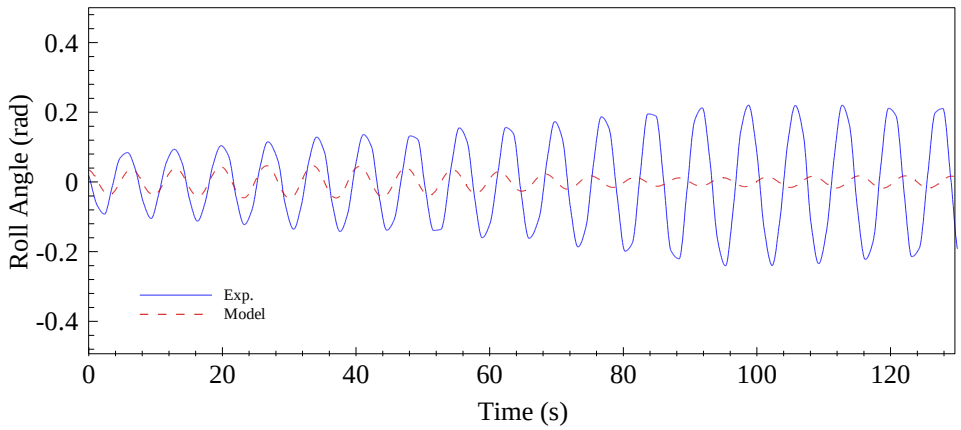

Figure 3.128. Roll data. GM = 0.370 m. Fn = 0. Freq. Ratio = 2.10. H_w = 1.005 m. λ = 19.9 m.

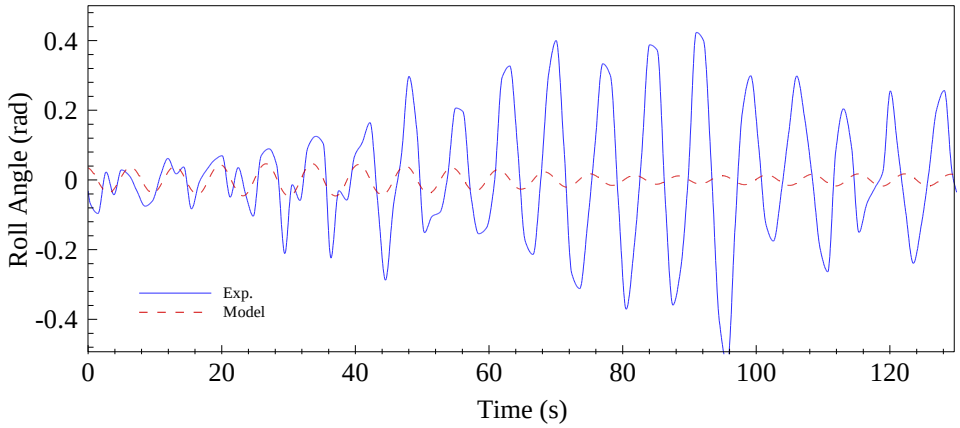

Figure 3.129. Roll data.GM = 0.370 m. Fn = 0.10. Freq. Ratio = 2.10. H_w = 0.630 m. λ =29.4 m.

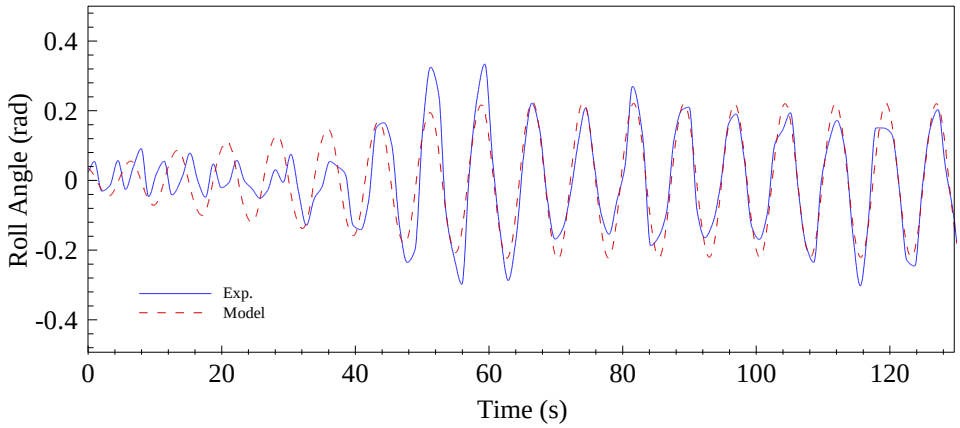

Figure 3.130. Roll data.GM = 0.370 m. Fn = 0.15. Freq. Ratio = 2.05. H_w = 0.750 m. λ =31.4 m.

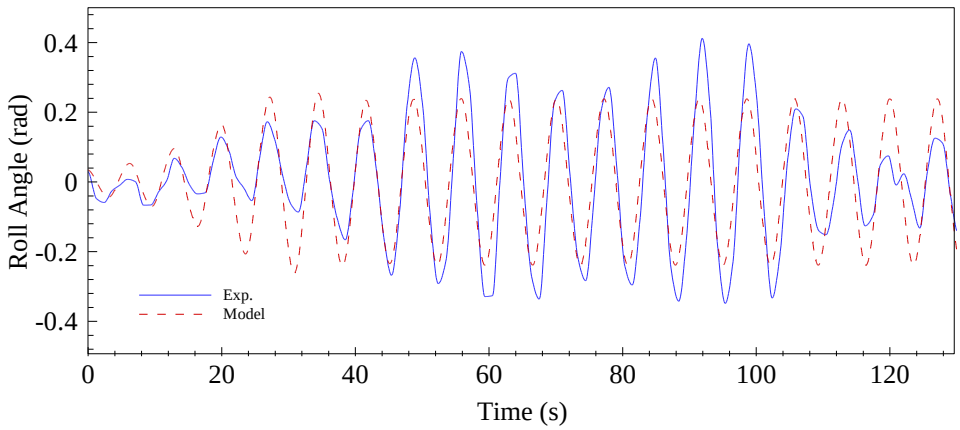

Figure 3.131. Roll data. GM = 0.370 m. Fn = 0.15. Freq. Ratio = 2.1. H_w = 0.750 m. λ =33.7m.

3.3.3.3 Ship Stability Analysis. Regular Waves.

Once the performance of the model has been evaluated for the different sailing conditions, it has been used for computing the complete stability diagrams that correspond to the previous conditions, together with additional ones which have not been tested in the towing tank, and that would be useful for analyzing the vessel behaviour in the whole range of operational conditions. Moreover, the comparison of these diagrams to the scatter ones obtained from the scale model tests, which were shown from Figure 3.64 to Figure 3.71, will also be helpful for completing the validation analysis carried out in the previous section. Again, for simplifying this comparison, the results obtained from these experiments have been superimposed to the corresponding mathematical plots; green dots represent non-resonant conditions, while resonance is shown by the red dots.

Taking this into account, the model has been recursively executed for a set of combinations of different wave frequencies and heights, covering the frequency ratio range from 1.70 to 2.40 and wave heights from 0.20 to 1.20 m, at each operational condition under consideration. These are composed by the two previously studied loading conditions (GM = 0.370 m and 0.436 m) and by five values of forward speed, corresponding to the zero speed case, the three values analyzed in the towing tank tests (Fn = 0.10, 0.15 and 0.20), and an additional value of Fn = 0.30, which could represent a typical cruising speed for such a ship (9 knots) and that has not been previously considered.

The obtained stability diagrams are presented from Figure 3.132 to Figure 3.136 for the low GM condition (GM = 0.370 m) and in figures from Figure 3.137 to Figure 3.141 for the higher GM one (GM = 0.436 m).

Regarding the low metacentric height case, the diagrams corresponding to the zero speed and the Fn = 0.1 conditions (Figure 3.132, Figure 3.133) show small unstable regions, which for the zero speed case do not coincide with the previously described experimental results but that for the Fn = 0.1 case are reasonably well tracked by the model. If speed is increased up to Fn = 0.15 (Figure 3.134), the unstable area significantly grows, extending from frequency ratios over 1.80 and reaching the largest amplitudes for the largest wave heights and ratios around 2.0. In this case, the shape of the unstable region matches the results obtained in the towing tank tests, that together with the accurate results obtained while computing roll amplitude at speeds over Fn = 0.15, show a good performance of the mathematical model. A rising in speed up to Fn = 0.2 (Figure 3.135), implies a reduction in its surface and a displacement of the unstable region to the right side of the diagram. The highest roll amplitudes take now place at frequency ratios over 2.10, also for the highest wave height values. This displacement to the right appears to be larger than the one observed in the towing tank tests, although not enough data is available for this condition as to determine the unstable region real shape. Finally, the unstable area computed for a Fn = 0.3 (Figure 3.136) spreads over the whole range of frequency ratios. Although the lower vertex is placed around a tuning ratio of 2.0, the worst conditions are also found at the upper-right corner of the diagram, for ratios of 2.20 and wave heights over 1.0 m.

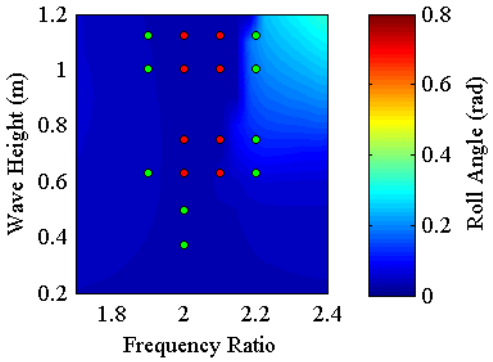

Figure 3.132. Stability Diagram.
Fn = 0. GM = 0.370 m.

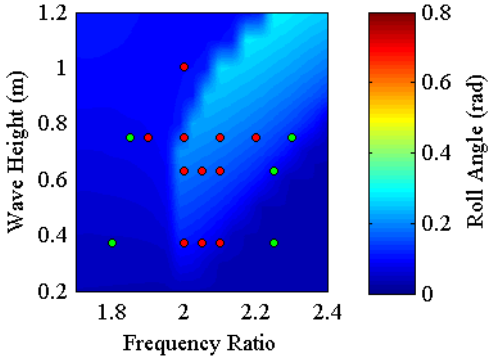

Figure 3.133. Stability Diagram.
Fn = 0.10. GM = 0.370 m.

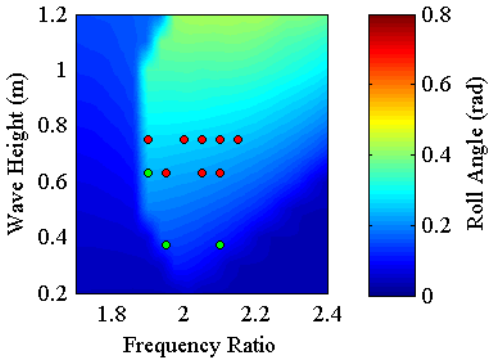

Figure 3.134. Stability Diagram.
Fn = 0.15. GM = 0.370 m.

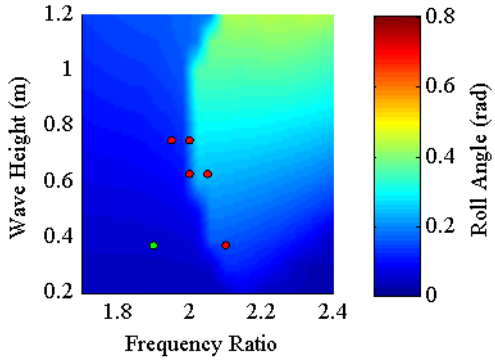

Figure 3.135. Stability Diagram.
Fn = 0.20. GM = 0.370 m.

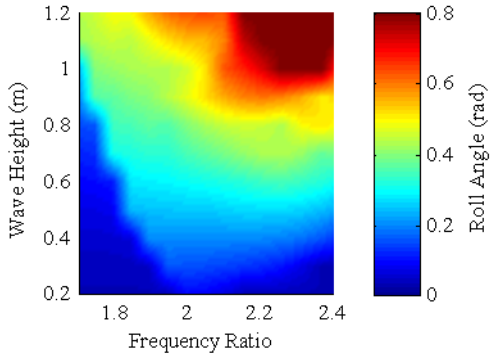

Figure 3.136. Stability Diagram.
Fn = 0.30. GM = 0.370 m.

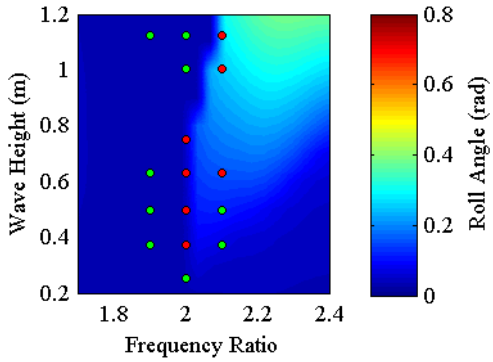

Figure 3.137. Stability Diagram.
Fn = 0. GM = 0.436 m.

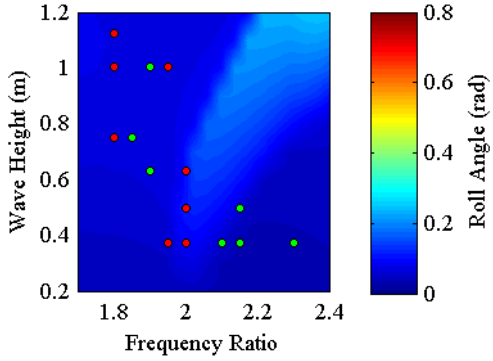

Figure 3.138. Stability Diagram.
Fn = 0.10. GM = 0.436 m.

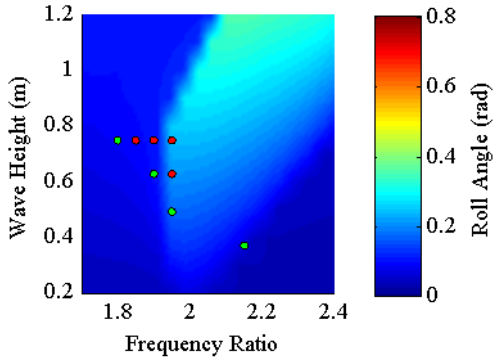

Figure 3.139. Stability Diagram.
Fn = 0.15. GM = 0.436 m.

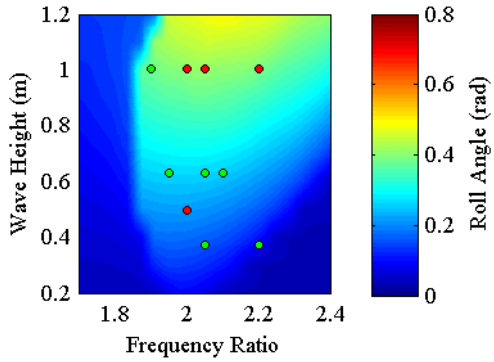

Figure 3.140. Stability Diagram.
Fn = 0.20. GM = 0.436 m.

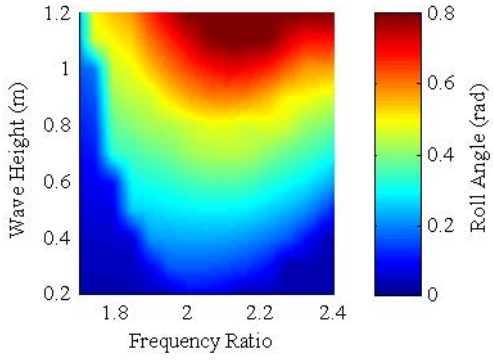

Figure 3.141. Stability Diagram.
Fn = 0.30. GM = 0.436 m.

Regarding the high GM condition, the unstable area for the zero speed case (Figure 3.137) is now larger and similar in shape to the one obtained from the towing tank tests, although the former is slightly drifted to higher frequencies. The results for the Fn = 0.1 condition (Figure 3.138) show a reduced unstable region, with light resonance present. According to the scale model results, resonance should be present at wave heights over 0.40 m at ratios around 2.0, which together with the resonant band centered at a tuning ratio of 1.80 are not reproduced by the model. For a Fn = 0.15 (Figure 3.139), although not much experimental data are available for comparison, the unstable area computed by the model is again drifting to higher frequencies, especially for the largest wave heights. Increasing the speed implies, both for Fn = 0.2 and 0.3, an increase in the unstable region, maintaining in the two conditions a lower vertex placed at frequency ratios around 2.00 and highest roll amplitudes at 2.10, corresponding to the largest wave heights. Moreover, the unstable region obtained from towing tank tests for the Fn = 0.2 condition seems to have its lower vertex placed at higher wave heights than the numerical one, which extends upwards from a wave height of 0.2 m.

From the previous analysis and the comparison of the results obtained for the two loading conditions, some conclusions may be obtained about the influence of the metacentric height, roll damping and forward speed on the shape, position and size of the unstable regions.

If the low metacentre condition is considered, the zero forward speed case is, from the five tested forward speeds, the one where the unstable region is smaller. An increase in speed, implies also an increasing of the size of the unstable area, that extends from the upper-right corner to its lower vertex, placed at a tuning ratio of 2.0 and a wave height of less than 0.40 m. If these diagrams (Figure 3.132 and Figure 3.133) are compared to those corresponding

to the high metacentre condition (Figure 3.137 and Figure 3.138) and the same speeds, it can be seen that the unstable area for a Fn = 0 is now much bigger, and an increase in speed up to a Fn = 0.1 implies a reduction in the size of this unstable area, instead of the increase previously seen.

The first fact may be explained by the higher damping present in the zero speed case, that exceeds that of the Fn = 0.1 condition and that compensates the possible effects of the shorter wavelengths present at the zero speed case, which are in the range of the ship length.

In the high GM case, the lower damping present in the zero speed case should be one of the causes of the larger unstable area. Moreover, wavelengths at the zero speed case are in the range of ship length, while those present at Fn = 0.1 are slightly longer. These two circumstances may compensate the possible influence of the larger pitch motions present at the higher speeds.

If speed is increased from Fn = 0.1 to Fn = 0.15, in both cases the unstable area grows; although roll damping increases, the larger effects of pitch motion (due to the encountering with steeper waves), which increase the amplitude of parametric excitation, compensate the higher damping.

This same behaviour takes place for the high GM condition, for speeds up to Fn = 0.3. However, if the low GM condition is considered, the increase in damping due to the speed rising from Fn = 0.15 to Fn = 0.2 seems to be enough for compensating the larger pitch motions, as the unstable area is smaller for the latter case. However, an even larger increase in speed, up to Fn = 0.3, leads again to bigger unstable areas, where roll – pitch coupling, together with wave passing, generate the largest parametric excitations.

3.3.4 Discussion

In this section, and by using a self-propelled scale model of the UK trawler, the strong tendency of this ship for developing parametric roll has been shown, and the phenomenon characterized for different sailing conditions.

Some difficulties have been described for obtaining accurate motion measurements from the IMU sensors inside the towing tank, due to magnetic disturbances. However, the developed scale model represents a valuable tool for carrying out not only parametric roll tests, but also any other type of seakeeping or resistance tests, where a complete monitoring of the model behaviour is needed.

The results of roll motion obtained by using this scale model have shown a higher variability in comparison with the results from more restrained models, as the one used in Section 3.2 of this work or that applied in (M.A.S. Neves,Rodríguez, 2006). This fact may be due to the influence of the other degrees of freedom in the development of parametric roll. In especial, very heavy pitching and large surging have been observed in the towing tank tests under the wave amplitudes and frequencies under analysis. Further research will be needed for studying the available recorded data to determine the extent of such influences.

Regarding the three degrees of freedom mathematical model applied in this section for predicting the ship roll amplitude, it can be concluded that the obtained results seem to be less accurate than those presented by the model developers. However, it has also been shown that these differences may also be due to the increase complexity of the roll motions experienced by the scale model.

The analysis carried out in this chapter should also be used for evaluating the suitability of this model to be used within an onboard guidance system. If the performance of this model for defining the vessel risk areas is compared to that of the single degree of freedom model (for fixed wavelengths), it could be appreciated that the former shows less accuracy, together with a higher complexity on its design, understanding and calibration. But the higher complexity of the scale model motions used in this chapter, makes this comparison inadequate.

Although the single degree of freedom model has shown under the described conditions relative accuracy on its performance, it will be necessary to apply the three degrees of freedom one to the “Spanish Trawler” case and the former to the “UK trawler” case. Once done, the comparison of the performance of both models could be correctly carried out and their applicability into a guidance system evaluated. Such an analysis has arisen as a possible future work to be carried out extending the research line presented in this dissertation.

4 PARAMETRIC ROLL PREDICTION

4.1 Introduction

As has been described in Section 2.4, the exigency of a system that can predict the inception of a parametric rolling episode soon enough as to give the crew time to take corrective actions and prevent heavy roll motions is clear and have been stated by the industry.

With the objective of obtaining such a system, different approximations have been undertaken; model based approaches have been proposed by (Holden et al., 2007) and (L. S. McCue,Bulian, 2007), whereas a signal based approach is the one selected in (R. Galeazzi et al., 2009a, 2009b; R. Galeazzi et al., 2012). A more detailed description of these works has been done in Section 2.4.2.

In the present work, a different approach is proposed, which relies on the use of artificial neural networks (ANNs) in order to forecast ship motions in parametric roll conditions. This line has been exploited by the author in the last years (López Peña et al., 2011; Míguez González, López Peña, Díaz Casás, Galeazzi, et al., 2011; Míguez González et al., 2010; Míguez González, López Peña, Díaz Casás,Neves, 2011) and also other research groups have started working in this same direction (Bellec et al., 2012).

ANNs are powerful mathematical tools capable of efficiently approximating any function, including nonlinear ones, by selecting the adequate number of layers and neurons (Cybenko, 1989) after a process of training with a set of examples.

This property has been broadly exploited for time series forecasting in different fields, including physics, engineering or economics (Zhang et al., 1998), but they have been successfully applied also in the field of marine engineering, for ship maneuvering and motion analysis (Ebada,Abdel-Maksoud, 2006; Xing,McCue, 2009, 2010), ship stability including anti-roll control systems (tanks, fin stabilizers, rudder roll stabilization) and auto pilots (Alarcin,Gulez, 2007; Jones et al., 2006; Li et al., 2005).

Among the advantages of the proposed alternative, the most representative is the fact that, instead of just making a detection, as the aforementioned methods, the forecasting system could predict in the short term the ship amplitude, speed and acceleration in roll, providing the crew or other onboard systems with valuable information to prevent and avoid the phenomenon of parametric roll resonance.

In this section, Artificial Neural Networks (ANN) have been used as a roll motion forecaster, exploiting their capabilities as nonlinear time series estimators, in order to subsequently detect any parametric roll event through the analysis of the forecasted time series (Golden, 1996). In particular, multilayer perceptron neural networks (MPNNs) have been the structures selected to predict ship roll motion in different situations.

The predictive capability of MPNN has been tested against parametric roll developed both in regular and irregular seas. The training and testing processes have been carried out in two of the scenarios presented in Chapter 3.

In the first one, the three degrees of freedom coupled model of the UK stern trawler, developed by (M.A.S. Neves,Rodríguez, 2006) has been applied for computing ship motions in heave, pitch and roll, in parametric rolling conditions in both regular and irregular seas.

In the second scenario, the more realistic roll motion data from the towing tank tests of the larger Spanish trawler have been used, in similar conditions to those described for the first one.

Different network set-ups have been considered by increasing the number of neurons per layer, or by increasing the number of hidden layers, in order to test their performance in the different situations.

The results obtained both in the mathematical model case and in the scale tests are very promising, and showed good agreement between the forecasted and the real values, for predictions of up to 40 seconds into the future in the best cases, confirming the good potential of using neural networks for the prediction of parametric roll.

4.2 Artificial Neural Networks

In this section we revisit some of the main aspects of artificial neural networks, providing the mathematical formalism about their working principles. The overview is based on (Haykin, 1998).

An ANN is an adaptive parallel distributed computational tool constituted by information-processing units called neurons, which has the capability of accumulating experiential knowledge to be used when needed. This fact has provided them with the property of being able to act as powerful non linear estimators, learning complex behaviours without the need of an explicit analytic model which describes them.

The structure of these algorithms is similar to the brain in two aspects:

- The acquisition of knowledge from the surroundings relies on a learning process.

- The strength of the interneuron links, called synaptic weights, are employed to accumulate the gathered knowledge.

The learning process is based on a learning algorithm, whose function is to change the synaptic weights to achieve a desired goal.

Each neuron performs the following operations: first each input is weighted by a synaptic weight w_{kj}, then all weighted inputs are added, and finally a bias b_k is added. This summation is then processed by an activation function, which limits the amplitude of the neuron output. Mathematically the neuron activity can be described as follows:

$$v_k = \sum_{j=1}^{m} w_{kj} x_j + b_k \tag{71}$$

$$y_k = f\left(v_k\right) \tag{72}$$

Where $x_1, x_2, \ldots, x_m$ are the input signals, $w_{k1}, w_{k2}, \ldots, w_{km}$ are the synaptic weights, b_k is the bias, v_k is the activation potential, $f(\ )$ is the activation function, and y_k is the neuron output.

The activation function should be selected depending on the analyzed data and the kind of problem to be solved. Three basic types of activation functions could be the Heaviside function (or threshold function), the piecewise linear function or the tan-sigmoid function.

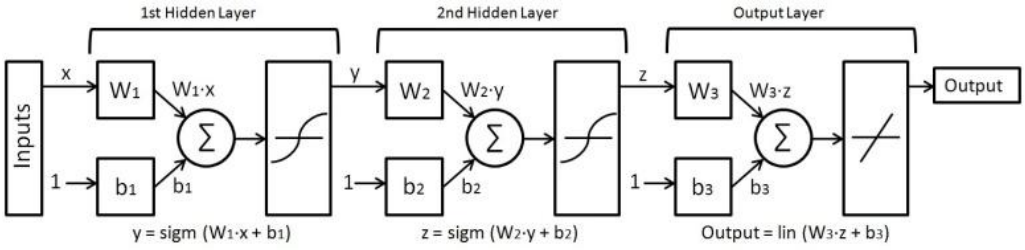

Figure 4.1. Multilayer Perceptron Neural Network Architecture.

The complexity of the problems that the network can deal with depends on the number of hidden layers and neurons in each layer. This capacity increases with the number of neurons and layers, but only up to a limit.

For a given function, no further improvements can be obtained by increasing the number of neurons and layers once the threshold is hit.

In this work, an ANN with multilayer perceptron architecture (MPNN) has been employed, which structure is shown in Figure 4.1. MPNNs are feedforward networks, also called backpropagation networks, because of the algorithm used for updating the weights and biases is called error backpropagation algorithm.

This algorithm consists of two phases: the forward pass and the backward pass. In the forward pass a certain pattern is inputted to the network, which generates a chain of effects that propagate throughout the network layer by layer up to the output layer, where the actual network response is produced. During this phase, the synaptic weights are kept fixed. In the backward pass instead the synaptic weights are changed accordingly with a cost function, which determines how close the network response is to the real output. The error signal is propagated backward through the network and the weights are adjusted such that the response of the network gets statistically closer to the desired response. Mathematically this is described as follows:

Consider a network with *N+1* layers of neurons, and *N* layers of synaptic weights. The input and bias vectors of each layer are given by

$$\mathbf{x}^l = \left[x_1, \ldots, x_{m_l}\right]^T \in \mathcal{R}^{m_l}, \qquad 0 \le l \le N \tag{73}$$

$$\mathbf{b}^l = \left[b_1^l, \ldots, b_{m_l}^l\right]^T \in \mathcal{R}^{m_l} \tag{74}$$

and the matrix of synaptic weights is

$$\mathbf{W}^l = \begin{bmatrix} w_{11}^l & w_{12}^l & \cdots & w_{1m_{l-1}}^l \\ w_{21}^l & \ddots & & \vdots \\ \vdots & & \ddots & \vdots \\ w_{m_l 1}^l & \cdots & \cdots & w_{m_l m_{l-1}}^l \end{bmatrix}, \quad \mathbf{W}^l \in \mathcal{R}^{m_l} \times \mathcal{R}^{m_{l-1}} \tag{75}$$

Forward pass: the input vector $\mathbf{x}^0$ is converted into the output vector $\mathbf{x}^N$ by calculating

$$\mathbf{x}^l = f\left(\mathbf{v}^l\right) = f\left(\mathbf{W}^l \mathbf{x}^{l-1} + \mathbf{b}^l\right), \qquad 0 \le l \le N \tag{76}$$

where $\mathbf{v}^l$ is the vector of activation potentials.

Output local gradient: the output local gradient vector δ^N is computed as function of the error between the desired output $\mathbf{y}^d$ and the actual output $\mathbf{x}^N$

$$\delta^N = f'\left(\mathbf{v}^N\right)\left(\mathbf{y}^d - \mathbf{x}^N\right) \tag{77}$$

Backward pass: the error signal is backpropagated through the network by computing the hidden layer local gradient vectors

$$\delta^{l-1} = f'\left(\mathbf{v}^{l-1}\right)\left(\mathbf{W}^l\right)^T \delta^l, \qquad N \ge l \ge 1 \tag{78}$$

Weights update: the synaptic weights and biases are updated according to the following relations

$$\Delta \mathbf{W}^l = \eta \delta^l \left(\mathbf{x}^l \right)^T \tag{79}$$

$$\Delta \mathbf{b}^l = \eta \delta^l \tag{80}$$

where η is the learning rate parameter.

It is possible to prove that equations (79) and (80) are found as gradient descent on the performance index

$$E = \frac{1}{2} \mathbf{e}^T \mathbf{e} \tag{81}$$

where $\mathbf{e} = \mathbf{y}^d - \mathbf{x}^N$ is the network output error (Haykin, 1998).

4.3 Prediction Algorithms

The base neural network architecture used in this work is a multilayer perceptron network with two hidden layers, 30 neurons per layer, and one output layer. This initial structure is modified by e.g. increasing the number of neurons per layer, or the number of layers, in order to compare the prediction performance of different architectures and according to the complexity of the cases under analysis.

The network is fed with time series of roll motion, which are 20 seconds long and sampled at a frequency F_s = 2 Hz; hence the input vector $\mathbf{x}^0$ has 40 components. The network has only one output, which is the one step-ahead prediction. By substituting part of the input vector with the network output values, and recursively executing the system, longer predictions can be obtained

from the initial 20 seconds. However, as the number of iterations grows, the prediction performance deteriorates accordingly.

The length of the roll time series has been selected taking into account two factors. On one hand, the natural roll periods of the vessels chosen for the testing. In the loading conditions considered for these tests, this value is 7.48 seconds for the UK trawler, while the natural roll period of the Spanish trawler is 11.16 seconds. On the other hand, parametric roll fully develops in a short period of time, usually no more than four rolling cycles (IMO, 2007). Therefore if the network prediction should be used e.g. together with a diagnostic system for the timely detection of parametric roll inception the time lapse that must be analyzed should be shorter than four roll periods.

As activation functions in the hidden layers, tan-sigmoid functions have been selected ($y = \tanh x$). These functions have proved to be more adequate for dealing with highly non linear systems than, for example, step or linear ones (Demuth et al., 2011) and they are the most commonly used in the multilayer perceptron architecture. A linear function ($y = x$) was instead selected in the output layer.

The performance of the neural network can be improved by normalizing the input and target data prior to being processed. During the training phase inputs and target values are normalized such that they fall in the range [-1,1], obtaining two scaling factors n_1 and n_2 respectively. Once trained, these factors are used for normalizing test inputs and de-normalizing their corresponding outputs.

As shown, the training algorithm is responsible of modifying the weights and biases in order to reduce the error between the network's prediction and the target value. In this work, the Levenberg-Marquardt (L-M) algorithm (Demuth et al., 2011), instead of using basic gradient descent, has been chosen.

L-M is a training method optimized for solving problems of function approximation. Based on the Gauss-Newton method, it overcomes the difficulties of computing the hessian matrix **H** of the performance index hessian by approximating it using the Jacobian matrix **J** (**H = J^{T}J**). In this case, the weights update is

$$\Delta \mathbf{W}^l = \left[J^T J + \mu I \right]^{-1} J^T \cdot e \cdot \left(\mathbf{x}^l \right)^T \tag{82}$$

$$\Delta \mathbf{b}^l = \left[J^T J + \mu I \right]^{-1} J^T \cdot e \tag{83}$$

where μ is a variable parameter called damping factor. When this parameter is large, the L-M is equivalent to gradient descent; when it is small, it becomes the Newton method. For measuring the aforementioned error, the mean squared error (MSE) was chosen as performance function.

Finally, and considering that the initialization of the training phase is a random process - the first set of weights and biases are randomly generated - the same set of training cases can generate different results for successive initializations. Consequently the performance of the network will also differ from training to training. Therefore the training process has been repeated 50 times, and the best network structure out of the 50 cases was selected based upon the network performance index.

4.4 Mathematical Model

In this first test, the mathematical model of the UK transom stern trawler described in Section 3.3, has been used for testing the proposed forecasting schemes. The loading condition is the one corresponding to the low GM (GM = 0.370 m) and the real ship speed considered is that corresponding to a Froude number of 0.3 (approximately 8.2 knots).

As have been already described, parametric roll is usually triggered when certain conditions are fulfilled simultaneously. On one hand, ship – wave encounter frequency should be about the double of the ship natural roll frequency. Taking into account that in our case ship speed, loading condition and heading (head seas) are kept constant, wave frequency is the only variable influencing encounter frequency. On the other hand, wave amplitude should be above a given threshold, which is ship dependant. In the following sections, different tests will be carried out by systematically modifying these parameters, with the objective of analyzing the performance of the proposed system.

Firstly, three different tests in regular waves will be presented; in the first one, wave amplitude is taken as constant as wave frequency is modified. In the second one, frequency is taken as constant while amplitude is modified. Finally, both parameters are taken as variable.

Secondly, another regular wave case where wave amplitude is considered as time dependant has been done, where wave conditions represent a time varying height wave with constant frequency, selected as the worst case regarding parametric rolling.

And finally, an irregular wave case will be presented, representing the highest level of complexity of the tests carried out with the mathematical simulator.

4.4.1 Regular Waves

As have been previously said, four different studies have been carried out in this section, in order to evaluate the system behavior under the variations of each one of those parameters. The area under consideration is that where parametric roll is more likely to occur for the ship conditions under analysis.

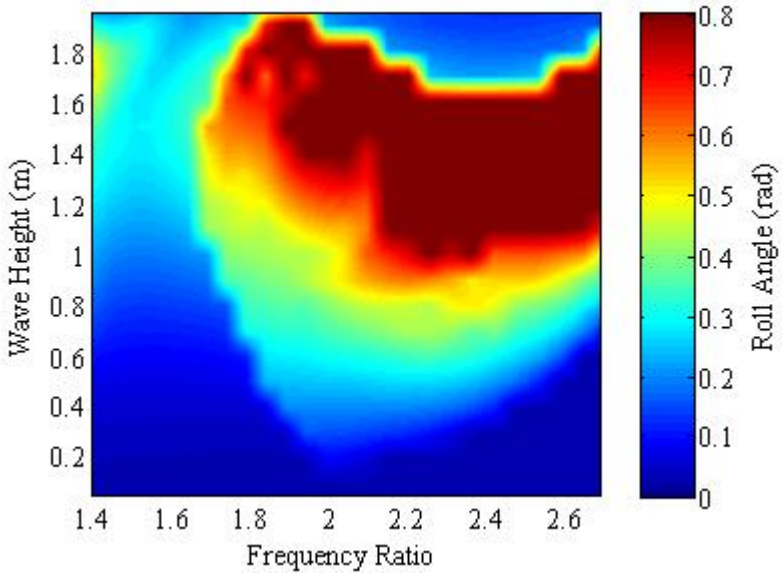

Figure 4.2. UK Trawler. Stability Diagram. Fn = 0.30. GM = 0.370 m.

This area could be seen in Figure 4.2, which has been previously computed in Section 3.3. In this test case, wave amplitude will be ranging from 0.3 m to 0.9 m, and the encounter frequency- natural roll frequency ratio will be ranging from 1.7 to 2.5.

In the different test cases, the prediction network has been recursively executed 10 and 20 times, in order to make predictions of 5 and 10 seconds in advance. After those 5 or 10 seconds, a new prediction is made based on another 20 seconds obtained from the real time series (simulating the effect of an onboard sensing system) and so on. This way we can generate a whole predicted time series of the same length as the original one.

The training cases have been obtained from the results of the aforementioned mathematical model, generating a 200 second time series for each of the combinations of wave frequency and amplitude considered.

These time series have been truncated when steady-state rolling is reached, in order to prevent the introduction of redundant data in the training process. These redundant values would give higher weights to these areas of the time series, reducing the performance of the prediction in the transient region.

In some cases, the whole predicted time series has been generated only from the first 20 seconds, by executing the network recursively until the complete length is generated.

4.4.1.1 Regular Waves. Constant Amplitude. Variable Frequency.

Here, the evaluation of the constant amplitude scenario is performed. A wave amplitude of 0.4 m has been selected, while encounter frequency – natural roll frequency ratio was chosen between 1.987 and 2.504, which cover an area where resonance takes place at an intermediate intensity. Seven combinations of frequency and amplitude where chosen to generate the training time series, which include 320 training cases. These combinations are shown in Table 4.1. Four other combinations have not been used for training and were chosen as test cases; these are located between training values. Test cases are also shown in Table 4.1.

In the test cases, steady-state is reached in 60 seconds, so the time series are truncated there. In these cases, three predictions have been performed for all of the three test cases: 5, 10 and 60 second predictions. As shown in Figure 4.3, Figure 4.4, Figure 4.5 and Figure 4.6, the obtained results from the three predictions are accurate enough to predict the appearance of the resonance phenomenon. The precision of the 40 second case is remarkable, as it accurately provides a prediction 40 seconds ahead in the four conditions tested.

The error values of the predictions for the different test cases and forecasting levels, are presented in Table 4.2.

Table 4.1. Constant amplitude (0.4 m) case. Training and testing conditions.

Case	ω_w (rad/s)	ω_e (rad/s)	ω_e/ω_n
Train 1	1.130	1.705	1.987
Test 1	1.145	1.735	2.022
Train 2	1.160	1.766	2.058
Train 3	1.190	1.827	2.130
Test 2	1.205	1.859	2.166
Train 4	1.220	1.890	2.203
Train 5	1.250	1.953	2.277
Test 3	1.265	1.985	2.314
Train 6	1.280	2.018	2.351
Train 7	1.310	2.083	2.427
Test 4	1.325	2.115	2.465
Train 8	1.340	2.148	2.504

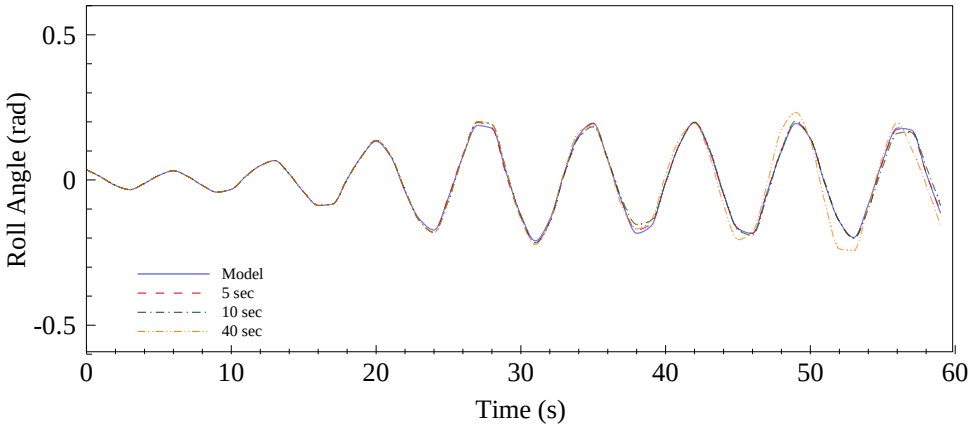

Figure 4.3. Constant amplitude case. Test 1. Predictions.

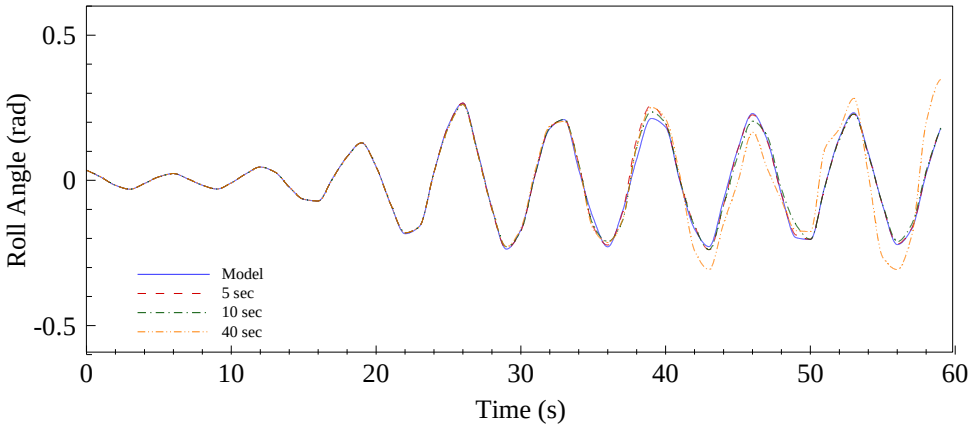

Figure 4.4. Constant amplitude case. Test 2. Predictions.

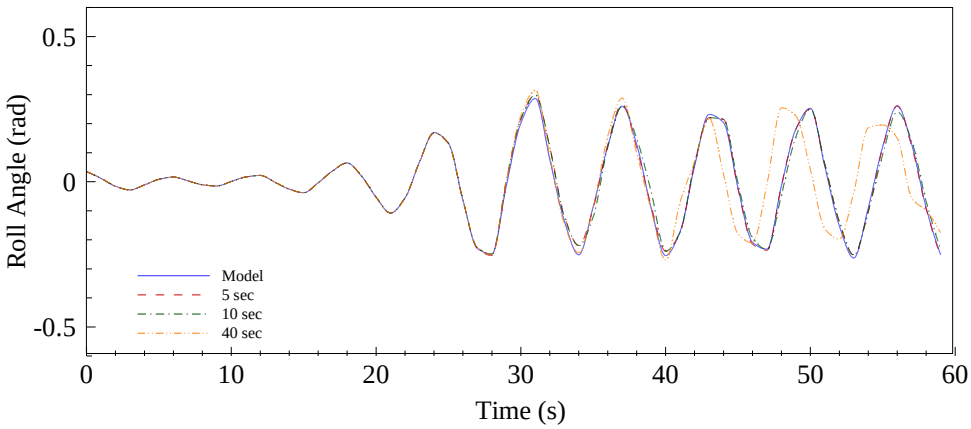

Figure 4.5. Constant amplitude case. Test 3. Predictions.

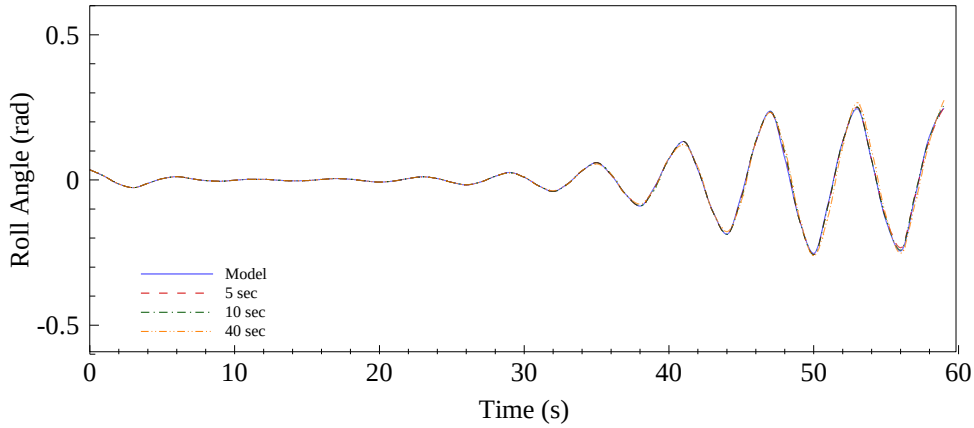

Figure 4.6. Constant amplitude case. Test 4. Predictions.

Table 4.2. Prediction performance. Constant amplitude case. MSE ($x10^{-4}$).

Prediction Horizon	5 seconds	10 seconds	40 seconds
Test 1	0.22	0.84	6.24
Test 2	1.50	1.67	29.89
Test 3	0.86	2.32	79.31
Test 4	0.12	0.16	1.30

4.4.1.2 Regular waves. Constant Frequency. Variable Amplitude.

In this test, the evaluation of the constant frequency case is presented. A wave frequency of 1.085 rad/s was selected, which implies an encounter frequency of 1.615 rad/s and an encounter frequency-natural roll frequency ratio of 1.9. At this ratio, parametric rolling is expected between the amplitudes of 0.2 and 0.8 m, as can be seen in Figure 4.2. Training and test amplitudes were chosen between those values, considering six training time series and two test series. These combinations generate 460 training cases. All the values are shown in Table 4.3. Again, a two hidden layer perceptron network architecture was selected, with 30 neurons in each of the hidden layers.

The first test case (Test 1), reaches steady-state in 60 seconds, and so it has been truncated in this value. Otherwise, the second case (Test 2) is at the limit of the capsizing area, where chaotic behavior and multiperiodicity start to take place and prediction is a lot more complicated (M.A.S. Neves, C.A. Rodríguez, et al., 2009). This test case has not been truncated, as steady-state is not well defined. In this case, three predictions were performed for the Test 1 case, including 5, 10 and 40 second predictions. In Test 2, only 5 and 10 second predictions have been performed, as a long term prediction is not possible in this chaotic scheme. In Figure 4.7 and Figure 4.8, the results obtained from both test cases are presented. The Test 1 is accurate, and the time series forecast is very good in all of the three predictions. The results obtained in Test 2 are not so good, but can be acceptable in the short term prediction case, taking in account the complexity of the behavior of these kinds of systems.

The error values of the predictions for the different test cases and forecasting levels, are presented in Table 4.4.

Table 4.3: Constant frequency case (Frequency Ratio = 1.90). Training and testing conditions.

Case	A_w (m)
Train 1	0.30
Train 2	0.35
Train 3	0.40
Train 4	0.50
Test 1	0.55
Train 5	0.60
Train 6	0.70
Train 7	0.75
Test 2	0.80

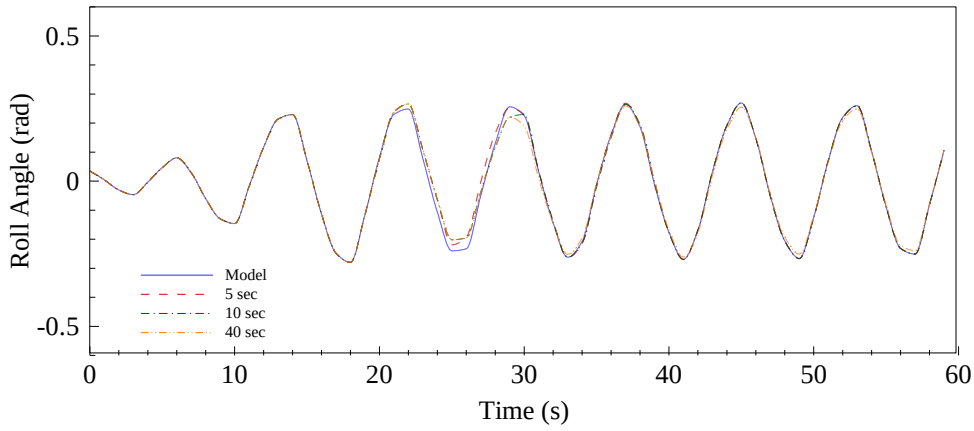

Figure 4.7. Constant frequency case. Test 1. Predictions.

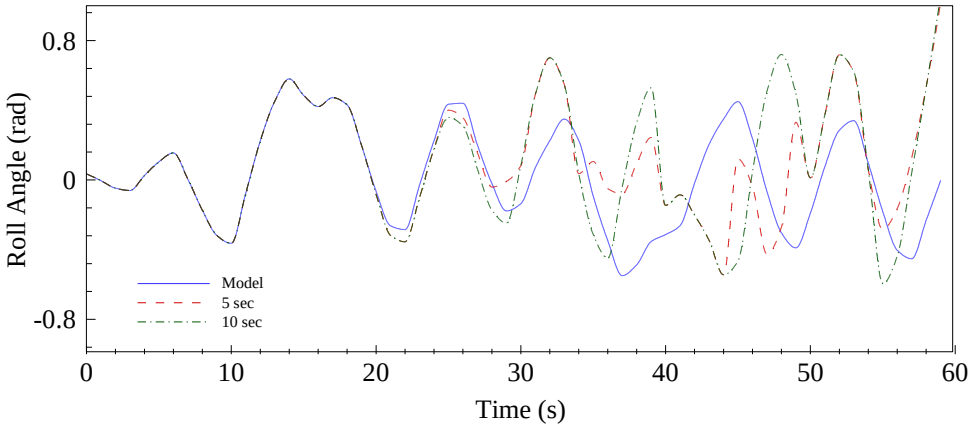

Figure 4.8. Constant frequency case. Test 2. Predictions.

Table 4.4. Predicton performance. Constant frequency case. MSE ($x10^{-4}$)

Prediction Horizon	5 seconds	10 seconds	40 seconds
Test 1	1.46	1.36	1.93
Test 2	1014.43	1522.02	-

4.4.1.3 Regular waves. Variable Amplitude and Frequency.

In this experiment, variable values for amplitude and wave frequency have been chosen, defining the test area inside the instability region, but outside the chaotic areas where capsizing is most likely to occur. The amplitude ranges from 0.33 to 0.6 m, while the frequency ratio ranges from 1.917 to 2.504 rad/s. 49 combinations of amplitude and frequency have been selected for training, generating 2660 training cases. These combinations are shown in Table 4.5. With the described training process, the system should be able to predict the behavior of the ship sailing in any of the wave conditions situated inside or in the surroundings of the rectangle limited by the aforementioned values. Test cases were chosen between these values; the five test combinations are presented in Table 4.6.

Table 4.5. Variable amplitude and frequency case. Training cases. Combinations.

ω_w (rad/s)	ω_e (rad/s)	ω_e / ω_n	A_w (m)
1.100	1.645	1.917	0.33
1.140	1.725	2.011	0.36
1.180	1.807	2.106	0.42
1.220	1.890	2.203	0.48
1.260	1.975	2.302	0.54
1.300	2.061	2.402	0.57
1.340	2.148	2.504	0.6

Table 4.6. Variable amplitude and frequency case. Test cases

Case	ω_w (rad/s)	ω_e (rad/s)	ω_e / ω_n	A_w (m)
Test 1	1.200	1.848	2.154	0.46
Test 2	1.200	1.848	2.154	0.41
Test 3	1.320	2.104	2.453	0.345
Test 4	1.320	2.104	2.453	0.585
Test 5	1.240	1.932	2.252	0.52

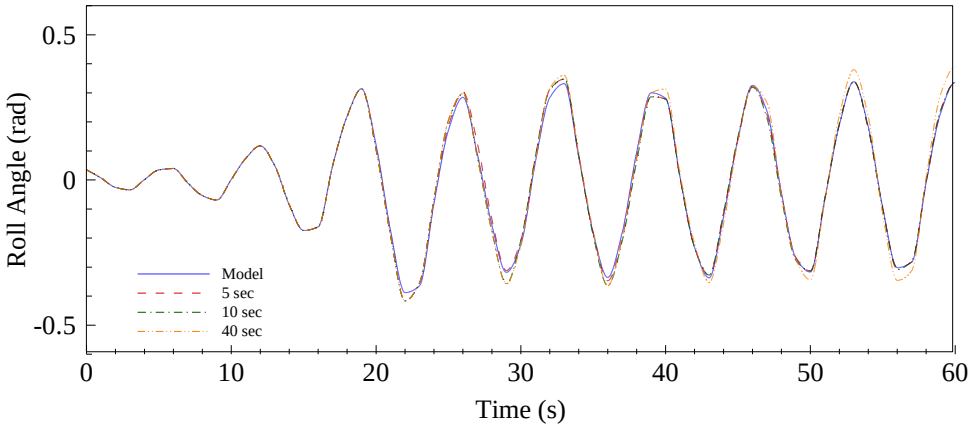

Figure 4.9. Test 1. Two hidden layers. 30 Neurons. Predictions

The same architecture as in the previous cases has been used; that is a multilayer perceptron, with two hidden layers and 30 neurons per layer. The five test cases have been truncated at 60 seconds and three predictions have been made, one for 5 seconds, another for 10 seconds and the last for 40 seconds, comprising the whole time series. The results of the described tests are shown in Figure 4.9, Figure 4.10, Figure 4.11, Figure 4.12 and Figure 4.13. As shown, the results are again very promising, although there are some punctual disturbances in Test 1, Test 3 and Test 5 and some difficulties for reproducing the model time series in Test 4, which is again near the capsizing area where chaotic and multiperiodic behavior appears. Taking into account that most training cases are out of this area and that ship behavior changes so drastically in these regions, the system is not so suitable for dealing with these cases.

The error values of the predictions for the different test cases and forecasting levels, are presented in Table 4.7.

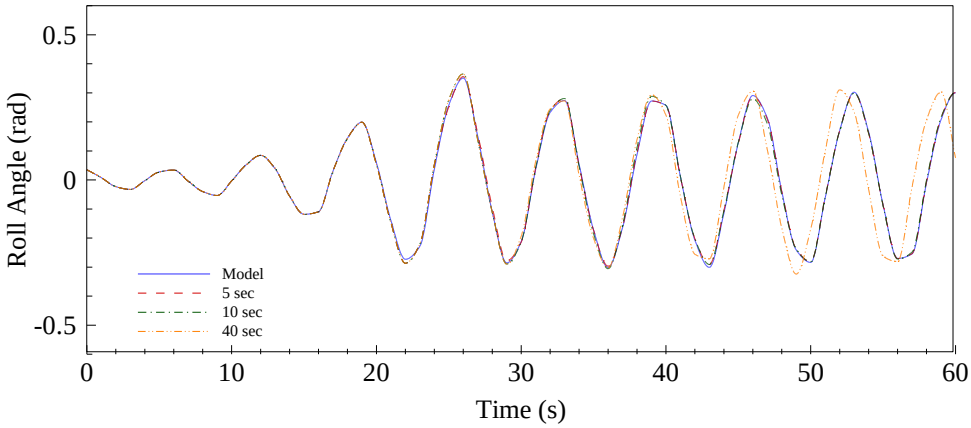

Figure 4.10. Test 2. Two hidden layers. 30 Neurons. Predictions

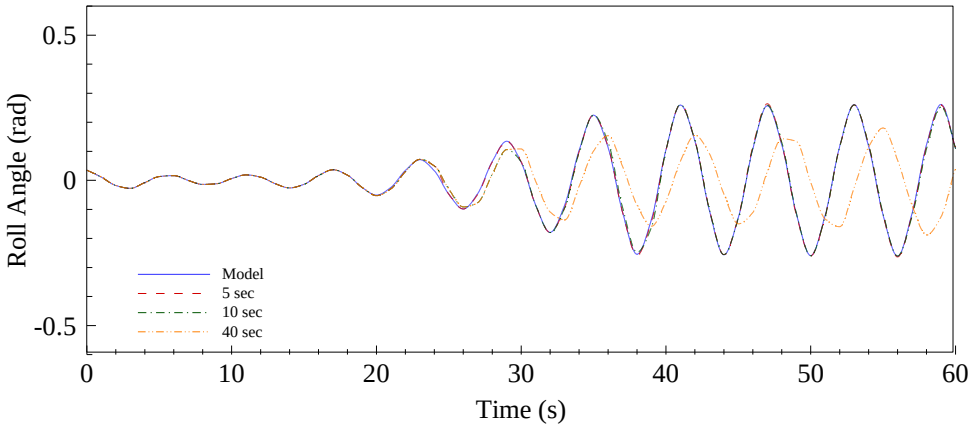

Figure 4.11. Test 3. Two hidden layers. 30 Neurons. Predictions

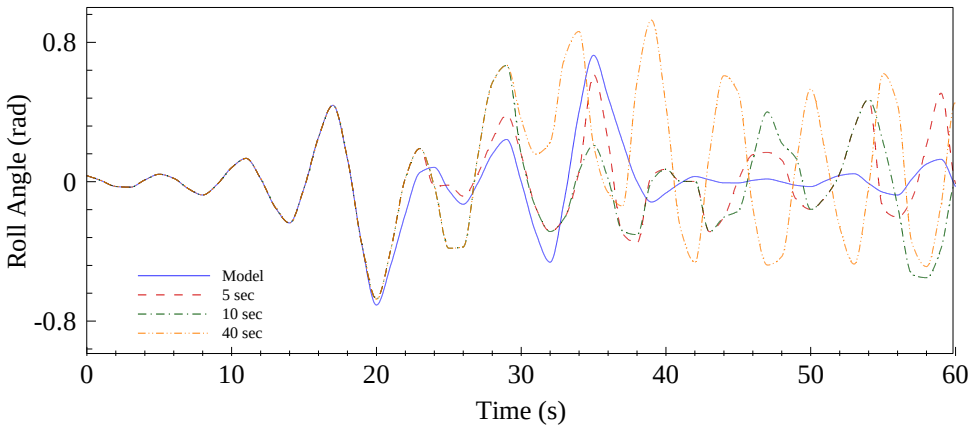

Figure 4.12. Test 4. Two hidden layers. 30 Neurons. Predictions

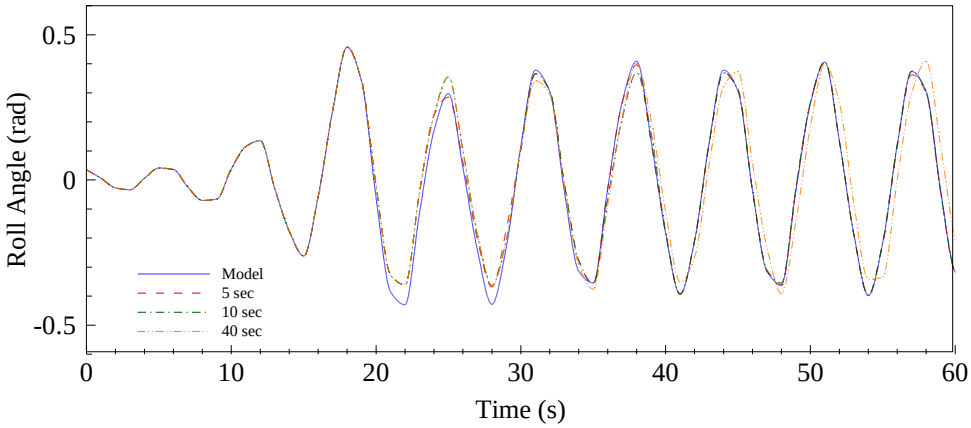

Figure 4.13. Test 5. Two hidden layers. 30 Neurons. Predictions

Table 4.7. Prediction performance. Variable amplitude and frequency case. Two hidden layers. 30 Neurons. MSE ($x10^{-4}$).

Prediction Horizon	5 seconds	10 seconds	40 seconds
Test 1	0.50	0.85	840.32
Test 2	0.17	0.51	772.12
Test 3	0.15	0.66	521.59
Test 4	138.21	207.69	2073.28
Test 5	1.97	3.18	534.04

It has to be said that the study of these cases is more complex than in the constant amplitude and frequency ones, as the number of training cases is bigger and the typology of the solutions more scattered. Taking this into account and also that the capacity of neural networks to deal with more complex functions increases with the number of layers and neurons in each of them, a new structure, increasing the number of neurons in the hidden layers from 30 to 40, has been developed and tested.

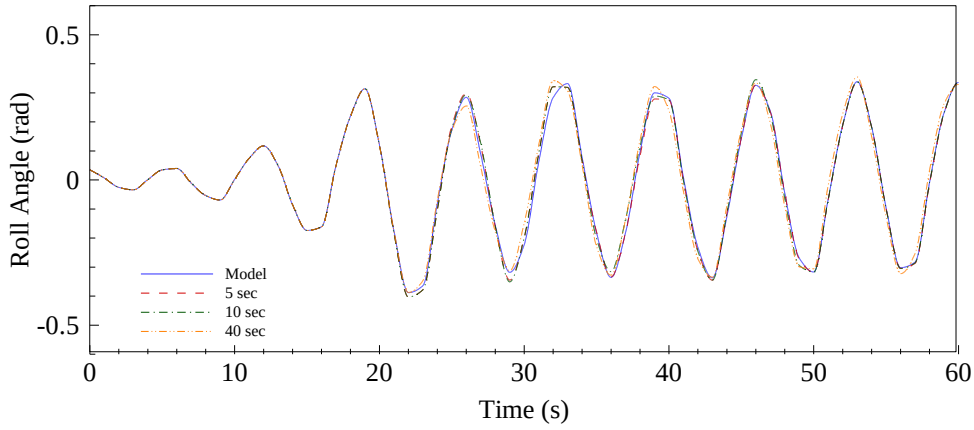

Figure 4.14. Test 1. Two hidden layers. 40 Neurons. Predictions

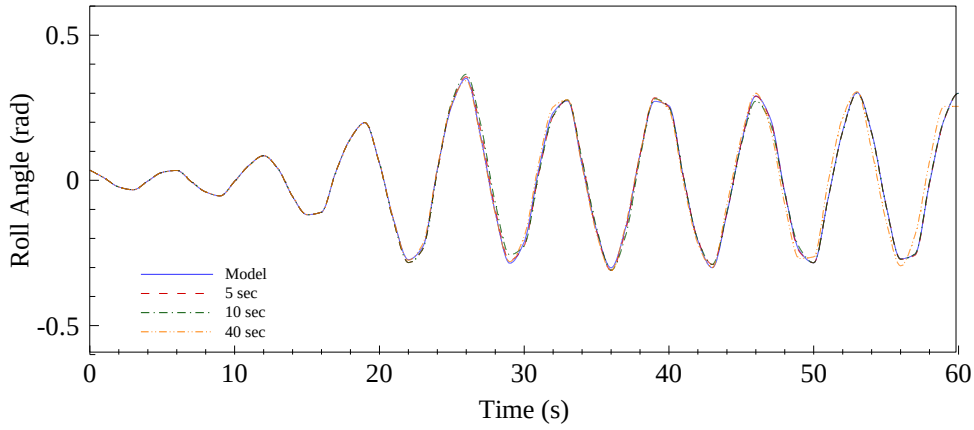

Figure 4.15. Test 2. Two hidden layers. 40 Neurons. Predictions

Again, as in the previous case, the 49 training cases and 5 test cases were used, in order to evaluate also its capacity to deal with cases where chaos and multiperiodicity start to develop. The results are shown in Figure 4.14, Figure 4.15, Figure 4.16, Figure 4.17 and Figure 4.18.

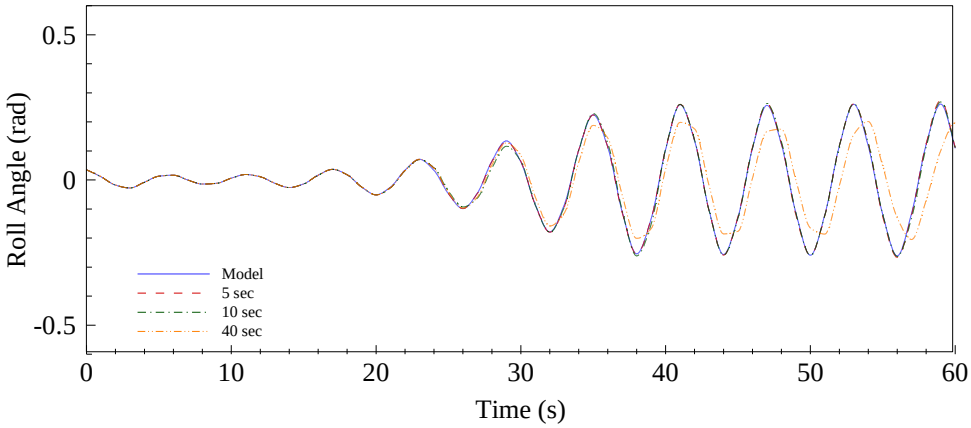

Figure 4.16. Test 3. Two hidden layers. 40 Neurons. Predictions

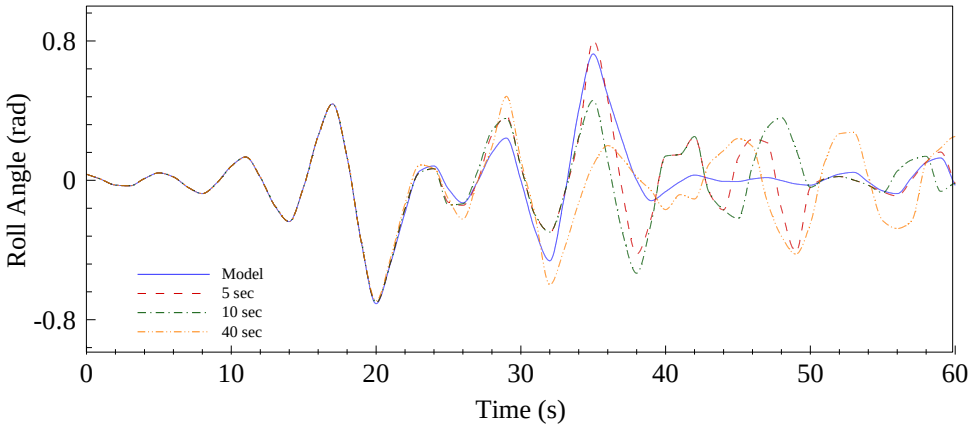

Figure 4.17. Test 4. Two hidden layers. 40 Neurons. Predictions

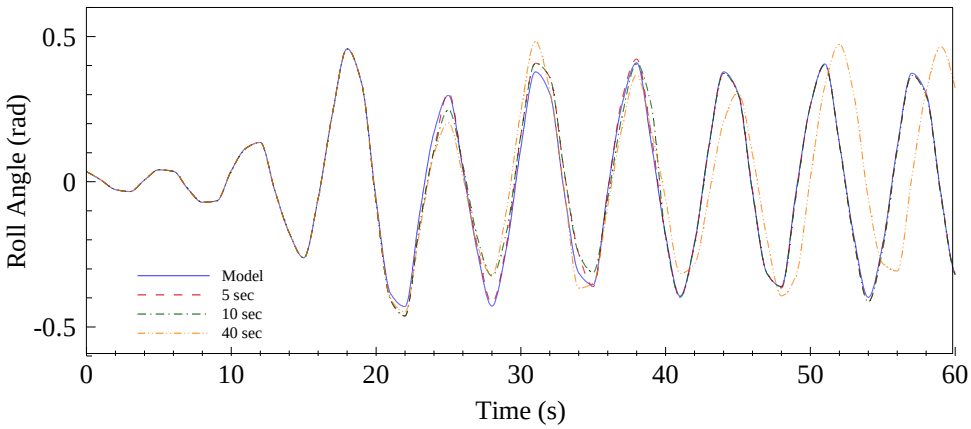

Figure 4.18. Test 5. Two hidden layers. 40 Neurons. Predictions

Table 4.8. Prediction performance. Variable amplitude and frequency case. Two hidden layers. 30 & 40 Neurons. MSE ($x10^{-4}$).

Prediction Horizon	5 seconds		10 seconds		40 seconds	
	30-30	40-40	30-30	40-40	30-30	40- 40
Test 1	0.50	0.33	0.85	0.74	840.32	564.59
Test 2	0.17	0.20	0.51	0.55	772.12	336.00
Test 3	0.15	0.16	0.66	0.46	521.59	399.22
Test 4	138.21	89.91	207.69	197.42	2073.28	1129.29
Test 5	1.97	1.22	3.18	3.39	534.04	916.16

As shown in the previous figures, the forecasts generated by the system track the model in a sufficiently accurate way, even in predictions of up to 40 seconds in advance, especially in Test 1. Although predictions in Test 4 and 5 are still presenting some divergences from the mathematical model, the results obtained in all the others are quite accurate and promising.

Observing the compared values of the MSE of the predictions obtained with the two tested architectures, described in Table 4.8, it can be concluded than results obtained with the larger MP (40 neuron) are better than those obtained with the 30 neuron one, except for the 5 and 10 second predictions in Test 2, where both are very similar.

Although these results are good, it is obvious that they are limited to a reduced experimental window; training has been performed only considering conditions where parametric roll was present, with the ship sailing in pure longitudinal

waves and with no external uncontrolled disturbances present (as a mathematical model is being used). Parametric roll fully develops in a few rolling cycles and then the steady state is indefectively reached.

4.4.1.4 Regular waves. Time Varying Amplitude.

As first attempt to approximate a realistic seaway scenario, which can induce the onset of parametric roll the following test case has been designed. The ship model was excited by a regular wave with time-varying amplitude ranging between 0.2 m and 0.5 m, and constant wave frequency equal to 1.26 rad/s, which corresponds to an encounter frequency of 1.98 rad/s (frequency ratio equal to 2.3). This gave rise to ship responses in roll where parametric resonance is always present, but with variable roll amplitude. The resulting roll time series can be seen in Figure 4.19. The corresponding wave amplitude in each time interval of the simulation is reported in Table 4.9.

The reason behind this approach was to evaluate the performance of the MPNN while dealing with a roll dynamics that does not reach a steady state response (typical of parametric rolling event in regular seas with constant wave amplitude and frequency), but that alternates growing and decaying oscillations in response to changes in the wave amplitude, similarly to what happens in a real seaway.

Regarding the training process and in order to feed the network with all possible representative cases, it has been necessary to use time series where resonance was fully developed and also time series without resonant behavior, equivalent to a roll decay condition. The former provides data for the case where roll amplitude increases, while the latter provides data for the cases where roll motion reduces, that is, transient behavior from a resonant to a non resonant roll motion.

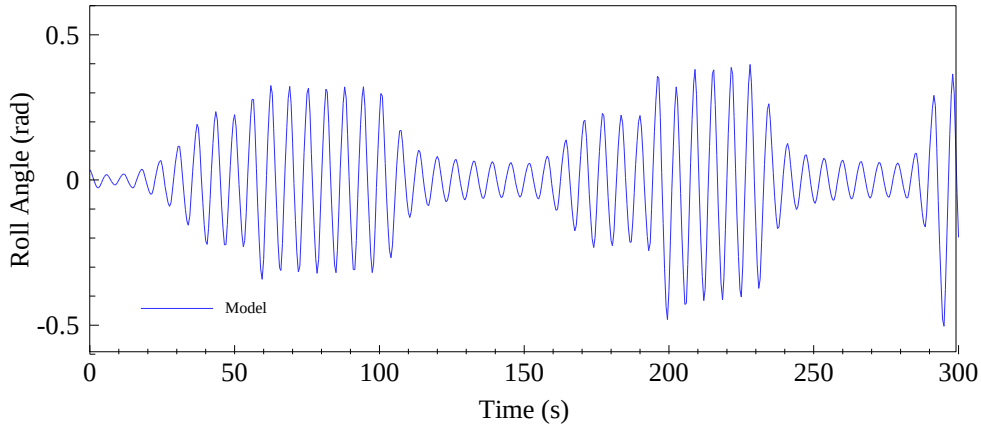

Figure 4.19. Time dependant amplitude regular waves. Roll motion test time series.

Table 4.9. Time intervals and corresponding wave amplitude .

Time (s)	Wave Amplitude (m)
0 - 50	0.30
50 - 100	0.40
100 -150	0.20
150 - 190	0.30
190 - 230	0.50
230 - 280	0.20
280 - 300	0.50

Taking into account that this transient depends on the initial roll amplitude (roll amplitude during the parametric roll event), several initial conditions were used for the generation of the training cases; this was done in order to feed the network with the largest possible amount of information about the ship's roll motion.

A training data set of 66 time series was generated, with wave amplitudes ranging from 0.1 m to 0.6 m in steps of 0.05 m, wave frequency equal to 1.26 rad/s, initial roll angles ranging from 5 degrees to 30 degrees, in steps of 5 degrees, and duration of 50 seconds. A total number of 4026 training cases were obtained.

The system has been recursively executed in order to obtain 5, 10 and 20 seconds long predictions. The obtained results for the three different prediction horizons, and their corresponding errors, are illustrated in Table 4.10 and Figure 4.20, Figure 4.21 and Figure 4.22.

The prediction made with 5 seconds horizon (Figure 4.20) accurately tracks the test time series. Analyzing the forecast, the parametric roll events that develop around the second 25, 150 and 280 can be predicted. Results of the 10 seconds prediction (Figure 4.21) are also quite good. However, around t = 250 s, the network slightly over predicts the roll amplitude, but just after one roll period the prediction is again well tracking the ship's roll motion. In the last case the prediction horizon is 20 seconds (Figure 4.22) and it can be observed that the general behavior is still rather good, but there exists three main areas around 120 s, 250 s and 280 s where the network fails. The last case is particularly interesting as the network prediction clearly underestimates the ship's roll oscillation.

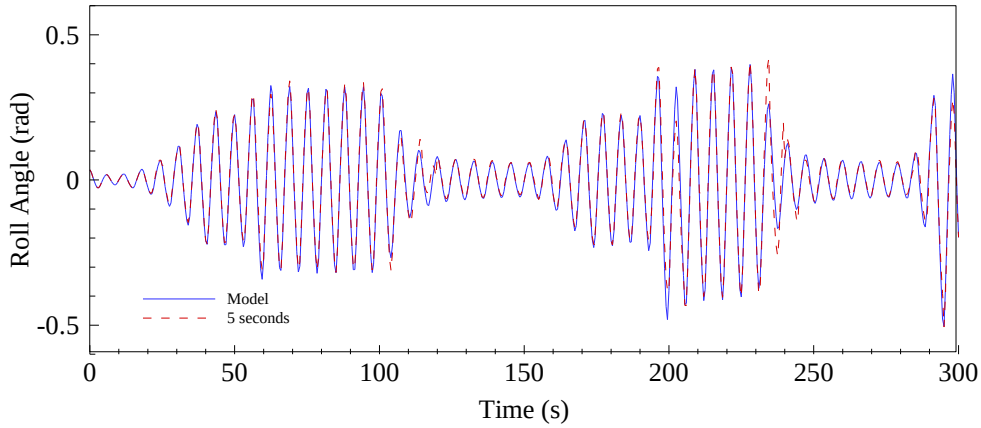

Figure 4.20. Time dependant amplitude regular waves. 5 seconds forecast.

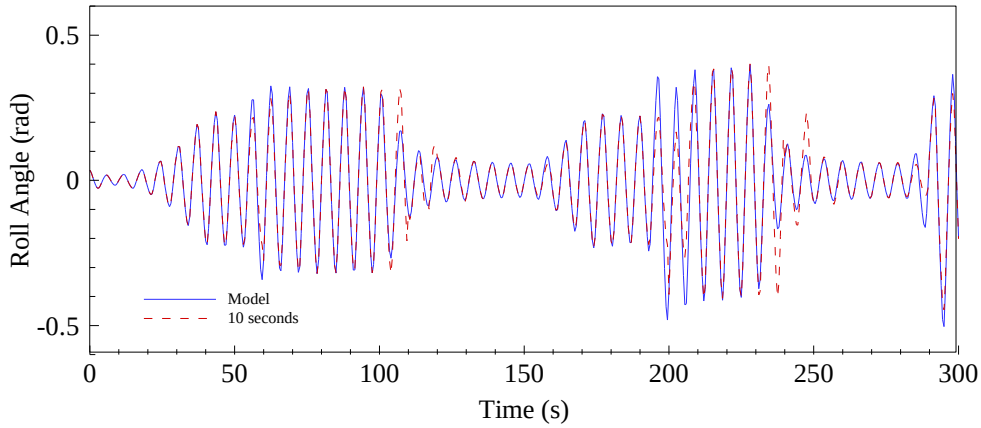

Figure 4.21. Time dependant amplitude regular waves. 10 seconds forecast.

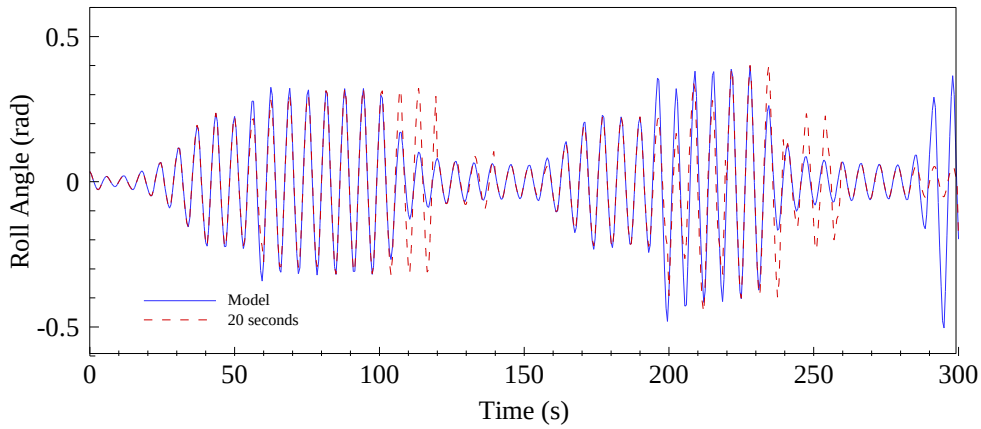

Figure 4.22. Time dependant amplitude regular waves. 20 seconds forecast.

Table 4.10. Prediction performance. Time dependant amplitude regular waves. MSE ($x10^{-4}$).

Forecast Horizon	MSE $x10^{-4}$
5 seconds	6.96
10 seconds	18.00
20 seconds	53.00

4.4.2 Irregular Waves.

Aiming at analyzing the performance of neural networks as predictors of ship's behavior in realistic sailing conditions, another simulation scenario was set up. While maintaining the head seas hypothesis, the UK trawler model was excited by irregular waves.

The wave motion is modeled applying the linear long crested model (DNV, 2007), where wave elevation as a function of time is computed as

$$\zeta(t) = \sum_{k=1}^{N} A_k \cos\left[\omega_k t + \varepsilon_k\right] \tag{84}$$

Where ε_k represent the uniformly distributed random phase, ω_k is the wave frequency selected for the spectrum computation, and A_k is the random wave amplitude, which follows a Rayleigh distribution with a mean squared value of

$$E\left[A_k^2\right] = 2S(\omega_k)\Delta\omega_k \tag{85}$$

where $S(\omega_k)$ is the selected wave spectrum and $\Delta\omega_k$ is the frequency resolution.

It has to be noted that some of the model coefficients were not recomputed for the irregular wave case; hence quantitative roll motion values will not be relevant, but the roll motion time series can be used for a qualitative analysis.

Considering the random nature of wave excitation in this simulation scenario, both training and test cases have been generated with the same wave conditions.

A Jonswap spectrum of peak frequency ω_p and significant wave height H_S has been selected, which definition is the following:

$$S_J(\omega) = A_\gamma \cdot S_{PM}(\omega) \cdot \gamma^{e^{-0.5\left(\frac{\omega-\omega_p}{\sigma\cdot\omega_p}\right)^2}} \tag{86}$$

Where S_{PM} is the Pierson – Moskowitz spectrum, so that:

$$S_{PM}(\omega) = \frac{5}{16} \cdot H_S^2 \cdot \omega_p^4 \cdot \omega^{-5} \cdot e^{\left(-\frac{5}{4}\left(\frac{\omega}{\omega_p}\right)^{-4}\right)} \tag{87}$$

And γ is the non – dimensional peak shape parameter, $A_\gamma = 1 - 0.287 \cdot \ln(\gamma)$ is a normalizing factor and σ is the spectral width diameter as a function of wave frequency:

$$\begin{aligned} \sigma &= \sigma_a \text{ for } \omega \le \omega_p \\ \sigma &= \sigma_b \text{ for } \omega > \omega_p \end{aligned} \tag{88}$$

The values selected were a peak shape parameter of 5, σ_a and σ_b values of 0.05 and 0.07 and 500 frequency values for its computation, ranging from 0.2 rad/s to 5 rad/s.

The peak period T_p was set to 3.2 seconds, coinciding with the encounter period used in the regular wave test case (encounter peak frequency of 1.98 rad/s,

frequency ratio equal to 2.3) and the significant wave height was set to 1.2 m, in order to define wave conditions where parametric roll is likely to occur.

The training data set is composed of 50 time series, each 200 seconds long. As in the regular wave scenario, the time series are split in groups of 40 inputs and 1 output, which correspond to a total number of 18050 training cases. Another three time series, shown in Figure 4.23, Figure 4.24 and Figure 4.25, were generated to be used as test cases.

In this scenario three different MPNN architectures were tested in a comparative study, to assess which configuration provides the best roll motion prediction. First, a two hidden layer MPNN with 40 neurons per layer has been set up and trained. By feeding the resulting structure with the three test cases, and recursively executing it for 20 times, 10 seconds ahead predictions were obtained.

The initial network structure was changed by increasing the number of neurons in the hidden layers up to 45. This, in turn, should also increase the network prediction accuracy, but only up to a certain limit. The third tested network has instead an increased number of hidden layers. To avoid that a deeper network entails a longer training time due to the larger number of network parameters (weights and biases) to be estimated, the increase in the number of layers was accompanied with a reduction in the number of neurons per layer. This generates a network with the same amount of parameters as the former two, but with a different structure and, hence with a different behavior. The proposed network has then three hidden layers and 30 neurons per layer.

Table 4.11. Irregular waves. Prediction performance. MSE ($x10^{-4}$).

Test Case	40-40	45-45	30-30-30
Test 1	89.00	32.00	28.00
Test 2	8.48	8.89	5.85
Test 3	5.24	4.99	3.48

After training the two new structures, the 10 seconds ahead forecasts for the three test cases were computed. The obtained predictions with the three different structures and their corresponding prediction errors are shown in Figure 4.26, Figure 4.27, Figure 4.28 and Table 4.11.

From the figures and the MSE values, it can be clearly seen that the best performing structure is that with three hidden layers, although it has a smaller number of neurons. Between the other two, the expected results were obtained, as the 45 neuron performs better or equal to that of 40 neurons. However, the difference in performance between these structures is much smaller than that between the two and the three hidden layers networks.

The predictions provided by the three layers network are accurate in all test cases, precisely tracking the ship roll response.

However, and taking into account that the ship model was not validated for the irregular wave scenario, to definitely assess the capability of neural networks to accurately forecast ship roll motion as parametric roll in realistic seaway conditions, it is necessary to include data from the model tank tests in irregular seas. These tests will be presented in the following section.

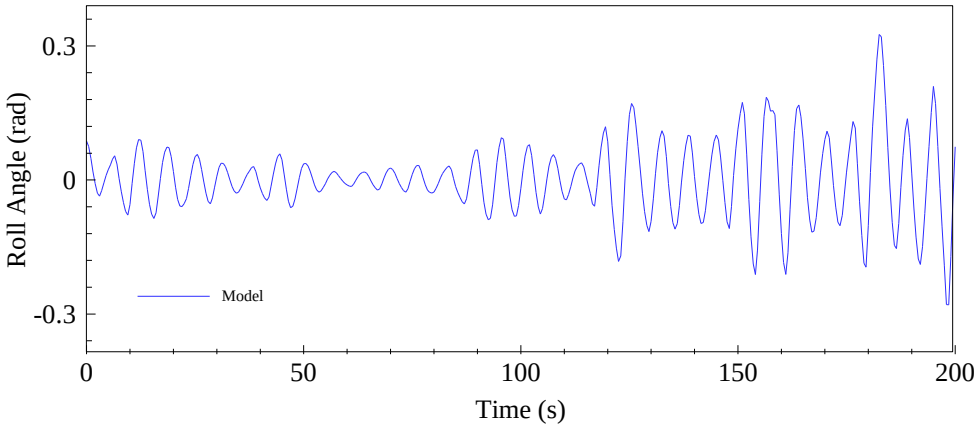

Figure 4.23. Irregular waves. Roll motion Test 1 time series.

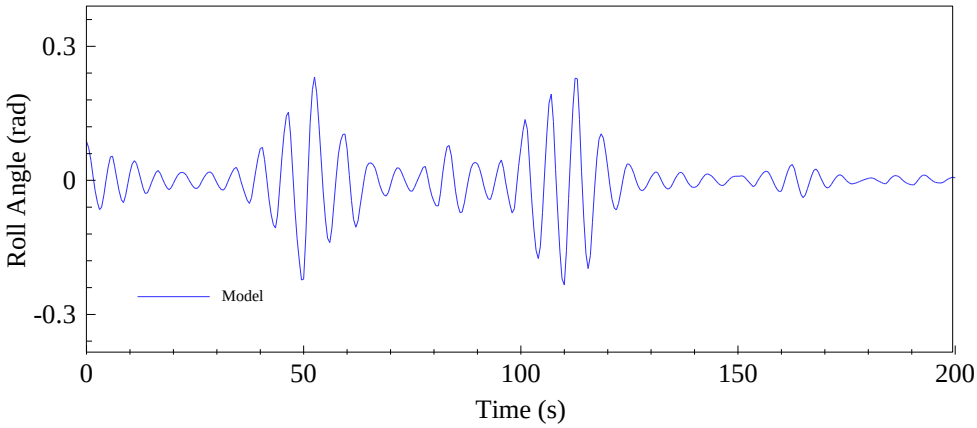

Figure 4.24. Irregular waves. Roll motion Test 2 time series.

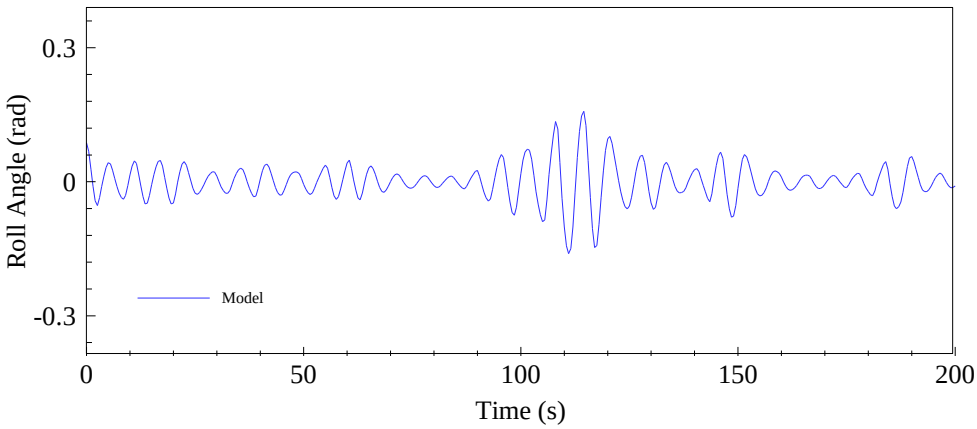

Figure 4.25. Irregular waves. Roll motion Test 3 time series.

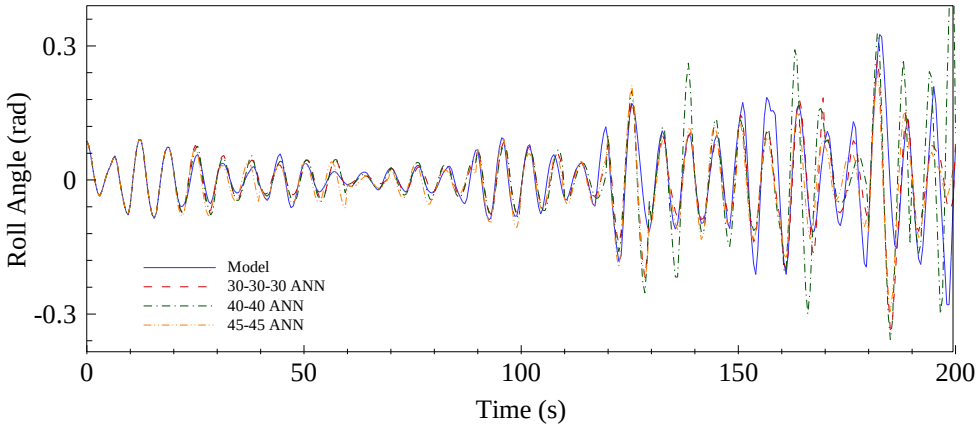

Figure 4.26. Irregular waves. Test 1 forecast results.

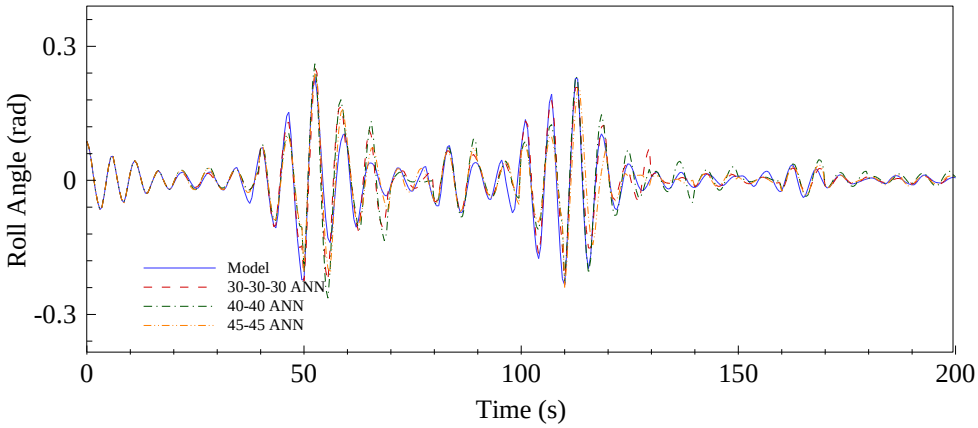

Figure 4.27. Irregular waves. Test 2 forecast results.

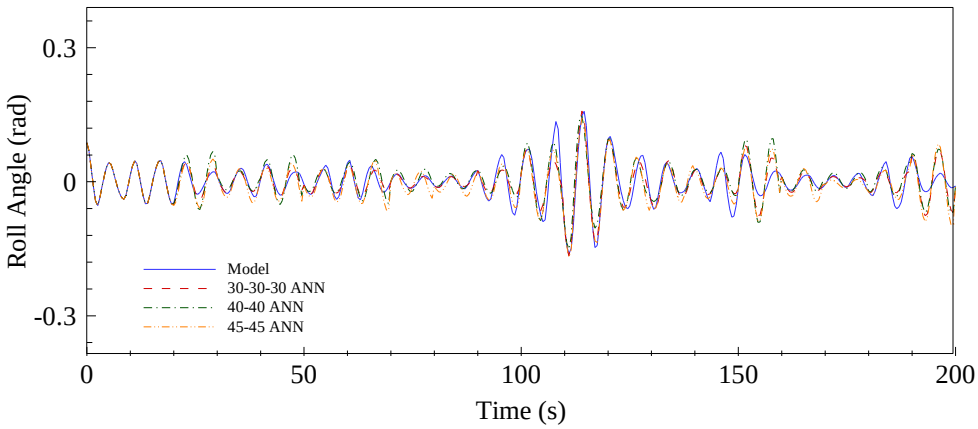

Figure 4.28. Irregular waves. Test 3 forecast results.

4.5 Towing Tank Tests

In order to test the behavior of the proposed system in a more realistic scenario to that provided by the mathematical model, the data obtained in the towing tank test of the Spanish trawler, described in Section 3.2, have been used.

In these tests, the ship is towed along the tank both in regular and irregular longitudinal waves, in 6 d.o.f. and under the influence of the disturbances generated by the carriage, wave interferences, wave iregularities generated by the wave-maker, etc.

The roll time series used for training and testing the ANN forecaster have been some of those obtained in the towing tanks tests, both in regular and irregular head seas, and the applied methodology has been the same as described for the mathematical model case. In order to evaluate the performance of the algorithm both in conditions where parametric rolling occurs and where it doesn´t, non resonant situations have also been included.

4.5.1 Regular Waves

As a first approximation, the forecasting system has been tested in regular head waves, for a real ship speed corresponding to a Froude number of 0.2 (around 7.0 knots).

The train and test cases have been obtained from the experiments that have been carried out with different values of wave frequency and amplitude at this Froude number, and that have been previously described in Section 3.2. These time series have an average full scale length of 420 seconds and can be seen in Figure 4.29.

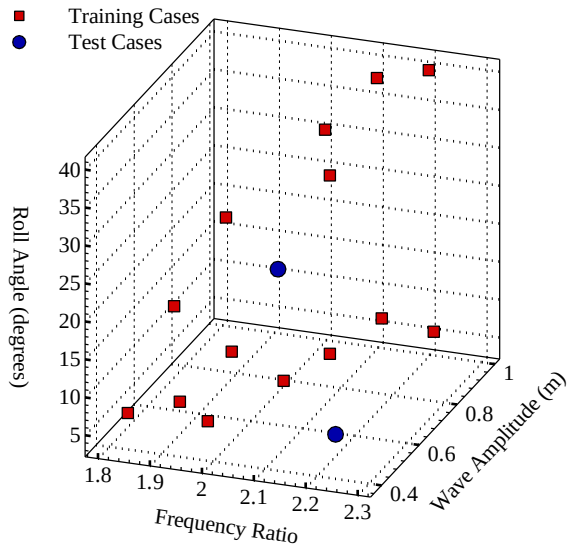

Figure 4.29. Regular waves. Towing tank experiments. Parameters.

In this occasion, encounter frequency – natural roll frequency ratio ranges from 1.8 to 2.3, implying that there would be cases where parametric roll is not present (see Figure 3.8). Due to this fact, the performance of the system in a condition where only small roll amplitudes appear due to small transversal excitations or when roll motions decrease (cases that were not present in the mathematical model tests as no other excitation was present appart from head waves) could have been evaluated.

From those experiments, two time series were chosen for testing the system (blue dots in Figure 4.29), including one with fully developed parametric roll, and another one without any resonant motions.

During the experiments, time series were sampled at a frequency of 50 Hz. For generating the ANN training and tests cases, time series were resampled at 2 Hz and following the same methodology of the previous section, divided into 40+1 time steps. 11169 training cases were obtained this way from the experimental data.

Table 4.12. Regular waves. Prediction performance. MSE ($x10^{-4}$).

Test case	40-40	45-45	50-50	30-30-30	40-40-40
Test 1	15.38	16.47	16.55	12.04	15.05
Test 2	4.11	4.20	4.33	4.73	3.76

As previously described, two test cases have been proposed, for combinations of wave frequency and amplitude not used during the training phase. The first one (Test 1), corresponds to a frequency ratio of 2.0 and a wave amplitude of 0.745 m (fully developed resonance). In the second one (Test 2), a frequency ratio of 2.2 and a wave amplitude of 0.5 m (no resonance condition) have been selected.

In order to increase the precision of the system, five different MP structures have been tested, modifying the initial one of two layers and 30 neurons per layer; these structures are three alternatives with two hidden layers and with the number of neurons ranging from 40 to 50, and two alternatives with three layers, with 30 and 40 neurons per layer. 10 seconds ahead predictions have been conducted for all test cases.

In Table 4.12, the error values (MSE) obtained with the five different MP structures for the two test cases, are presented. In Figure 4.31 and Figure 4.33, the results obtained with the best alternative for each of the test cases (three layers and 30 neurons per layer in Test 1, and three layers and 40 neurons per layer in Test 2), are included.

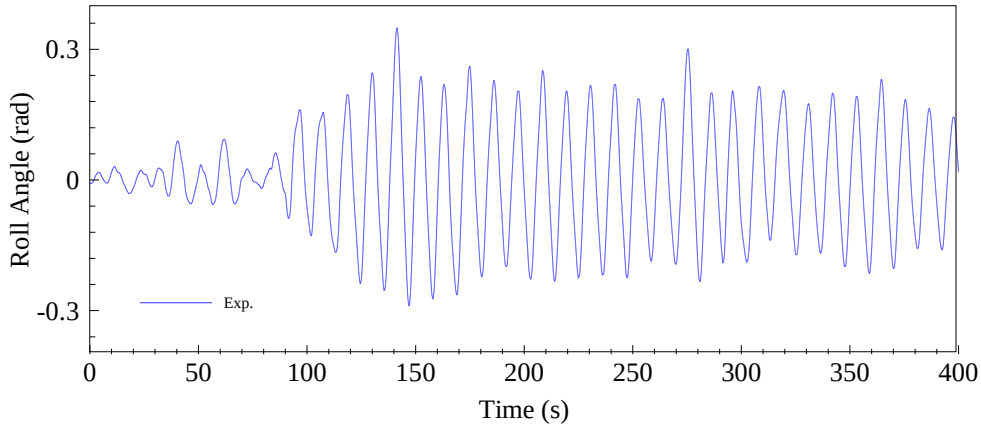

Figure 4.30. Regular waves. Roll motion Test 1 time series.

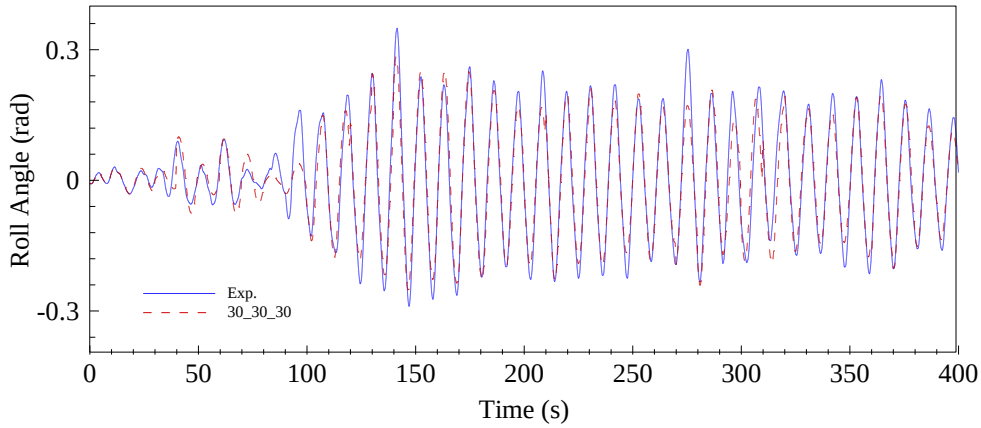

Figure 4.31. Regular waves. Test 1. Forecast results. 30 neuron, 3 layer MP.

As it can be seen from the error values and the presented graphs, the predictions obtained in both test cases are quite accurate. These cases include both resonant and non resonant behaviour in more realistic conditions than those observed in the mathematical model case, as small roll motions due to external disturbances and natural roll motion are included.

Again, it has to be emphasized that ANN performance increases with the number of layers and neurons, but up to a limit, over which its performance remains constant.

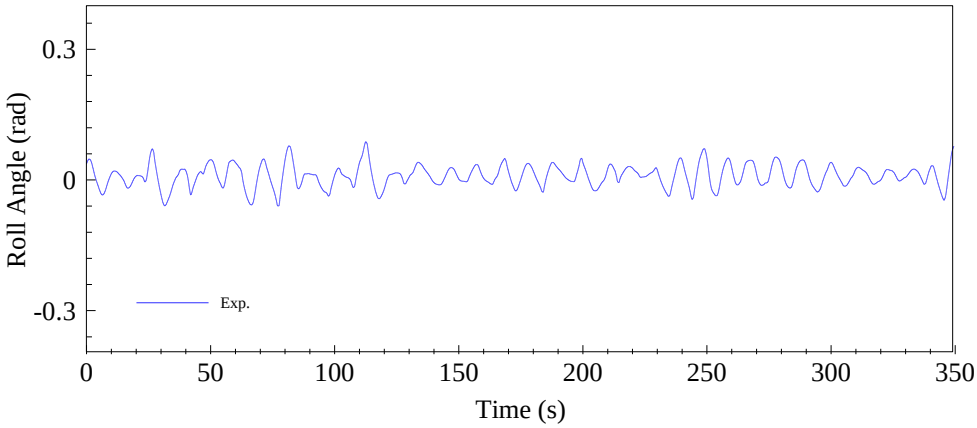

Figure 4.32. Regular waves. Roll motion Test 2 time series.

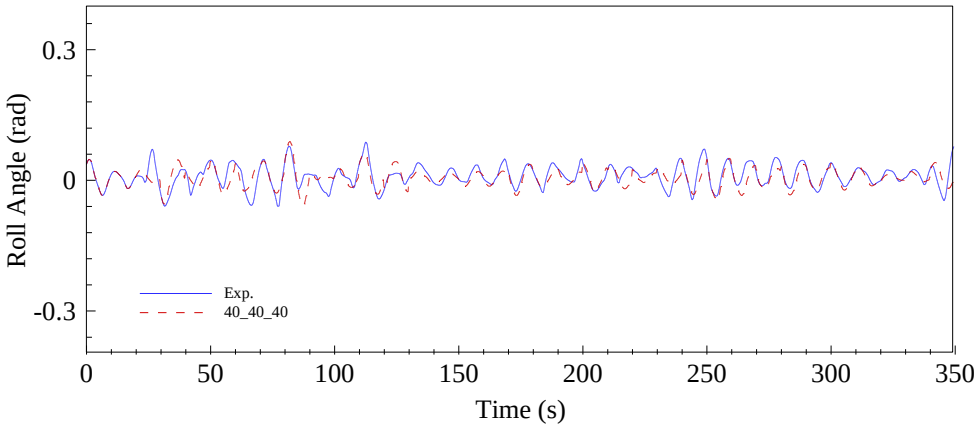

Figure 4.33. Regular waves. Test 2. Forecast results. 40 neuron, 3 layer MP.

This fact could be appreciated in the two hidden layer alternatives, where in both cases, the best results are obtained with the 30 neuron structure, and also in the three hidden layer alternative in Test 1, where the best results correspond to the 30 neurons case.

4.5.2 Irregular Waves

Finally, in order to test the behavior of the forecasting system in a condition as closer as possible to a real sailing situation, the irregular head waves case was considered.

Again, as in the previous case, the loading condition of the ship was kept constant (and equal to the one described in Section 3.2) and the vessel speed was also set to a Froude number of 0.2 (7 knots of real ship speed).

For training and testing the MPNN forecasting system, the experiments corresponding to the irregular wave case and TMA spectrum, with a peak shape parameter of 7 and a significant wave height of 1.5 meters, have been selected (see Table 3.5). In these experiments, the spectrum peak frequency is modified, in order to get peak encounter frequency – natural roll frequency ratios of between 1.9 and 2.2, where parametric roll resonance may appear according to the previously presented results.

The whole set of training cases has been obtained from 15 time series where roll resonance either takes place or not, with an average real scale length of about 380 seconds. For testing the system, two time series have been selected, corresponding to frequency ratios of 2 (Test 1) and 2,1 (Test 2); in the first one, parametric roll doesn´t appear, while in the second, a large amplitude episode is present.

In Figure 4.34 and Figure 4.35, the selected test time series are presented. As can be seen, in Test 1 no parametric rolling events develop, being only present small amplitude roll motions due to the natural roll motion of the ship and the effects of the present external disturbances (towing device, wall rebounds, etc.). The maximum roll amplitude reaches approximately 0.13 rad (7.4 degrees) around the second 225, and soon dissipates into the average of 1.2 degrees that could be found along the whole time series.

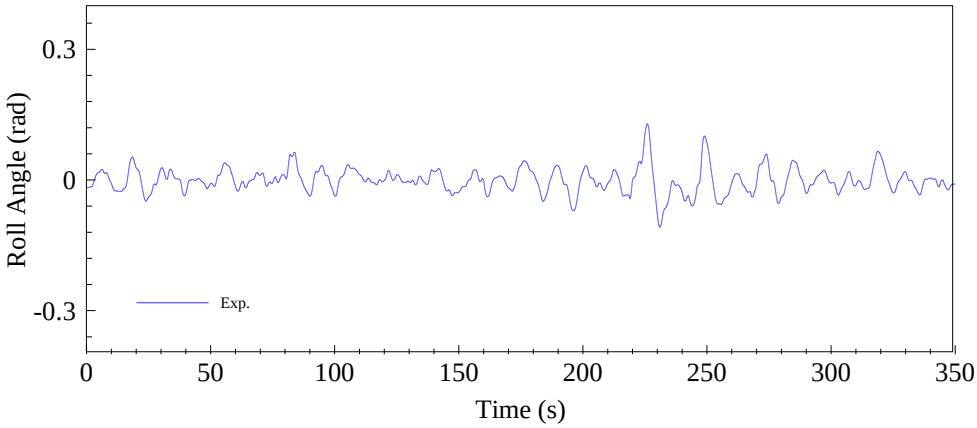

Figure 4.34. Irregular waves. Roll motion Test 1 time series.

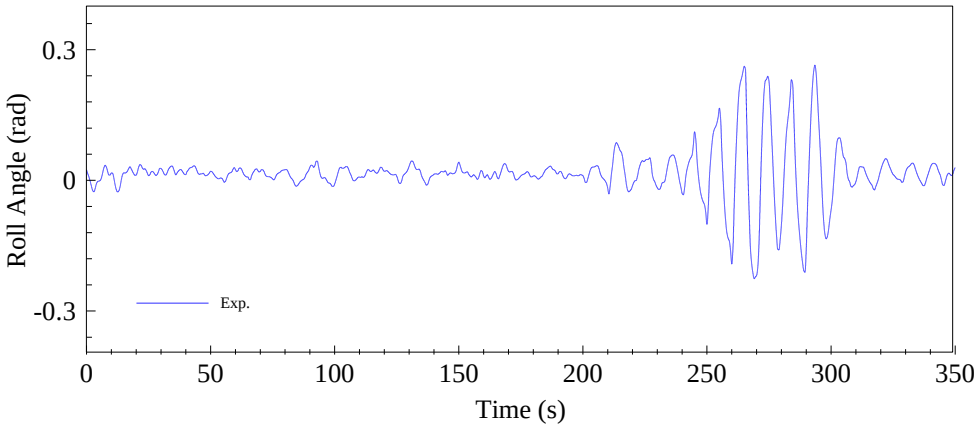

Figure 4.35. Irregular waves. Roll motion Test 2 time series.

In Test 2, no large roll motions appear until a slightly larger roll to port around second 215 and an adequate wave sequence, excite an episode of parametric roll, that lasts for 6 rolling cycles (approximately from second 240 to 310) and that dissipates when wave conditions change.

Again, and following the same methodology described in the regular waves case, time series have been re-sampled from 50 to 2 Hz and divided in the 40 + 1 time steps that are used as inputs and output of the network. This way, 10898 cases were obtained and used in the training process.

The same five structures that were proposed in the regular waves case, have also been tested here. So, three two hidden layer structures with 40, 45 and 50 neurons per layer and two three layer ones, with 30 and 40 neurons, have been trained (50 training processes each, selecting the best performing one) and a 10 seconds forecast obtained with each one for the two test cases.

The error values (MSE) of the ten predictions are included in Table 4.13. As can be seen from these values, the fact that increasing the number of layers and neurons not necessarily implies and increase in the network performance is specially reflected in Test 1. In this case, the best performing structure is the two layer 45 neurons one, which is not the largest of the set. This fact could also be seen in Test 2. Although in this occasion the largest structure (three layer, 40 neuron) is the best performing one, its performance is very similar to that of the two layer, 40 neuron one.

In Figure 4.36 and Figure 4.37, the results obtained with the best alternative for each of the test cases (two layers and 45 neurons per layer in Test 1, and three layers and 40 neurons per layer in Test 2), are included.

Table 4.13. Irregular waves. Prediction performance. MSE ($x10^{-4}$).

Test case	40-40	45-45	50-50	30-30-30	40-40-40
Test 1	6.32	5.60	6.00	5.94	6.35
Test 2	16.70	40.80	31.70	22.50	16.66

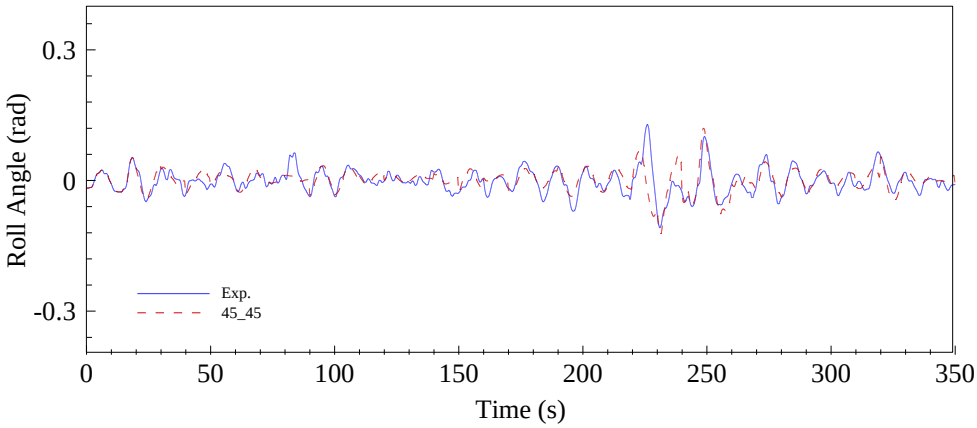

Figure 4.36. Test 1. Forecast results. 45 neuron, 2 layer MP.

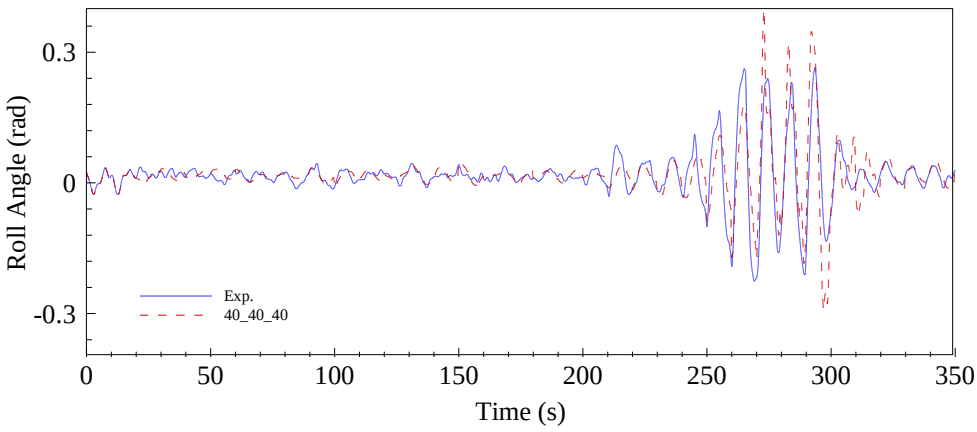

Figure 4.37. Test 2. Forecast results. 40 neuron, 3 layer MP.

4.6 Discussion

In this section, an innovative roll motion forecasting system has been presented, with the capacity of also predicting the short term appearance of parametric roll resonance. It has been shown that the systems performed well in most of the tested situations, making forecast of up to 40 seconds in advance for the simplest cases, while also accurate predictions of up to 10 seconds in advance have been obtained for the most complex cases obtained from irregular waves tests in the towing tank.

Two aspects are crucial for the proposed roll motion forecasting system: the time horizon in which reliable predictions are made, and the high accuracy of these predictions. Two scenarios are feasible: the prediction system is directly used by the fisherman/captain in the wheel house to monitor the ship's behavior and eventually alert the rest of crew busy in the fishing activities; the prediction system provides roll motion forecasts to a diagnostic system used for automatic detection of parametric roll.

In the first situation, to have a sufficiently long prediction horizon is a condition sine qua non the crew cannot take countermeasures to guarantee their safety and bring the vessel out of the risky zone. It is also essential to have accurate predictions because the captain would not like to put in alert his crew if there is no need for that; a false alarm could determine e.g. the loss of catch, or crew's member injuries due to the spread of panic, or even the execution of rough maneuvers, which may really lead the vessel into unstable motions.

In the second scenario the two aspects are as important as in the first. The time span of the forecasting is an issue even if it is a detection system processing the predictions simply because it will still be the captain who will have to promptly respond to an issued alarm. In fact current regulations prohibit to any system to

directly inject control signals into the autopilot, in case one was available onboard. The accuracy of the predictions is substantial because, although it is not possible to infer a priori that a poor prediction will determine poor detection performances, it is sensible to think that a highly accurate forecast may require a less robust diagnostic system.

Considering the prediction performance showed by the MPNN in the analyzed sailing conditions, and by taking in account the small size and inertias of the test vessel, the authors think that a combined predictor could be employed, using a (20 - 10) prediction scheme. The 20 seconds forecast would be used to display preventive alarms, which could be used to alert the crew about possible large roll oscillations; whereas the 10 seconds accurate predictions would be used to confirm or reject the alert situation. A time span of 10 seconds could also be enough for the master to change ship's speed or course.

Moreover, and although in the work presented in these dissertation the proposed methodology has been applied to two small-medium sized fishing vessels, it can be straightforwardly applied to any other kind of ship, for example the resonance-prone large containerships, with the only need of a modification on the sampling rate and the subsequent change in the time span of the input vector of the system; this increase in the input time span, will also imply an increase in the output, and so in the prediction times. Considering that the obtained 40 seconds predictions approximately correspond to 5 complete roll periods of the UK trawler, and that one whole period is predicted with a 10 seconds forecast for the Spanish trawler, equivalent prediction horizons could be obtained for other types of ships.

5 CONCLUSIONS AND FUTURE WORK

As have been established in Chapter 1, the main objectives of this work were focused onto two different topics. On one hand, on the study of the phenomenon of parametric roll resonance, with the objective of analyzing how the different parameters involved influence the appearance and intensity of the phenomenon and designing prevention systems. And on the other hand, on the development of short term detection schemes that could alert the crew about the appearance of parametric roll resonance. In this chapter, the main conclusions and contributions of this work will be presented.

As a brief summary of the work carried out in this work it will be said that, regarding the first of the main objectives, two research lines have been adopted and exploited for the analysis of parametric roll resonance in head seas: the experimental approach, through the design and carrying out of two scale model tests in head waves, and the analytical one, implementing, validating and applying two mathematical models of ship motion, capable of simulating parametric roll resonance, to the study of the phenomenon.

Regarding the design of the detection schemes, in the present work an original approach, consisting on the application of artificial neural networks to the forecasting of the ship roll motion, has been taken. The proposed system has shown to be able to obtain accurate predictions of the ship roll motions in different degrees of advance, which could be applied to an onboard parametric roll detection system.

The work presented in this dissertation has been based on the study of two different fishing vessels. They have been selected due to the importance of this fleet and the fishing sector in Spain and also to its higher risk in comparison with other types, which make them and their crews more vulnerable to dynamic stability issues. Finally, also due to the fact that up to date, they have been remained less studied than larger ships, such as containerships, because of their relative smaller economical importance. Below, a more detailed description of the conclusions corresponding to each of the main objectives of this thesis, are presented.

5.1 Parametric Roll Stability Analysis

In Chapter 3, the work aimed at analyzing the behaviour of the two selected ships in parametric roll resonance conditions have been carried out. From the background analysis contained in Chapter 2, it can be concluded that two main research lines, i.e. analytical or experimental, could be taken for analyzing the phenomenon. Mathematical codes provide a relatively easy to use, low cost and less time consuming tool, that allows extensive analysis of ship dynamics in a seaway. However, the accuracy of these methods is correct for qualitative analysis, but, depending on their complexity, may lack precision for quantitative analysis. On the other hand, towing tank tests provide much more realistic data, but experiments are costly and very time consuming, and so just a limited set of conditions can be evaluated.

In this work, both techniques have been applied for analyzing the behaviour of the previously mentioned stern trawlers, under conditions likely to induce parametric resonance.

Regarding the experimental approach, two towing tank testing campaigns have been carried out. Both of them have been as extensive as possible, aimed at

collecting the largest amount of data; the more than 250 test runs are representative of this fact.

In the first case, a Spanish type trawler has been analyzed both in regular and irregular waves. The characterization of parametric roll for this ship in both cases has been done, including the representation of the stability diagrams (which are a good indicator of the risk of developing parametric roll as a function of the prevailing sea state and ship loading parameters) and the analysis of the influence that the different parameters have on the amplitude of parametric roll events.

In the second case, a UK type stern trawler has been studied. In order to do so, an advanced scale model of the vessel was developed. This model was designed to be mainly applied to the conducting of seakeeping tests, not only parametric resonance, but also broaching, loss of stability or any others. It is completely watertight, its dynamical behaviour is fully monitored by an IMU, torque, thrust, rpm and rudder position sensors, and can be auto controlled by using an onboard mounted PC. A similar analysis to the previously described has been done for this second ship. The characterization of parametric rolling in this case has been only done in regular waves and two different loading conditions have been tested.

In both cases, the analyzed data is limited to roll motion. However, and especially in the second case, a very large amount of data corresponding to ship motions, speeds and accelerations, is available for future analyses. From the observations in the towing tank tests, the presence of very large pitch motions for certain waves has been noticed and their influence on parametric roll development could be the objective of future research.

Although towing tank tests provide more realistic dynamical data, in order to develop an onboard prevention system it is necessary to have a fast and quite accurate tool which can be used for analyzing the risk level of the ship in a given seaway. Two non linear models have been implemented and tested in this work. A one degree of freedom model and the three degrees of freedom model developed by (M.A.S. Neves,Rodríguez, 2006). The data obtained with the models have been compared to that from the towing tank tests, in order to evaluate their performance at the different sea and vessel conditions, and to evaluate the possibility of the application of these models into an onboard system.

The obtained results have shown that the one degree of freedom fails in simulating the parametric roll events present at the highest speed tests, while accurate results are obtained for the rest of the conditions. An underestimation of the large pitching motions observed in the towing tank, may be the cause of this matter. The higher order model has performed better in a wider range of situations, as the couplings between pitch, heave and roll are directly included in this approach.

5.2 Parametric Roll Prediction

The analysis carried out in Chapter 2, has shown that parametric roll resonance in head seas is a real issue affecting large fleets, of different kind of ships, and that the appearance of these events may lead to catastrophic consequences, including not only economical losses, but also human lives. Moreover, it has also been shown that in the last years, the maritime community has stated the need of developing systems that could detect, on the short term, the appearance of a parametric roll episode shortly before it develops. This could avoid damage to the crew, the vessel or the cargo, and also the inconvenient of heading or

speed changes that could be derived from the use of long term predictions of traditional guidance systems.

Taking as a basis the existing detection strategies, which in any case are very limited in number, a novel alternative has been proposed, implemented and tested in this work. Taking profit from the well known capabilities of artificial neural networks for reproducing the behaviour of complex non linear systems, these algorithms have been applied into a roll motion forecasting system, which from the analysis of the rolling of the ship, is capable of forecasting this time series in different degrees of advance.

The performance of these schemes has been tested by using data obtained with the previously mentioned 3 d.o.f. mathematical model in head regular and irregular seas, but also with much more realistic data obtained from the towing tank testing of a scale model.

In both cases, the presented results have indicated a very good accuracy of the predictions, which in the best cases have a forecasting horizon of more than four rolling cycles, showing the suitability of the proposed approach for its use within an onboard parametric roll prevention and prediction system.

Moreover, the developed system has a main advantage respecting the existing approaches. While the latter are limited to analyzing the motions of the vessel and issuing a detection signal if a set of prescribed conditions are fulfilled, the former provides a motion forecast. This may be analyzed for determining if roll resonance is developing, but that could also be taken into account for optimizing any possible stabilizing measures that could be undertaken.

Finally, the proposed methodology, although implemented for the case of the two stern trawlers, is straightforwardly applicable to any other type of ship with similar accuracy, fact which largely increases its real possibilities.

5.3 Future Work

The presented work had been mainly focused as an approximation to the design and development of a parametric roll prevention system, that installed onboard could guide the masters, detect the appearance of resonance and prevent it from developing. As such an approximation, there is still a broad research field until that system could be installed onboard. This research can be divided into three main topics, which are described below:

- **Improvement of the forecasting times**. Although the obtained results are very promising, longer predictions would be desirable for improving the efficiency of the system. The study of other different neural network structures, together with the analysis of other parameters which may enable the earlier detection of the phenomenon, related with the roll, heave or pitch motions, are among the possible approaches to this issue.

- **Real time measurement of wave and ship conditions**. In order to evaluate the level of risk of a given seaway, it is necessary to know which are the real sailing conditions of the ship to determine, by using the implemented mathematical models, if parametric roll is likely to occur. The development of algorithms able to accurately determining these values from the analysis of ship motions would be extremely important to obtain a low cost guidance system to install, for example, in the small ships studied along this work. Collected data from the towing tank tests, where both wave and ship sailing parameters are known, could be used for the design and the validation of such algorithms.

- **Implementation on an onboard system.** The implementation of the proposed algorithms into an onboard system, to carry out real scale tests, would be the last stage of the development of the proposed preventive strategy. The design of a data acquisition and processing unit, together with the implementation of the ANN based algorithms into a real time environment, would be also an important topic for future work.

But apart from the aforementioned lines, which are largely related to the initial objective of this thesis, in the course of this work some other future research topics have been identified. Among them, broaching analysis or deeper parametric roll and other ship dynamics studies could be highlighted and are described below.

- **Broaching analysis.** From the dynamic instabilities a ship can experience, broaching in following seas is among the less known, and an increase of the studies on this matter has been noticed in the last years. In the same way as with parametric roll, experimental analysis is the best way of obtaining accurate data for studying the phenomenon, but due to its characteristics, not all scale models are prepared for broaching testing. The one developed in this work is, and so its appliance into broaching analysis would be an extremely helpful tool.

- **Further analysis of parametric roll resonance and other dynamical issues.** In this work, only a limited part of the data obtained from the towing tank tests has been used, which is that corresponding to roll motions. So, and considering the huge amount of data available, the analysis of the pitch and heave influence on roll motion, together with a study of the performance of the proposed mathematical models as a

function of both degrees of freedom, may be future work lines. Moreover, the incidence of wavelength and wave slope on the development of roll resonance could also be a future field of reserach.

REFERENCES

Abramowitz, M.,Stegun, I. A. (1964). *Handbook of mathematical functions with formulas, graphs, and mathematical tables* (Vol. 55): Dover Publications.

ABS. (2000). Giants in the Container Industry. Ultra Large Containerships: American Bureau of Shipping.

ABS. (2004). Guide for the Assessment of Parametric Roll Resonance in the Design of Container Carriers: American Bureau of Shipping.

ABS. (2008). ABS Awards First Containership Parametric Roll Notation. *ABS press releases 2008*, from www.eagle.org

Alarcin, F.,Gulez, K. (2007). Rudder roll stabilization for fishing vessel using neural network approach. *Ocean Engineering, 34*(13), 1811-1817.

Amarcon-BV. (2011a). Amarcon and Technical University of Denmark Develop System for Parametric Roll Warnings Retrieved 3/06/2012, 2012, from http://www.ship-technology.com

Amarcon-BV. (2011b). Amarcon OCTOPUS - Onboard. Retrieved from http://www.amarcon.com

AMI. (2001). AMI Seware EnRoute Live. Retrieved from http://www.amiwx.com/seawareenroutelive.html

BEAmer. (2006). Report on the technical inquiry into the case of the CMA CGM Otello. Bay of Biscay. 17th February 2006. Paris: Bureau d'enquêtes sur les évènements de mer.

Beck, R. F.,Reed, A. M. (2000). *Modern Seakeeping Computations for Ships.* Paper presented at the Twenty-Third Symposium on Naval Naval Hydrodynamics, Val de Reuil, France.

Belenky, V. L.,Sevastianov, N. B. (2007). *Stability and Safety of Ships. Risk of Capsizing. Second Edition*: The Society of Naval Architects and Marine Engineers (SNAME).

Belenky, V. L., Yu, H.,Weems, K. M. (2006). *Numerical Procedures and Practical Experience of Assessment of Parametric Roll of Container Carriers*. Paper presented at the International Conference on Stability of Ships and Ocean Vehicles, Rio de Janeiro, Brazil.

Bellec, J. R., Rodríguez, C. A.,Neves, M. A. S. (2012). An investigation on parametric rolling prediction using neural networks *Sustainable Maritime Transportation and Exploitation of Sea Resources* (pp. 157–163). London, UK: CRC Press. Taylor & Francis Group.

Bernoulli, D. (1810). *Mémoire sur la manière de diminuer le roulis et le tangage d'un naivre*. Paris: Bachelier.

Bhattacharyya, R. (1978). *Dynamics of Marine Vehicles*. New York: Wiley - Interscience.

Birikh, R. V., Briskman, V. A., Cherepanov, A. A.,Velarde, M. G. (2001). Faraday ripples, parametric resonance, and the Marangoni effect. *Journal of Colloid and Interface Science, 238*(1), 16-23.

Blocki, W. (1980). Ship Safety in Connection with Parametric Resonance of the Roll. *International Shipbuilding Progress, 27*, 36.

BMA. (2007). The combined report of the investigations into the disablement of the passenger vessels Explorer & Voyager, due to the failure of the bridge front windows, during severe weather conditions, on the 27 January & 14 February 2005. London, UK: The Bahamas Maritime Authority.

Bouguer, P. (1746). *Traité du Navire, de sa Construction et de ses Mouvemens*. Paris: Chez Jombert.

Bouws, E., Günther, H., Rosenthal, W.,Vincent, C. (1985). Similarity of the wind wave spectrum in finite depth water. 1 - Spectral form. *Journal of Geophysical Research, 90*(C1), 975-986.

Breu, D., Fossen, T. I. (2010). *Extremum seeking speed and heading control applied to parametric roll resonance.* Paper presented at the IFAC Conference on Control Applications in Marine System (CAMS), Germany.

Breu, D. A.,Fossen, T. I. (2011). *L1 adaptive and extremum seeking control applied to roll parametric resonance in ships.* Paper presented at the IEEE International Conference on Control & Automation (ICCA), Sanitago, Chile.

Brown, D. K. (2006). *The way of a ship in the midst of the sea: the life and work of William Froude*. Penzanze, UK: Periscope Publishing Ltd.

Bulian, G. (2005). Nonlinear parametric rolling in regular waves--a general procedure for the analytical approximation of the GZ curve and its use in time domain simulations. *Ocean Engineering, 32*(3-4), 309-330.

Bulian, G. (2006a). *Development of analytical nonlinear models for parametric roll and hydrostatic restoring variations in regular and irregular waves.* PhD Thesis, Universitá Degli Studi di Trieste, Trieste, Italy.

Bulian, G. (2006b). Nonlinear parametric rolling in regular waves: An approximate analytical solution for the response curve in the region of first parametric resonance. *Journal of Ship Research, 50*(3), 239-249.

Bulian, G., Francescutto, A.,Lugni, C. (2004). On the nonlinear modeling of parametric rolling in regular and irregular waves. *International Shipbuilding Progress, 51*(2), 173-203.

Bulian, G., Francescutto, A.,Lugni, C. (2006). Theoretical, numerical and experimental study on the problem of ergodicity and practical ergodicity'with an application to parametric roll in longitudinal long crested irregular sea. *Ocean Engineering, 33*(8-9), 1007-1043.

Bulian, G., Francescutto, A., Umeda, N.,Hashimoto, H. (2008). Qualitative and quantitative characteristics of parametric ship rolling in random waves in the light of physical model experiments. *Ocean Engineering, 35*(17-18), 1661-1675.

Butikov, E. I. (2005). Parametric resonance in a linear oscillator at square-wave modulation. *European Journal of Physics, 26*, 157.

Carmel, S. M. (2006). Study of parametric rolling event on a panamax container vessel. *Transportation Research Record: Journal of the Transportation Research Board, 1963*(-1), 56-63.

Cipriano Quinteros, W. M. (2005). *Estabilidade do navio em condições extremas: estudo de um modelo numérico não-linear de terceira ordem, acoplado em seis graus de liberdade* Master Thesis, Universidade Federal do Rio de Janeiro, Rio de Janeiro.

Cybenko, G. (1989). Approximation by superpositions of a sigmoidal function. *Mathematics of Control, Signals, and Systems (MCSS), 2*(4), 303-314.

Chang, B. C. (2008). On the parametric rolling of ships using a numerical simulation method. *Ocean Engineering, 35*(5), 447-457.

Damgov, V. (2004). *Nonlinear and parametric phenomena: theory and applications in radiophysical and mechanical systems* (Vol. 49). Singapore: World Scientific Publishing Co.

de Juana Gamo, J., Rodrigo, C. A.,Rojas, L. P. (2005). *On the parametric rolling of fishing vessels*. Paper presented at the International Conference on Marine Research and Transportation, Ischia, Italy.

Demuth, H., Beale, M.,Hagan, M. (2011). *Neural Network Toolbox™ 6. User´s Guide*. Natick, MA, USA.: The MathWorks Inc. .

DNV. (2007). Recommended practice - Environmental conditions and environmental loads (Vol. DNV-RP-C205). Høvik, Norway: Det Norske Veritas.

Døhlie, K. (2006). Parametric Roll - a problem solved? *DNV Container Ship Update, 1*.

Ebada, A.,Abdel-Maksoud, M. (2006). *Prediction of ship turning manoeuvre using Artificial Neural Networks (ANN).* Paper presented at the Fifth International Conference on Computer Applications and Information Technology in the Maritime Industries, Oegstgeest, The Netherlands.

Euler, L. (1749). Scientia navalis: sev Tractatvs de constrvendis ac dirigendis navibvs.

Euler, L. (1759). Sur le roulis et le tangage: Examen des efforts qu'ont à soutenir toutes les parties d'un Vaisseau dans le Roulis et dans le Tangage. *On Rolling and Pitching…", Académie Royale des Sciences, Paris, prize treatise*, 1-47.

Europa-Press. (2005, 26/03/2006). Fallece una pasajera ibicenca del crucero 'Gran Voyager', accidentado en febrero entre Cerdeña y Menorca, *El Mundo*. Retrieved from http://www.elmundo.es/elmundo/2005/03/26/sociedad/1111855209.html

Evangelou, S., Limebeer, D. J. N., Sharp, R. S.,Smith, M. C. (2006). Control of motorcycle steering instabilities. *Control Systems Magazine, IEEE, 26*(5), 78-88.

Faltinsen, O. M. (1993). *Sea loads on ships and offshore structures*: Cambridge University Press.

Faraday, M. (1831). On a peculiar class of acoustical figures and on certain forms assumed by groups of particles upon vibrating elastic surfaces. *Philosophical Transactions of the Royal Society of London, 121*, 299.

Fincham, J. (1851). *History of naval architecture: to which is prefixed, an Introductory disertation on the application of mathematical science to the art of naval construction*. London: Whittaker & Co.

Fossen, T. I. (2011). *Handbook of Marine Craft Hydrodynamics and Motion Control*. UK: John Wiley & Sons.

Fossen, T. I., Nijmeijer, H. (2012). *Parametric Resonance in Dynamical Systems*. New York, USA: Springer.

Fossen, T. I.,Smogeli, Ø. N. (2004). Nonlinear time-domain strip theory formulation for low-speed manoeuvering and station-keeping. *Modeling, Identification and Control, 25*(4), 201-221.

France, W. N., Levadou, M., Treakle, T. W., Paulling, J. R., Michel, R. K.,Moore, C. (2003). An investigation of head-sea parametric rolling and its influence on container lashing systems. *Marine Technology, 40*(1), 1-19.

Francescutto, A. (2001). An experimental investigation of parametric rolling in head waves. *Journal of Offshore Mechanics and Arctic Engineering, 123*, 65.

Francescutto, A., Bulian, G.,Lugni, C. (2004). Nonlinear and stochastic aspects of parametric rolling modeling. *Marine Technology, 41*(2), 74-81.

Froude, W. (1861). On the rolling of ships. *Transactions of the Institute of Naval Architects, 2*, 180-227.

Froude, W. (1863). Remarks on Mr. Scott Russell's paper on rolling. *Transactions of the Institute of Naval Architects, 4*, 232–275.

Fujiwara, T.,Ikeda, Y. (2007). *Effects of Roll Damping and Heave Motion on Heavy Parametric Rolling of a Large Passenger Ship in Beam Waves*. Paper presented at the 9th International Ship Stability Workshop, Hamburg, Germany.

Galeazzi, R.,Blanke, M. (2007). *On the feasibility of stabilizing parametric roll with active bifurcation control.* Paper presented at the 7th IFAC Conference on Control Applications in Marine Systems, Bol, Croatia.

Galeazzi, R., Blanke, M.,Poulsen, N. K. (2009a). *Parametric Roll Resonance Detection on Ships from Nonlinear Energy Flow Indicator*. Paper presented at the 7th IFAC Symposium on Fault Detection, Supervision and Safety of Technical Processes, Barcelona, Spain.

Galeazzi, R., Blanke, M.,Poulsen, N. K. (2009b). *Parametric roll resonance detection using phase correlation and log-likelihood testing techniques.* Paper presented at the 8th IFAC International Conference on Manoeuvring and Control of Marine Craft, Guaruja, Brazil.

Galeazzi, R., Blanke, M.,Poulsen, N. K. (2012). Early Detection of Parametric Roll Resonance on Container Ships. *IEEE Transactions on Control Systems Technology*, *PP*(99).

Galeazzi, R., Holden, C., Blanke, M., Fossen, T. I. (2009). *Stabilisation of parametric roll resonance by combined speed and fin stabiliser control.* Paper presented at the Proceedings of the European Control Conference 2009, Budapest, Hungary.

Galeazzi, R.,Perez, T. (2011). *A Nonlinear Observer for Estimating Transverse Stability Parameters of Marine Surface Vessels.* Paper presented at the 18th IFAC World Congress, Milano, Italy.

Gimson, G. S. (1975). Report of Court No. S 497. Formal investigation on M.F.V. Trident (on PD111). London, UK.

GL. (2011). Certification of Hull Response Monitoring Systems for Container Ships (Vol. GL Rules & Guidelines I, Pt. 1 Ch. 5): Germanischer Lloyd.

Golden, R. M. (1996). *Mathematical methods for neural network analysis and design*. Cambridge, USA: The MIT Press.

Graff, W.,Heckscher, E. (1941). Widerstands und Stabilitäts versuche mit drei Fischdampfermodellen. *Werft-Reederei-Hafen, 22*.

Grim, O. (1952). Rollschwingungen, stabilität und sicherheit im seegang. *Schiffstechnik, 1*(1), 10-21.

Günther, H., Tränkmann, I.,Kluwe, F. (2008). *ADOPT DSS - Ocean Environment Modelling for Use in Decision Making support.* Paper presented at the 7th International Conference on Computer Applications and Information Technology in the Maritime Industries, Liege, Belgium.

Hashimoto, H.,Umeda, N. (2004). Nonlinear analysis of parametric rolling in longitudinal and quartering seas with realistic modeling of roll-restoring moment. *Journal of Marine Science and Technology, 9*(3), 117-126.

Hayashi, C. (1964). *Nonlinear oscillations in physical systems* (Vol. 33). New York, USA: McGraw-Hill New York.

Haykin, S. (1998). *Neural Networks. A comprehensive foundation*: Prentice Hall.

Himeno, Y. (1981). Prediction of Ship Roll Damping. A State of the Art. Michigan, USA: Department of Naval Architecture and Marine Engineering. The University of Michigan College of Engineering.

Holden, C., Galeazzi, R., Fossen, T. I.,Perez, T. (2009). *Stabilization of Parametric Roll Resonance with Active U-Tanks via Lyapunov Control Design.* Paper presented at the European Control Conference, Budapest, Hungary.

Holden, C., Perez, T.,Fossen, T. I. (2007). *Frequency-motivated observer design for the prediction of parametric roll resonance.* Paper presented at the IFAC Conference on Control Applications in Marine Systems, Bol, Croatia.

Holden, C., Perez, T.,Fossen, T. I. (2011). A Lagrangian approach to nonlinear modeling of anti-roll tanks. *Ocean Engineering, 38*(2-3), 341-359.

Ikeda, Y., Katayama, T., Fujiwara, T.,Munif, A. (2008). *Prediction Methods for Parametric Rolling Under Drifting Condition and their Validation - Final Report of SCAPE Committee (Part 3).* Paper presented at the 6th Osaka Colloquium on Seakeeping and Stability of Ships, Osaka, Japan.

IMO. (1995). Guidance to the Master for Avoiding Dangerous Situations in Following and Quartering Seas (Vol. IMO MSC/Circ. 707): IMO Maritime Safety Committee. 65th session.

IMO. (2002a). List of documents issued in connection with the forty-fifth session of the Sub-committee on Stability and Load Lines and on Fishing Vessels Safety (Vol. SLF 45/INF.4): IMO Sub-Committee on Stability and Load Lines and on Fishing Vessels Safety. 45th Session.

IMO. (2002b). Proposals with regard to the scope of revising the IS Code and teh related MSC/Circ. 707. Submitted by Germany. (Vol. SLF 45/6/2): IMO Sub-Committee on Stability and Load Lines and on Fishing Vessels Safety. 45th Session.

IMO. (2007). Revised Guidance to the Master for Avoiding Dangerous Situations in Adverse Weather and Sea Conditions (Vol. IMO MSC.1/Circ. 1228): IMO Maritime Safety Committee. 82nd session.

Insperger, T.,Stépán, G. (2003). Stability of the Damped Mathieu Equation With Time Delay. *Journal of Dynamic Systems, Measurement, and Control, 125*.

ITTC. (2005). Testing and Extrapolation Methods Loads and Responses, Stability. Predicting the Occurrence and Magnitude of Parametric Rolling (Vol. ITTC 7.5–02-07–04.3): Stability in Waves Committee of the 24th International Towing Tank Conference.

ITTC. (2008a). Testing and Extrapolation Methods Loads and Responses, Stability. Model Tests on Intact Stability (Vol. ITTC 7.5–02-07–04.1): Stability in Waves Committee of the 25th International Towing Tank Conference.

ITTC. (2008b). Testing and Extrapolation Methods. Loads and Responses, Stability. Model Tests on Intact Stability (Vol. ITTC 7.5-02-07-04.1): International Towing Tank Conference.

Jensen, J. J. (2007). Efficient estimation of extreme non-linear roll motions using the first-order reliability method (FORM). *Journal of Marine Science and Technology, 12*(4), 191-202.

Jensen, J. J., Pedersen, P. T.,Vidic-Perunovic, J. (2008). *Estimation of Parametric Roll in a Stochastic Seaway.* Paper presented at the IUTAM Symposium on Fluid-Structure Interaction in Ocean Engineering, Adelaide, Australia.

Jones, E. B., Roskilly, A., Webster, B.,Birmingham, R. (2006). Adaptive roll stabilization of fishing vessels. *Proceedings of the Institution of Mechanical Engineers, Part M: Journal of Engineering for the Maritime Environment, 220*(1), 13-27.

Journee, J. M. J.,Adegeest, L. J. M. (2003). Theoretical Manual of Strip Theory Program SEAWAY for Windows. Delft, The Nederlands: Delft University of Technology.

Juan, J.,Navia, J. G. (1793). *Examen marítimo teórico práctico ó Tratado de Mecánica aplicado á la construccion, conocimiento y manejo de los navíos y demás embarcaciones* (Vol. 689). Spain: Imprenta Real.

Kempf, G. (1938). Die Stabilität Beanspruchung der Schiffe Durch Wellen und Schwingungen. *Werft-Reederei-Hafen, 19*.

Kerwin, J. E. (1955). Notes on Rolling in Longitudinal Waves. *International. Shipbuilding Progress, 16*.

Kinney, W. D. (1961). On the unstable rolling motions of ships resulting from nonlinear coupling with pitch including the effect of damping in roll. San Diego, USA: University of California, Institute of Engineering Research.

Kroeger, P. (1987). Simulation der Rollbewegung von Schiffen im Seegang. Report No. 473. Hamburg: Institut fuer Schiffbau.

Krüger, S.,Kluwe, F. (2008). A Simplified Method for the Estimation of the Natural Roll Frequency of Ships in Heavy Weather. *HANSA International Maritime Journal*(9).

Krüger, S., Kluwe, F.,Vorhölter, H. (2008). *Decision support for large amplitude roll motions based on nonlinear time-domain simulations.* Paper presented at the Computer Applications and Information Technology in the Maritime Industries (COMPIT), Liege, Belgium.

Lewandowski, E. M. (2004). *The dynamics of marine craft: maneuvering and seakeeping*. Singapore: World Scientific Publishing Co.

Leybourne, M. T., Batten, W. M. J., Bahaj, A. S., O'Nians, J.,Minns, N. (2009). *A parametric experimental study of the 2D performance of a ducted wave energy converter.* Paper presented at the 8th European Wave and Tidal Energy Conference, Uppsala, Sweden.

Li, H., Guo, C.,Jin, H. (2005). *Design of Adaptive Inverse Mode Wavelet Neural Network Controller of Fin Stabilizer.* Paper presented at the International Conference on Neural Networks and Brain, Beijing, China.

Longhi, S. (2000). Parametric resonance in periodic paraxial optical systems. *Optics Communications, 176*(4-6), 327.

López Peña, F., Míguez González, M., Díaz Casás, V.,Duro Fernández, R. J. (2011). *Ship roll motion time series forecasting using neural networks.* Paper presented at the International Conference on Computational Intelligence for Measurement Systems and Applications, Ottawa, Canada.

Lloyd, A. R. J. M. (1989). *Seakeeping: ship behaviour in rough weather*. Sussex, UK: A.R.J.M. Lloyd.

MAIB. (2006). Report on the investigation of the loss of cargo containers overboard from P&O Nedlloyd Genoa, North Atlantic Ocean on 27 January 2006. Southampton: Marine Accident Investigation Branch.

MAIB. (2009). Report on the investigation of heavy weather encountered by the cruise ship Pacific Sun 200 miles north north east of North Cape, New Zealand on 30 July 2008 resulting in injuries to 77 passengers and crew. Southampton: Marine Accident Investigation Branch.

Malenica, Š., Chen, X. B.,Xia, J. Z. (2006). *Parametric Roll–Validation of a Numerical Model.* Paper presented at the 7th International Conference on Hydrodynamics, Ischia, Italy.

Marsig. (2011). ARROW. Retrieved from http://www.marsig.com

McCue, L. S.,Bulian, G. (2007). A numerical feasibility study of a parametric roll advance warning system. *Journal of Offshore Mechanics and Arctic Engineering, 129*, 165.

McCue, L. S., Campbell, B. L.,Belknap, W. F. (2007). On the Parametric Resonance of Tumblehome Hullforms in a Longitudinal Seaway. *Naval Engineers Journal, 119*(3), 35-44.

Mégel, J.,Kliava, J. (2009). On the buoyancy force and the metacentre. *arXiv Cornel University, arXiv:0906.1112*.

Míguez González, M., Caamaño Sobrino, P., Tedín Álvarez, R., Díaz Casás, V., Martínez López, A.,López Peña, F. (2012). Fishing vessel stability assessment system. *Ocean Engineering, 41*, 67-78.

Miguez González, M., Díaz Casás, V., López Peña, F.,Duro, R. J. (2008). Buques de Pesca y Eficiencia Energética: Proyecto Peixe Verde Actividad del Grupo Integrado de Ingeniería. *Ingeniería Naval*(857), 94-107.

Míguez González, M., López Peña, F., Díaz Casás, V., Galeazzi, R.,Blanke, M. (2011). *Prediction of Parametric Roll Resonance by Multilayer Perceptron Neural Network.* Paper presented at the 21st International Offshore (Ocean) and Polar Engineering Conference (ISOPE), Maui, USA.

Míguez González, M., López Peña, F., Díaz Casás, V.,Neves, M. A. S. (2010). *An Artificial Neural Network Approach for Parametric Rolling Prediction.* Paper presented at the The 11th international symposium on practical design of ships and other floating structures, Río de Janeiro, Brazil.

Míguez González, M., López Peña, F., Díaz Casás, V.,Neves, M. A. S. (2011). *Large Amplitude Roll Motion Forecasting through an Artificial Neural Network System.* Paper presented at the 12th International Ship Stability Workshop, Washington D.C., USA.

Mook, D. T., Marshall, L. R.,Nayfeh, A. H. (1974). Subharmonic and Superharmonic Resonances in the Pitch and Roll Modes of Ship Motions. *Journal of Hydronautics, 8*, 32.

Moreno-Moreno, M., Raman, A., Gomez-Herrero, J.,Reifenberger, R. (2006). Parametric resonance based scanning probe microscopy. *Applied Physics Letters, 88*(19), 193108-193108-193103.

Munif, A., Katayama, T.,Ikeda, Y. (2005). Numerical Prediction of Parametric Rolling of a Large Passenger Ship in Beam Seas. *Conference proceedings, the Japan Society of Naval Architects and Ocean Engineers, 1*(2005-11), 95-98.

Munif, A.,Umeda, N. (2006). Numerical prediction on parametric roll resonance for a ship having no significant wave-induced change in hydrostatically-obtained metacentric height. *International Shipbuilding Progress, 53*(3), 183-203.

Nayfeh, A. (1988). On the undesirable roll characteristics of ships in regular seas. *Journal of Ship Research, 32*(2).

Nayfeh, A. H.,Mook, D. T. (2004). *Nonlinear oscillations* (Vol. 31). USA: John Wiley & Sons.

Nayfeh, A. H., Mook, D. T.,Marshall, L. R. (1973). Nonlinear coupling of pitch and roll modes in ship motions. *Journal of Hydronautics, 7*(4).

Neves, M. A. S. (2004). *Dinâmica do Navio*. Rio de Janeiro: Departamento de Enghenheria naval e Oceânica. Universidade Federal do Rio de Janeiro.

Neves, M. A. S., Merino, J. A.,Rodríguez, C. A. (2009). A nonlinear model of parametric rolling stabilization by anti-roll tanks. *Ocean Engineering, 36*(14), 1048-1059.

Neves, M. A. S., Muñoz, J. A. M., Castillo, C. A. R.,Soares, L. F. N. (2007). *Estabilización de Rolido Paramétrico Utilizando un Tanque de Estabilización Pasivo Tipo U*. Paper presented at the Congreso Panamericano de Ingeniería Naval (COPINAVAL).

Neves, M. A. S., Perez, N.,Lorca, O. (2003). Analysis of roll motion and stability of a fishing vessel in head seas. *Ocean Engineering, 30*(7), 921-935.

Neves, M. A. S., Pérez, N.,Lorca, O. (2002). *Experimental analysis on parametric resonance for two fishing vessels in head seas.* Paper presented at the 6th International Ship Stability Workshop, Webb Institute, New York.

Neves, M. A. S., Perez, N.,Valerio, L. (1999). Stability of small fishing vessels in longitudinal waves. *Ocean Engineering, 26*(12), 1389-1420.

Neves, M. A. S.,Rodriguez, C. A. (2005). *A coupled third order model of roll parametric resonance.* Paper presented at the 12th International Congress of the International Maritime Association of the Mediterranean (IMAM), Lisbon, Portugal.

Neves, M. A. S.,Rodriguez, C. A. (2007). Influence of non-linearities on the limits of stability of ships rolling in head seas. *Ocean engineering, 34*(11-12), 1618-1630.

Neves, M. A. S.,Rodríguez, C. A. (2006). On unstable ship motions resulting from strong non-linear coupling. *Ocean Engineering, 33*(14-15), 1853-1883.

Neves, M. A. S., Rodríguez, C. A., Merino, J. A., Mañuico Vivanco, J. E., Villagómez Rosales, J. C.,Agarwal, R. (2009). *Efecto de la Aplicación de Tanques Estabilizadores Anti-Roll para prevenir la resonancia parametrica*. Paper presented at the Congreso Panamericano de Ingeniería Naval (COPINAVAL).

Neves, M. A. S., Rodríguez, C. A.,Vivanco, J. E. M. (2009). On the limits of stability of ships rolling in head seas. *Journal of Engineering for the Maritime Environment, 223*(4), 517-528.

Neves, S., Perez, N.,Lorca, O. (2003). Analysis of roll motion and stability of a fishing vessel in head seas. *Ocean Engineering, 30*(7), 921-935.

noticiasdecruceros.com. (2011). El Costa Voyager Retrieved 12/02/2012, 2012, from http://noticiasdecruceros.com.ar/index.php/2011/11/09/el-costa-voyager/#

Nowacki, H. (2006). *Developments in fluid mechanics theory and ship design before Trafalgar*: Max-Planck-Institute for the History of Science.

Nowacki, H. (2008). Leonhard Euler and the theory of ships. *Journal of Ship Research, 52*(4), 274-290.

Nowacki, H.,Ferreiro, L. D. (2011). Historical roots of the theory of hydrostatic stability of ships *Contemporary Ideas on Ship Stability and Capsizing in Waves*. London: Springer.

Oh, I.,Nayfeh, A. (1996). *Nonlinearly Interacting Responses of the Two Rotational Modes of Motion-Roll and Pitch Motions.* Paper presented at the Twenty-First Symposium on Naval Hydrodynamics, Trondheim, Norway.

Oh, I. G., Nayfeh, A. H.,Mook, D. T. (1993). *Theoretical and experimental study of the nonlinearly coupled heave, pitch and roll motions of a ship in longitudinal waves.* Paper presented at the 14th Biennial Conference on Mechanical Vibration and Noise.

Oh, I. G., Nayfeh, A. H.,Mook, D. T. (2000). A theoretical and experimental investigation of indirectly excited roll motion in ships. *Philosophical Transactions of the Royal Society of London. Series A: Mathematical, Physical and Engineering Sciences, 358*(1771), 1853-1881.

Olvera, A., Prado, E.,Czitrom, S. P. R. (2001). *Performance improvement of OWC systems by Parametric Resonance.* Paper presented at the Fourth European Wave Energy Conference.

Olvera, A., Prado, E.,Czitrom, S. P. R. (2007). Parametric resonance in an oscillating water column. *Journal of Engineering Mathematics, 57*(1), 1-21.

Oueini, S. S.,Nayfeh, H. A. (1999). Single-Mode Control of a Cantilever Beam Under Principal Parametric Excitation. *Journal of Sound and Vibration, 224*(1), 33.

Ovegård, E. (2009). *Numerical simulation of parametric rolling in waves.* Master thesis, KTH Royal Institute of Technology, Stockholm.

Paffett, J. A. H. (1976). Experiments with a model of MFV Trident and an alternative round-stern design. Feltham, UK: National Maritime Institute (NMI) Ltd.

Palmquist, M.,Nygren, C. (2004). Recordings of head-sea parametric rolling on a PCTC, SLF 47/INF.5. SLF 47th Session, document SLF 47/6/6: IMO Sub-Committee on Stability and Load Lines and on Fishing Vessels Safety, London.

Pauling, J. R.,Rosenberg, R. M. (1959). On Unstable Ship Motions Resulting from Nonlinear Coupling. *Journal of Ship Research, 3*, 36.

Pérez Meza, N. A.,Sanguinetti, C. F. O. (2006). Scale model tests of a fishing vessel in roll motion parametric resonance. *Síntesis Tecnológica, 3*(1), 33-37.

Perez, T. (2005). *Ship motion control. Course keeping and roll stabilisation using rudder and fins*. London: Springer Verlag.

Petey, F. (1988). Ermittlung der Kentersicherheit lecker Schiffe im Seegang aus Bewegungssimulationen (Bericht Nr. 487). Hamburg: Institut fuer Schiffbau.

Pierson, W. J.,St Denis, M. (1953). On the motion of ships in confused seas. *Transactions SNAME 61*, 280-354.

Ribeiro e Silva, S.,Guedes Soares, C. (2008). *Non-Linear Time Domain Simulation of Dynamic Instabilities in Longitudinal Waves.* Paper presented at the 27th International Conference on Offshore Mechanics and Arctic Engineering (OMAE 2008), Estoril, Portugal.

Ribeiro e Silva, S., Santos, T. A.,Guedes Soares, C. (2005). Parametrically excited roll in regular and irregular head seas. *International Shipbuilding Progress, 52*(1), 29-56.

Ribeiro e Silva, S., Turk, A., Guedes Soares, C.,Prpić-Oršić, J. (2010). On the parametric rolling of container vessels. *Brodo Gradnja, 61*, 347-358.

Rodríguez, C. A. (2008). *Análisis de la estabilidad de pesqueros en olas regulares de proa.* Master Thesis, Universidad Nacional de Ingeniería, Lima, Perú.

Rodríguez, C. A. (2010). *Análise Não Linear da Ressonância Paramétrica do Balanço de Navios.* PhD thesis, Universidade Federal do Rio de Janeiro, Rio de Janeiro, Brazil.

Rodríguez, C. A., Holden, C., Perez, T., Drummen, I., Neves, M. A. S.,Fossen, T. I. (2007). *Validation of a container ship model for parametric rolling.* Paper presented at the 9th International Ship Stability Workshop, Hamburg, Germany.

Sadat-Hosseini, H., Stern, F., Olivieri, A., Campana, E. F., Hashimoto, H., Umeda, N., . . . Francescutto, A. (2010). Head-wave parametric rolling of a surface combatant. *Ocean Engineering, 37*(10), 859-878.

Salvador, M.,Fabris, D. (2004). *Study of stability of a two wheeled vehicle through experiments on the road and in laboratory*. Paper presented at the Mostra-Convegno Automobili e Motori High-Tech, Modena, Italy.

Salvesen, N., Tuck, E. O.,Faltinsen, O. (1970). Ship motions and sea loads. *Transactions SNAME, 78*, 250-287.

Sanchez, N. E.,Nayfeh, A. H. (1990). Nonlinear rolling motions of ships in longitudinal waves. *International Shipbuilding Progress, 37*(411), 247-272.

Schreuder, M. (2008). Research study on the sinking sequence of MV Estonia. WP 4.1- 4.3. Numerical simulations of foundering scenarios. Gothenburg, Sweden: Chalmers University of Technology. Department of Shipping and Marine Technology.

Shaeri, A., Limebeer, D. J. N.,Sharp, R. S. (2004). *Nonlinear steering oscillations of motorcycles.* Paper presented at the 43rd IEEE Conference on Decision and Control, Nassau, Bahamas.

Sharp, R. S. (2001). Stability, control and steering responses of motorcycles. *Vehicle System Dynamics, 35*(4), 291-318.

Shaw, S., Turner, K., Rhoads, J.,Baskaran, R. (2003). *Parametrically excited MEMS-based filters.* Paper presented at the Proceedings of the IUTAM Symposium On Chaotic Dynamics And Control Of Systems And Processes In Mechanics, Rome, Italy.

Shin, Y. S., Belenky, V. L., Paulling, J. R., Weems, K. M.,Lin, W. M. (2004). Criteria for parametric roll of large containerships in longitudinal seas. *Transactions of the Society of Naval Architects and Marine Engineers, 112*, 14-47.

Skomedal, N. G. (1982). *Parametric excitation of roll motion and its influence on stability.* Paper presented at the 2nd Interanational Conference on Stability of Ships and Ocean Vehicles, Tokyio, Japan.

Spanos, D.,Papanikolaou, A. (2005). *Numerical Simulation of a Fishing Vessel in Parametric Roll in Head Seas.* Paper presented at the 8th International Workshop on Stability and Operational Safety of Ships Istambul, Turkey.

Spanos, D.,Papanikolaou, A. (2009). SAFEDOR International Benchmark Study on Numerical Simulation Methods for the Prediction on Parametric Rolling of Ships in Waves. Athens, Greece: National Technical University of Athens. School of Naval Architecture and Marine Engineering. http://www.naval.ntua.gr/sdl/sibs/intact.htm

Spyrou, K. J. (2000). On the parametric rolling of ships in a following sea under simultaneous nonlinear periodic surging. *Philosophical Transactions of the Royal Society of London. Series A: Mathematical, Physical and Engineering Sciences, 358*(1771), 1813-1834.

Spyrou, K. J. (2005). Design criteria for parametric rolling. *Oceanic Engineering International, 9 (1)*, 11-27.

Thomas, G. A., Duffy, J., Lilienthal, T., Watts, R.,Gehling, R. (2008). *Parametric rolling in head seas - an Australian perspective*. Paper presented at the 6th Osaka Colloquium on Seakeeping and Stability of Ships, Osaka, Japan.

Tondl, A.,Nabergoj, R. (1990). Model simulation of parametrically excited ship rolling. *Nonlinear Dynamics, 1*(2), 131-141.

Tondl, A., Ruijgrok, T., Verlhust, F.,Nabergoj, R. (2000). *Autoparametric resonance in mechanical systems*. Cambridge, UK: Cambridge University Press.

Treakle III, T. W. (1998). *A Time-Domain Numerical Study of Passive and Active Anti-Roll Tanks to Reduce Ship Motions.* Master thesis, Virginia Tech, Blacksburg, Virginia, USA.

Umeda, N. (1999). Nonlinear dynamics of ship capsizing due to broaching in following and quartering seas. *Journal of Marine Science and Technology, 4*(1), 16-26.

Umeda, N., Hashimoto, H., Minegaki, S.,Matsuda, A. (2008). An investigation of different methods for the prevention of parametric rolling. *Journal of Marine Science and Technology, 13*(1), 16-23.

Umeda, N., Hashimoto, H., Vassalos, D., Urano, S.,Okou, K. (2004). Nonlinear dynamics on parametric roll resonance with realistic numerical modelling. *International Shipbuilding Progress, 51*(2), 205-220.

Umeda, N., Iskandar, B., Hashimoto, H., Urano, S.,Matsuda, A. (2002). *Comparison of European and Asian Trawlers–Stability in Seaways.* Paper presented at the Asia Pacific Workshop on Marine Hydrodynamics, Kobe, Japan.

Valle Cabezas, J. (1999). *Estudio experimental de las no linealidades del amortiguamiento en el movimiento de balance de buques.* PhD thesis, Escuela Técnica Superior de Ingenieros Navales. Universidad Politécnica de Madrid, Madrid, Spain.

van Laarhoven, B. J. H. (2009). *Stability Analysis of Parametric Roll Resonance.* Master Thesis, Eindhoven University of Technology, Eindhoven.

Vidic-Perunovic, J. (2009). Ship Dynamic Intact Stability Focus on Parametric Roll. Lyngby, Denmark: Technical University of Denmark. Dept. of Mechanical Engineering. Coastal, Maritime and Structural Engineering

Vidic-Perunovic, J.,Jensen, J. J. (2009). Parametric roll due to hull instantaneous volumetric changes and speed variations. *Ocean Engineering, 36*(12), 891-899.

Vivanco, J. E. M. (2009). *Análise da Dinâmica Não-Linear no Balanço Paramétrico de Uma Embarcação Pesqueira.* Master thesis, Universidade Federal do Rio de Janeiro, Rio de Janeiro, Brazil.

Watts, P. (1883). On a method of reducing the rolling of ships at sea. *Transactions of Institution of Naval Architects, 24*, 165.

Watts, P. (1885). The use of water chambers for reducing the rolling of ships at sea. *Transactions of Institution of Naval Architects, 26*, 30.

Windén, B. (2009). *Anti Roll Tanks in Pure Car and Truck Carriers.* Master thesis, KTH Royal Institute of Technology, Stockholm.

Xing, Z.,McCue, L. (2009). *Modeling Ship Equations of Roll Motion Using Neural Networks*. Paper presented at the 10th International Conference on Stability of Ships and Ocean Vehicles, St. Petersburg, Russia.

Xing, Z.,McCue, L. (2010). Modeling Ship Equations of Roll Motion Using Neural Networks. *Naval Engineers Journal, 122*(3), 49-60.

Young, S. T. (2011). Report on the Rehearing of the formal investigation into the loss of the motor fishing vessel "Trident", registered at Peterhead (Official number PD111). Aberdeen, UK.

Zhang, G., Eddy Patuwo, B.,Y Hu, M. (1998). Forecasting with artificial neural networks: The state of the art. *International Journal of Forecasting, 14*(1), 35-62.

APPENDIX A. Spanish Trawler Test Conditions & Results

Table a. Regular waves. Fn = 0. Wave parameters and roll results.

H_w (m)	ω_w / ω_n	ω_w (rad/s)	T_w (s)	λ (m)	Slope (deg)	Φ_{max} (rad)	Φ_{avg} (rad)	Φ_{dev} (rad)
0.281	2.00	1.126	5.582	48.640	1.041	0.114	0.053	0.038
0.497	1.90	1.069	5.875	53.895	1.659	0.003	0.001	0.001
	2.00	1.126	5.582	48.640	1.838	0.216	0.093	0.072
0.745	1.90	1.069	5.875	53.895	2.488	0.143	0.083	0.043
	2.00	1.126	5.582	48.640	2.756	0.262	0.089	0.085
	2.10	1.182	5.316	44.118	3.038	0.022	0.004	0.004
1.000	1.70	0.957	6.567	67.322	2.672	0.012	0.004	0.002
	1.80	1.013	6.202	60.050	2.995	0.011	0.005	0.003
	1.90	1.069	5.875	53.895	3.336	0.220	0.096	0.078
	2.00	1.126	5.582	48.640	3.696	0.312	0.115	0.103
	2.10	1.182	5.316	44.118	4.073	0.132	0.039	0.036
	2.20	1.238	5.074	40.199	4.469	0.125	0.011	0.016
	2.30	1.295	4.854	36.779	4.882	0.011	0.004	0.002
1.200	2.00	1.126	5.582	48.640	10.966	0.375	0.156	0.111
1.491	1.70	0.957	6.567	67.322	3.979	0.008	0.003	0.002
	1.80	1.013	6.202	60.050	4.459	0.014	0.004	0.003
	1.90	1.069	5.875	53.895	4.966	0.319	0.142	0.096
	2.00	1.126	5.582	48.640	5.499	0.447	0.192	0.131
	2.10	1.182	5.316	44.118	6.059	0.364	0.143	0.105
	2.20	1.238	5.074	40.199	6.645	0.021	0.007	0.005
	2.30	1.295	4.854	36.779	7.256	0.018	0.006	0.004

H_w (m)	ω_w / ω_n	ω_w (rad/s)	T_w (s)	λ (m)	Slope (deg)	Φ_{max} (rad)	Φ_{avg} (rad)	Φ_{dev} (rad)
1.988	2.00	1.126	5.582	48.640	7.315	0.480	0.232	0.142
2.513	2.00	1.126	5.582	48.640	9.217	0.554	0.272	0.153
3.000	2.00	1.126	5.582	48.640	10.966	0.586	0.303	0.165

Table b. Regular waves. Fn = 0.1. Wave parameters and roll results.

H_w (m)	ω_e / ω_n	ω_w (rad/s)	T_w (s)	ω_e (rad/s)	λ (m)	Slope (deg)	Φ_{max} (rad)	Φ_{avg} (rad)	Φ_{dev} (rad)
0.745	2.00	0.965	6.509	1.126	66.145	2.027	0.110	0.033	0.023
1.000	1.90	0.923	6.807	1.070	72.341	2.487	0.251	0.061	0.043
	2.00	0.965	6.509	1.126	66.145	2.719	0.256	0.078	0.061
	2.10	1.007	6.237	1.182	60.741	2.961	0.276	0.052	0.048
	2.20	1.049	5.989	1.238	55.997	3.211	0.186	0.032	0.026
1.491	1.80	0.880	7.141	1.013	79.616	3.366	0.189	0.047	0.037
	1.90	0.923	6.807	1.070	72.341	3.704	0.352	0.113	0.076
	2.00	0.965	6.509	1.126	66.145	4.050	0.475	0.167	0.117
	2.10	1.007	6.237	1.182	60.741	4.409	0.695	0.223	0.152
	2.20	1.049	5.989	1.238	55.997	4.780	0.364	0.057	0.057
	2.30	1.090	5.764	1.294	51.876	5.158	0.342	0.041	0.049
1.988	1.80	0.880	7.141	1.013	79.616	4.484	0.111	0.023	0.018
	1.90	0.923	6.807	1.070	72.341	4.933	0.480	0.183	0.102
	2.00	0.965	6.509	1.126	66.145	5.393	0.607	0.258	0.151
	2.10	1.007	6.237	1.182	60.741	5.869	0.659	0.273	0.167
	2.20	1.049	5.989	1.238	55.997	6.362	0.564	0.141	0.115

Table c. Regular waves. Fn = 0.2. Wave parameters and roll results.

H_w (m)	ω_e / ω_n	ω_w (rad/s)	T_w (s)	ω_e (rad/s)	λ (m)	Slope (deg)	Φ_{max} (rad)	Φ_{avg} (rad)	Φ_{dev} (rad)
0.745	2.00	0.867	7.246	1.126	81.965	1.636	0.143	0.025	0.022
	1.80	0.796	7.898	1.013	97.380	1.848	0.072	0.021	0.016
	1.90	0.832	7.555	1.069	89.126	2.019	0.113	0.022	0.020
1.000	2.00	0.867	7.246	1.126	81.965	2.195	0.244	0.044	0.043
	2.10	0.902	6.964	1.182	75.712	2.376	0.198	0.032	0.035
	2.20	0.937	6.708	1.238	70.251	2.561	0.088	0.022	0.017
	1.80	0.796	7.898	1.013	97.380	2.753	0.218	0.031	0.030
	1.90	0.832	7.555	1.069	89.126	3.008	0.429	0.075	0.064
	2.00	0.867	7.246	1.126	81.965	3.270	0.349	0.104	0.075
1.491	2.10	0.902	6.964	1.182	75.712	3.539	0.572	0.177	0.149
	2.20	0.937	6.708	1.238	70.251	3.814	0.253	0.066	0.060
	2.30	0.971	6.473	1.295	65.423	4.094	0.248	0.040	0.040
	2.00	0.867	7.246	1.126	81.965	4.356	0.548	0.163	0.141
1.988	2.10	0.902	6.964	1.182	75.712	4.714	0.683	0.289	0.159
	2.20	0.937	6.708	1.238	70.251	5.079	0.711	0.221	0.165

Table d. Regular waves. Fn = 0.3. Wave parameters and roll results.

H_w (m)	ω_e / ω_n	ω_w (rad/s)	T_w (s)	ω_e (rad/s)	λ (m)	Slope (deg)	Φ_{max} (rad)	Φ_{avg} (rad)	Φ_{dev} (rad)
1.000	2.00	0.797	7.879	1.125	96.930	1.856	0.106	0.034	0.024
	2.20	0.858	7.322	1.238	83.695	2.150	0.168	0.036	0.026
1.491	1.80	0.735	8.553	1.013	114.215	2.348	0.149	0.035	0.027
	1.90	0.766	8.197	1.070	104.915	2.556	0.311	0.076	0.059
	2.00	0.797	7.879	1.125	96.930	2.766	0.153	0.040	0.031
	2.10	0.828	7.587	1.182	89.873	2.983	0.141	0.035	0.025
	2.20	0.858	7.322	1.238	83.695	3.203	0.645	0.235	0.160
1.988	2.00	0.797	7.879	1.125	96.930	3.686	0.209	0.057	0.044
	1.80	0.735	8.553	1.013	114.215	3.129	0.152	0.044	0.031
	1.90	0.766	8.197	1.070	104.915	3.406	0.206	0.050	0.042
	2.10	0.828	7.587	1.182	89.873	3.974	0.251	0.045	0.044
	2.20	0.858	7.322	1.238	83.695	4.267	0.687	0.197	0.190
	2.30	0.888	7.076	1.295	78.173	4.567	0.256	0.052	0.048

Table e. Irregular waves. Fn = 0. Wave parameters and roll results.

ω_{pe} / ω_n	ω_p (rad/s)	T_p (s)	Spectrum	H_S (m)	PEF	Φ_{max} (rad)	Φ_{avg} (rad)	Φ_{dev} (rad)
2.00	1.126	5.582	Jonswap	1.800	5.0	0.208	0.026	0.030
2.00	1.126	5.582	Jonswap	1.988	3.5	0.302	0.026	0.031
						0.279	0.033	0.034
						0.413	0.036	0.045
2.00	1.126	5.582	TMA	0.994	7.0	0.017	0.022	0.994
2.00	1.126	5.582	TMA	1.500	7.0	0.045	0.053	1.500
2.00	1.126	5.582	TMA	1.988	3.5	0.045	0.049	1.988
					7.0	0.080	0.080	1.988
2.00	1.126	5.582	TMA	2.438	7.0	0.100	0.096	2.438

Table f. Irregular waves. Fn = 0.1. H_S = 1.491. TMA spectrum.
Wave parameters and roll results.

ω_{pe} / ω_n	ω_p (rad/s)	ω_{pe} (rad/s)	T_p (s)	PEF	Φ_{max} (rad)	Φ_{avg} (rad)	Φ_{dev} (rad)
2.00	0.965	1.126	6.509	3.5	0.223	0.044	0.038
					0.126	0.018	0.017
					0.188	0.027	0.031
					0.119	0.020	0.017
2.00	0.965	1.126	6.509	7.0	0.370	0.069	0.077
					0.543	0.067	0.082
					0.191	0.039	0.035
					0.319	0.057	0.058
					0.331	0.057	0.052
2.10	1.007	1.182	6.237	7.0	0.080	0.013	0.011
					0.186	0.019	0.017
2.20	1.049	1.238	5.989	3.5	0.137	0.021	0.019
					0.132	0.025	0.021
2.20	1.049	1.238	5.989	7.0	0.272	0.039	0.048
					0.140	0.016	0.017

Table g. Irregular waves. Fn = 0.2. H_S = 1.491. TMA spectrum.
Wave parameters and roll results.

ω_{pe} / ω_n	ω_p (rad/s)	ω_{pe} (rad/s)	T_p (s)	PEF	Φ_{max} (rad)	Φ_{avg} (rad)	Φ_{dev} (rad)
1.90	0.832	1.069	7.555	3.5	0.409	0.115	0.092
					0.088	0.022	0.017
					0.122	0.032	0.023
					0.271	0.050	0.047
1.90	0.832	1.069	7.555	7.0	0.149	0.045	0.035
					0.219	0.047	0.038
2.00	0.867	1.126	7.246	3.5	0.163	0.022	0.022
					0.089	0.017	0.014
					0.137	0.030	0.025
					0.298	0.029	0.034
2.00	0.867	1.126	7.246	7.0	0.190	0.040	0.035
					0.118	0.024	0.020
					0.187	0.027	0.027
					0.290	0.041	0.043
					0.143	0.024	0.023
					0.129	0.022	0.021
2.10	0.902	1.182	6.964	3.5	0.064	0.016	0.013
					0.108	0.024	0.020
					0.370	0.058	0.068
					0.253	0.031	0.036

ω_{pe} / ω_n	ω_p (rad/s)	ω_{pe} (rad/s)	T_p (s)	PEF	Φ_{max} (rad)	Φ_{avg} (rad)	Φ_{dev} (rad)
2.10	0.902	1.182	6.964	7.0	0.154	0.036	0.028
					0.134	0.025	0.020
					0.193	0.032	0.031
					0.157	0.029	0.027
					0.483	0.049	0.068
					0.151	0.031	0.028
					0.268	0.036	0.050
2.20	0.937	1.238	6.708	3.5	0.148	0.034	0.028
					0.137	0.039	0.029
					0.301	0.069	0.064
					0.107	0.022	0.019
2.20	0.937	1.238	6.708	7.0	0.101	0.023	0.019
					0.254	0.058	0.049
					0.216	0.039	0.041
					0.222	0.038	0.035

Table h. Irregular waves. Fn = 0.3. H_S = 1.491. TMA spectrum.
Wave parameters and roll results.

ω_{pe} / ω_n	ω_p (rad/s)	ω_{pe} (rad/s)	T_p (s)	PEF	Φ_{max} (rad)	Φ_{avg} (rad)	Φ_{dev} (rad)
2.00	0.797	1.125	7.879	3.5	0.255	1.724	0.049
					0.156	1.901	0.028
					0.144	2.748	0.030
					0.196	3.126	0.040
					0.209	1.791	0.044
					0.111	2.800	0.018
2.00	0.797	1.125	7.879	7.0	0.145	1.619	0.030
					0.146	1.719	0.033
					0.235	4.052	0.048
					0.277	2.318	0.071
					0.284	1.450	0.055
					0.181	0.734	0.031
					0.139	2.549	0.025
					0.072	1.051	0.013
2.10	0.828	1.182	7.587	3.5	0.041	0.418	0.007
					0.073	0.813	0.014
					0.079	0.720	0.013
					0.076	0.988	0.017

ω_{pe} / ω_n	ω_p (rad/s)	ω_{pe} (rad/s)	T_p (s)	PEF	Φ_{max} (rad)	Φ_{avg} (rad)	Φ_{dev} (rad)
2.10	0.828	1.182	7.587	7.0	0.165	1.800	0.031
					0.091	0.953	0.017
					0.129	1.344	0.023
					0.108	1.203	0.021

APPENDIX B. UK Trawler Test Conditions & Results

Table i. Regular waves. Fn = 0. GM = 0.370 m. Wave parameters and roll results.

H_w (m)	ω_w / ω_n	ω_w (rad/s)	T_w (s)	λ (m)	Slope (deg)	Φ_{max} (rad)	Φ_{avg} (rad)	Φ_{dev} (rad)
0.375	2.00	1.678	3.744	21.890	3.081	0.035	0.006	0.006
0.495	2.00	1.678	3.744	21.890	4.064	0.015	0.003	0.002
	2.00	1.678	3.744	21.890	4.064	0.107	0.015	0.019
0.630	1.90	1.594	3.941	24.255	4.665	0.097	0.008	0.014
	2.00	1.678	3.744	21.890	5.166	0.157	0.011	0.022
	2.10	1.762	3.566	19.855	5.693	0.189	0.065	0.063
	2.20	1.846	3.404	18.090	6.244	0.048	0.007	0.007
0.750	2.00	1.678	3.744	21.890	6.144	0.230	0.040	0.056
	2.10	1.762	3.566	19.855	6.768	0.204	0.083	0.068
	2.20	1.846	3.404	18.090	7.421	0.115	0.007	0.011
1.005	1.90	1.594	3.941	24.255	7.416	0.099	0.006	0.009
	2.00	1.678	3.744	21.890	8.207	0.456	0.079	0.116
	2.10	1.762	3.566	19.855	9.036	0.241	0.103	0.073
	2.20	1.846	3.404	18.090	9.900	0.090	0.006	0.008
1.125	1.90	1.594	3.941	24.255	8.290	0.085	0.008	0.013
	2.00	1.678	3.744	21.890	9.172	0.177	0.069	0.046
	2.00	1.678	3.744	21.890	9.172	0.478	0.078	0.113
	2.10	1.762	3.566	19.855	10.093	0.230	0.093	0.075
	2.20	1.846	3.404	18.090	11.055	0.146	0.011	0.017
1.245	2.00	1.678	3.744	21.890	10.131	0.133	0.027	0.029

Table j. Regular waves. Fn = 0.1. GM = 0.370 m. Wave parameters and roll results.

H_w (m)	ω_e / ω_n	ω_w (rad/s)	T_w (s)	ω_e (rad/s)	λ (m)	Slope (deg)	Φ_{max} (rad)	Φ_{avg} (rad)	Φ_{dev} (rad)
0.375	1.80	1.270	4.946	1.525	38.195	1.767	0.045	0.009	0.008
	2.00	1.330	4.725	1.665	34.860	1.936	0.081	0.014	0.013
	2.05	1.389	4.525	1.708	31.967	2.111	0.194	0.035	0.039
	2.10	1.448	4.338	1.784	29.377	2.296	0.182	0.035	0.043
	2.25	1.510	4.160	1.893	27.016	2.497	0.036	0.008	0.006
0.630	2.00	1.330	4.725	1.679	34.860	3.250	0.248	0.045	0.031
	2.05	1.389	4.525	1.708	31.967	3.543	0.459	0.075	0.075
	2.10	1.448	4.338	1.762	29.377	3.854	0.529	0.086	0.097
	2.25	1.510	4.160	1.880	27.016	4.190	0.123	0.042	0.026
0.750	1.85	1.270	4.946	1.563	38.195	3.530	0.159	0.047	0.030
	1.90	1.330	4.725	1.619	34.860	3.867	0.562	0.089	0.103
	2.00	1.389	4.525	1.678	31.967	4.216	0.624	0.142	0.133
	2.10	1.448	4.338	1.755	29.377	4.586	0.280	0.056	0.045
	2.20	1.510	4.160	1.839	27.016	4.984	0.458	0.111	0.068
	2.30	1.562	4.022	1.926	25.260	5.329	0.113	0.036	0.023
1.005	2.00	1.448	4.338	1.680	29.377	6.134	0.430	0.097	0.098
	2.00	1.389	4.525	1.660	31.967	5.641	0.559	0.097	0.124

Table k. Regular waves. Fn = 0.15. GM = 0.370 m. Wave parameters and roll results.

H_w (m)	ω_e / ω_n	ω_w (rad/s)	T_w (s)	ω_e (rad/s)	λ (m)	Slope (deg)	Φ_{max} (rad)	Φ_{avg} (rad)	Φ_{dev} (rad)
0.375	1.95	1.299	4.838	1.658	36.543	1.846	0.059	0.012	0.009
	2.10	1.352	4.648	1.781	33.737	2.000	0.049	0.016	0.011
0.630	1.90	1.246	5.043	1.595	39.714	2.853	0.071	0.032	0.016
	1.95	1.299	4.838	1.645	36.543	3.100	0.174	0.029	0.026
	2.05	1.352	4.648	1.734	33.737	3.357	0.349	0.078	0.073
	2.10	1.402	4.482	1.775	31.357	3.612	0.459	0.055	0.071
0.750	1.90	1.246	5.043	1.595	39.714	3.395	0.200	0.074	0.045
	2.00	1.299	4.838	1.678	36.543	3.689	0.134	0.053	0.032
	2.05	1.402	4.482	1.736	31.357	4.297	0.434	0.104	0.108
	2.10	1.352	4.648	1.763	33.737	3.995	0.195	0.043	0.034
	2.10	1.352	4.648	1.763	33.737	3.995	0.720	0.124	0.114
	2.15	1.402	4.482	1.806	31.357	4.297	0.412	0.102	0.098

Table l. Regular waves. Fn = 0.2. GM = 0.370 m. Wave parameters and roll results.

H_w (m)	ω_e / ω_n	ω_w (rad/s)	T_w (s)	ω_e (rad/s)	λ (m)	Slope (deg)	Φ_{max} (rad)	Φ_{avg} (rad)	Φ_{dev} (rad)
0.375	1.90	1.226	5.123	1.612	40.978	1.647	0.092	0.025	0.016
	2.10	1.274	4.931	1.742	37.963	1.777	0.107	0.037	0.023
0.630	2.00	1.226	5.123	1.666	40.978	2.765	0.236	0.092	0.055
	2.05	1.274	4.931	1.729	37.963	2.984	0.138	0.040	0.030
0.750	1.95	1.226	5.123	1.624	40.978	3.291	0.091	0.025	0.019
	2.00	1.274	4.931	1.691	37.963	3.551	0.075	0.020	0.014

Table m. Regular waves. Fn = 0. GM = 0.436 m. Wave parameters and roll results.

H_w (m)	ω_w / ω_n	ω_w (rad/s)	T_w (s)	λ (m)	Slope (deg)	Φ_{max} (rad)	Φ_{avg} (rad)	Φ_{dev} (rad)
0.255	2.00	1.828	3.437	18.445	2.487	0.014	0.002	0.002
0.375	1.90	1.735	3.621	20.474	3.293	0.013	0.003	0.002
	2.00	1.828	3.437	18.445	3.655	0.135	0.024	0.030
	2.10	1.918	3.275	16.748	4.024	0.018	0.002	0.002
0.495	1.90	1.735	3.621	20.474	4.344	0.012	0.003	0.002
	2.00	1.828	3.437	18.445	4.819	0.171	0.025	0.041
	2.10	1.918	3.275	16.748	5.305	0.027	0.003	0.004
0.630	1.90	1.735	3.621	20.474	5.522	0.051	0.005	0.006
	2.00	1.828	3.437	18.445	6.125	0.187	0.049	0.044
	2.10	1.918	3.275	16.748	6.740	0.072	0.007	0.010
0.750	2.00	1.828	3.437	18.445	7.280	0.092	0.030	0.020
1.005	2.00	1.828	3.437	18.445	9.714	0.031	0.006	0.005
	2.10	1.918	3.275	16.748	10.676	0.059	0.017	0.015
1.125	1.90	1.735	3.621	20.474	9.794	0.040	0.006	0.005
	2.00	1.828	3.437	18.445	10.847	0.034	0.007	0.006
	2.10	1.918	3.275	16.748	11.916	0.075	0.013	0.013

Table n. Regular waves. Fn = 0.1. GM = 0.436 m. Wave parameters and roll results.

H_w (m)	ω_e / ω_n	ω_w (rad/s)	T_w (s)	ω_e (rad/s)	λ (m)	Slope (deg)	Φ_{max} (rad)	Φ_{avg} (rad)	Φ_{dev} (rad)
0.375	1.95	1.498	4.196	1.772	27.484	2.454	0.304	0.034	0.055
	2.00	1.498	4.196	1.825	27.484	2.454	0.037	0.009	0.007
	2.00	1.498	4.196	1.825	27.484	2.454	0.182	0.018	0.028
	2.10	1.498	4.196	1.905	27.484	2.454	0.034	0.007	0.006
	2.15	1.557	4.036	1.959	25.428	2.653	0.022	0.006	0.004
	2.30	1.616	3.887	2.086	23.593	2.859	0.016	0.004	0.003
0.495	2.00	1.498	4.196	1.816	27.484	3.238	0.000	0.000	0.000
	2.15	1.601	3.925	1.955	24.052	3.699	0.040	0.009	0.007
0.630	1.90	1.498	4.196	1.763	27.484	4.119	0.097	0.021	0.018
	2.00	1.498	4.196	1.852	27.484	4.119	0.216	0.028	0.029
0.750	1.80	1.325	4.744	1.636	35.132	3.837	0.210	0.045	0.037
	1.85	1.394	4.506	1.701	31.707	4.250	0.145	0.050	0.031
1.005	1.80	1.498	4.196	1.675	27.484	6.553	0.258	0.051	0.044
	1.90	1.498	4.196	1.745	27.484	6.553	0.109	0.029	0.024
	1.95	1.498	4.196	1.776	27.484	6.553	0.419	0.063	0.077
1.125	1.80	1.325	4.744	1.615	35.132	5.745	0.187	0.052	0.037

Table o. Regular waves. Fn = 0.15. GM = 0.436 m. Wave parameters and roll results.

H_w (m)	ω_e / ω_n	ω_w (rad/s)	T_w (s)	ω_e (rad/s)	λ (m)	Slope (deg)	Φ_{max} (rad)	Φ_{avg} (rad)	Φ_{dev} (rad)
0.375	2.15	1.498	4.196	1.985	27.484	2.454	0.020	0.006	0.004
0.495	1.95	1.394	4.506	1.797	31.707	2.808	0.023	0.006	0.005
0.630	1.90	1.325	4.744	1.726	35.132	3.224	0.065	0.014	0.012
	1.95	1.394	4.506	1.778	31.707	3.572	0.252	0.076	0.066
0.750	1.80	1.343	4.680	1.651	34.193	3.942	0.127	0.027	0.022
	1.85	1.325	4.744	1.678	35.132	3.837	0.240	0.050	0.045
	1.90	1.394	4.506	1.740	31.707	4.250	0.467	0.090	0.106
	1.95	1.394	4.506	1.778	31.707	4.250	0.286	0.041	0.051

Table p. Regular waves. Fn = 0.2. GM = 0.436 m. Wave parameters and roll results.

H_w (m)	ω_e / ω_n	ω_w (rad/s)	T_w (s)	ω_e (rad/s)	λ (m)	Slope (deg)	Φ_{max} (rad)	Φ_{avg} (rad)	Φ_{dev} (rad)
0.375	2.05	1.325	4.744	1.872	35.132	1.921	0.000	0.000	0.000
	2.20	1.325	4.744	2.003	35.132	1.921	0.062	0.013	0.010
0.495	2.00	1.325	4.744	1.802	35.132	2.534	0.221	0.024	0.035
0.630	1.95	1.278	4.916	1.775	37.734	3.003	0.065	0.018	0.013
	2.05	1.325	4.744	1.858	35.132	3.224	0.054	0.015	0.011
	2.10	1.376	4.566	1.944	32.545	3.480	0.068	0.014	0.011
1.005	1.90	1.325	4.744	1.775	35.132	5.135	0.159	0.032	0.032
	2.00	1.325	4.744	1.796	35.132	5.135	0.290	0.079	0.055
	2.05	1.325	4.744	1.854	35.132	5.135	0.321	0.099	0.062
	2.20	1.394	4.506	2.008	31.707	5.687	0.345	0.057	0.053

LIST OF TABLES

LIST OF FIGURES